Seismic Risk

Stefano Parolai

stefano.parolai@units.it

https://www.dmg.units.it/it/dipartimento/persone/personale-docente?q=it/node/27958

Seismic Risk Assessment and Mitigation

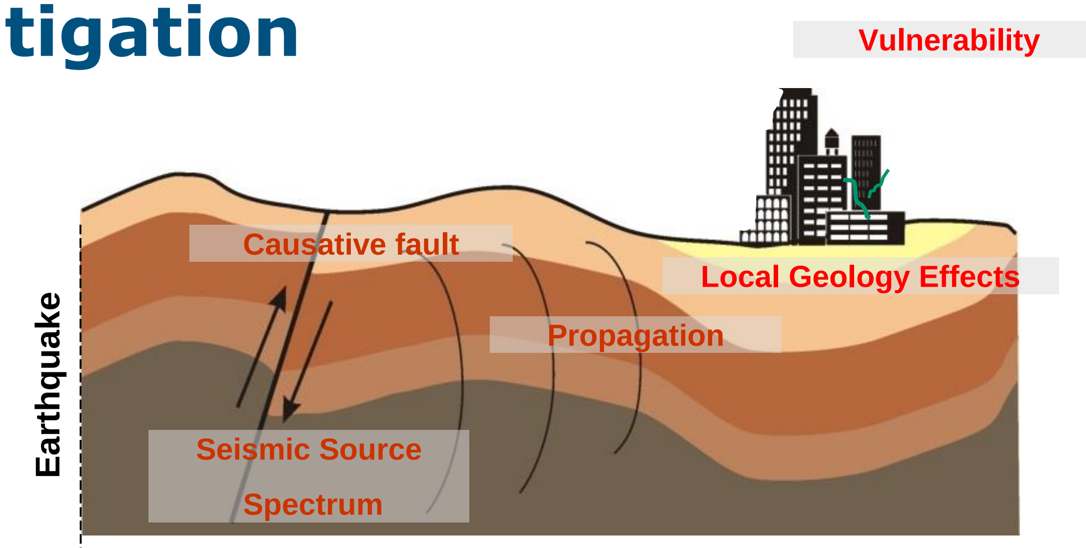

Decades | Years | Days to minutes | 0 | seconds | Minutes to hours

Long Term Seismic and landslides Risk mapping

Long Term Forecasting

Short Term Forecasting

Earthquake and landslides Early Warning

Real time and rapid loss estimation

Aftershock Forecasting

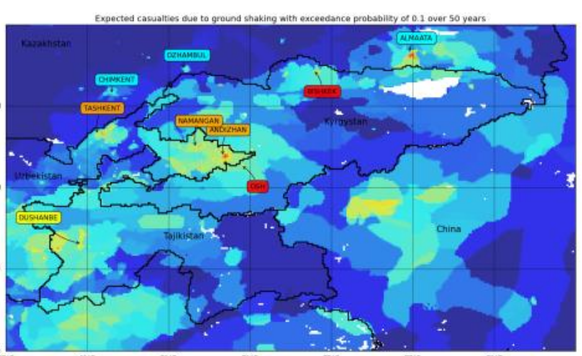

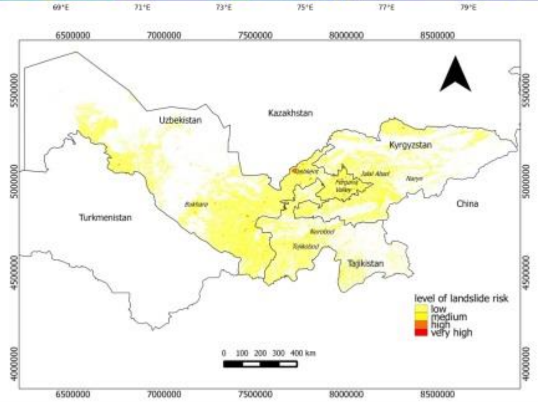

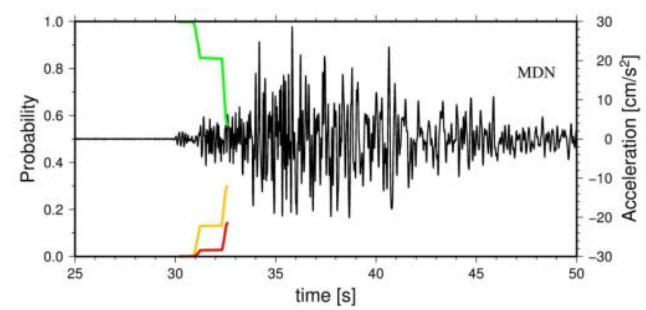

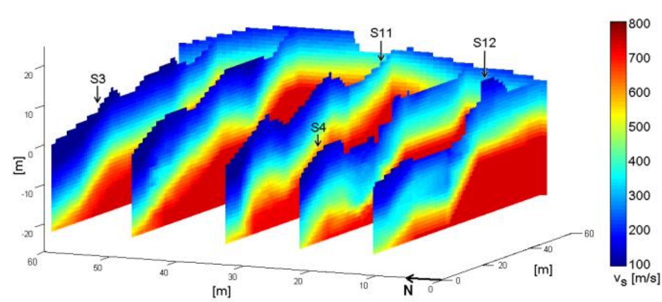

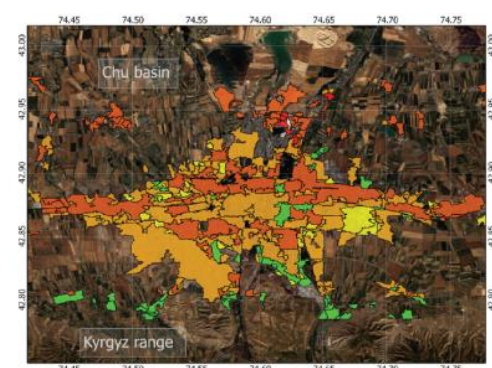

UNIVERSITÀ DEGLI STUDI DI TRIESTE

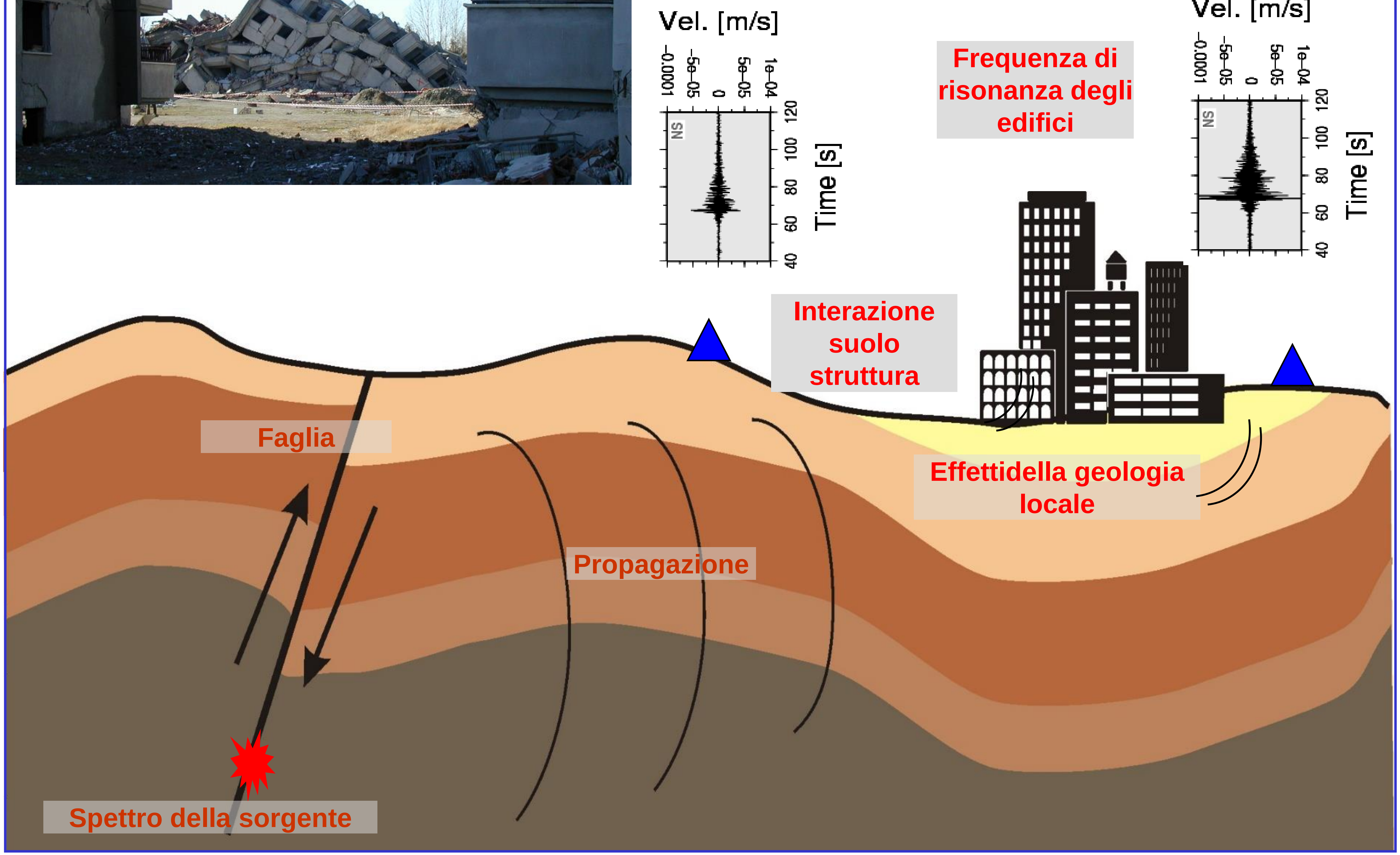

Vel. [m/s]
Time [s]
Frequenza di risonanza degli edifici
Interazione suolo struttura
Faglia
Propagazione
Effettidella geologia locale
Spettro della sorgente

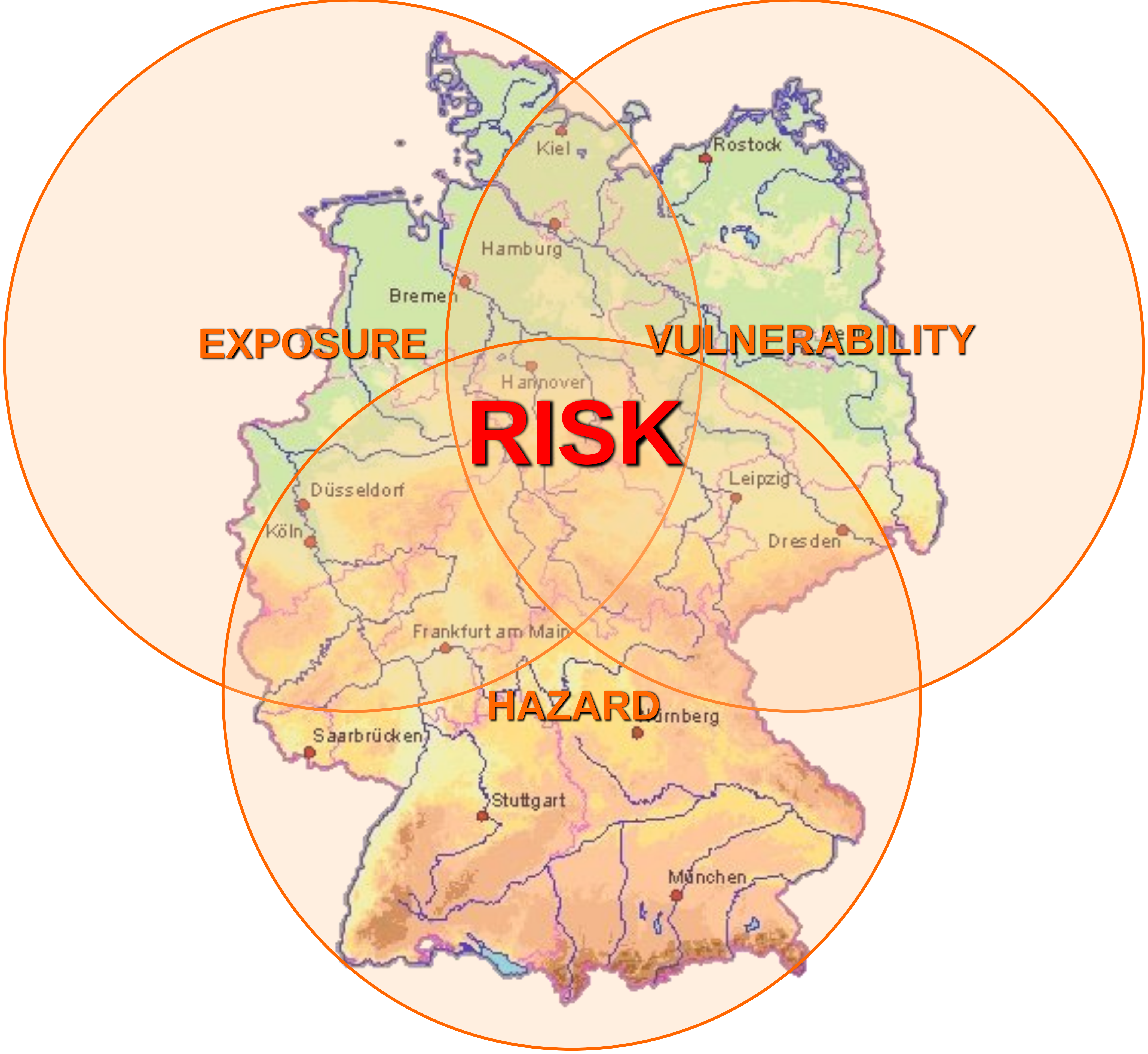
EXPOSURE
VULNERABILITY
RISK
HAZARD
Kiel
Rostock
Hamburg
Bremen
Hannover
Düsseldorf
Köln
Leipzig
Dresden
Frankfurt am Main
Saarbrücken
Stuttgart
München

Some terminology

Hazard: A dangerous phenomenon, substance, human activity or condition that may cause loss of life injury, or other health impacts, property damage, loss of livelihoods and services, social and economic disruption, or environmental damage (UNISDR, 2009).

Exposure: People, property, systems or other elements present in hazard zones that are thereby subject to potential losses (UNISDR, 2009).

Vulnerability: Characteristics and circumstances of a community, system or asset that make it susceptible to the damaging effects of a hazard (UNISDR, 2009).

Risk: The combination of the consequences of an event (hazard) and the associated likelihood/probability of its occurrence (ISO 31010, 2009).

Global Seismic Hazard Assessment Program (1)

The ***Global Seismic Hazard Assessment Program*** (GSHAP) was completed in 1999.

Of the continental land masses, it was found that

- *ca.* 70% have low hazard, 0-8% of *g* being exceeded;
- *ca.* 22% have moderate hazard, 8-24%;
- *ca.* 6% have high hazard, 24-40%;
- *ca.* 2% have very high hazard, >40%.

HOWEVER . . Remember that while plate boundaries make up only 15% of the Earth’s surface, 40% of the human population is located in their vicinity.

Seismic hazard maps (1)

Seismic hazard maps describe the ***probability*** (e.g., 2, 5 or 10%) that a given ***ground motion*** (e.g., peak horizontal acceleration) will be ***exceeded*** over a certain period (e.g., 50 years).

Evaluating seismic hazard requires characterising ***seismic cycles***, where the ***recurrence times*** range from 10 to 10^3 years (active areas) to 10^3 to 10^5 years (low deformation).

The generation of seismic hazard maps may employ a group of methodologies under the general term ***probabilistic seismic hazard assessment*** (PSHA).

Global Earthquake Model

GEM
GLOBAL EARTHQUAKE MODEL
working together to assess risk

Global Seismic Hazard Map

Version 2018.1

OQ OPENQUAKE

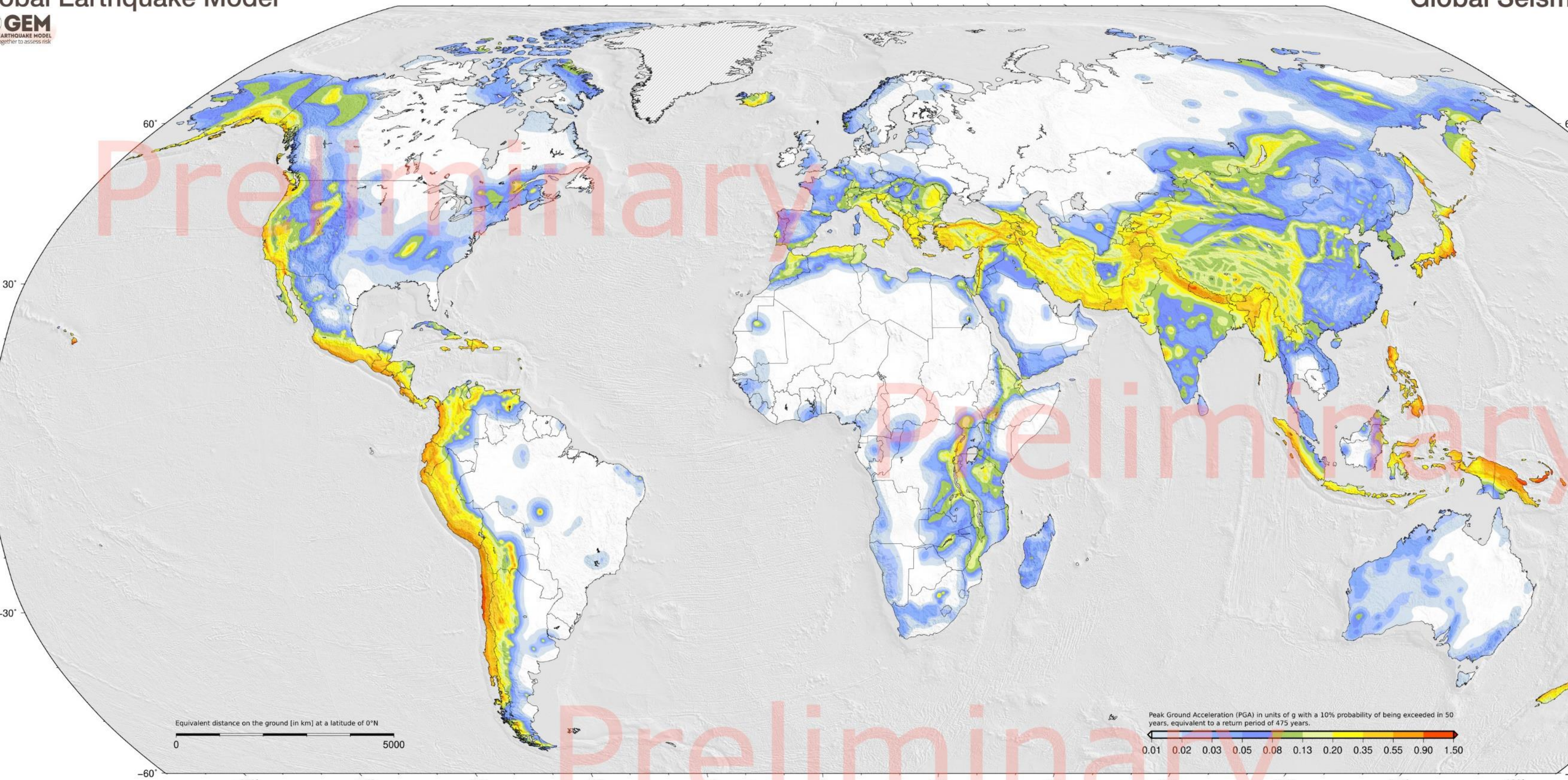

Global Earthquake Model (GEM) Seismic Hazard Map

The Global Earthquake Model (GEM) Seismic Hazard Map depicts the geographic distribution of the Peak Ground Acceleration (PGA) with a 10% probability of being exceeded in 50 years, equivalent to a return period of about 475 years, the internationally agreed reference for building safety regulation. The map was created by collating maps computed using national and regional probabilistic seismic hazard models developed by various institutions and projects, and by scientists working at the GEM Foundation. The OpenQuake engine, an open source seismic hazard and risk calculation software principally developed by the GEM Foundation, was used to calculate the hazard values. A smoothing methodology was applied to homogenise hazard values between adjacent models within buffer zones symmetrically distributed across the model borders. The map is based on a database of hazard models described using the OpenQuake engine and data format. Scientists working at the GEM Secretariat converted the models originally described using other formats. The models that were translated are: Alaska, Arabian Peninsula, Canada (translation completed by the Canada Geological Survey), China (translation completed by CEA in collaboration with GEM and the Swiss Seismological Service), Hawaii, India (translation completed by Nick Ackerley), Japan (translation completed by GEM in collaboration with NIED), New Zealand (translation completed by GNS Science), and United States of America. While translating these models various checks were performed to test the compatibility between the original results and the new results computed using the OpenQuake engine. Overall the differences between the original and translated model results are small, notwithstanding some diversity in modelling methodologies implemented in different hazard modelling software. The map and the underlying database of models are designed as a dynamic framework, capable to incorporate the most recent open models. The GEM Foundation plans to release future updates of this map on a regular basis as new information becomes available.

Acknowledgements

This map is the result of a collaborative effort and extensively relies on the determination of various organisations and projects to openly share resources. The creation of this map would not have been possible without the support provided by several public and private organisations during GEM's second implementation phase (2015-2018). These key contributions are profoundly acknowledged. The map was plotted using the GMT plotting software; the authors of this tool are acknowledged.

How to use and cite this work

Please cite this work as: M. Pagani, L. Danciu, J. Garcia, R. Gee, K. Johnson, D. Monelli, V. Poggi, R. Styron, G. Weatherill (2018). Global Earthquake Model (GEM) Seismic Hazard Map (version 2018.1 - December 2018). doi:

Contacts:
Fondazione GEM
via Ferrata, 127100 Pavia, Italy
info@globalquakemodel.org

More information available at:
http://www.globalquakemodel.org/gem

→ **Alaska (US) [ALS] - 2007**
Developed by the United States Geological Survey and converted into the OpenQuake engine by GEM.
• Authors: R.L. Wesson, O.S. Boyd, C.S. Mueller, C.G. Bufe, A.D. Frankel, M.D. Petersen
• Website: https://earthquake.usgs.gov/hazards/hazmaps/

→ **Arabian Peninsula [ARB] - 2018**
Developed by the Saudi Geological Survey and converted into the OpenQuake engine by GEM.
• Authors: H. Zahran, V. Sokolov, S. El-Hadidy Youssef, W. W. Alraddadi, M. J. Roobol, I. C. F. Stewart, M. El-Hadidy
• Website: https://www.sgs.org.sa/english/naturalhazards/pages/ncev.aspx

→ **Australia [AUS] - 2018**
Developed by Geoscience Australia.
• Authors: T. Allen, J. Griffin, M. Leonard, D. Clark, H. Ghasemi
• Website: http://www.ga.gov.au/about/projects/safety/nsha

→ **Canada [CAN] - 2015**
Developed by Natural Resources Canada, partly adjusted to the OpenQuake engine by GEM.
• Authors: J. Adams, S. Halchuk, T. Allen, G. Rogers
• Website: http://www.earthquakescanada.nrcan.gc.ca

→ **Caribbean and Central America [CCA] - 2018**
Developed within the USAID-funded project CCARA. Cuba and Puerto Rico were included a posteriori by GEM. Organisations involved in CCARA: GEM - University of Costa Rica, Costa Rica - Costa Rican Institute of Electricity, Costa Rica - Nicaraguan Institute of Territorial Studies, Nicaragua - Catholic University of El Salvador, El Salvador - Ministry of Environment and Natural Resources, El Salvador - Panama University, Panama.
• Authors: J. Garcia-Pelaez, R. Gee, R. Styron, V. Poggi
• Website: https://www.globalquakemodel.org/

→ **Central Asia [CEA] - 2018**
Developed within the EMCA project. Organisations involved: Helmholtz German Research Centre for Geosciences, Germany - Institute of Geology, Earthquake Engineering and Seismology of the Academy of Sciences of the Republic of Tajikistan - Institute of Geophysical Research, Kazakhstan - International University of Innovation Technologies, Kyrgyzstan - Kyrgyzstan Institute of Seismology, Kyrgyzstan - Central-Asian Institute of Applied Geosciences, Kyrgyzstan - Institute of Mechanics and Seismic Stability of Structures of the Academy of Sciences of Uzbekistan, Uzbekistan - Mavlyanov Institute of Seismology, Uzbekistan.
• Authors: S. Ullah, D. Bindi, M. Pilz, L. Danciu, G.A. Weatherill, E. Zuccolo, A. Ischuk, N.N. Mikhailova, K. Abdrakhmatov, S. Parolai, K. Fleming
• Website: http://www.emca-gem.org/

→ **China [CHN] - 2015**
Developed by the Institute of Geophysics of the China Earthquake Administration and converted into the OpenQuake engine by Changlong Li within a collaboration between the Institute of Geophysics of the China Earthquake Administration, the Swiss Seismological Service, Swiss Federal Institute of Technology, Switzerland and GEM.
• Authors: M. Gao, G. Chen, F. Xie, X. Xu, X. Li, Y. Yu, S. Li, B. Zhou, H. Pan, Y. Lu, F. Zhao, J. Wu
• Website: http://www.gb18306.cn/

→ **Europe [EUR] - 2013**
Developed within the EU-funded SHARE project, coordinated by the Swiss Federal Institute of Technology, Zurich, Switzerland. Organisations involved: Helmholtz Zentrum Potsdam Deutsches GeoForschungsZentrum GFZ - Istituto Nazionale di Geofisica e Vulcanologia, Italy - Université Joseph Fourier Grenoble, France - Università degli Studi di Pavia, Italy - Aristotelio Panepistimio Thessalonikis, Greece - Bureau de Recherches Géologiques et Minières, France - Centre de Recherche en Astronomie Astrophysique et Géophysique, Algeria - Instituto Superior Tecnico, Portugal - Bogazici University, Turkey - Laboratorio Nacional de Engenharia Civil, Portugal - Middle East Technical University, Turkey - Seizmoloski Zavod Crne Gore, Montenegro - Natural Environment Research Council, United Kingdom - Institutul National de Cercetare-Dezvoltare Pentru Fizica Pamantului, Romenia - Ethniko kai Kapodistriako Panepistimio Athinon, Greece - Stiftelsen Norsar, Norway - Koninklijke Sterrenwacht van Belgie, Belgium
• Authors: J. Woessner, L. Danciu, D. Giardini, H. Crowley, F. Cotton, G. Grünthal, G. Valensise, R. Arvidsson, R. Basili, M. Betül Demircioglu, S. Hiemer, Carlo Meletti, R. W. Musson, A.N. Rovida, K. Sesetyan, M. Stucchi
• Website: http://www.share-eu.org/

→ **Hawaii (US) [HAW] - 1998**
Developed by the United States Geological Survey and converted into the OpenQuake engine by GEM.
• Authors: F. W. Klein, A.D. Frankel, C.S. Mueller, R.L. Wesson, P.G. Okubo
• Website: https://earthquake.usgs.gov/hazards/hazmaps/

→ **Indonesia [IDN] - 2017**
National seismic hazard model for Indonesia created by the Team for Updating of Seismic Hazard Maps of Indonesia. The team belongs to the National Center for Earthquake Studies under the Center for Research and Development of Housing and Settlements of the Ministry of Public Works and People Housing. Ministries involved: Ministry of Public Works and People Housing; Ministry of Energy and Mineral resources; Ministry of Transportation; Ministry of Research, Technology and Higher Education; and National Disaster Management Authority of Indonesia. Organizations involved: Bureau of Meteorology, Climatology and Geophysics; Indonesian Research Institute; Geospatial Information Agency; Center for Research and Development of Housing and Settlements; Centre of Volcanology and Geological Hazard Mitigation; Indonesian Academy of Sciences; Bandung Institute of Technology; University of Indonesia; University of Gajah Mada; University of Diponegoro; Indonesian Society for Geotechnical Engineering; and Indonesian Disaster Expert Association. The team collaborated internationally with Geoscience Australia, Australia.
• Authors: M. Irsyam., L. Faizal, D. Natawidjaja, I. Meilano, S. Widiyantoro, W. Triyoso, A. Rudiyanto, S. Hidayati, M. Asrurifak, M. Ridwan, P. Cummins

→ **India and surroundings [IND] - 2012**
Developed by Thingbaijam and Nath (2012), revised and implemented in OpenQuake by N. Ackerley (Natural Resources Canada).
• Authors: N. Ackerley, K.K.S. Thingbaijam, and S.K. Nath

→ **Japan [JPN] - 2014**
National hazard model implemented by the Headquarters for Earthquake Research Promotion (HERP) and converted into the OpenQuake engine format within a collaboration between the National Research Institute for Earth Science and Disaster Resilience (NIED), Japan, and GEM.
• Authors: - H. Fujiwara, N. Morikawa, S. Kawai, S. Aoi, S. Senna, T. Maeda, H. Azuma, K. X. Hao, A. Iwaki, K. Wakamatsu, M. Imoto, N. Hasegawa, T. Okumura, T. Hayakawa, and M. Takahashi
• Website: http://www.j-shis.bosai.go.jp/en/

→ **Korean Peninsula [KOR] - 2018**
Assembled by GEM.
• Website: https://www.globalquakemodel.org/

→ **Mexico [MEX] - 2018**
Developed by GEM.
• Authors: J. Garcia-Pelaez, R. Gee, R. Styron
• Website: https://www.globalquakemodel.org/

→ **Middle East [MIE] - 2016**
Developed within the EMME project, jointly coordinated by the Swiss Federal Institute of Technology, Switzerland, and the Kandilli Observatory and Earthquake Research Institute, Turkey. Institutions involved:International Institute for Earthquake Engineering ans Seismology, Iran; Middle East Technical University, Turkey; Sakarya University, Turkey; University of Peshawar, Pakistan; Yarmouk University, Jordan; American University of Beirut, Lebanon; Ivane Javakhishvili Tbilisi State University, Georgia; National Academy of Sciences, Armenia; National Academy of Sciences, Azerbaijan.
• Authors: D. Giardini, L. Danciu, M. Erdik, K. Sesetyan, MB Demircioğlu, S. Akkar, L. Gulen, M. Zare, S. Adamia, A. Ansari, A. Arakelyan, A. Askan, M. Avanesyan, H. Babayan, T. Chelidze, R. Durgaryan, A. Elias, H. Hamzehloo, K. Hessami, D. Kalafat, O. Kale, A. Karakhanyan, MA. Khan, T. Mamadli, M. Al-Qarouti, M. Sayab, N. Tsereteli, M. Utkucu, O. Varazanashvili, M. Waseem, H. Yalçın, MT. Yilmaz
• Website: http://www.efehr.org

→ **Northern Africa [NAF] - 2018**
Developed by GEM.
• Authors: V. Poggi, J. Garcia-Pelaez, R. Styron
• Website: https://www.globalquakemodel.org/

→ **Northeast Asia [NEA] - 2018**
Developed by GEM.
• Authors: V. Poggi, J. Garcia-Pelaez, R. Styron
• Website: https://www.globalquakemodel.org/

→ **Northwestern Asia [NWA] - 2018**
Developed by GEM and the Swiss Federal Institute of Technology, Switzerland.
• Authors: V. Poggi, L. Danciu
• Website: https://www.globalquakemodel.org/

→ **New Zealand [NZL] - 2010 corrected**
GNS Science led the development of the model and converted it into the OpenQuake engine.
• Authors: E.R. Abbott, N. Horspool, M. Gerstenberger, R. Huso, C. Van Houtte, G. McVerry, S. Canessa
• Website: https://www.gns.cri.nz/

Contributing models

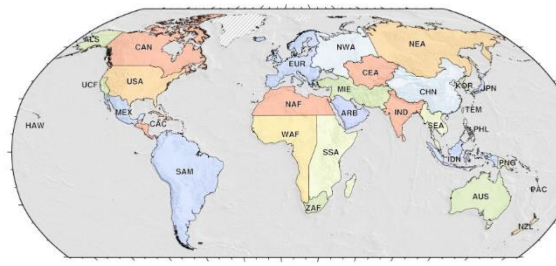

→ **Pacific Islands [PAC] - 2018**
Developed by GEM.
• Authors: K. Johnson
• Website: https://www.globalquakemodel.org/gem

→ **Philippines [PHL] - 2018**
Developed jointly by the Philippine Institute of Volcanology and Seismology and GEM.
• Authors: PHIVOLCS, K. Johnson and R. Styron
• Website: https://www.phivolcs.dost.gov.ph/ and https://www.globalquakemodel.org/gem

→ **Papua New Guinea [PNG] - 2015**
Developed within a collaboration between the Port Moresby Geophysical Observatory and Geoscience Australia.
• Authors: H. Ghasemi, C. McKee, M. Leonard, P. Cummins, M. Moihoi, S. Spiliopoulos, F. Taranu, E. Buri

→ **South America [SAM] - 2018**
Initially developed within the Swiss Re Foundation sponsored project SARA and updated by GEM. Organisations involved: GEM, Colombian Geological Survey, Colombia - National University of Colombia, Colombia - University of Valle, Colombia - Venezuelan Foundation for Seismological Research, Venezuela - University of Merida, Venezuela - National Observatory, Brazil, Institute of Astronomy, Geophysics and Atmospheric Sciences, Brazil - Federal University of Rio Grande do Norte, Brazil - National Polytechnic University, Ecuador - San Calixto Observatory - Bolivia - University of Chile, Chile - University of Concepción, Chile - Pontifical Catholic University of Chile, Chile - Research Center for Disaster Risk Management, Chile - Peruvian Geological Service, Peru - University of San Luis, Argentina - University of Antofagasta, Argentina - National Institute of Seismic Prevention, Argentina - National Institute of Geophysics and Volcanology, Italy.
• Authors: J. Garcia-Pelaez, M. Pagani, K. Johnson, R. Styron, V. Poggi
• Website: https://www.globalquakemodel.org/gem

→ **Continental Southeast Asia [SEA] - 2018**
Developed by the Earth Observatory of Singapore and Mahidol University.
• Authors: C.-H. Chan, T. Ornthammarath

→ **Sub-Saharan Africa [SSA] - 2018**
Developed by GEM in collaboration with AfricaArray within the USAID sponsored project SSAHARA.
• Authors: V. Poggi, R. Durrheim, G.M. Tuluka, G.A. Weatherill, R. Gee, M. Pagani, A. Nyblade, D. Delvaux
• Website: https://www.globalquakemodel.org/

→ **Taiwan [TWN] - 2015**
Developed within the Taiwan Earthquake Model initiative, a collaboration between various Taiwanese research institutions operating in the field of seismic hazard and risk assessment.
• Authors: Y.-J. Wang, C.-H. Chan, Y.-T. Lee, K.-F. Ma, J.-H. Shyu, R.-J. Rau, and C.-T. Cheng
• Website: http://tec.earth.sinica.edu.tw/TEM/index.php

→ **California (US) [UCF] - 2014**
Developed within a project supported by the United States Geological Survey, the Southern California Earthquake Center, the California Geological Survey and the California Earthquake Authority. The model was converted into the OpenQuake engine by GEM.
• Authors: E.H. Field, G.P. Biasi, P. Bird, T.E. Dawson, K.R. Felzer, D.D. Jackson, K.M. Johnson, T.H. Jordan, C. Madden, A.J. Michael, K.R. Milner, M.T. Page, T. Parsons, P.M. Powers, B.E. Shaw, W.R. Thatcher, R.J. Weldon II, Y. Zeng
• Website: http://wgcep.org/ucerf3

→ **United States of America [USA] - 2014**
Developed the United States Geological Survey and converted into the OpenQuake engine by GEM.
• Authors: M.D. Petersen, M.P. Moschetti, P.M. Powers, C.S. Mueller, K. M. Haller, A.D. Frankel, Y. Zeng, S. Rezaeian, S.C. Harmsen, O.S. Boyd, E.H. Field, R. Chen, K.S. Rukstales, N. Luco, R.L. Wheeler, R.A. Williams, A.H. Olsen
• Website: https://earthquake.usgs.gov/hazards/hazmaps/

→ **Western Africa [WAF] - 2018**
Developed by GEM.
• Authors: V. Poggi
• Website: https://www.globalquakemodel.org/

→ **South Africa [ZAF] - 2018**
Developed by scientists working at the Council of Geoscience, South Africa.
• Authors: V. Midzi, B. Manzunzu, T. Mulabisana, B.S. Zulu, T. Pule, S. Myendeki, G. W. Rathod
• Website: http://www.geoscience.org.za/

Global Earthquake Model (GEM) Foundation

The GEM Global Seismic Hazard Map is a product of the GEM Foundation. Initiated by the OECD's Global Science Forum in 2006, GEM was formed in 2009 as a non-profit foundation in Pavia, Italy, funded through a public-private sponsorship with the vision to create a world that is resilient to earthquakes. Participants represent national research, applied science or disaster management institutions, the private sector and international organisations. GEM continues the tradition of the Global Seismic Hazard Assessment Program (GSHAP), which produced the first global seismic hazard map arising from a global collaborative effort of scientists in 1999 in support of the UN International Decade of Natural Disaster Reduction (IDNDR). GEM's collaborative network comprises more than 70 public and private institutions organized under more than 25 regional, national and multilateral projects. Observing its core values of collaboration, transparency, openness, credibility and serving the public good, the GEM initiative extends the scope of work of GSHAP to the risk domain, providing an institutional framework for continuous updates and fostering direct applications to risk reduction and prevention projects. GEM's OpenQuake platform provides access to data, models, tools and software behind the maps. GEM's heart is the open-source OpenQuake engine, which enables probabilistic hazard and risk calculations worldwide and at all scales, from global down to regional, national, local, and site-specific in a single software package.

The Sendai Framework for Disaster Risk Reduction (SFDRR) calls for "decision-making on disaster risk reduction to be based on solid and openly accessible scientific work". GEM supports the SFDRR goals by contributing its openly accessible products, its capabilities for hazard and risk assessment, for training and capacity development, and for application in risk reduction projects. GEM also serves as a baseline or exemplar for the development of a broader multi-hazard framework for risk assessment in support of a holistic and comprehensive approach to disaster risk reduction. Technical details on the compilation of the hazard and risk maps and the underlying models are available on GEM's website at http://www.globalquakemodel.org/gem

Legal statements

Sponsors and major contributors:

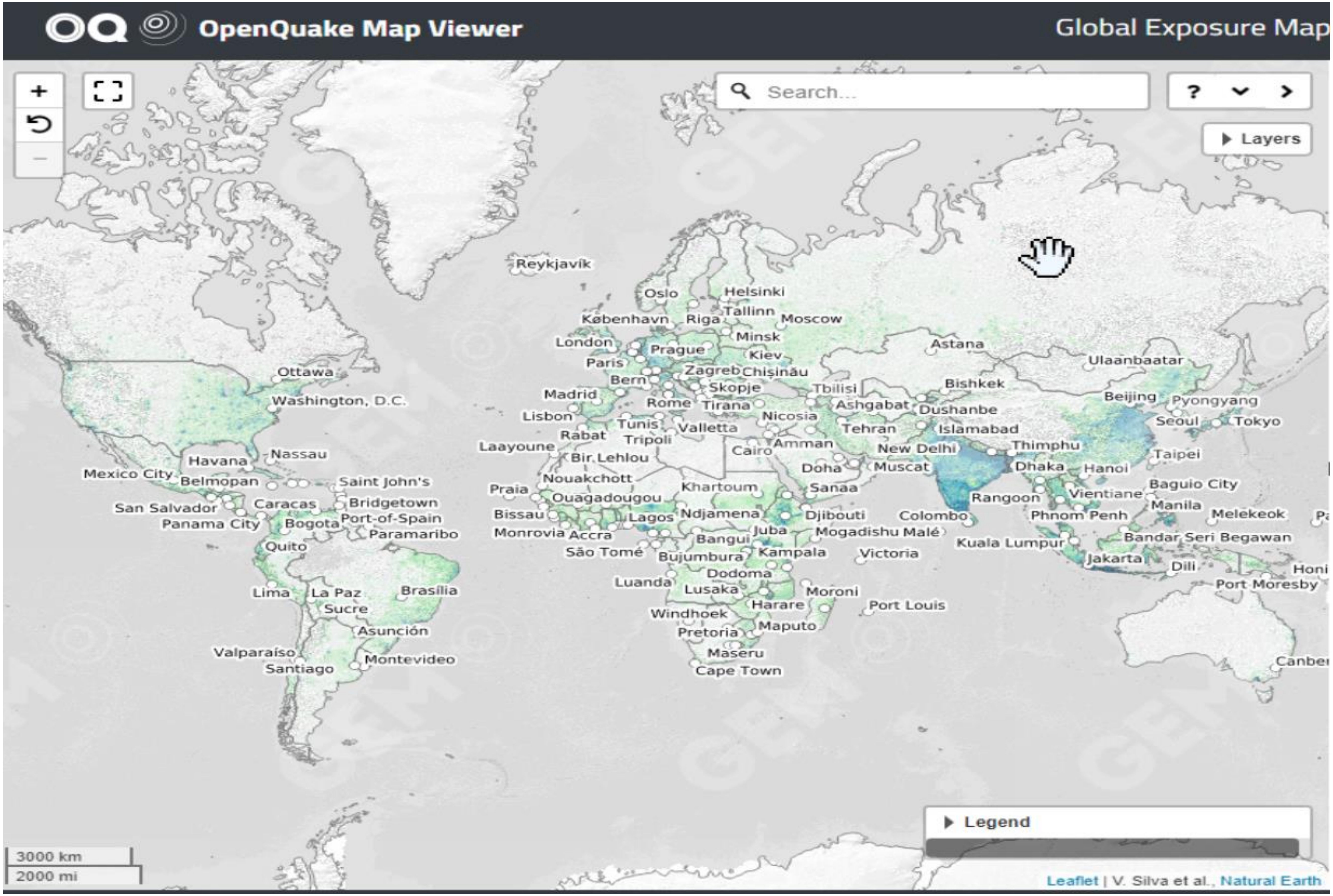
OpenQuake Map Viewer
Global Exposure Map
Search...
Layers
Legend
3000 km
2000 mi
Leaflet | V. Silva et al., Natural Earth
Reykjavík
Oslo
Helsinki
Tallinn
København
Riga
Moscow
Minsk
London
Prague
Kiev
Paris
Zagreb
Chişinău
Bern
Skopje
Madrid
Rome
Tirana
Tbilisi
Lisbon
Nicosia
Tunis
Valletta
Rabat
Tripoli
Laayoune
Cairo
Amman
Bir Lehlou
Nouakchott
Praia
Ouagadougou
Bissau
Monrovia
Accra
Lagos
São Tomé
Khartoum
Ndjamena
Bangui
Juba
Kampala
Bujumbura
Dodoma
Luanda
Lusaka
Harare
Windhoek
Pretoria
Maputo
Maseru
Cape Town
Moroni
Port Louis
Victoria
Mogadishu
Malé
Djibouti
Sanaa
Doha
Muscat
Tehran
Ashgabat
Dushanbe
Islamabad
New Delhi
Thimphu
Dhaka
Colombo
Astana
Bishkek
Ulaanbaatar
Beijing
Pyongyang
Seoul
Tokyo
Taipei
Hanoi
Rangoon
Vientiane
Phnom Penh
Baguio City
Manila
Melekeok
Bandar Seri Begawan
Kuala Lumpur
Jakarta
Dili
Port Moresby
Ottawa
Washington, D.C.
Havana
Nassau
Mexico City
Belmopan
San Salvador
Panama City
Caracas
Saint John's
Bridgetown
Port-of-Spain
Paramaribo
Bogota
Quito
Lima
La Paz
Sucre
Brasília
Asunción
Valparaíso
Santiago
Montevideo

Global Earthquake Model

Global Seismic Risk Map

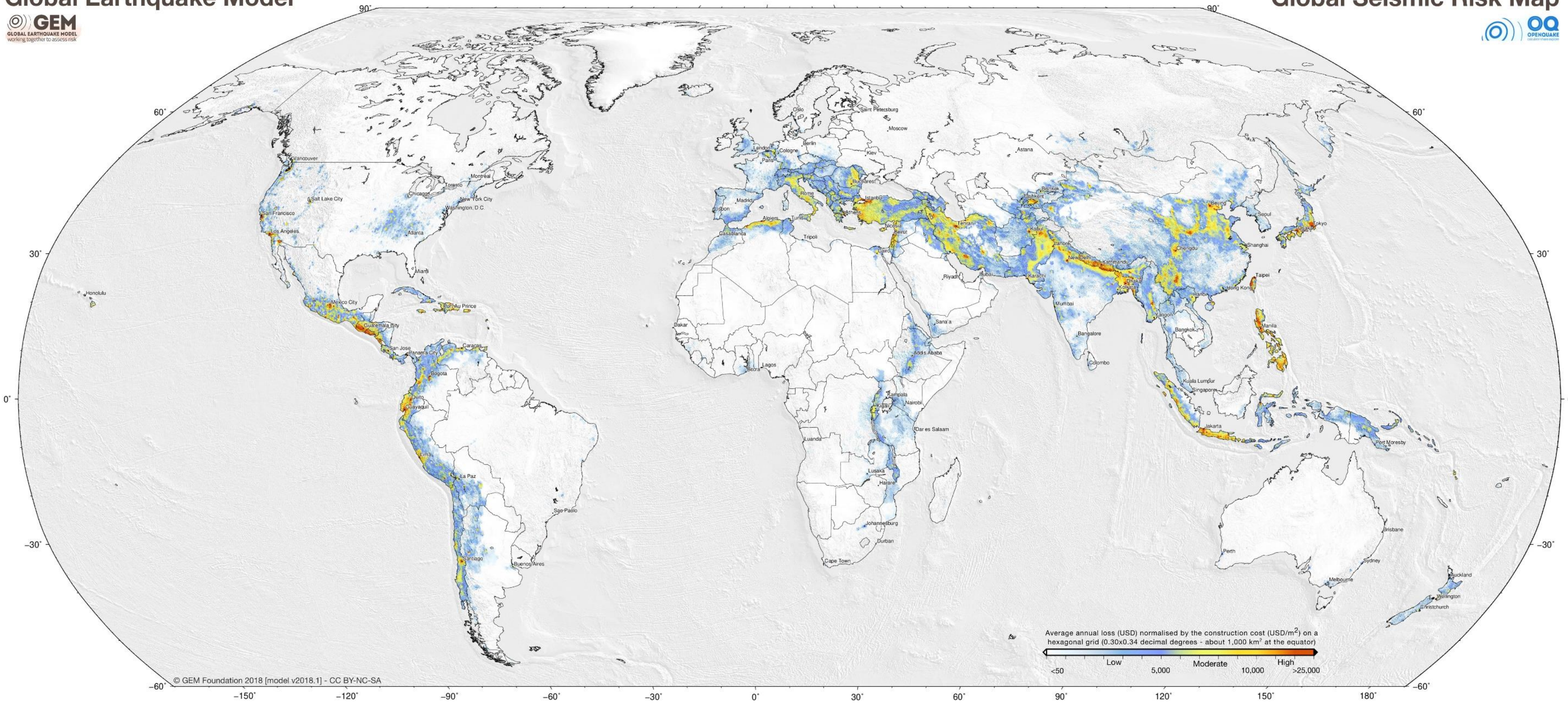

Global Seismic Hazard Map

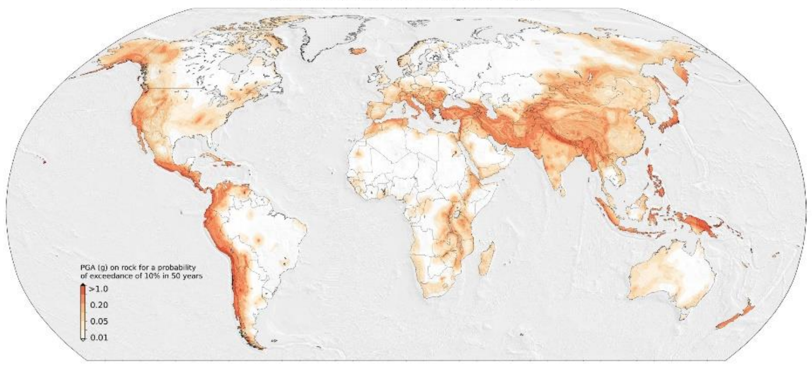

Global Exposure Map

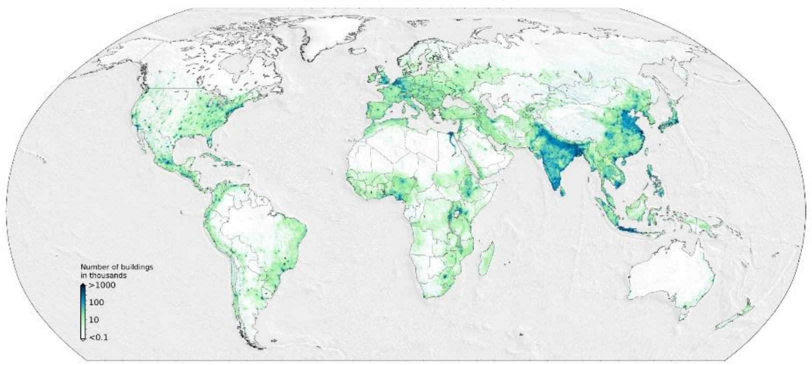

Global Seismic Fatalities Map

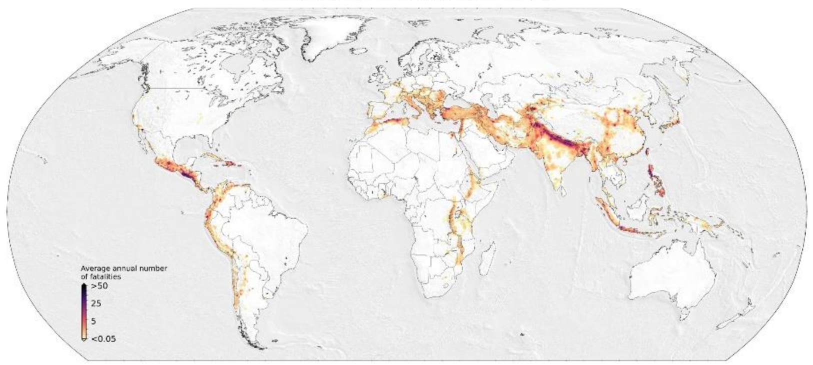

Global Earthquake Model (GEM) Global Seismic Risk Map

The Global Seismic Risk Map (v2018.1) comprises four global maps. The main map presents the geographic distribution of average annual loss (USD) normalised by the average construction costs of the respective country (USD/m^2) due to ground shaking in the residential, commercial and industrial building stock, considering contents, structural and non-structural components. The normalised metric allows a direct comparison of the risk between countries with widely different construction costs. It does not consider the effects of tsunamis, liquefaction, landslides, and fires following earthquakes. The loss estimates are from direct physical damage to buildings due to shaking, and thus damage to infrastructure or indirect losses due to business interruption are not included. The Global Seismic Hazard Map depicts the geographic distribution of the Peak Ground Acceleration (PGA) with a 10% probability of being exceeded in 50 years, computed for reference rock conditions (shear wave velocity of 760-800 m/s). The Global Exposure Map depicts the geographic distribution of residential, commercial and industrial buildings. The Global Seismic Fatalities Map depicts an estimate of average annual human losses due to earthquake-induced structural collapse of buildings. The results for human losses do not consider indirect fatalities such as those from post-earthquake epidemics. The average annual losses and number of buildings are presented on a hexagonal grid, with a spacing of 0.30 x 0.34 decimal degrees (approximately 1,000 km^2 at the equator). The average annual losses were computed using the event-based calculator of the OpenQuake engine, an open-source software for seismic hazard and risk analysis developed by the GEM Foundation. The seismic hazard, exposure and vulnerability models employed in these calculations were provided by national institutions, or developed within the scope of regional programs or bilateral collaborations. These global maps and the underlying databases are based on best available and publicly accessible datasets and models. Due to possible model limitations, regions portrayed with low risk may still experience potentially damaging earthquakes. The GEM Risk Map is intended to be a dynamic product, such that it may be updated when new datasets and models become available. Releases of updated versions of the seismic risk map are anticipated on a regular basis. Additional hazard and risk metrics for each country can be explored at globalquakemodel.org/gem.

The Global Earthquake Model (GEM) Foundation

The Earthquake Risk Map 2018 is a product of the GEM Foundation. Initiated by the Organisation for Economic Co-operation and Development (OECD) Global Science Forum in 2006, GEM was formed in 2009 as a non-profit foundation in Pavia (Italy), funded through a public-private sponsorship with the vision to create a world that is resilient to earthquakes. Participants represent national research or disaster management institutions, the private sector and international organisations. GEM expands the assessment of seismic hazard at the global scale initially started by the Global Seismic Hazard Assessment Program (GSHAP) in support of the UN International Decade of Natural Disaster Reduction in 1999 to the consideration of direct economic and human losses. Observing its core values of collaboration, transparency, openness, credibility, and serving the public good, GEM goes beyond GSHAP by extending the scope of work to the risk domain, providing an institutional framework for continuous updates, and fostering direct applications to risk reduction and prevention projects. GEM's collaborative network comprises more than 70 public and private institutions organised under more than 25 regional, national and multilateral projects.

GEM's OpenQuake platform (platform.openquake.org) provides access to all data, models, tools and software behind the maps. GEM's open-source OpenQuake engine enables probabilistic hazard and risk calculations worldwide and at all scales, from global down to regional, national, local, and site-specific in a single software package.
The Sendai Framework for Disaster Risk Reduction (SFDRR) calls for "decision-making on disaster risk reduction to be based on solid and openly accessible scientific work". GEM supports the SFDRR goals by contributing openly accessible products for hazard and risk assessment and capacity development in risk reduction projects. GEM also serves as a baseline or exemplar for the development of a broader multi-hazard framework for risk assessment in support of a holistic and comprehensive approach to disaster risk reduction. Technical details on the development and compilation of the hazard and risk maps, underlying models and the list of contributors can be found at globalquakemodel.org/gem.

How to use and cite this work

Please cite this work as: V. Silva, D. Amo-Oduro, A. Calderon, J. Dabbeek, V. Despotaki, L. Martins, A. Rao, M. Simionato, D. Viganò, C. Yepes-Estrada, A. Acevedo, H. Crowley, N. Horspool, K. Jaiswal, M. Journeay, M. Pittore (2018). Global Earthquake Model (GEM) Seismic Risk Map (version 2018.1), DOI: 10.13117/GEM-GLOBAL-SEISMIC-RISK-MAP-2018.

Acknowledgements

This map is the result of a collaborative effort and extensively relies on the enthusiasm and commitment of various organisations to openly share and collaborate. The creation of this map would not have been possible without the support provided by several public and private organisations during GEM's second working programme (2014-2018). None of this would have been possible without the extensive support of all GEM Secretariat staff. These key contributions are profoundly acknowledged. A complete list of the contributors can be found at globalquakemodel.org/gem.

Legal statements

This map is an informational product created by the GEM Foundation for public dissemination purposes. The information included in this map must not be used for the design of earthquake-resistant structures or to support any important decisions involving human life, capital and movable and immovable properties. The values of seismic hazard and risk in this map do not constitute an alternative nor do they replace building actions defined in national building codes or earthquake risk estimates derived nationally. Readers seeking this information should contact the national authorities tasked with seismic hazard and risk assessment. The seismic risk map results from an integration process that is solely the responsibility of the GEM Foundation.

Contacts

GEM (Global Earthquake Model) Foundation
Via Ferrata, 1 – 27100, Pavia, Italy
info@globalquakemodel.org

More information available at globalquakemodel.org/gem

Sponsors and major contributors

Response spectra

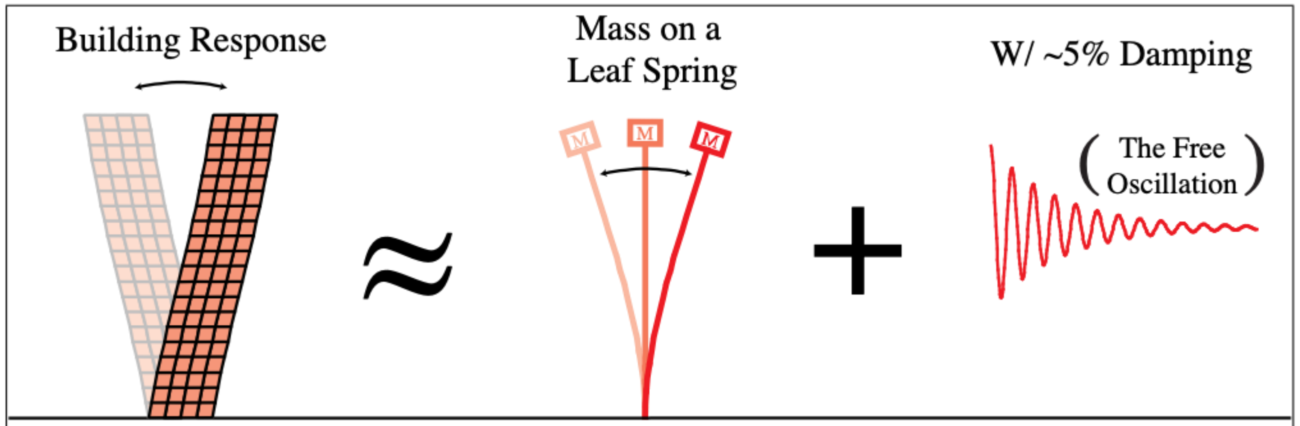

Figure 1. The response-spectrum value is the peak motion (displacement, velocity, or acceleration) of a damped single-degree of freedom harmonic oscillator (with a particular damping and resonant period) subjected to a prescribed ground motion.

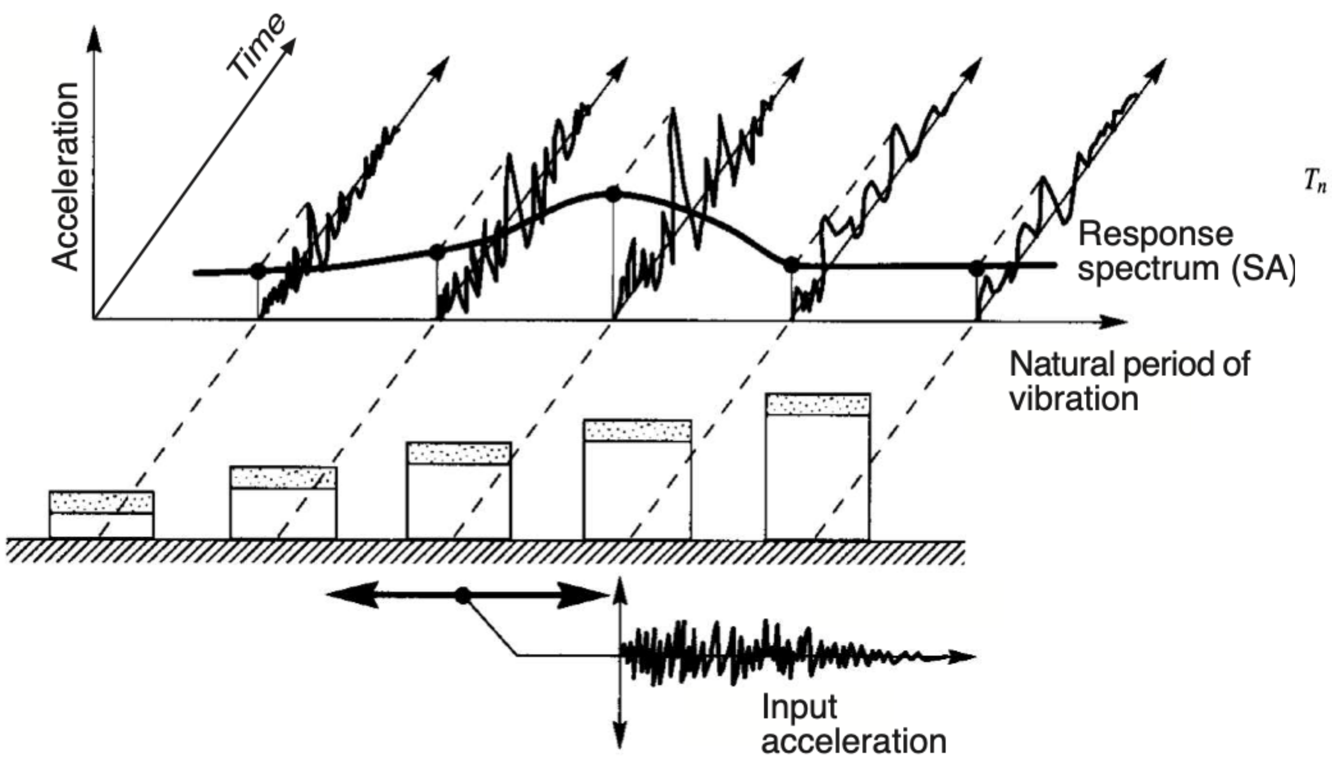

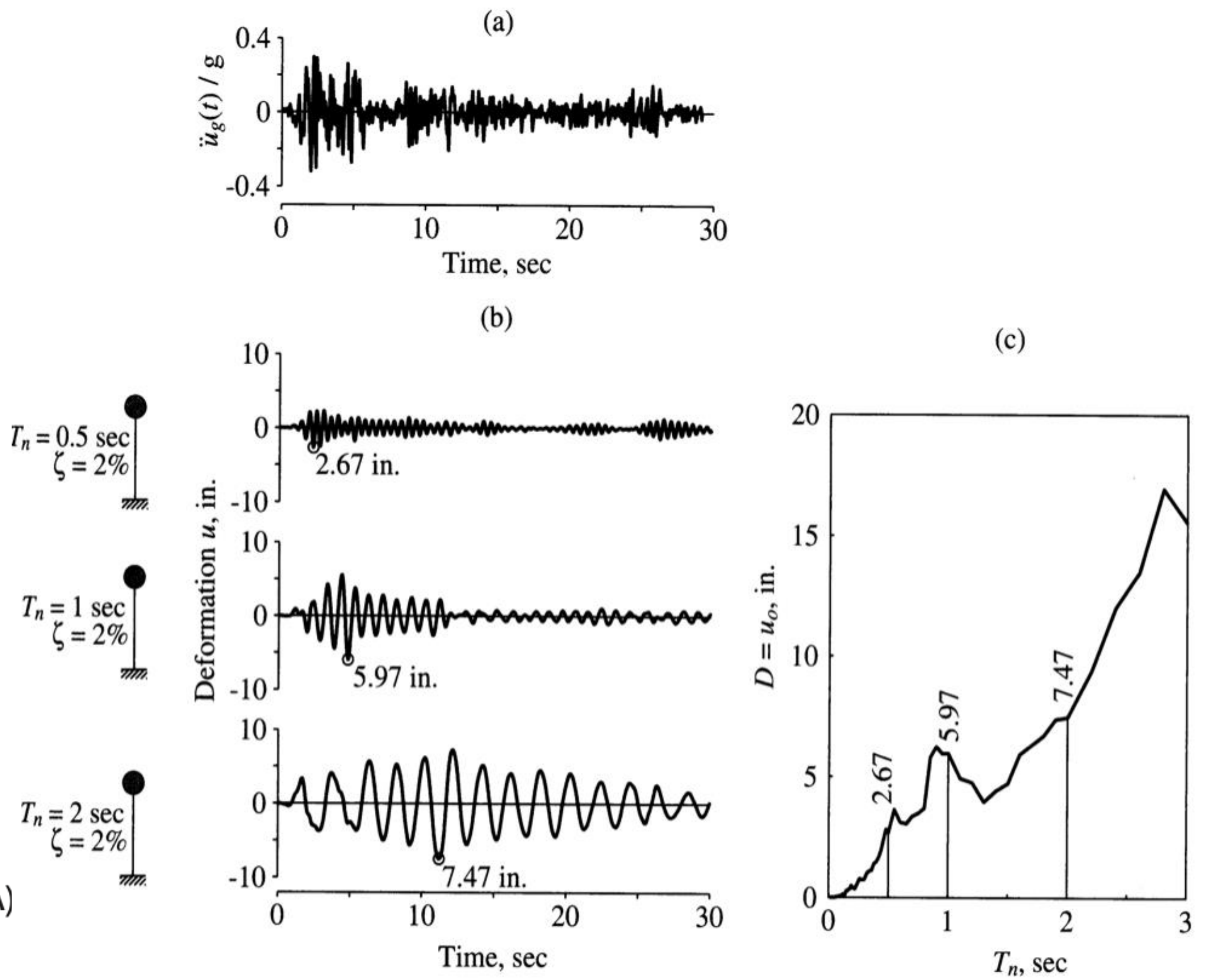

Figure 6.6.1 (a) Ground acceleration; (b) deformation response of three SDF systems with $\zeta = 2\%$ and $T_n = 0.5$, 1, and 2 sec; (c) deformation response spectrum for $\zeta = 2\%$.

Relative displacement

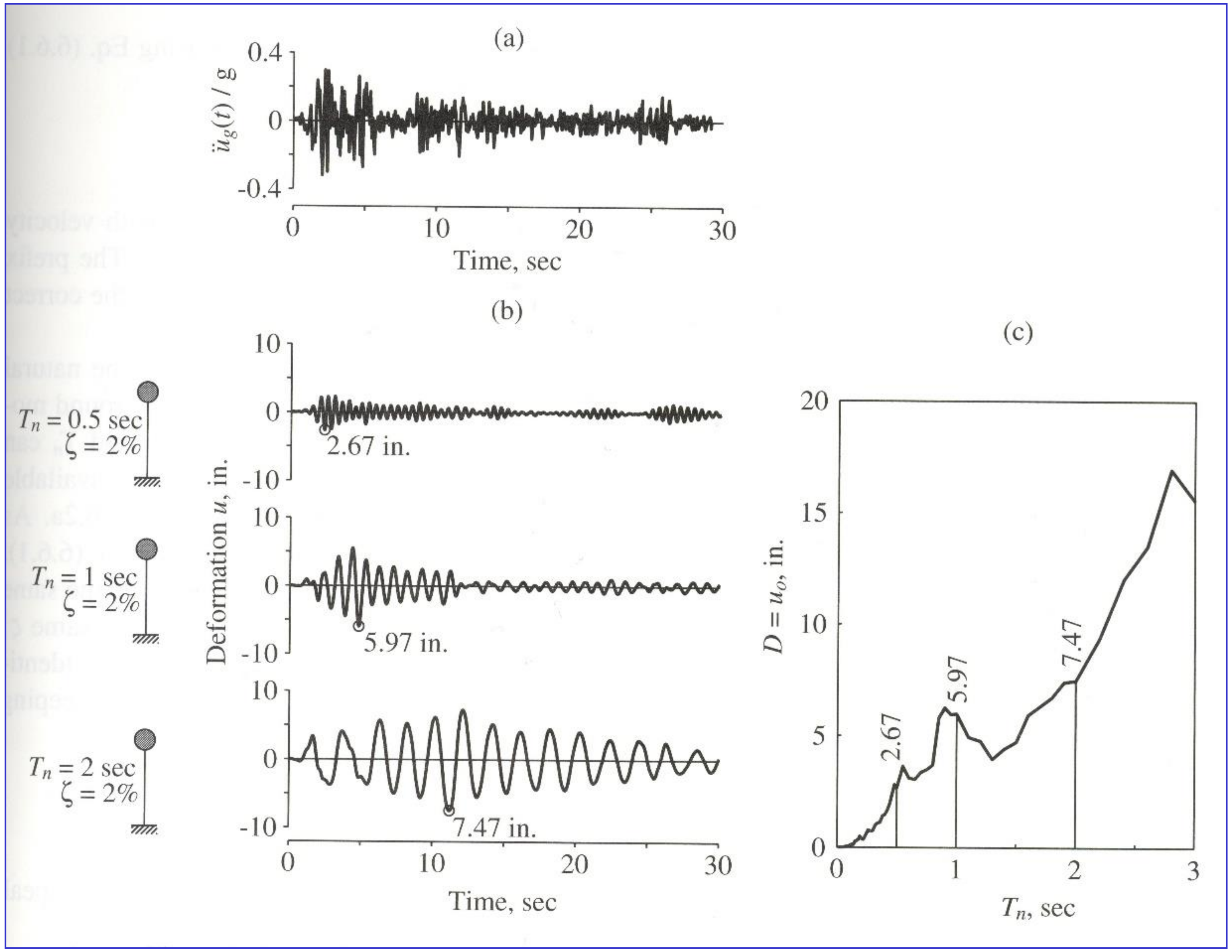

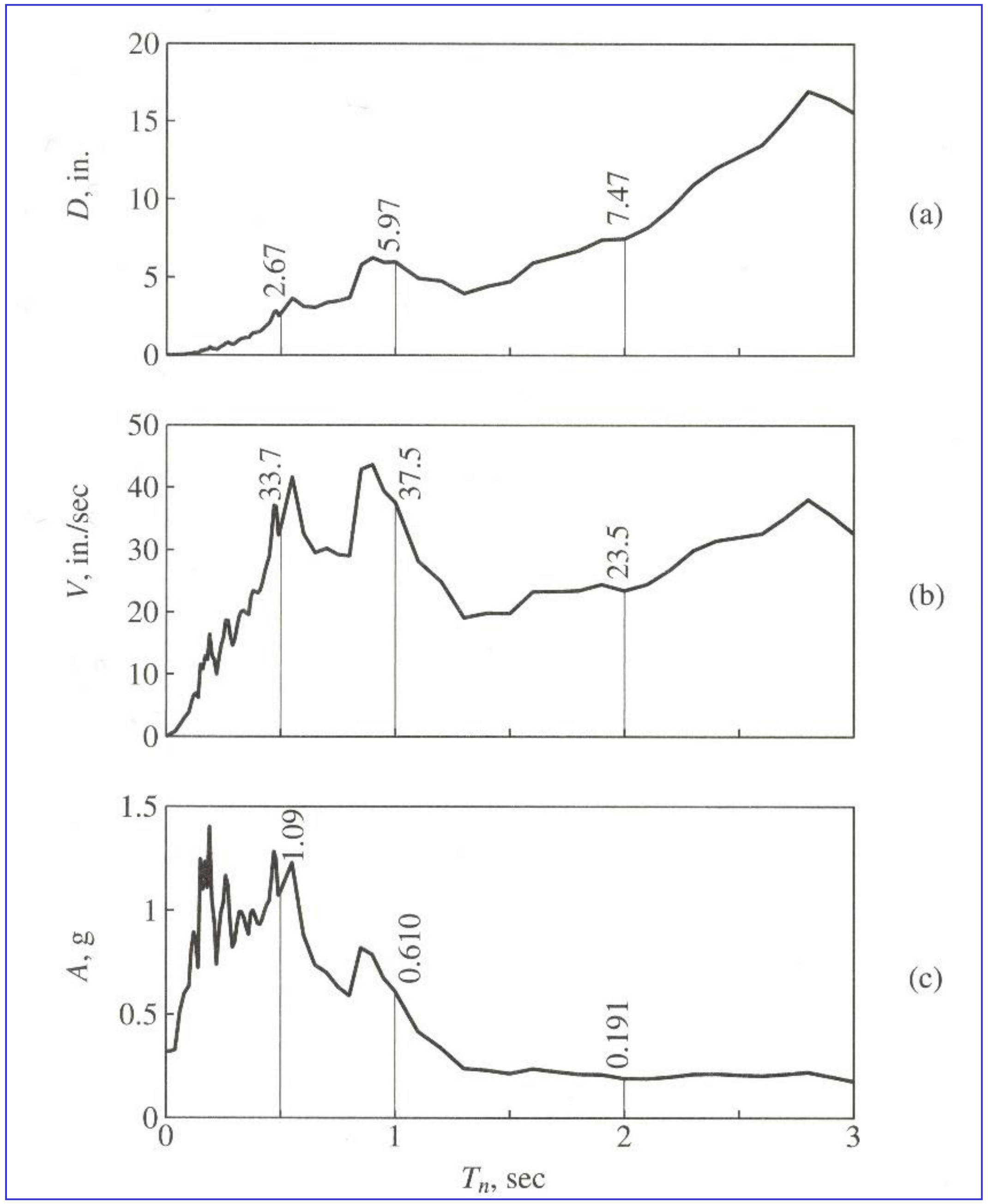

Pseudo Velocity and
Pseudo accelerations

UNIVERSITÀ DEGLI STUDI DI TRIESTE

Since PSV and PSA are obtained by SD simply multiplying for a factor □

The 3 spectra can be diplayed on the same plot

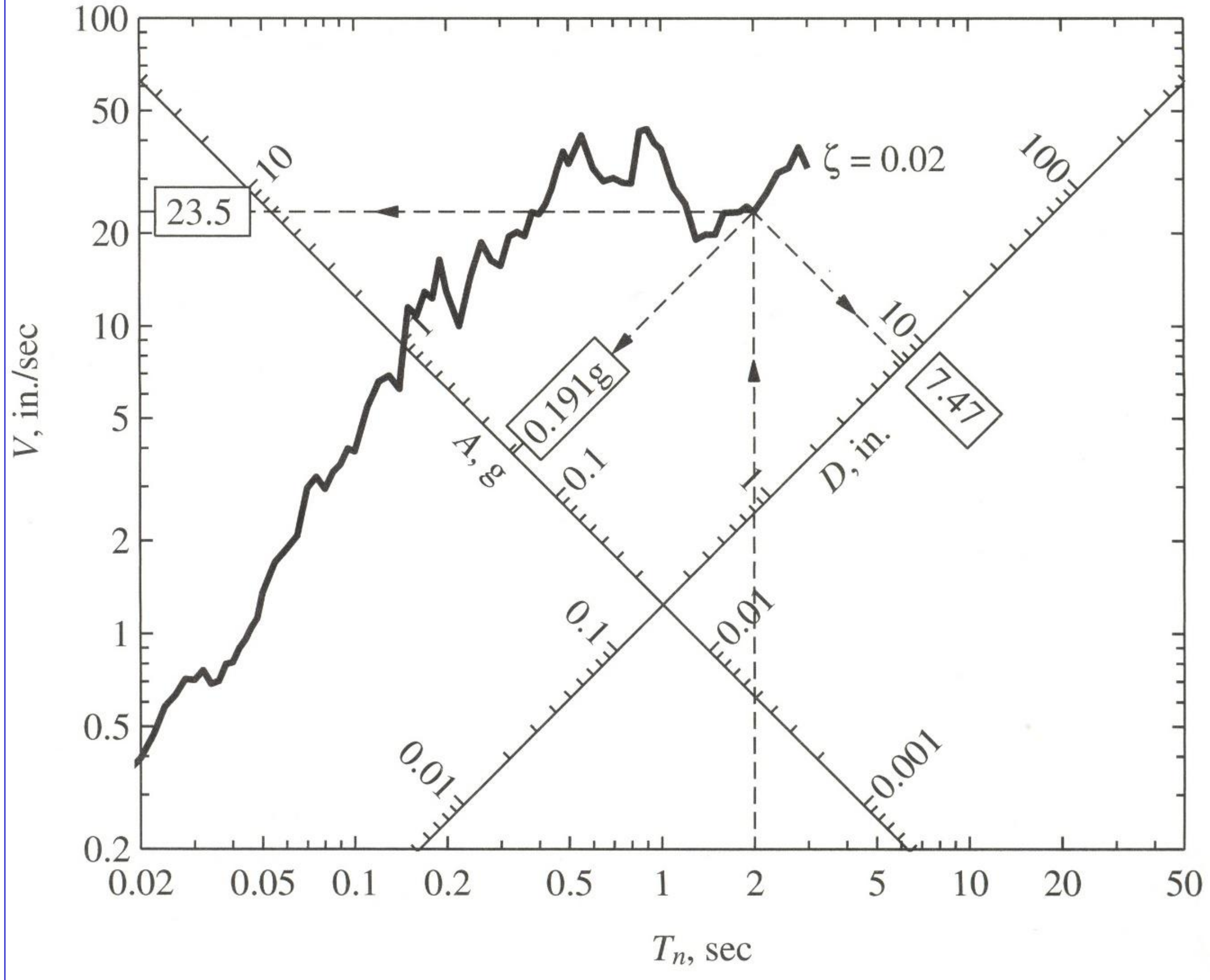

Response spectra

ritically damped system $(\xi = 1)$.
2. Overdamped system $(\xi > 1)$.
3. Underdamped system $(\xi < 1)$

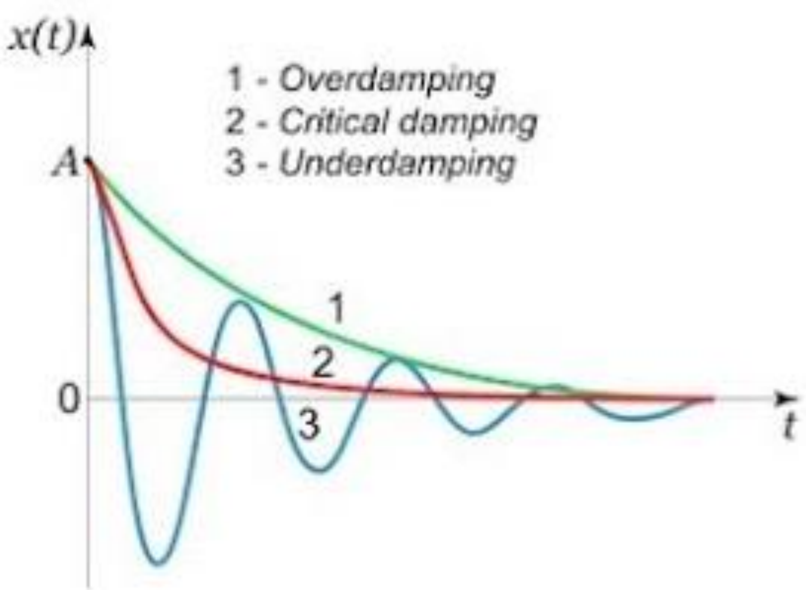

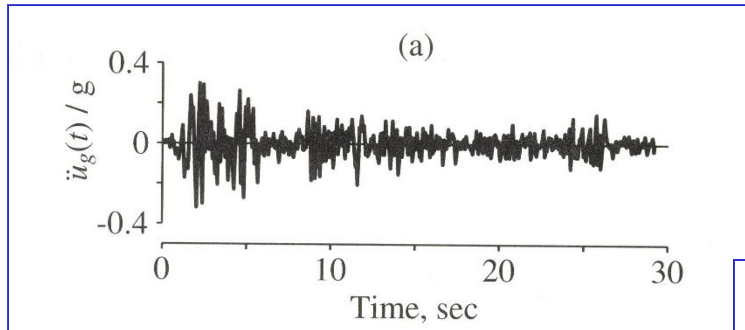

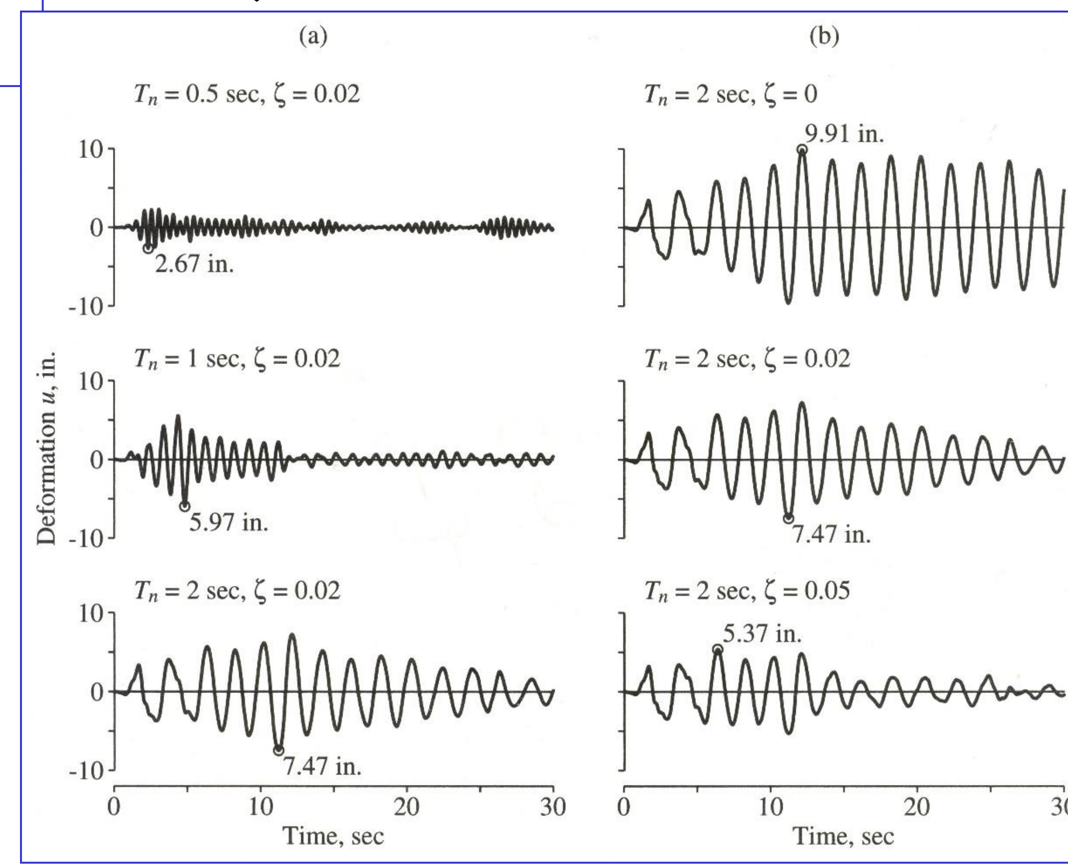

La risposta dell'oscillatore dipende dalla sua frequenza e dallo smorzamento!

Scheme of intensity estimation for scenario earthquakes

1. Epicentral intensity
as a function of **magnitude and depth**

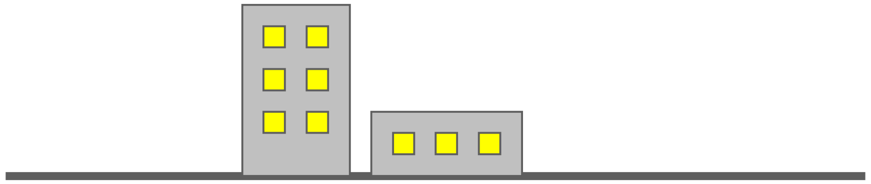

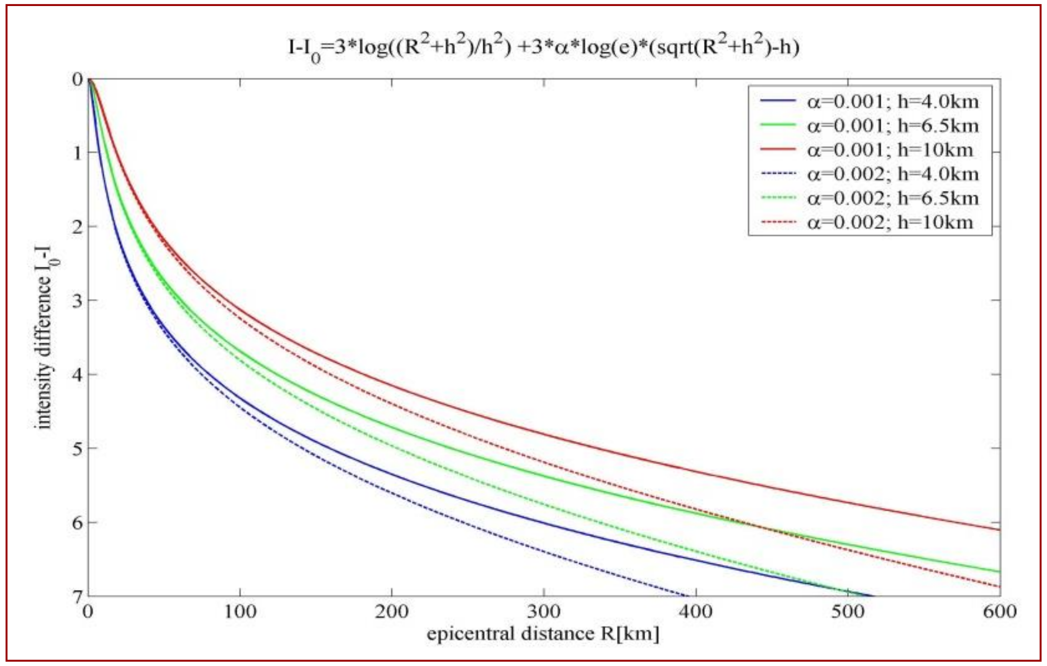

2. Site intensity from **attenuation relationships**

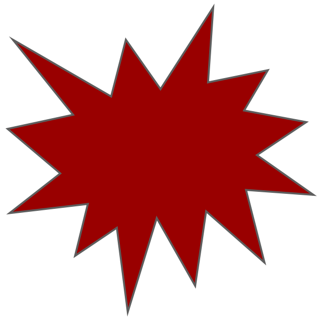

Scheme of intensity estimation for scenario earthquakes

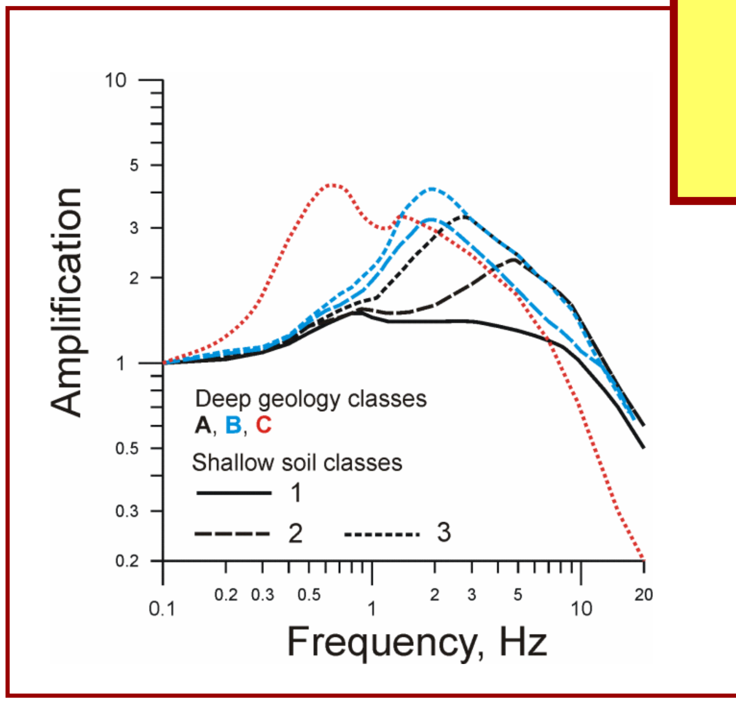

3. Modification of the Spectrum **– Local Site Amplification**

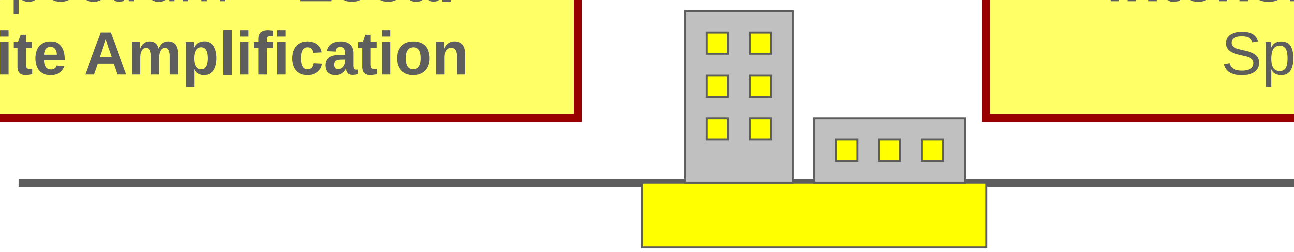

4. Estimation of **site intensity** from the Spectrum

2. Modification of the Spectrum **– distance attenuation**

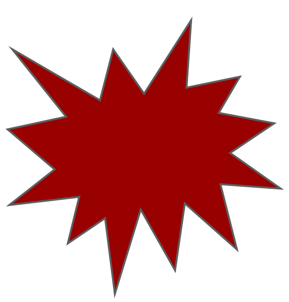

1. Source Spectrum – function of **magnitude** and **stress parameter**

Typical site classes (A1 – C3) that correspond to particular locations are estimated from correspondent geology maps

UNIVERSITÀ DEGLI STUDI DI TRIESTE

Probabilistic Seismic Hazard Analysis

All possible distances are considered - contribution of each is weighted by its probability of occurrence

$$\lambda_{y^*} = \sum_{i=1}^{N_S} \sum_{j=1}^{N_M} \sum_{k=1}^{N_R} \nu_i \int\int P[Y > y^* \mid m_j, r_k] P[M = m_j] P[R = r_k]$$

All sites are considered

All possible effects are considered - each weighted by its conditional probability of occurrence

All possible magnitudes are considered - contribution of each is weighted by its probability of occurrence

Probabilistic Seismic Hazard Analysis

Seismic Zonation

$$\lambda_{y^*} = \sum_{i=1}^{N_S} \sum_{j=1}^{N_M} \sum_{k=1}^{N_R} \nu_i \int\int P[Y > y^* \mid m_j, r_k] P[M = m_j] P[R = r_k]$$

All sites are considered

Ground Motion Prediction Equations - GMPEs

Seismic Catalogs

Random events

Sample Space

$S = \{1, 2, 3, 4, 5, 6\}$

$E_1 = \{1, 3, 5\}$ $E_2 = \{4, 5, 6\}$

Union

$E_1 \cup E_2 = \{1, 3, 4, 5, 6\}$

Intersection

$E_1 \cap E_2 = \{5\}$

Or E_1E_2

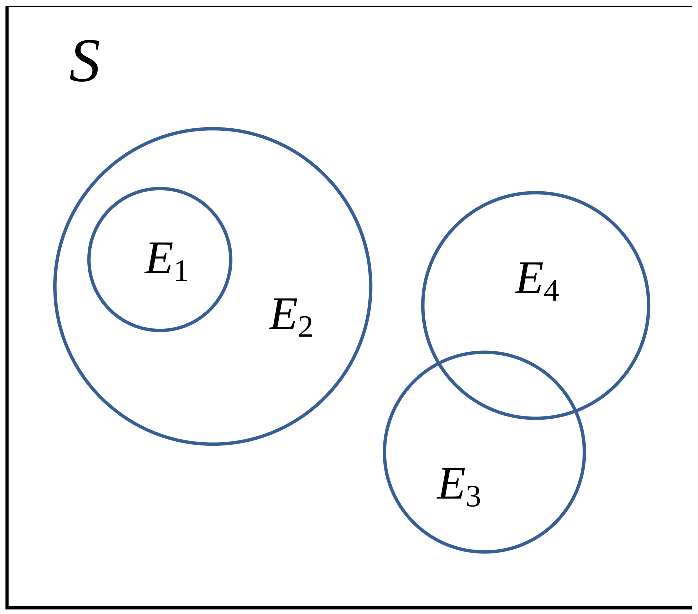

Baker, Bradley and Stafford (2021), "Seismic Hazard and Risk Analysis." These images are provided for instructional and research use, with attribution. Not for commercial use.

1. Events E_1 and E_2 are *mutually exclusive* when they have no common outcomes (i.e., $E_1E_2 = \phi$, where ϕ is the *null event*).
2. Events $E_1, E_2 \ldots E_n$ are *collectively exhaustive* when their union contains every possible outcome of the random event (i.e., $E_1 \cup E_2 \cup, \ldots, \cup E_n = S$).
3. The *complementary event*, $\overline{E_1}$, of an event E_1, contains all outcomes in the sample space that are not in event E_1. By this definition, $\overline{E_1} \cup E_1 = S$ and $\overline{E_1}E_1 = \phi$. That is, $\overline{E_1}$ and E_1 are mutually exclusive and collectively exhaustive.

Random events

We will be interested in the probabilities of occurrence of various events. These probabilities must follow three axioms of probability:

$$0 \leq P(E) \leq 1, \tag{A.1}$$

$$P(S) = 1, \tag{A.2}$$

and, for mutually exclusive events E_1 and E_2,

$$P(E_1 \cup E_2) = P(E_1) + P(E_2). \tag{A.3}$$

$$P(\bar{E}) = 1 - P(E) \tag{A.4}$$

$$P(\phi) = 0 \tag{A.5}$$

$$P(E_1 \cup E_2) = P(E_1) + P(E_2) - P(E_1 E_2). \tag{A.6}$$

Conditional Probability

$$P(E_1|E_2) = \begin{cases} \frac{P(E_1E_2)}{P(E_2)} & \text{if } P(E_2) > 0 \\ 0 & \text{if } P(E_2) = 0. \end{cases}$$

Ground-motion intensity measure

Seismic sources

Ground-motion model

Site properties

$$\lambda(IM > im) = \sum_{i=1}^{n_{rup}} P(IM > im \mid rup_i, site)\, \lambda(rup_i)$$

Individual rupture

Consider all possible ruptures

for the nontrivial case of $P(E_2) > 0$, gives

$$P(E_1E_2) = P(E_1|E_2)P(E_2).$$

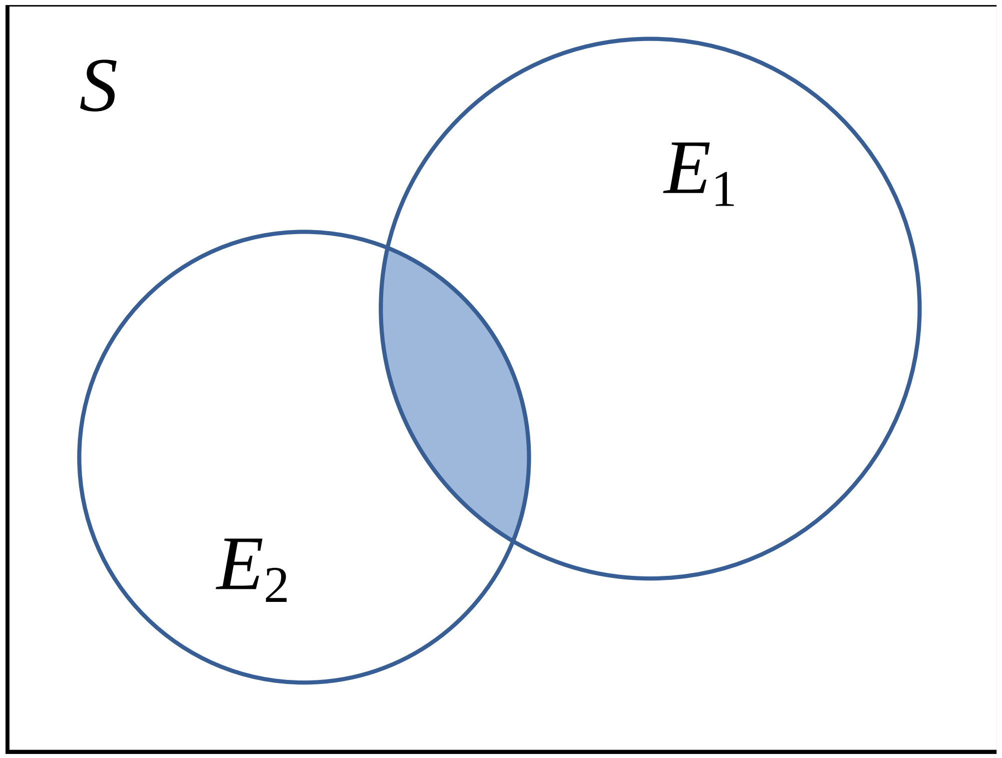

Independence

$$P(E_1|E_2) = P(E_1). \qquad \text{(A.9)}$$

$$P(E_1E_2) = P(E_1)P(E_2),$$

Conditional Probability

Total Probabilty Theorem

Ground-motion intensity measure

Seismic sources

Ground-motion model

Site properties

$$\lambda(IM > im) = \sum_{i=1}^{n_{rup}} P(IM > im \mid rup_i, site)\, \lambda(rup_i)$$

Individual rupture

Consider all possible ruptures

Consider an event A and a set of mutually exclusive and collectively exhaustive events $E_1, E_2, \ldots, E_n$. The Total Probability Theorem states that

$$P(A) = \sum_{i=1}^{n} P(A|E_i)P(E_i). \qquad \text{(A.11)}$$

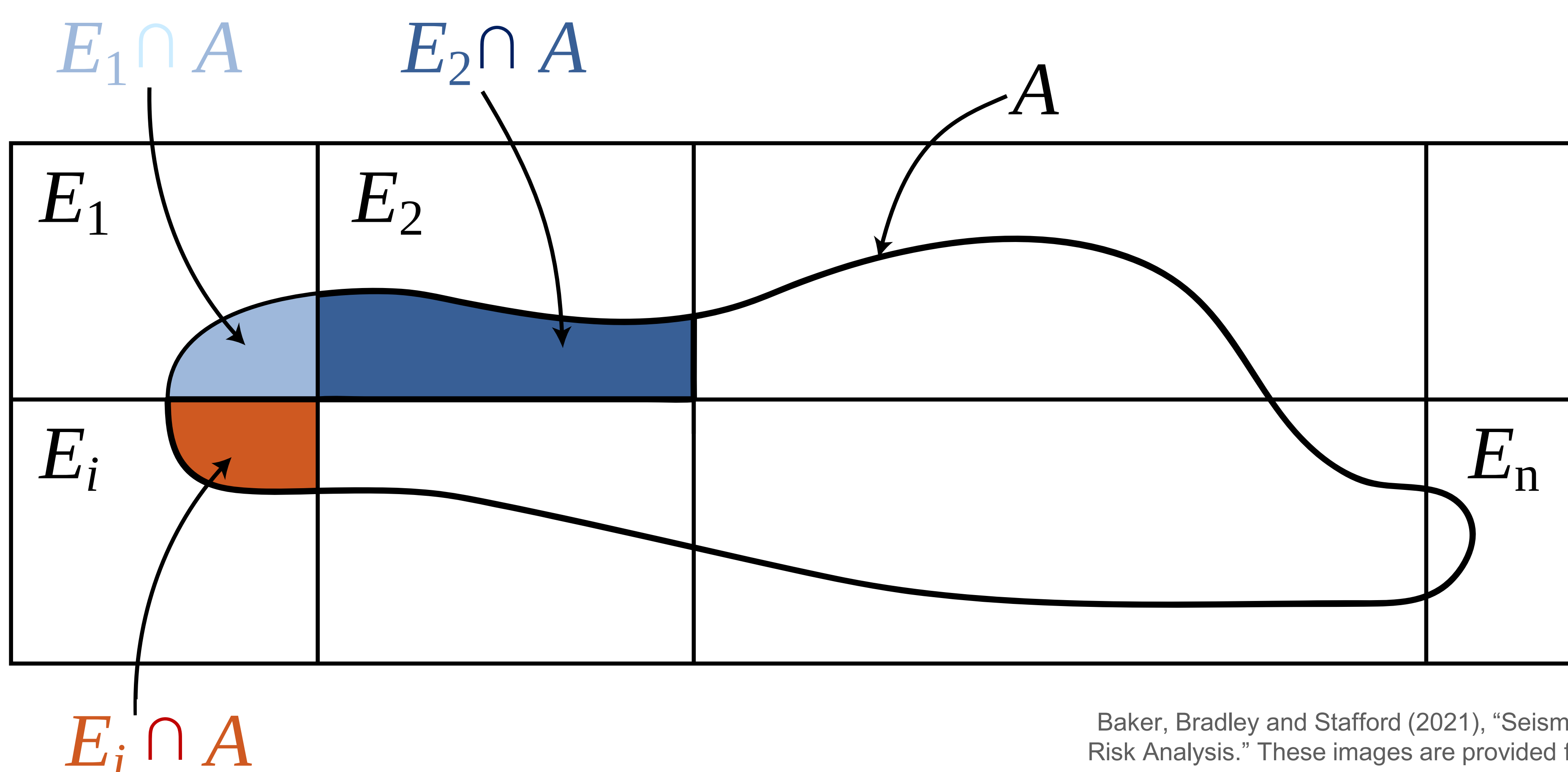

Baker, Bradley and Stafford (2021), "Seismic Hazard and Risk Analysis." These images are provided for instructional and research use, with attribution. Not for commercial use.

UNIVERSITÀ DEGLI STUDI DI TRIESTE

Conditional Probability

Bayes' Rule

$$P(E_1|E_2) = P(E_1). \qquad \text{(A.9)}$$

Consider an event A and a set of mutually exclusive and collectively exhaustive events $E_1, E_2, \ldots, E_n$. Using Equation A.9, we can write

$$P(AE_j) = P(E_j|A)P(A) = P(A|E_j)P(E_j). \qquad \text{(A.12)}$$

Rearranging the last two terms gives

$$\boxed{P(E_j|A) = \frac{P(A|E_j)P(E_j)}{P(A)}.} \qquad \text{(A.13)}$$

Random Variables

Ground-motion intensity measure
Seismic sources
Ground-motion model
Site properties

$$\lambda(IM > im) = \sum_{i=1}^{n_{rup}} P(IM > im \mid rup_i, site)\,\lambda(rup_i)$$

Individual rupture
Consider all possible ruptures

A **random variable** is a numerical variable whose specific value cannot be predicted with certainty before the occurrence of an event

x1,x2,x3 …denote possible outcome of X

P(X=x1) is the probability of X of assuming the value x1

Random variable can be **discrete** (e.g. number of earthquakes occurring in a region in a certain amount of time) or **continuous**

The probabilty distribution of a discrete random variable is quantified by the **probability mass function (PMF):**

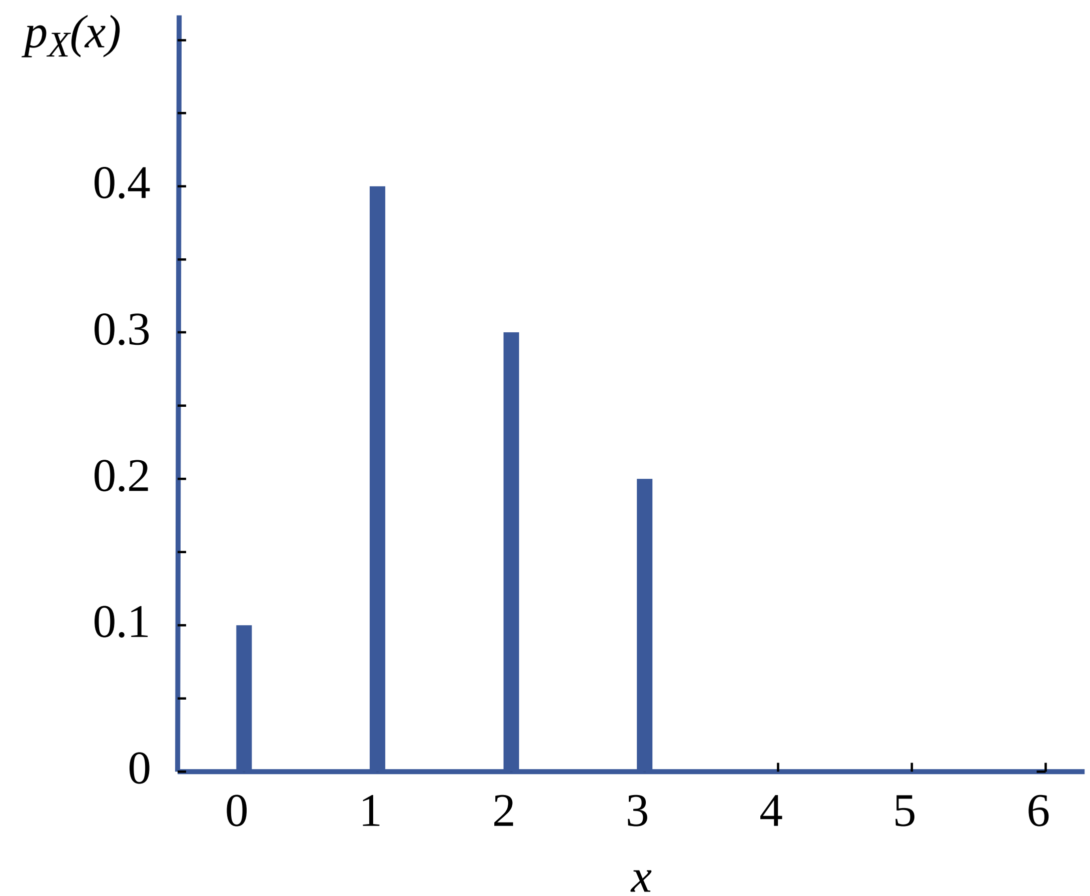

(a)

$$p_X(x) = P(X = x).$$

Random Variables

Ground-motion intensity measure
Seismic sources
Ground-motion model
Site properties

$$\lambda(IM > im) = \sum_{i=1}^{n_{rup}} P(IM > im \mid rup_i, site)\, \lambda(rup_i)$$

Individual rupture
Consider all possible ruptures

The **cumulative distribution function (CDF)** is defined as the probability of the event that the random variable takes a value less than or equal to the value of the argument:

$$F_X(x) = P(X \leq x).$$

PMF and **CDF** are related by:

$$F_X(a) = \sum_{\text{all } x_i \leq a} p_X(x_i).$$

In many cass (see equation on the top right) we are interested in the probability of **X** $\geq$ **x**:

$$P(X > x) = 1 - P(X \leq x)$$

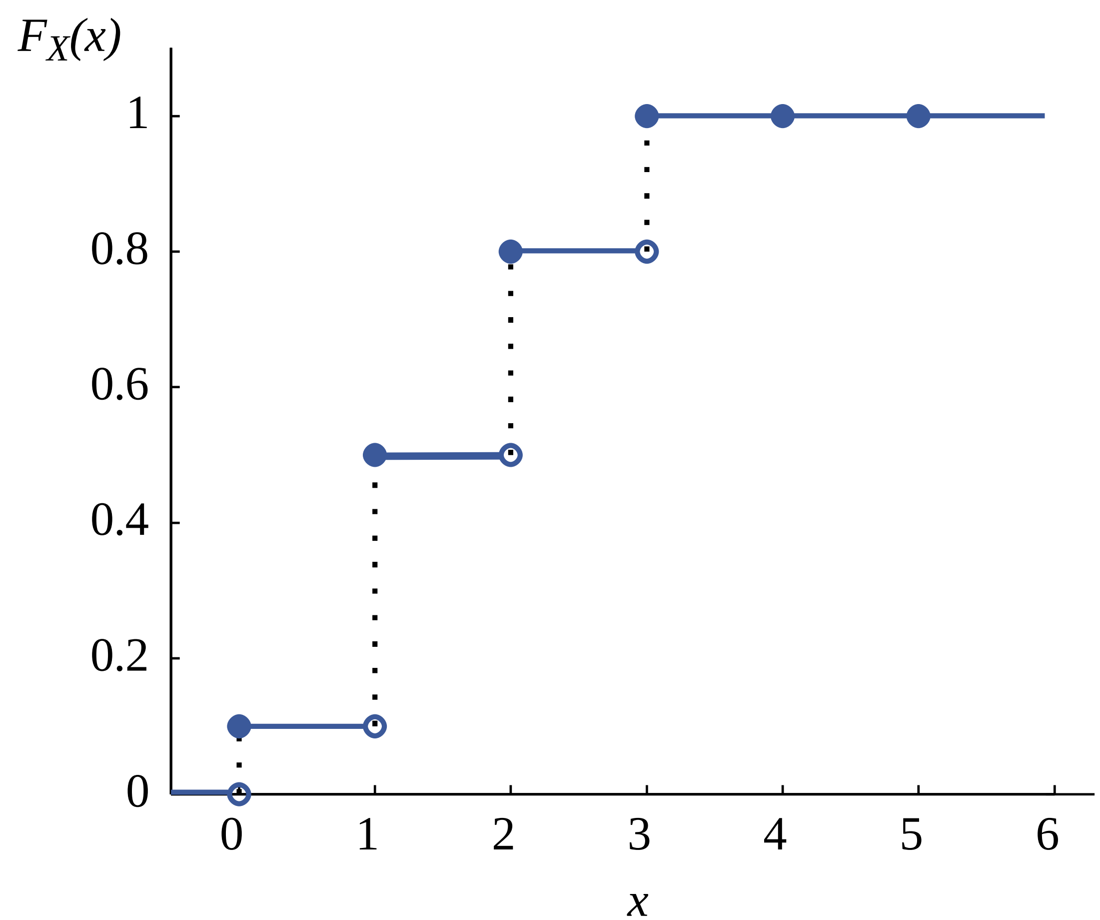

(b)

Random Variables

Ground-motion intensity measure
Seismic sources
Ground-motion model
Site properties

$$\lambda(IM > im) = \sum_{i=1}^{n_{rup}} P(IM > im \mid rup_i, site)\,\lambda(rup_i)$$

Individual rupture
Consider all possible ruptures

In the case of a **continuous** variable the **Probability Density Function (PDF)** is defined:

$$f_X(x)\,dx = P(x < X \le x + dx)$$

$f_X(x)\,dx$ represents the probability of the random variable X taking values between x and x+dx

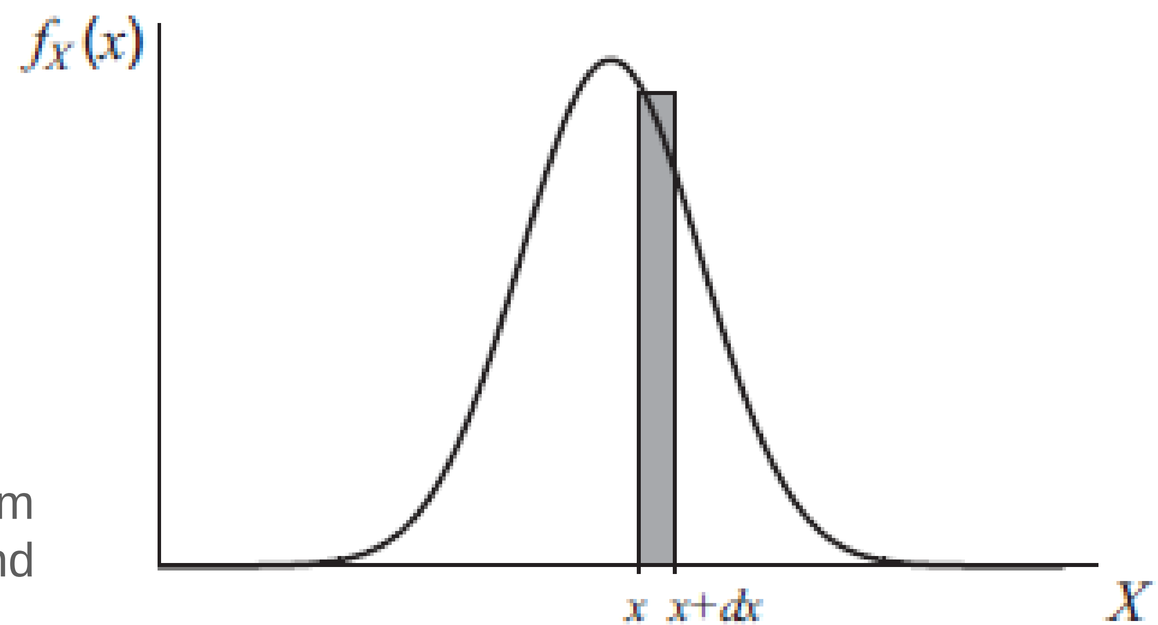

Baker, Bradley and Stafford (2021), “Seismic Hazard and Risk Analysis.” These images are provided for instructional and research use, with attribution. Not for commercial use.

Random Variables

Probability that the outcome of X is in the interval between and **b**

$$P(a < X \le b) = \int_a^b f_X(x)\,dx.$$

For discrete random variables

$$p_{\tilde{X}}(x) = f_X(x)\,\Delta x = P(x < X \le x + \Delta x)$$

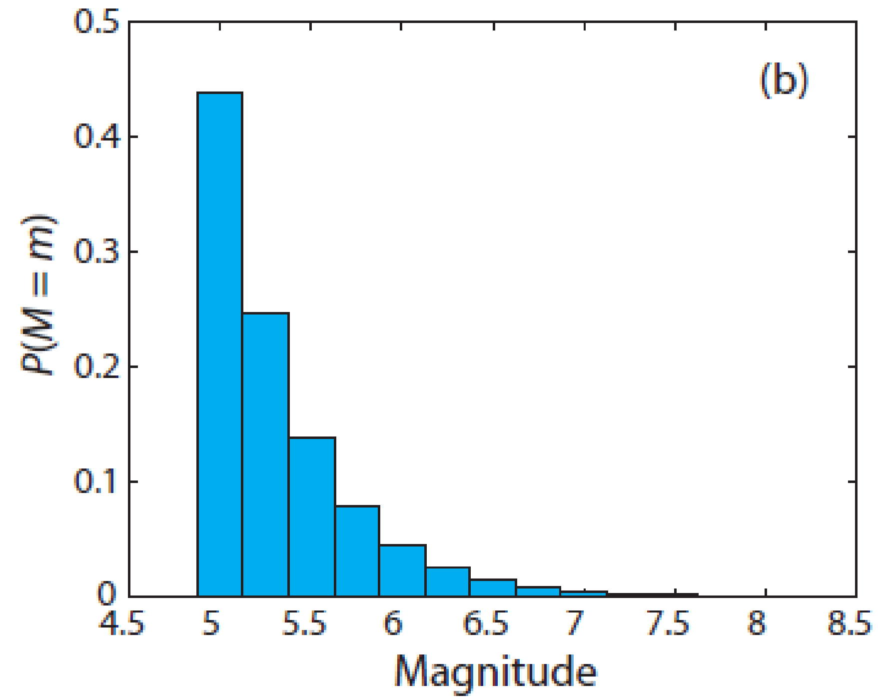

Relation between PDF and CDF

CDF $$F_X(x) = P(X \le x).$$

CDF $$F_X(x) = P(X \le x) = \int_{-\infty}^{x} f_X(u)\,du$$

$-\infty$

PDF $$f_X(x) = \frac{d}{dx}F_X(x).$$

Common Probability Distributions

Normal Distribution

PDF $$f_X(x) = \frac{1}{\sigma_X\sqrt{2\pi}}\exp\left(-\frac{1}{2}\left(\frac{x-\mu_X}{\sigma_X}\right)^2\right) \qquad -\infty \le x \le \infty$$

where μ_X and σ_X denote the mean value and standard deviation, respectively, of X.

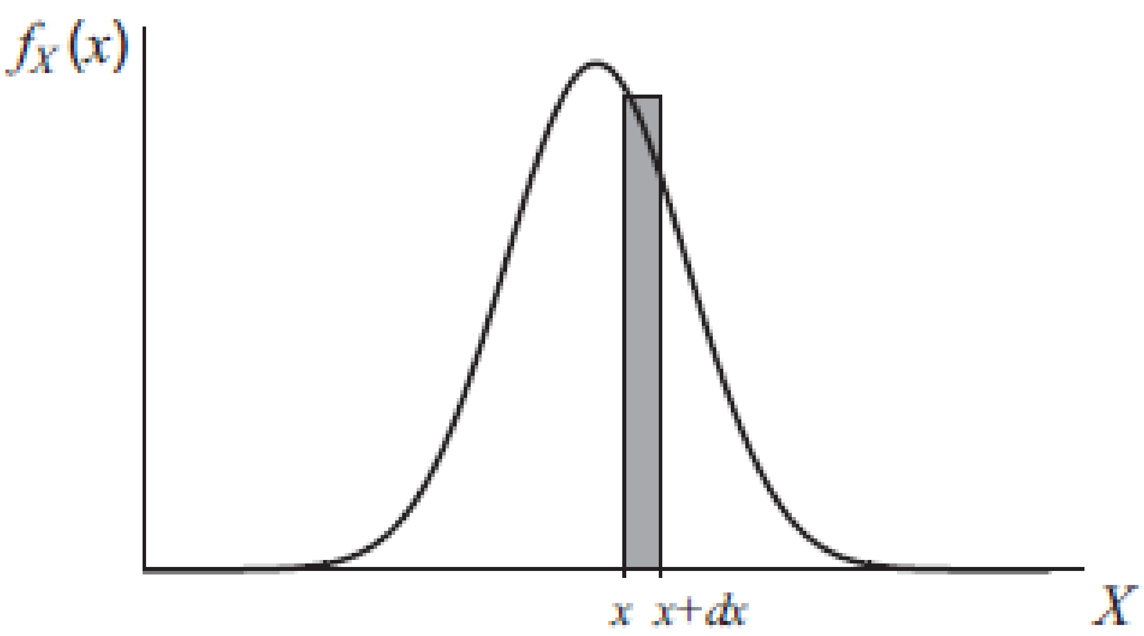

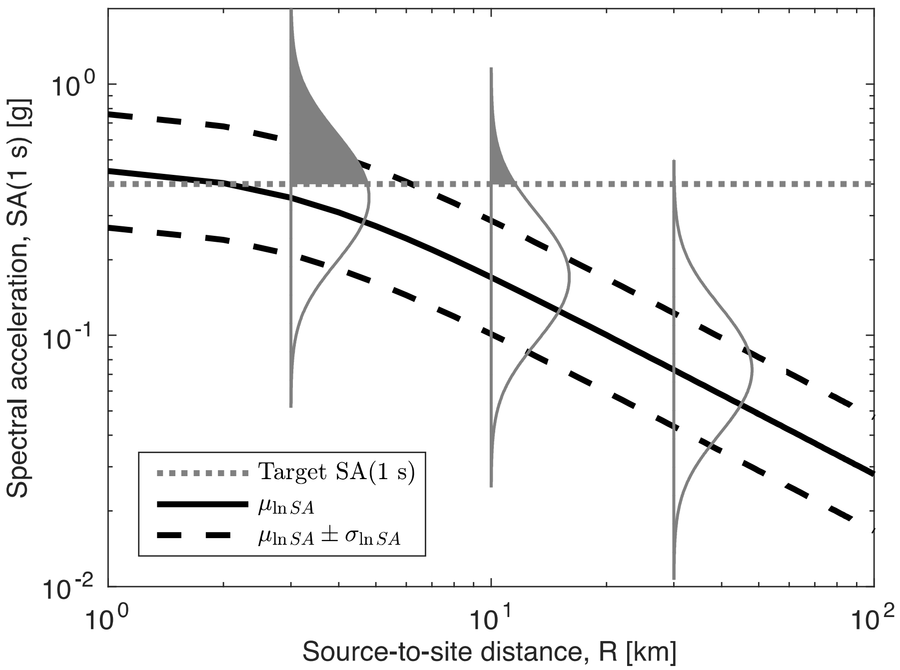

Baker, Bradley and Stafford (2021), "Seismic Hazard and Risk Analysis." These images are provided for instructional and research use, with attribution. Not for commercial use.

Common Probability Distributions

Normal Distribution

A normal random variable, X, can be transformed into a standard normal random variable as

$$U = \frac{X - \mu_X}{\sigma_X} \tag{A.51}$$

where U is a standard normal random variable.

The CDF for general normal random variable can be written as:

$$P(X \leq x) = \Phi\left(\frac{X - \mu_X}{\sigma_X}\right)$$

UNIVERSITÀ DEGLI STUDI DI TRIESTE

Common Probability Distributions

Bivariate Normal Distribution

Normal distribution of 2 random variables

$$f_{X,Y}(x,y) = \frac{1}{2\pi\sigma_X\sigma_Y\sqrt{1-\rho_{X,Y}^2}} \exp\left\{-\frac{z}{2(1-\rho_{X,Y}^2)}\right\} \qquad -\infty \le x, y \le \infty$$

where $\rho_{X,Y}$ is the correlation coefficient between X and Y, and

$$z = \frac{(x-\mu_X)^2}{\sigma_X^2} - \frac{2\rho_{X,Y}(x-\mu_X)(y-\mu_Y)}{\sigma_X\sigma_Y} + \frac{(y-\mu_Y)^2}{\sigma_Y^2}.$$

A useful property of random variables having this distribution is that if X and Y are jointly normal, then their marginal distributions ($f_X(x)$ and $f_Y(y)$) are normal, and their conditional distributions are also normal. Specifically, the distribution of X given $Y = y$ has conditional mean

$$\mu_{X|Y=y} = \mu_X + \rho_{X,Y}\,\sigma_X\left(\frac{y-\mu_Y}{\sigma_Y}\right) \qquad \text{(A.55)}$$

and conditional standard deviation

$$\sigma_{X|Y=y} = \sigma_X\sqrt{1-\rho_{X,Y}^2}. \qquad \text{(A.56)}$$

These properties are convenient when computing joint distributions of ground-motion parameters.

Common Probability Distributions

Lognormal Distribution

A random variable Y has a lognormal distribution if its logarithm, X=ln Y has a normal distribution

$$f_Y(y) = \frac{1}{y\sigma_{\ln Y}\sqrt{2\pi}} \exp\left(-\frac{1}{2}\left(\frac{\ln y - \mu_{\ln Y}}{\sigma_{\ln Y}}\right)^2\right) \quad 0 \le y \le \infty$$

$$F_Y(y) = \Phi\left(\frac{\ln y - \mu_{\ln Y}}{\sigma_{\ln Y}}\right) \quad 0 \le y \le \infty$$

Relation to the mean and standard deviation of Y

$$\mu_Y = e^{\mu_{\ln Y}} e^{\frac{1}{2}\sigma^2_{\ln Y}}$$

$$\sigma_Y = \mu_Y \sqrt{e^{\sigma^2_{\ln Y}} - 1}.$$

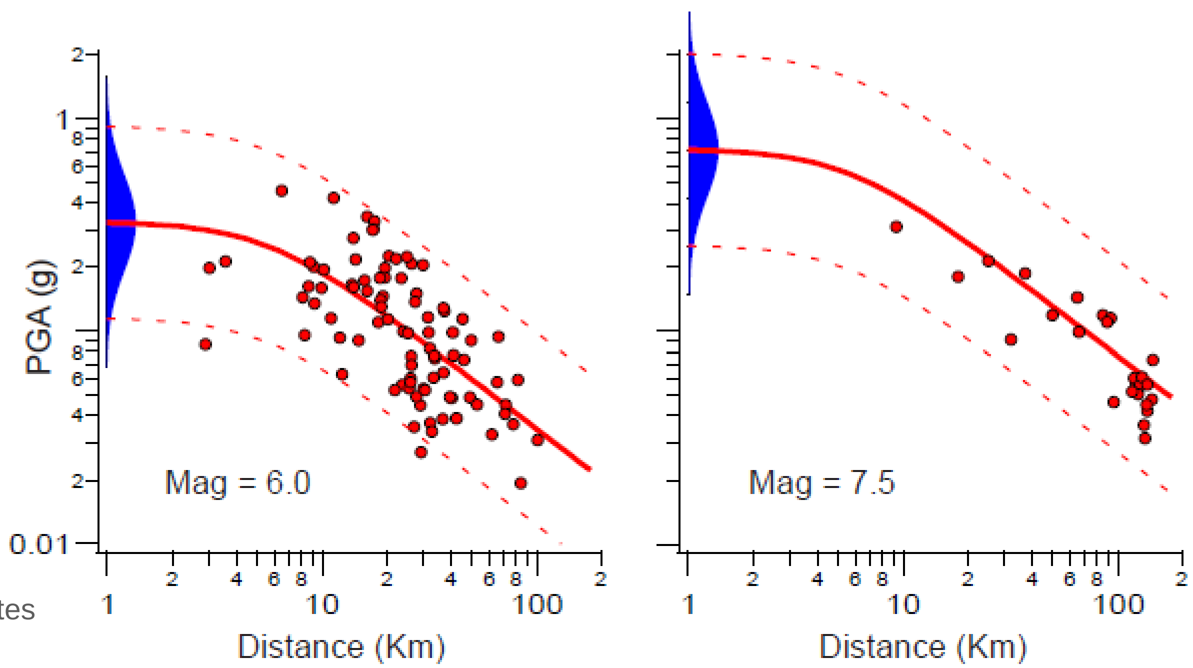

E.H. Field notes

The relationship between the median of Y, y_{50}, and $\mu_{\ln Y}$ can be determined by setting the CDF of Equation A.69 equal to 0.5 when y equals the median, y_{50}:

$$0.5 = \Phi\left(\frac{\ln y_{50} - \mu_{\ln Y}}{\sigma_{\ln Y}}\right) \quad \rightarrow \quad y_{50} = e^{\mu_{\ln Y}}. \qquad (A.72)$$

The equivalence of $\ln y_{50}$ and $\mu_{\ln Y}$ can be stated in words as "the log of the median is equal to the logarithmic mean."

Common Probability Distributions

The poisson process

A *Poisson process* is a sequence of discrete events having the following properties:

1. Stationarity: the probability of an event in a short interval from time t to $t + h$ is approximately λh, for any t.
2. Nonmultiplicity: the probability of two or more events in a short time interval is negligible compared with λh.
3. Independence: the number of events in any interval of time is independent of the number of events in any other (nonoverlapping) interval of time.

The number of events observed in time t froma poisson process has a Poisson distribution.

Poisson PMF $$p_X(x) = \frac{(\lambda t)^x}{x!}\exp(-\lambda t), \qquad x = 0, 1, 2, \ldots$$

X is the number of success in time t
The process has a mean rate of events λ

Mean $$\mu_X = \lambda t$$

Standard deviation $$\sigma_X = \sqrt{\lambda t}.$$

Baker, Bradley and Stafford (2021), "Seismic Hazard and Risk Analysis." These images are provided for instructional and research use, with attribution. Not for commercial use.

E.H. Field notes

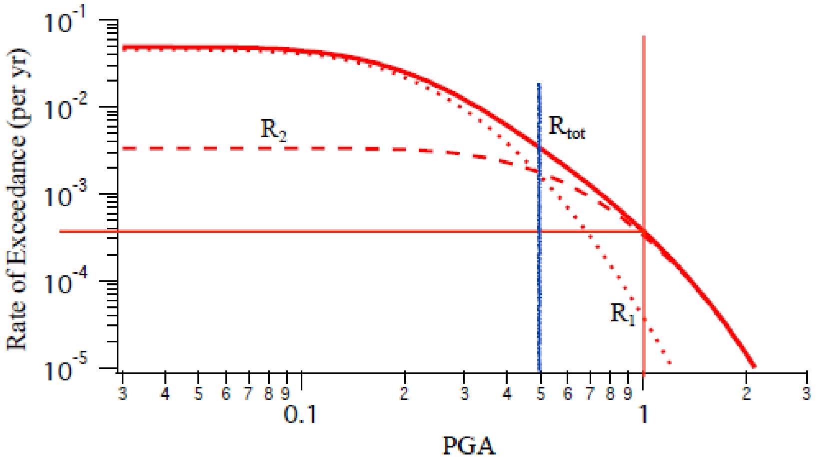

Poissonian probability of exceeding each ground motion level in the next T years from the annual rate

Modified from Probabilistic Seismic Hazard Analysis (PSHA)
A Primer Written by Edward (Ned) H. Field

Basic of Probabilistic Seismic Hazard Assessment (1)

Hazard is the mean rate of exceedence of a certain ground motion measure (PGA, SA, PGV) etc   UNIT is $(\text{years})^{-1}$

Risk is the mean annual loss (dollars, properties, lives) UNITS dollars/years lives/years

Sesimic Source Zone (SSZ) $=5\text{X}10^6$ km^2

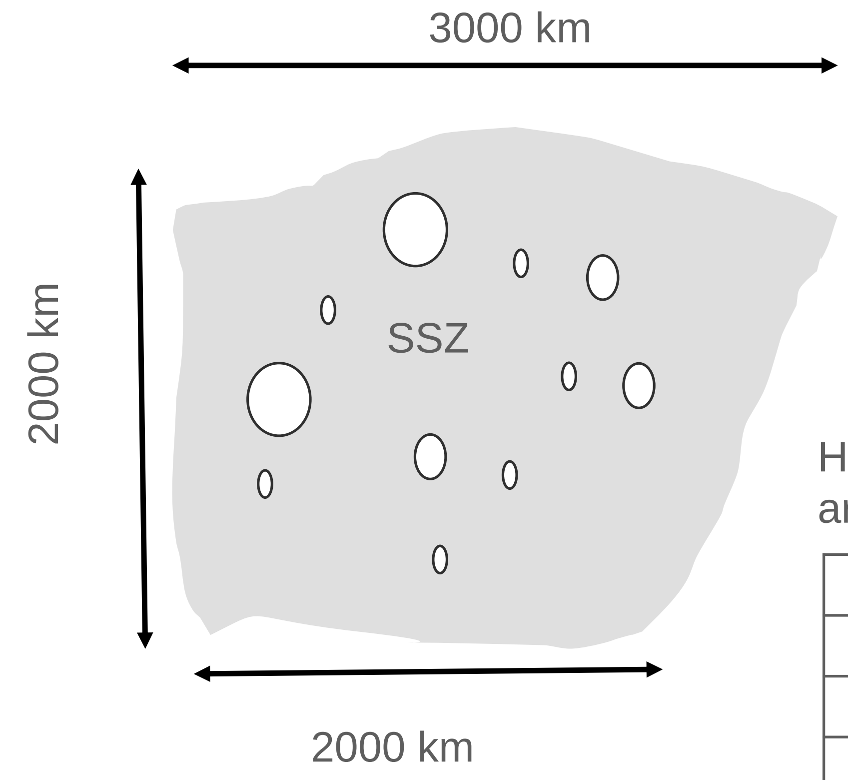

One M=5   per year
One M=6 per decade
One M=7 per century

Horizontal distance (km) within which the given pga's are achieved or exceeded for the given magnitudes

	M=5	M=6	M=7
0.1 g	14	25	41
0.2 g	3.2	12	22
0.4 g	0	0	10

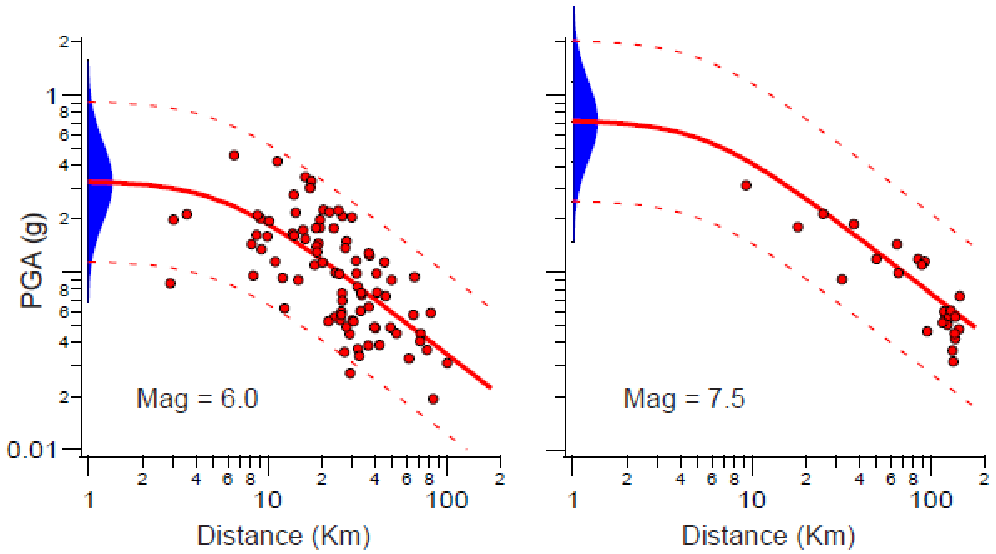

Mean rate of exceedance (MROES) x 10-4 per year, for given pga's for the given magnitudes

	M=5	M=6	M=7	$\sum$	$\sum^{\sigma}$
0.1 g	1.23	0.39	0.11	1.73	1.47
0.2 g	0.06	0.09	0.03	0.18	0.41
0.4 g	0	0	0.006	0.006	0.034

UNIVERSITÀ DEGLI STUDI DI TRIESTE

Modified from probabilistic seismic hazard analysis: a beginner's guide T.C Hanks, C.A. Cornell

Basic of Probabilistic Seismic Hazard Assessment (1)

Example for MROE
M=5
Pga=0.1

The PGA will be greater than or equal to the given value of PGA within each distance R
That is where exceedance comes!

Likelihood that the place of interest will be affected by the level of pga or higher

$$\text{MROE}=\underbrace{((\pi 14^2)\ \text{km}^2/(5\text{X}10^6)\ \text{km}^2)}_{\text{Likelihood}}*\underbrace{1/\text{year}}_{\text{Occurrence}} = 1.23\text{x}10^{-4}$$

Occurrence rate of each Magnitude

One M=5 per year
One M=6 per decade
One M=7 per century

Horizontal distance R (km) within which the given pga's are achieved or exceeded for the given magnitudes

	M=5	M=6	M=7
0.1 g	14	25	41
0.2 g	3.2	12	22
0.4 g	0	0	10

Mean rate of exceedance (MROES) x 10-4 per year, for given pga's for the given magnitudes

	M=5	M=6	M=7	$\sum$	$\sum^{\sigma}$
0.1 g	1.23	0.39	0.11	1.73	1.47
0.2 g	0.06	0.09	0.03	0.18	0.41
0.4 g	0	0	0.006	0.006	0.034

Numerical integration with ΔM=1

Modified from probabilistic seismic hazard analysis: a beginner's guide T.C Hanks, C.A. Cornell

Basic of Probabilistic Seismic Hazard Assessment (1)

Example for MROE
M=5
Pga=0.1

The mean rate in the order of 10^{-4} /year does not mean that we need data for 10.000 year.

The small value is not due to the seismicity rate but to the ratio of the area!

The earthquakes are occurring at the rate of 1/year for M=5 and 10^{-2} year for M=7

One M=5 per year
One M=6 per decade
One M=7 per century

Horizontal distance R (km) within which the given pga's are achieved or exceeded for the given magnitudes

	M=5	M=6	M=7
0.1 g	14	25	41
0.2 g	3.2	12	22
0.4 g	0	0	10

Mean rate of exceedance (MROES) x 10-4 per year, for given pga's for the given magnitudes

	M=5	M=6	M=7	$\sum$	$\sum^{\sigma}$
0.1 g	1.23	0.39	0.11	1.73	1.47
0.2 g	0.06	0.09	0.03	0.18	0.41
0.4 g	0	0	0.006	0.006	0.034

Numerical integration with ΔM=1

UNIVERSITÀ DEGLI STUDI DI TRIESTE

Modified from probabilistic seismic hazard analysis: a beginner's guide T.C Hanks, C.A. Cornell

Basic of Probabilistic Seismic Hazard Assessment (1)

Consider that two subregions are more active than the rest

Three different seismicty rate but with whole region with the same value as in the previous case

In Region 1 the seismicity rate is dow by **0.5** but the (area)-1 is up (for example) of a factor **100**

Therefore, for this region the exceedence rate is **50** time larger with respect to the previous case

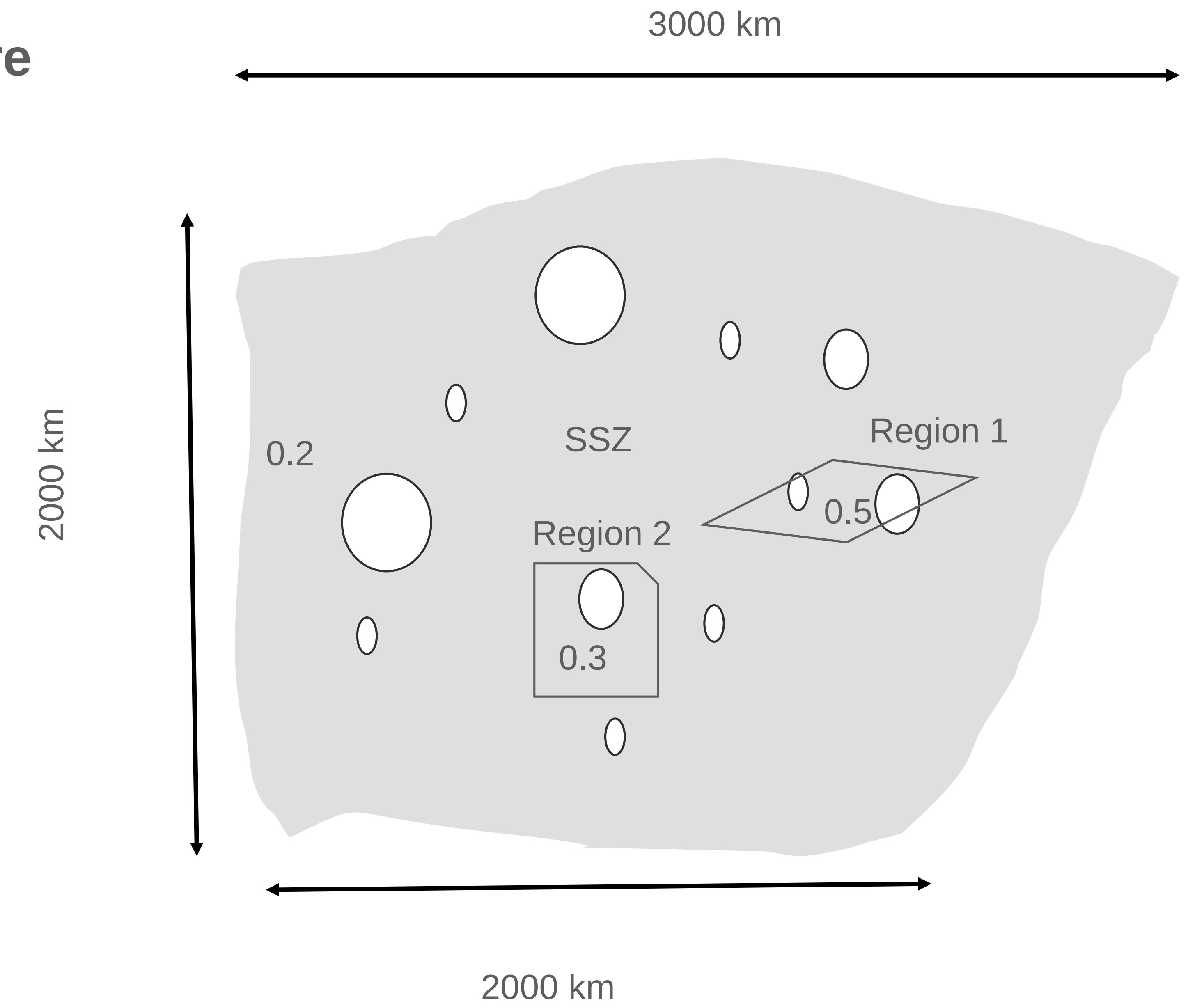

UNIVERSITÀ DEGLI STUDI DI TRIESTE

Modified from probabilistic seismic hazard analysis: a beginner's guide T.C Hanks, C.A. Cornell

Basic of Probabilistic Seismic Hazard Assessment (2)

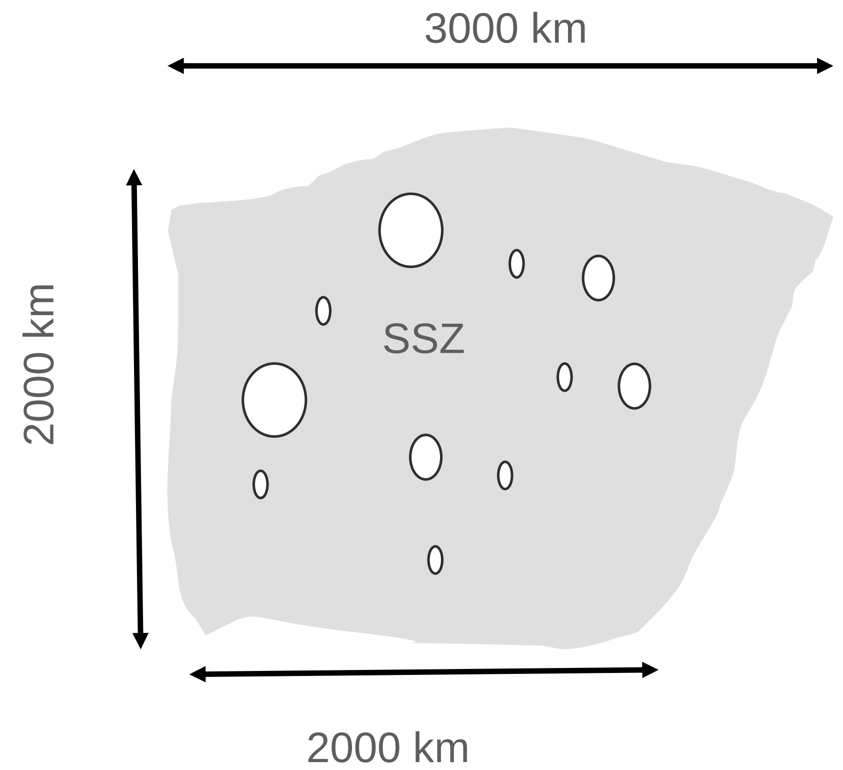

Consider that the source model is made by N earthquake scenarion E_n, each one with its magnitude (m_n,) location (L_n) and rate (r_n)

$$E_n = E(m_n, L_n, r_n).$$

r_n represents the annual rate of the earthquake scenario

The probability of the scenario over some specified time period should be given; this would allow the implementation of time-dependent models.

Time dependent models are usually implemented by converting the conditional probability into an equivalent Poissonian time-dependent rate

Example

An average repeat time of an earthquake ona fault is 147 years→ r=0.007 events per year

The Poissonian probability of having more than one event over T years is:

$$P_{pois} = 1 - \exp(-rT)$$

The Poissonian probability for an event in the next 30 years is 19%

Modified from Probabilistic Seismic Hazard Analysis (PSHA)
A Primer Written by Edward (Ned) H. Field

Basic of Probabilistic Seismic Hazard Assessment (2)

The target is to calculate the PSHA at a certain site
The Seismic source model provide the N earthquake scenarios E_n, each one with its magnitude (m_n,) location (L_n) and rate (r_n)

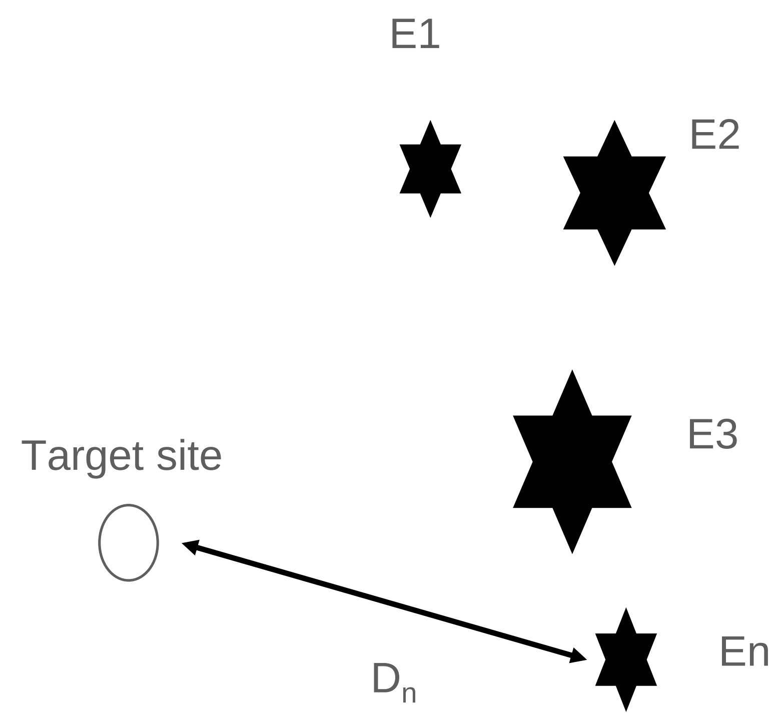

From the scenario L_n we can calculate the distance D_n to the target site.

Given m_n and D_n and using a Ground Motion Prediction equation.

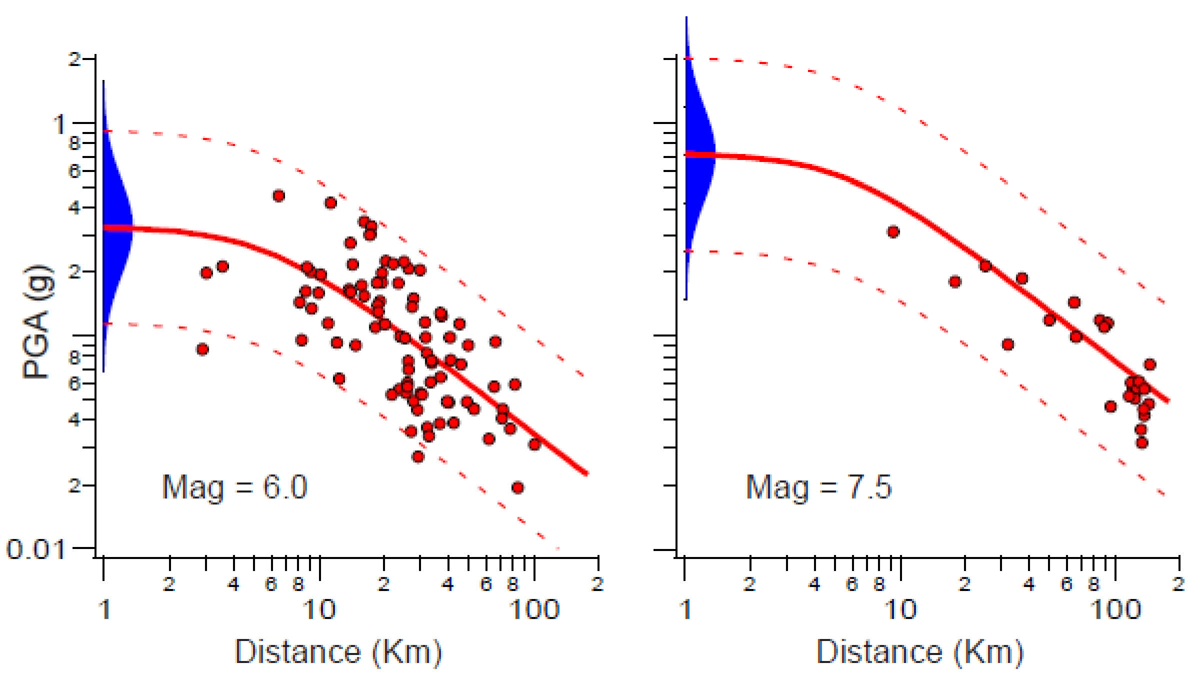

$$p_n(\ln PGA) = \frac{1}{\sigma_n\sqrt{2\pi}} e^{-(\ln PGA - g(m_n, D_n))^2/2\sigma_n} =$$

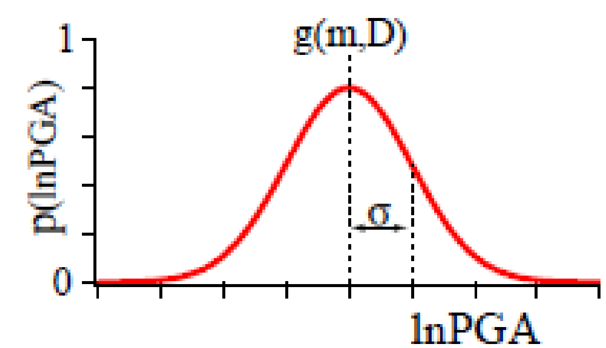

Basic of Probabilistic Seismic Hazard Assessment (2)

Probabiliy of exceeding a certain lnPGA

$$P_n(> \ln PGA) = \frac{1}{\sigma_n \sqrt{2\pi}} \int_{\ln PGA}^{\infty} e^{-(\ln PGA - g(m_n, D_n))^2 / 2\sigma_n} d\ln PGA =$$

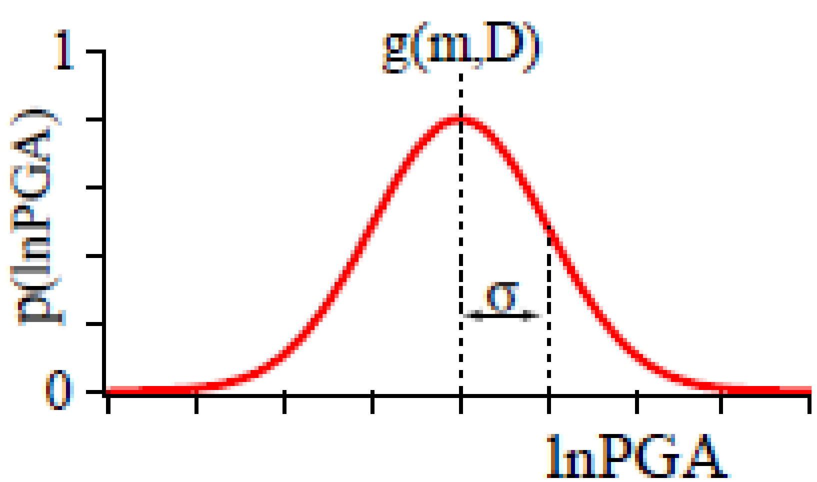

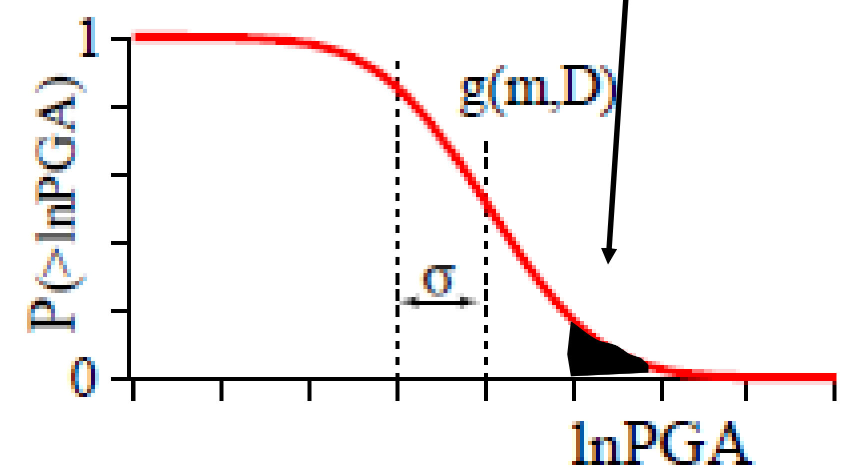

Modified from Probabilistic Seismic Hazard Analysis (PSHA)
A Primer Written by Edward (Ned) H. Field

Basic of Probabilistic Seismic Hazard Assessment (2)

Multiplying for the annual rate r_n one get **annual rate R_n at which a certain lnPGA will be exceeded** for that specific M and Location scenario at the considered site

$$R_n(>\ln PGA) = r_n P_n(>\ln PGA)$$

Summing over the N scenarios (all considered Magnitudes and locations, and rates) one get the

Total annual rate of exceeding a certain ln PGA

$$R_{tot}(>\ln PGA) = \sum_{n=1}^{N} R_n(>\ln PGA) = \sum_{n=1}^{N} r_n P_n(>\ln PGA)$$

Modified from Probabilistic Seismic Hazard Analysis (PSHA)
A Primer Written by Edward (Ned) H. Field

Basic of Probabilistic Seismic Hazard Assessment (2)

Considering the Poissonian distribution one can compute the **Probability of exceeding each ground motion level in T years** using the total annual rate

$$P_{pois}(> \ln PGA, T) = 1 - e^{-R_{tot}T}$$

If P_{pois}=10% in 50 years

T= 50 years

R_{tot}=(-ln(1-0.1))/T=0.00210721

From which one get a **return period of 475 years**

Modified from Probabilistic Seismic Hazard Analysis (PSHA)
A Primer Written by Edward (Ned) H. Field

Basic of Probabilistic Seismic Hazard Assessment (2)

Example
Two scenarios only

R1=M=6 every 22 years

R2=M= 7.8 every 300 years

$$\ln(PGA) = 0.53(M\text{-}6) - 0.39\ln(D^2+31) + 0.25$$

→ 0.19 g

→ 0.5 g

Both at 10 km from the target site

σ (lnpga)= 0.52

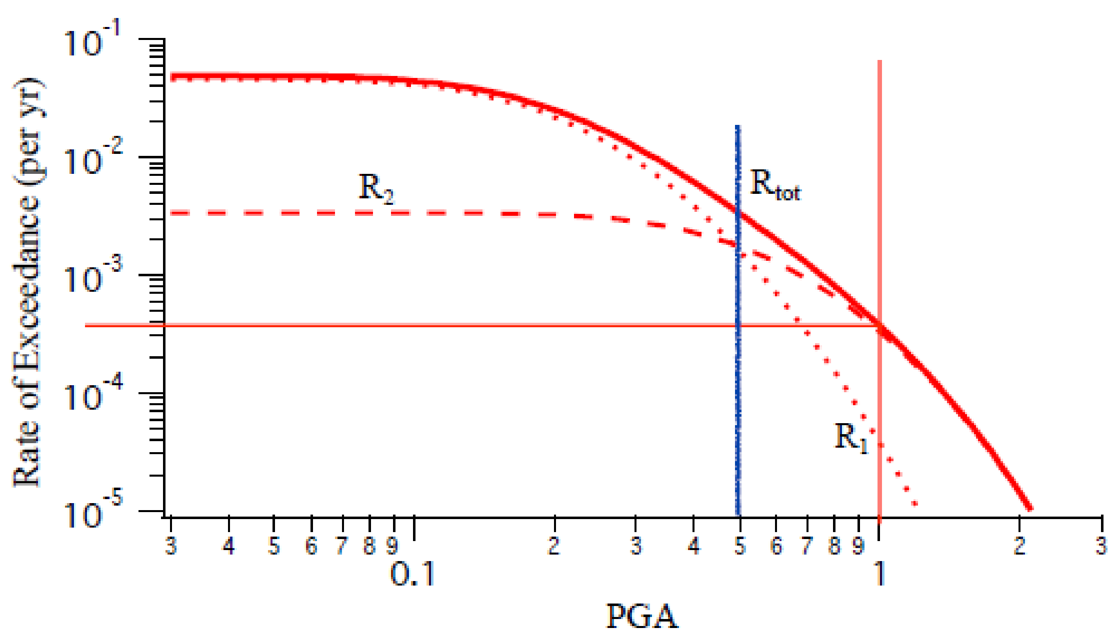

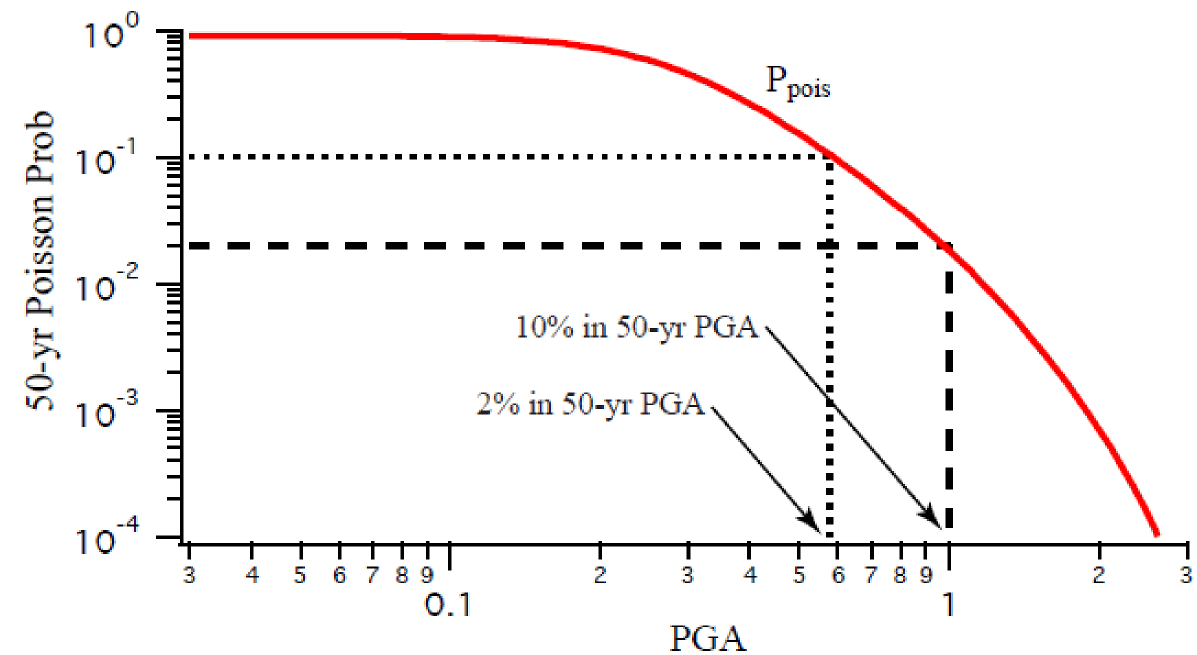

Modified from Probabilistic Seismic Hazard Analysis (PSHA)
A Primer Written by Edward (Ned) H. Field

Basic of Probabilistic Seismic Hazard Assessment (2)

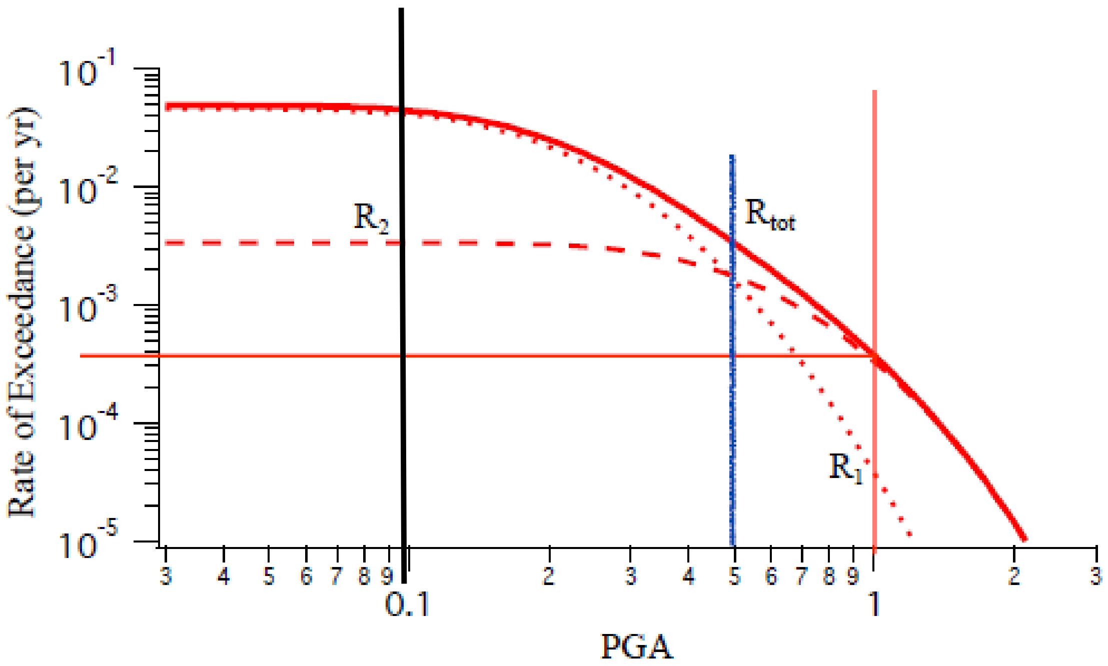

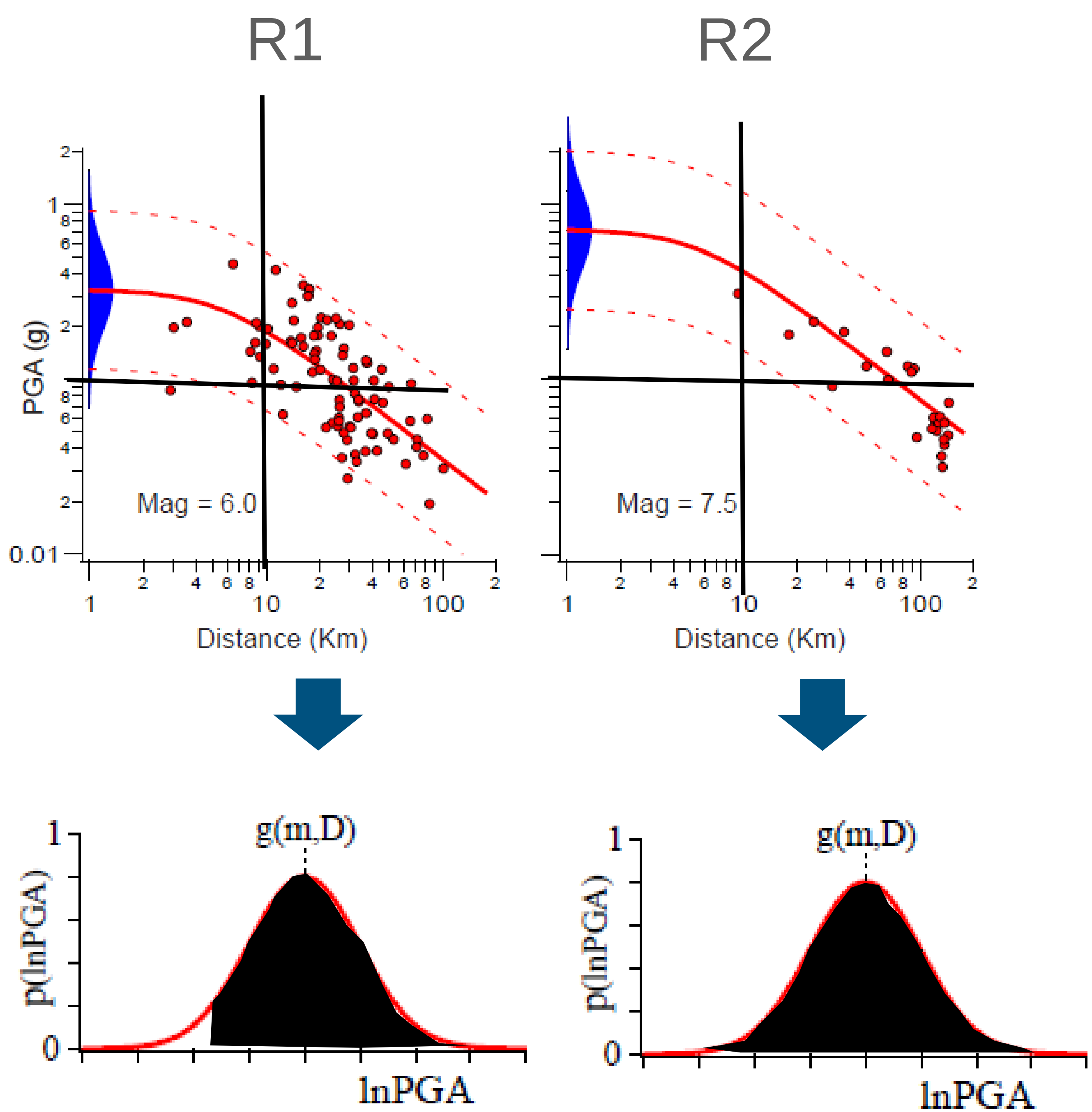

For small PGA (e.g. 0.1 g) although the **probability of exceedence** is larger for the M6, the **annual rate of exceedence** of R1 is larger than that of R2 because the **annual rate** of R1, r1=1/22 is much larger than the **annual rate** of R2, r2=1/300!

Basic of Probabilistic Seismic Hazard Assessment (2)

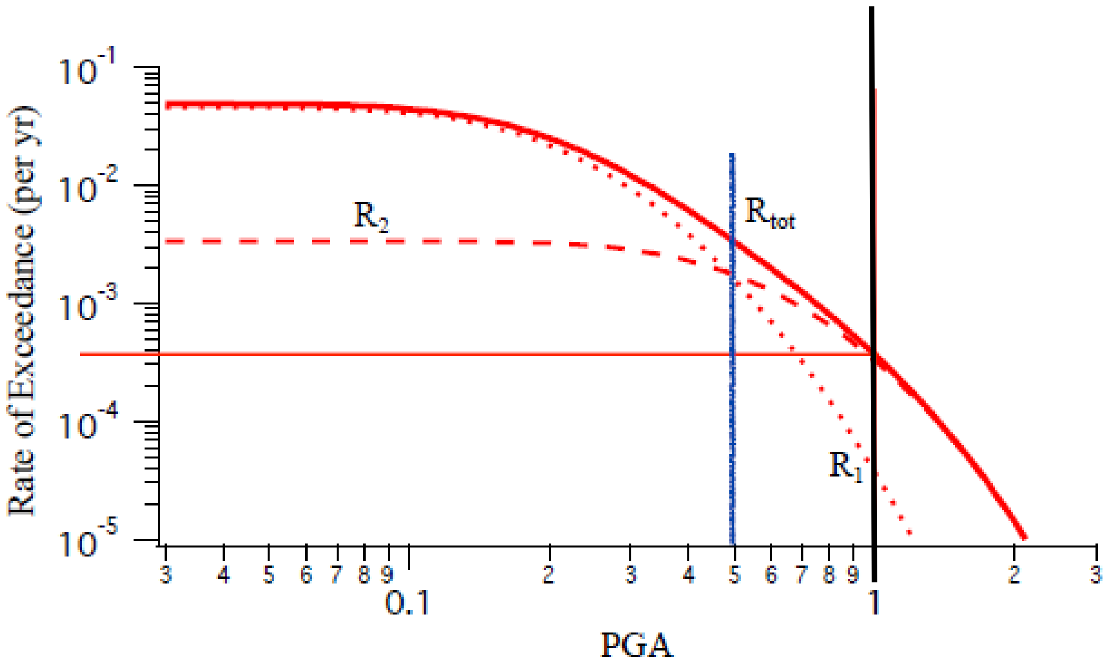

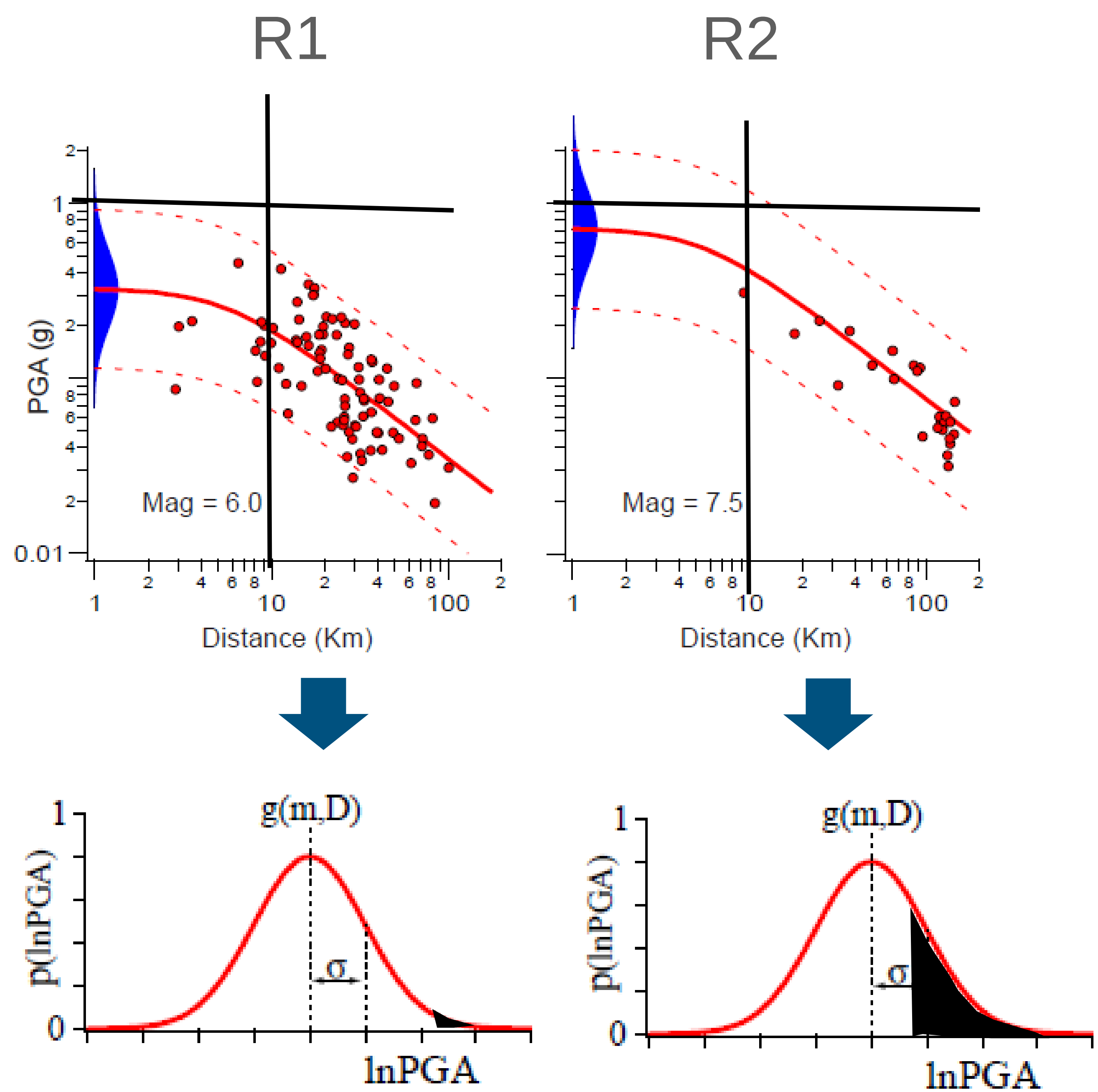

For large PGA (e.g. 1 g) the **probability of exceedence** is larger for the M7.8, **although** the **annual rate** of R1 is larger than that of R2, because **probability of exceedence** of R1 is very small

Basic of Probabilistic Seismic Hazard Assessment (2)

Rtot=sum of the two scenario is dominated at low PGA by the small but frequent events and for high pga by the strong but rare events

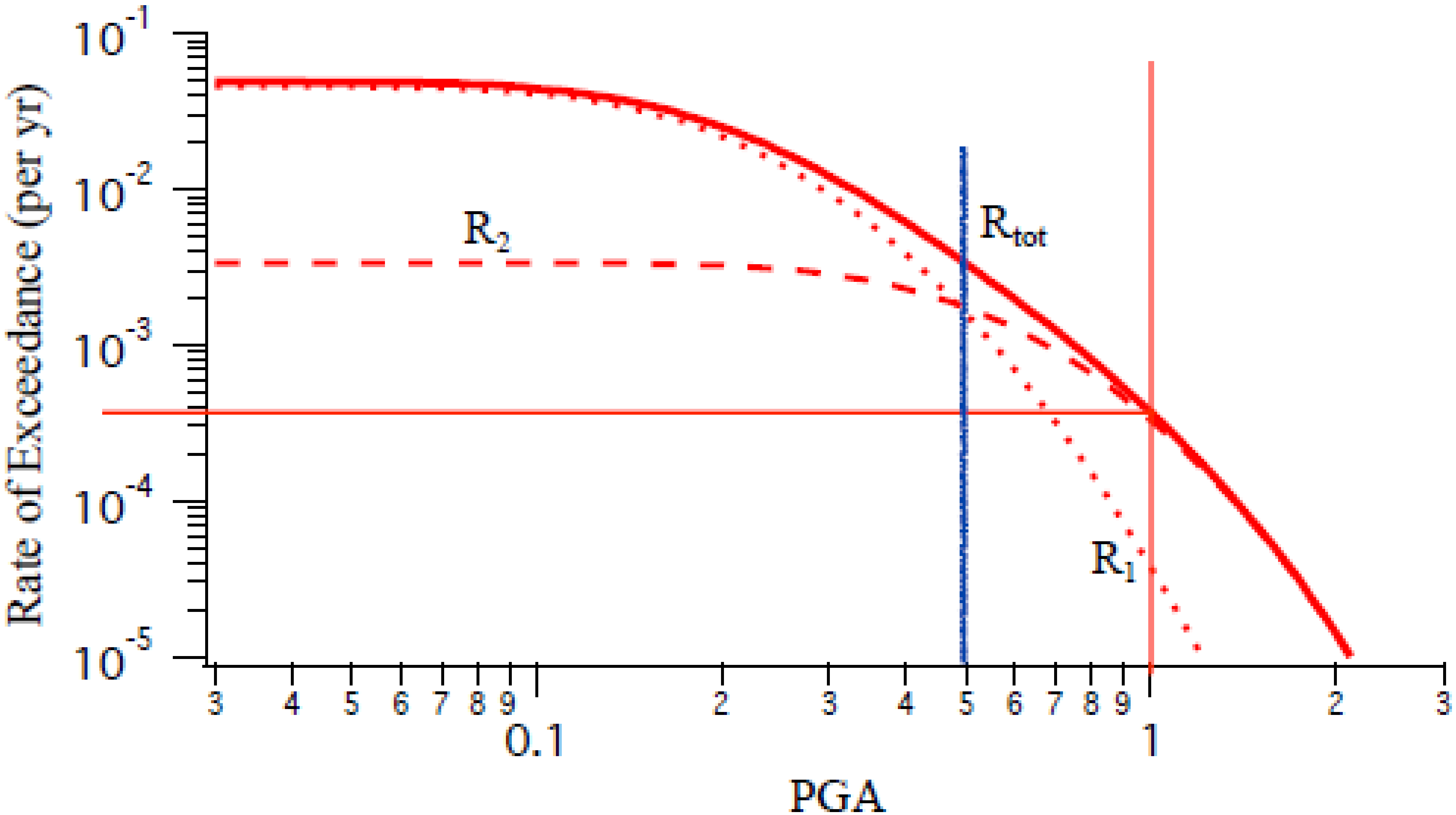

Modified from Probabilistic Seismic Hazard Analysis (PSHA)
A Primer Written by Edward (Ned) H. Field

Basic of Probabilistic Seismic Hazard Assessment (2)

$$P_{pois}(>\ln PGA, T) = 1 - e^{-R_{tot}T}$$

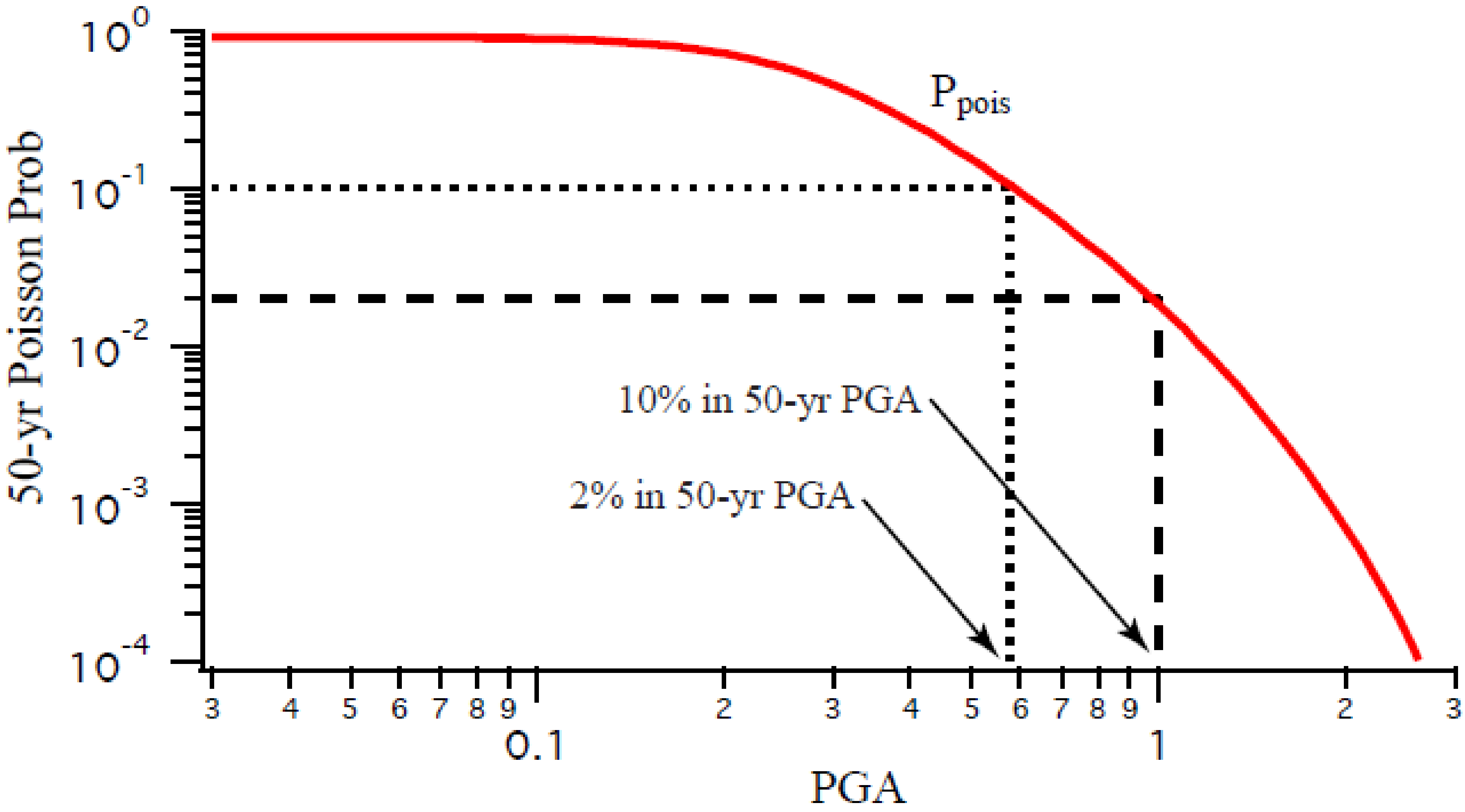

Extending this analysis for several sites we obtain the seismic hazard maps

Modified from Probabilistic Seismic Hazard Analysis (PSHA)
A Primer Written by Edward (Ned) H. Field

Earthquake Magnitude

The concept of magnitude was introduced by Richter (1935) to provide an objective instrumental measure of the size of earthquakes. Contrary to seismic intensity, I, which is based on the assessment and classification of shaking damage and human perceptions of shaking, the magnitude M uses instrumental measurements of earth ground motion adjusted for epicentral distance and source depth.

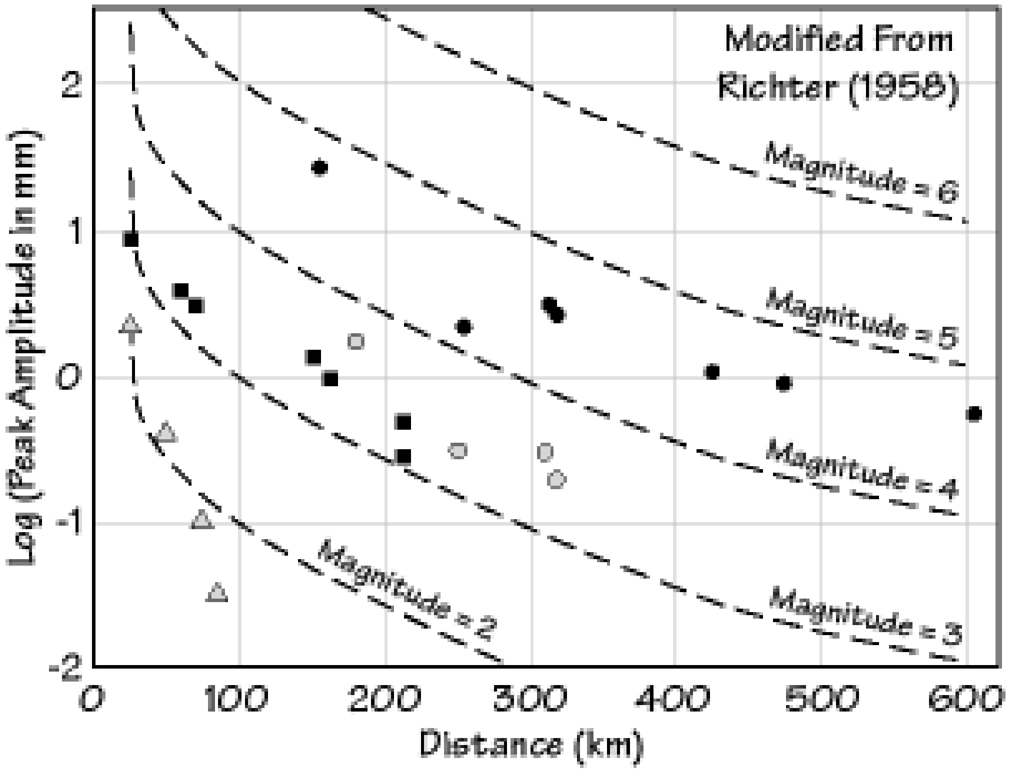

The original Richter scale was based on the observation that the amplitude of seismic waves systematically decreases with epicentral distance.

Data from local earthquakes in California

The relative size of events is calculated by comparison to a reference event, with M_L=0, such that A_0 was 1 μm at an epicentral distance, Δ, of 100 km with a Wood-Anderson instrument:

$$\mathbf{M_L=\log(A/A_0)=\log A-2.48+2.76\Delta.}$$

Hazard Inputs

“I found a paper by Professor K. Wadati of Japan in which he compared large earthquakes by plotting the maximum ground motion against distance to the epicenter. I tried a similar procedure for our stations, but the range between the largest and smallest magnitudes seemed unmanageably large. Dr. Beno Gutenberg then made the natural suggestion to plot the amplitudes logarithmically. I was lucky because **logarithmic plots are a device of the devil**. I saw that I could now rank the earthquakes one above the other. Also, quite unexpectedly the attenuation curves were roughly parallel on the plot. By moving them vertically, a representative mean curve could be formed, and individual events were then characterized by individual logarithmic differences from the standard curve. This set of logarithmic differences thus became the numbers on a new instrumental scale. Very perceptively, Mr. Wood insisted that this new quantity should be given a distinctive name to contrast it with the intensity scale. My amateur interest in astronomy brought out the term "magnitude," which is used for the brightness of a star.”

Charles F. Richter - An Interview by Henry Spall, Earthquake Information Bulletin. Vol. 12, No. 1, January - February, 1980

[CHAP. 22] MAGNITUDE, STATISTICS, ENERGY 341

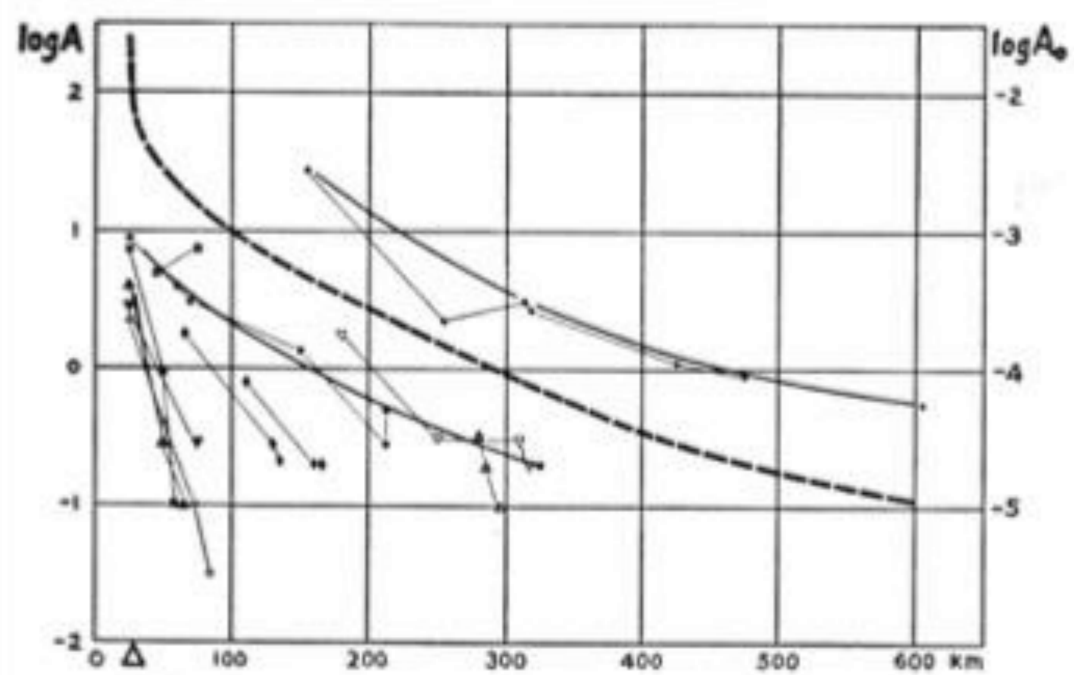

FIGURE 22-2 *Origin of the magnitude scale. Data for Southern California earthquakes of January, 1932. [Redrafted from the original notes.]*

Hazard Inputs

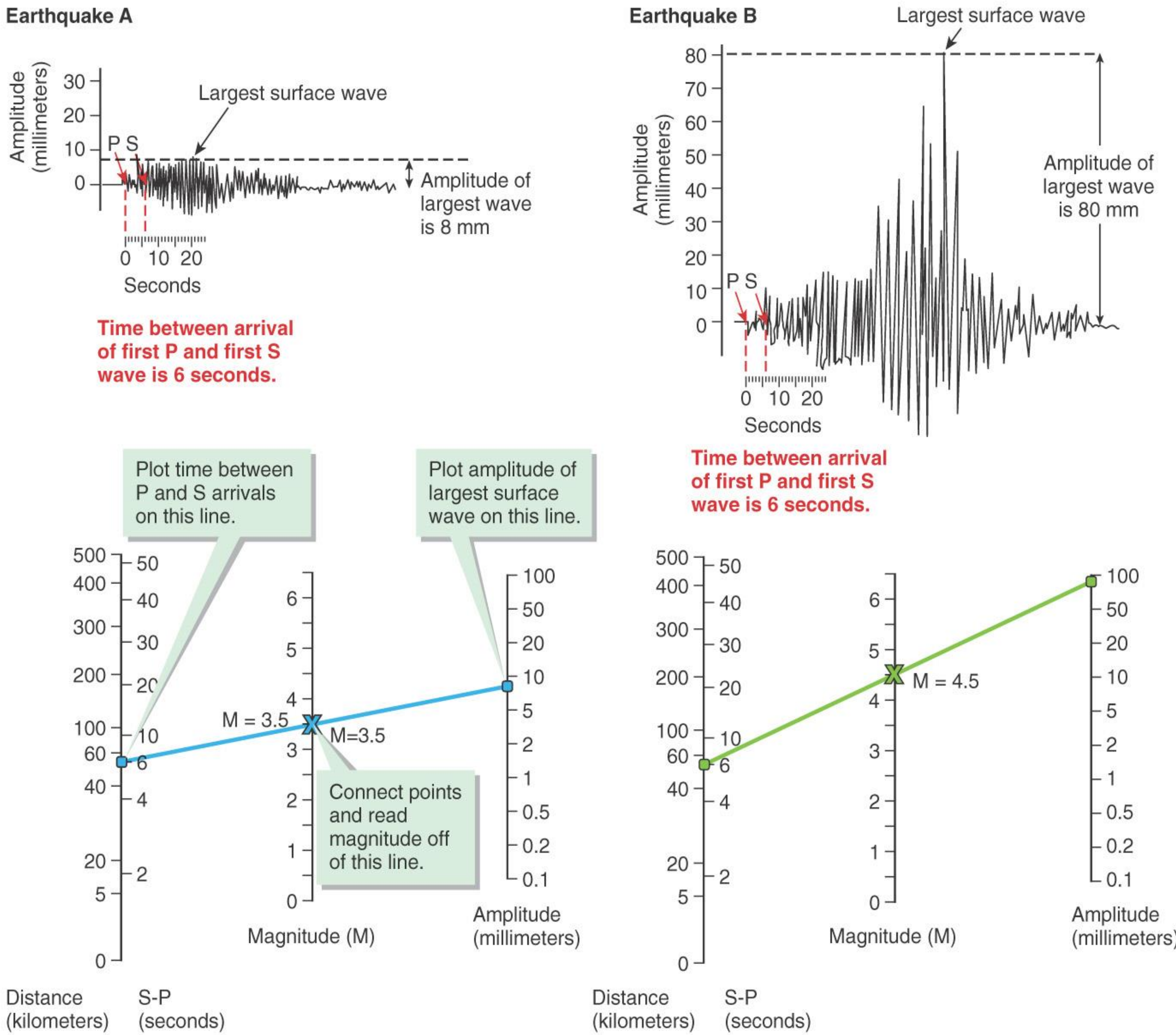

Hazard Inputs

Wood-Anderson Seismometer

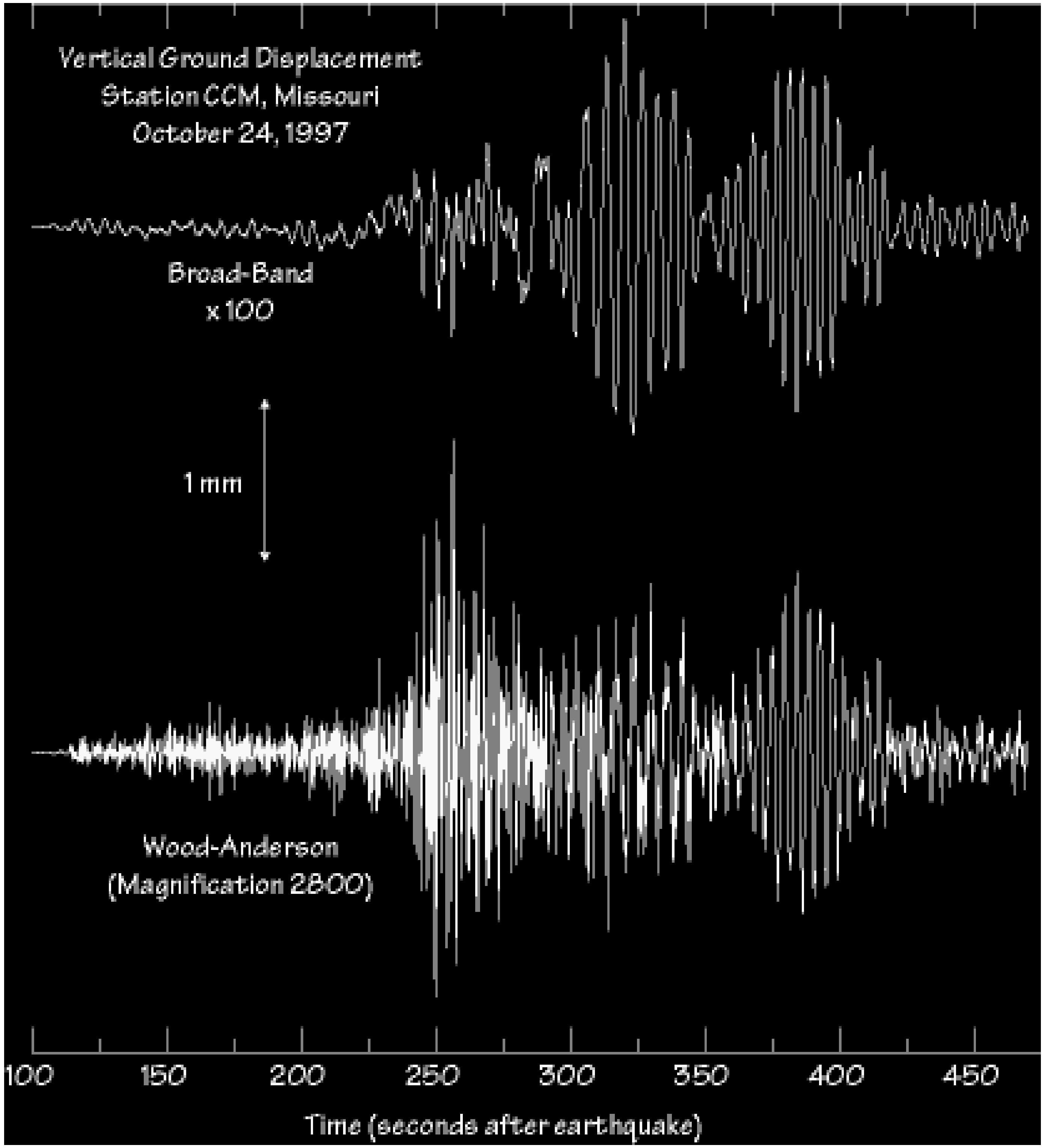

Richter also tied his formula to a specific seismic instrument.

$M_L = \log(A/A_0) = \log A - 2.48 + 2.76\Delta$.

Magnitude Scales

The original M_L is suitable for the classification of local shocks in Southern California only since it used data from the standardized short-period Wood-Anderson seismometer network. The magnitude concept has then been extended so as to be applicable also to ground motion measurements from medium- and long-period seismographic recordings of both surface waves (M_s) and different types of body waves (m_b) in the teleseismic distance range.

The general form of all magnitude scales based on measurements of ground displacement amplitudes A and periods T is:

$$M = \log\left(\frac{A}{T}\right) + f(\Delta, h) + C_r + C_s$$

M seismic magnitude
A amplitude
T period
f correction for distance and depth
C_s correction for site
C_r correction for source region

M_L **Local magnitude**
m_b **body-wave magnitude** (1s)
M_s **surface wave magnitude** (20s)

Teleseismic M_S and mb

The two most common modern magnitude scales are:

- M_S, Surface-wave magnitude (Rayleigh Wave, 20s)
- m_b, Body-wave magnitude (P-wave)

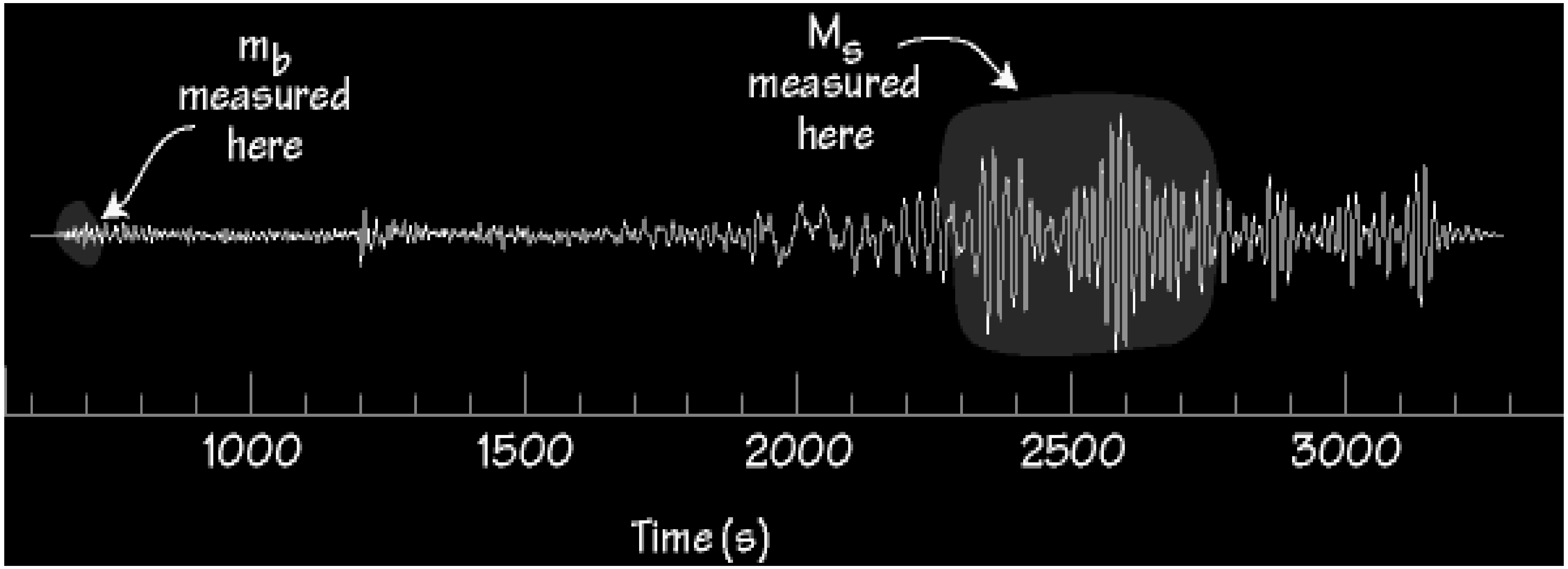

Example: m_b "Saturation"

m_b seldom gives values above 6.7 - it "saturates".

m_b must be measured in the first 5 seconds - that's the rule.

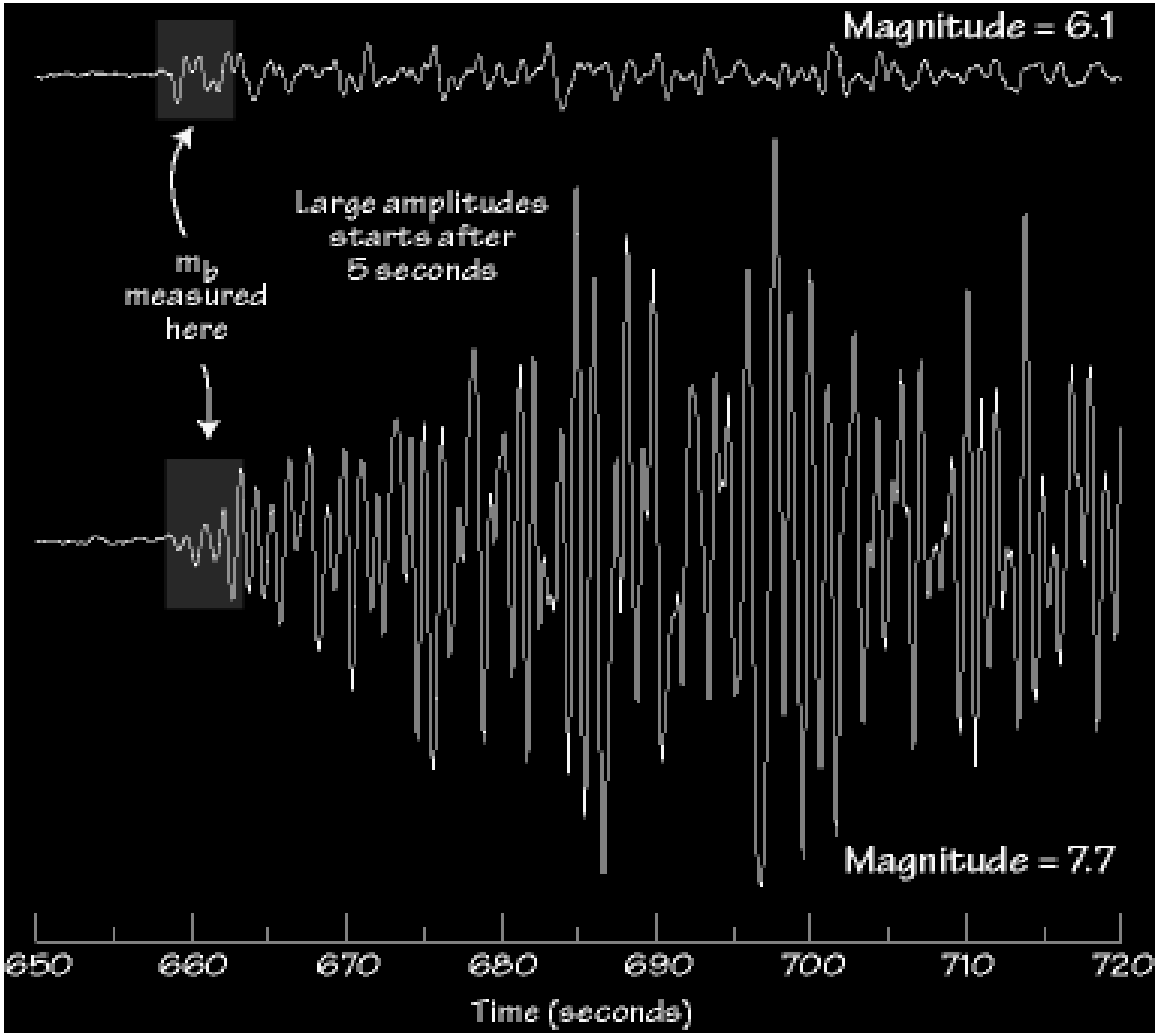

Saturation

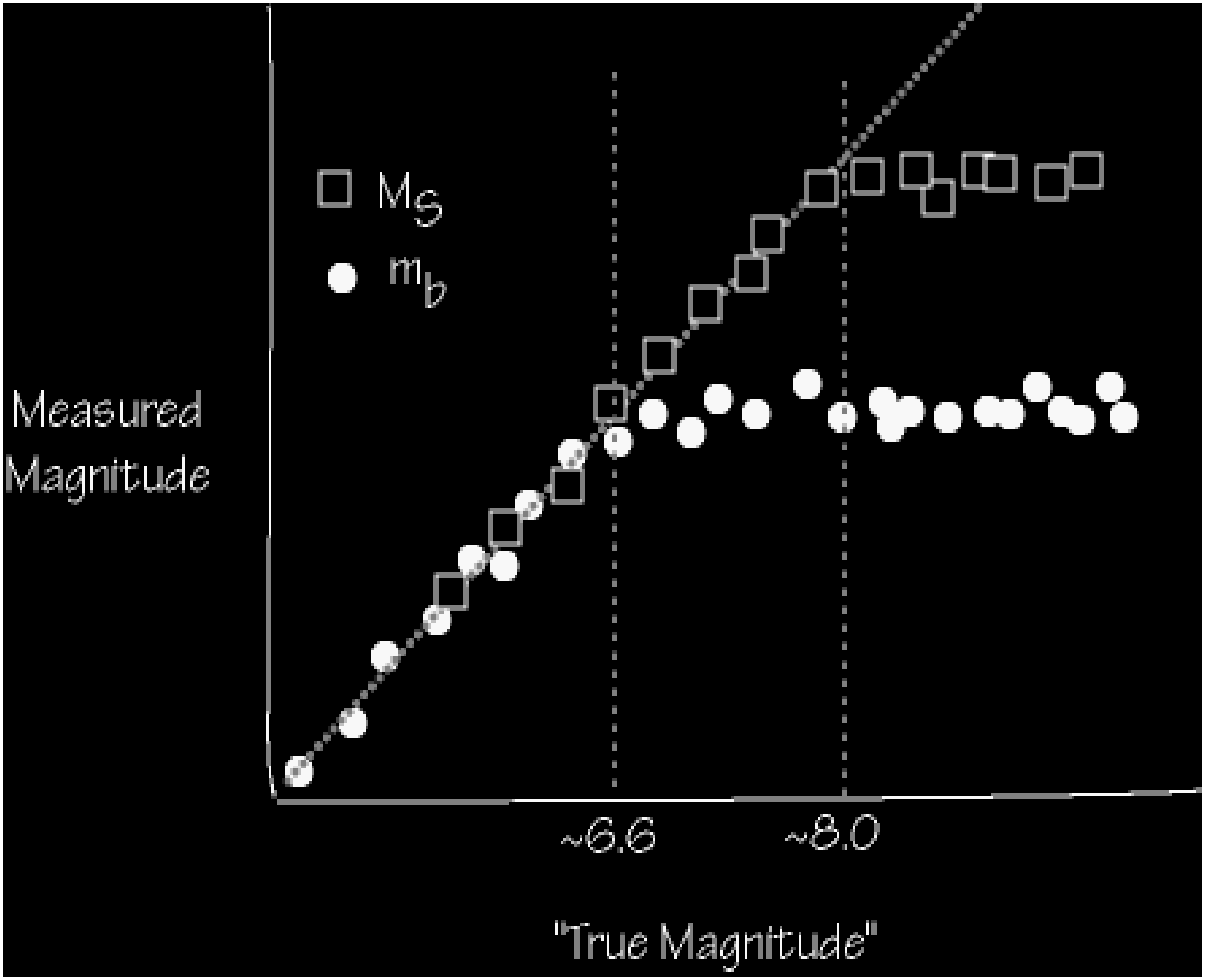

UNIVERSITÀ DEGLI STUDI DI TRIESTE

Magnitude saturation

Nature limits the maximum size of tectonic earthquakes which is controlled by the maximum size of a brittle fracture in the lithosphere. A simple seismic shear source with linear rupture propagation has a typical "source spectrum".

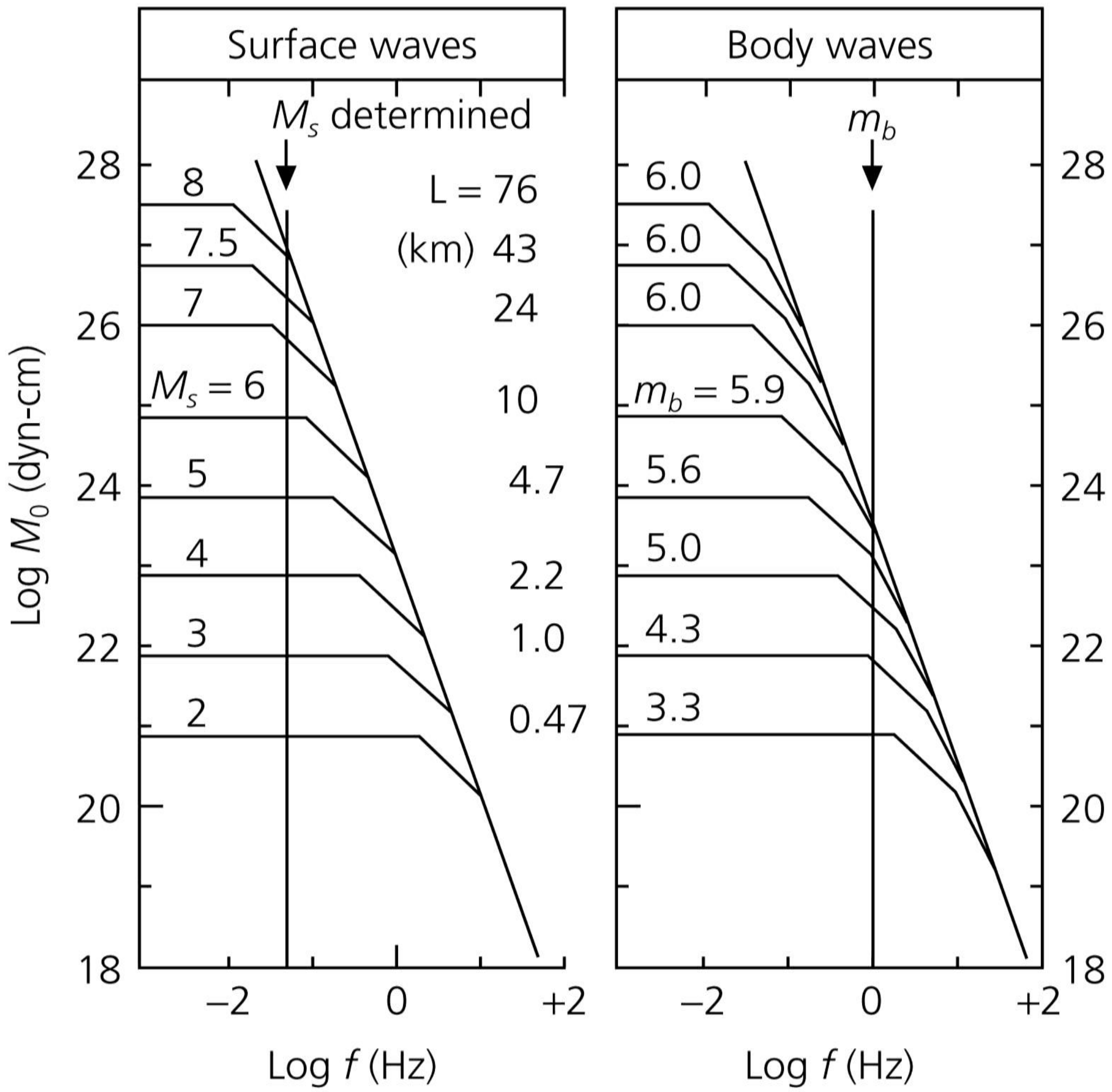

Ms is not linearly scaled with M_0 for $M_s > 6$ due to the beginning of the so-called saturation effect for spectral amplitudes with frequencies $f > f_c$. This saturation occurs already much earlier for m_b which are determined from amplitude measurements around 1 Hz.

Moment magnitude

Empirical studies (Gutenberg & Richter, 1956; Kanamori & Anderson, 1975) lead to a formula for the released seismic energy (in Joule), and for moment, with magnitude:

$\log E = 4.8 + 1.5 M_s$ $\log M_0 = 9.1 + 1.5 M_s$
resulting in

$M_w = 2/3 \log M_0 - 6.07$

when the Moment is measured in N·m (otherwise the intercept becomes 10.73); it is related to the final static displacement after an earthquake and consequently to the tectonic effects of an earthquake.

$$u(x,t) = A\cos\left(\frac{2\pi t}{T}\right) \Rightarrow v(x,t) \propto \frac{A}{T}u$$

$$\Rightarrow e \propto v^2 \propto \left(\frac{A}{T}\right)^2 \Rightarrow \log E = C + 2\log\left(\frac{A}{T}\right)$$

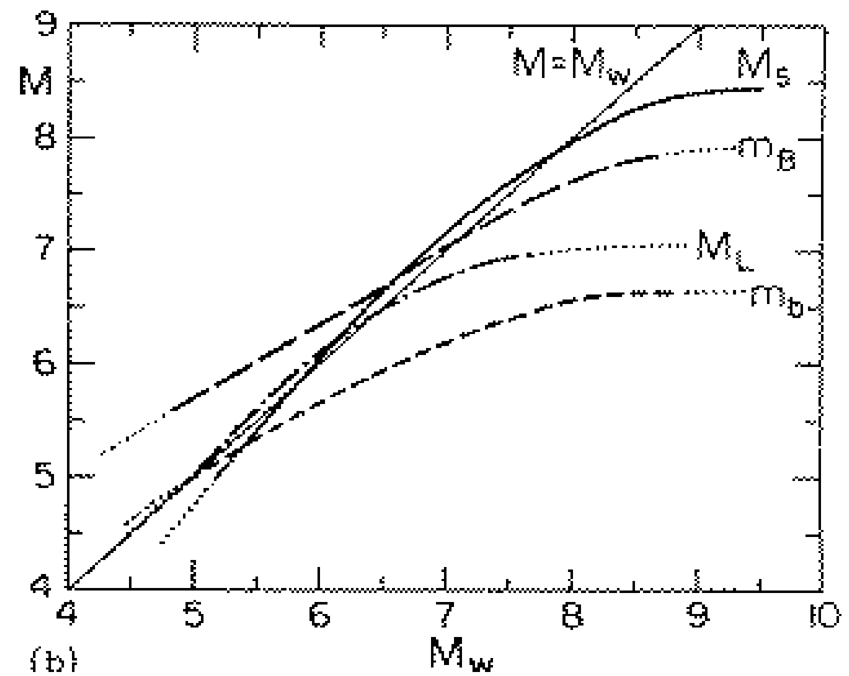

Earthquake	Body wave magnitude m_b	Surface wave magnitude M_s	Fault area (km^2) length × width	Average dislocation (m)	Moment (dyn-cm) M_0	Moment magnitude M_w
Truckee, 1966	5.4	5.9	10 × 10	0.3	8.3×10^{24}	5.8
San Fernando, 1971	6.2	6.6	20 × 14	1.4	1.2×10^{26}	6.7
Loma Prieta, 1989	6.2	7.1	40 × 15	1.7	3.0×10^{26}	6.9
San Francisco, 1906		8.2	320 × 15	4	6.0×10^{27}	7.8
Alaska, 1964	6.2	8.4	500 × 300	7	5.2×10^{29}	9.1
Chile, 1960		8.3	800 × 200	21	2.4×10^{30}	9.5

Seismic moment (1)

Remember . . . the displacement equation for the P and S wave radiation patterns:

$$u_r = \frac{1}{4\pi\alpha^3 r} \dot{M}\left(t - r/\alpha\right) \sin\left(2\theta\right)\cos(\varphi)$$ e.g. P waves

Amplitude term

Source time function

Describes the pattern

Considering the ***seismic moment rate function*** or ***source time function***

$$\dot{M}\left(t - r/v\right)$$

which is the time derivative of the ***seismic moment function***

$$M(t) = \mu D(t) S(t)$$

where μ is rigidity, and *D(t)* and *S(t)* are the slip and fault area histories, respectively.

(*Lay & Wallace, 1995; Stein & Wysession, 2003*)

Seismic moment (2)

This leads to the best measure of an earthquake's size and energy,

$$M(t) = \mu D_{av} S$$

the ***seismic moment***, where D_{av} is the average slip or dislocation and S is the fault area.

which in turn gives the ***moment magnitude*** M_w

$$M_w = \frac{\log M_o}{1.5} - 10.73$$

where M_o is in dyn-cm.

and which we will discuss again with respect to other magnitude scales.

(*Lay & Wallace, 1995; Stein & Wysession)*

Hazard Inputs

$$E_S = \left[\frac{1}{15\pi\rho\alpha^5} + \frac{1}{10\pi\rho\beta^5}\right] \int_{f1}^{f2} \left|\frac{\dot{u}(f)}{G(f)/2\pi f}\right|^2 df,$$

$$Me = 2/3(\log_{10} E_S - 4.4), \text{ with } E_S \text{ given in Joule.}$$

Importance of comparing Mw and Me

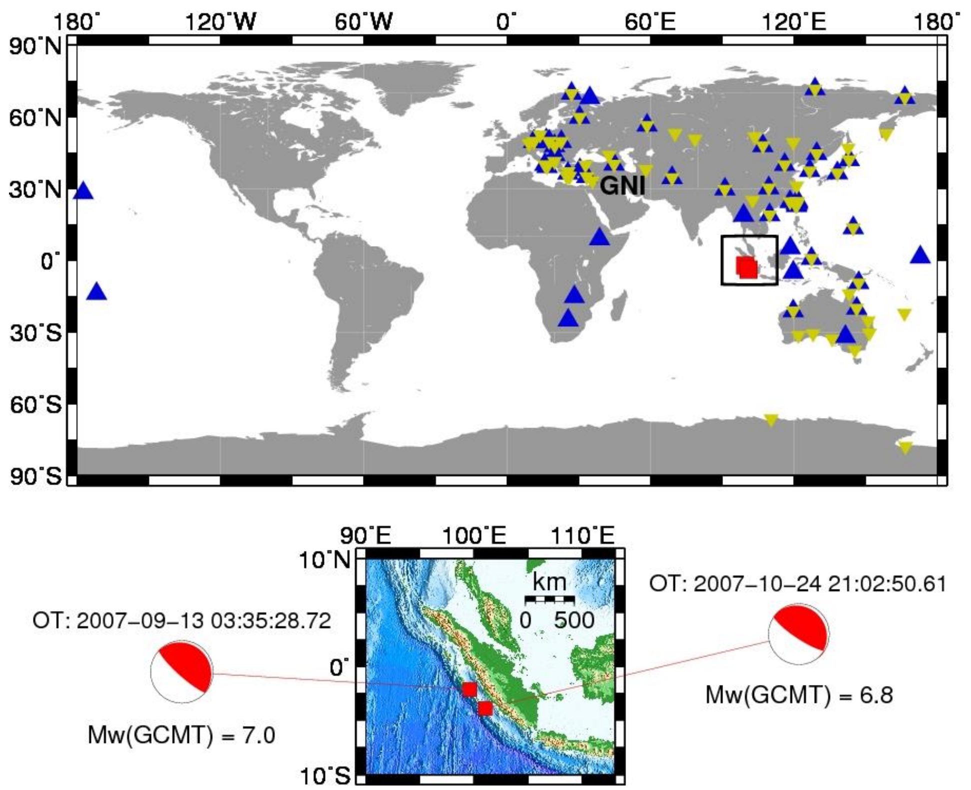

Mw(GCMT) = 7.0
Me(GFZ) = 7.1

Mw(GCMT) = 6.8
Me(GFZ) = 6.4

The locations differ by about 250 km and the moment magnitudes Mw and the fault plane solutions are very similar.

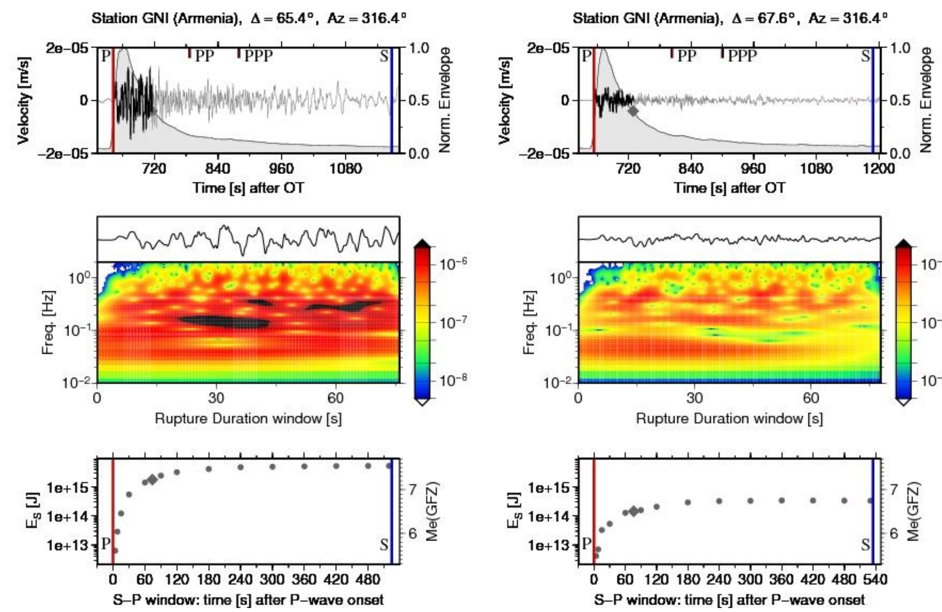

However, the high frequency content observed in the seismograms is significantly different and cannot be explained by Mw only.

UNIVERSITÀ DEGLI STUDI DI TRIESTE

Di Giacomo and Bindi (2009)

Hazard Inputs

Importance of comparing Mw and Me

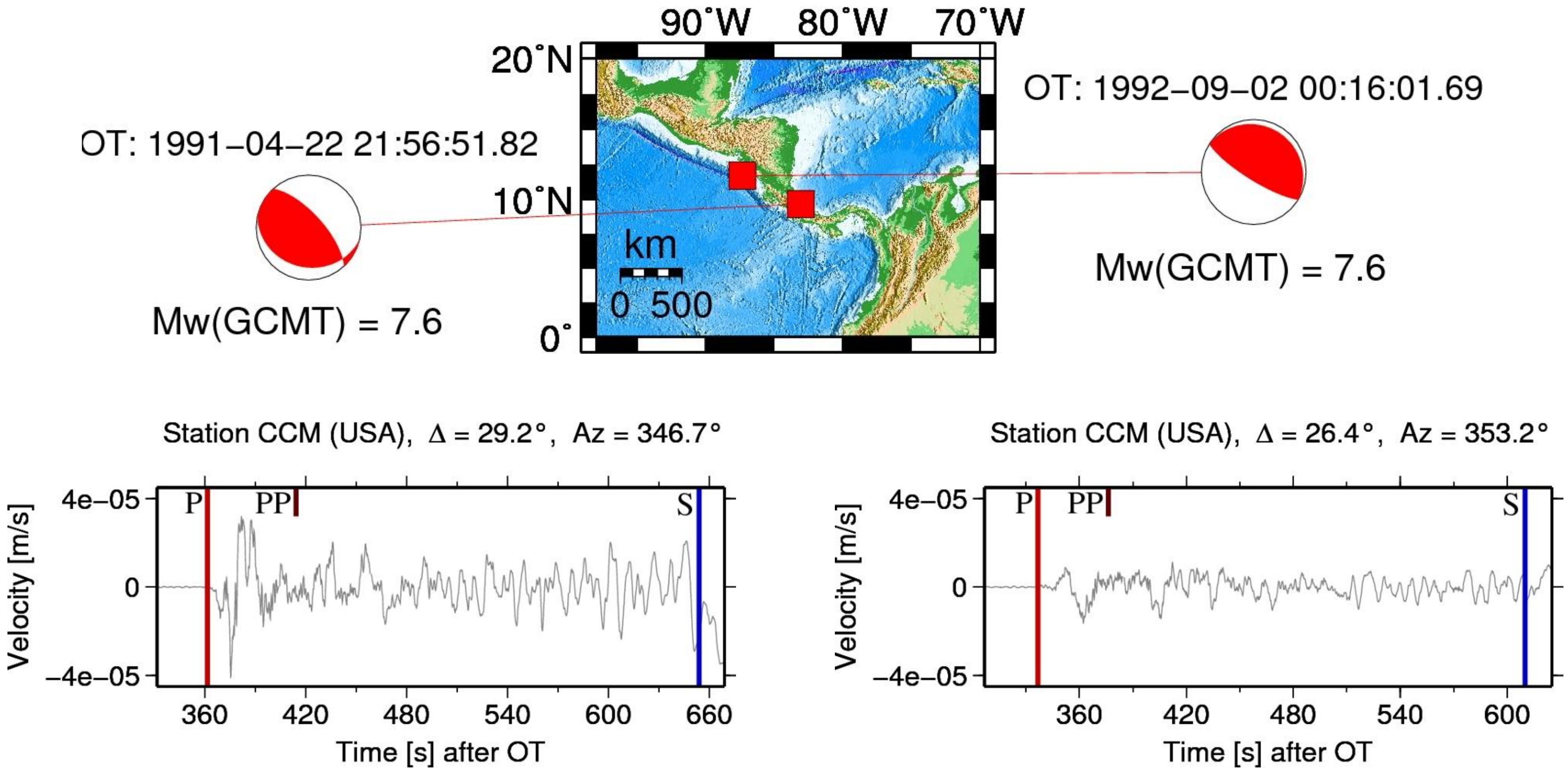

Mw(GCMT) = 7.6, Me(GFZ) = 7.19

Mw(GCMT) = 7.6, Me(GFZ) = 6.75

The locations differ by about 500 km and the moment magnitudes Mw are nearly identical, therefore the differences in the high frequency content observed in the seismograms can be attributed to different source characteristics.

Di Giacomo and Bindi (2009)

Hazard Inputs

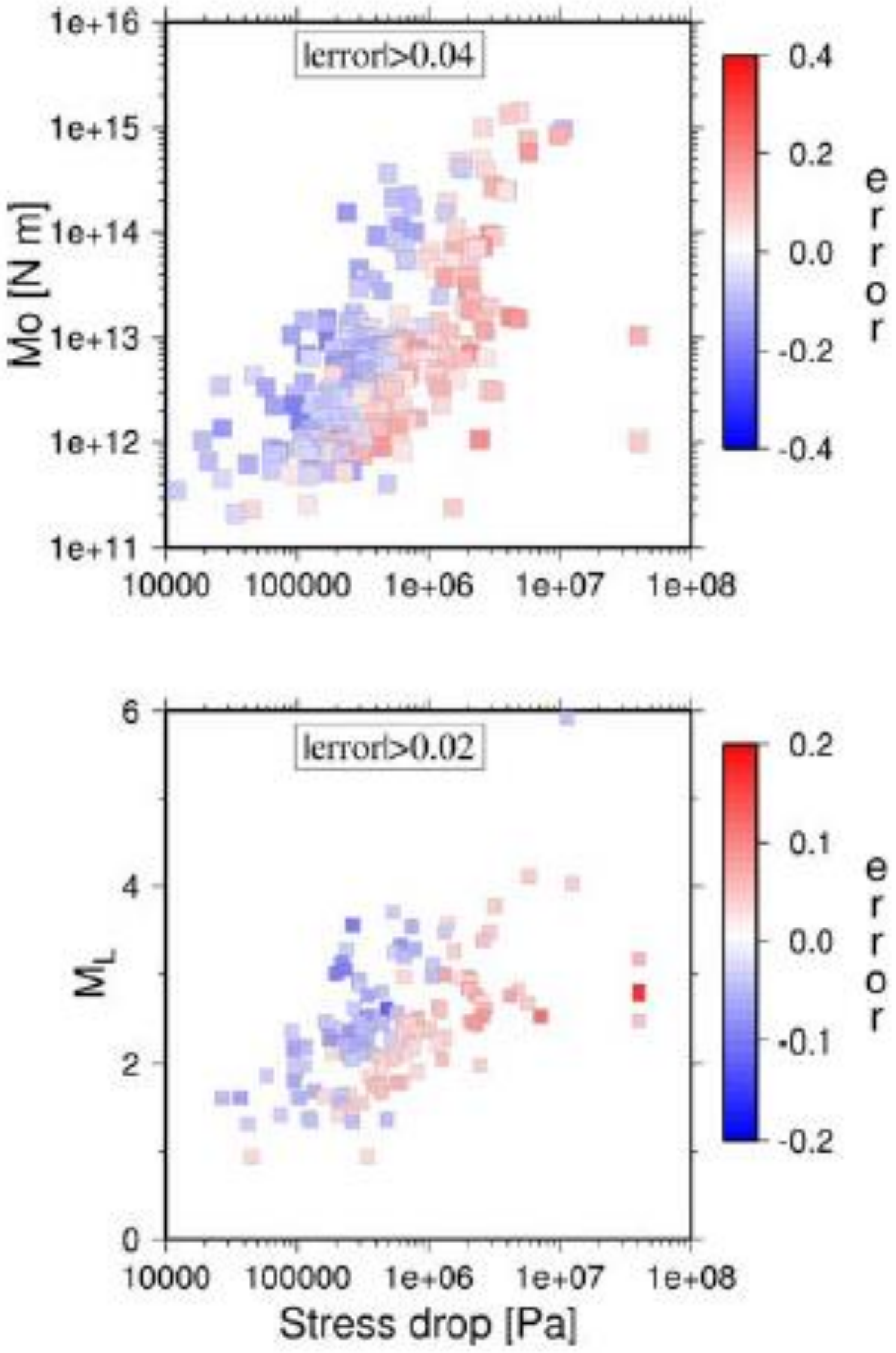

Figure 3. Inter-event errors for the maximum horizontal PGA model, considering epicentral distance. The amount of error is given by the color of the symbol. (top) Mw is considered in the regression. The errors having absolute values >0.04 are shown as a function of the stress drop $\Delta\sigma$ and the seismic moment Mo of each earthquake. (bottom) M_L is considered in the regression. The errors having absolute values >0.02 are shown as a function of $\Delta\sigma$ and M_L. The source parameters are taken from *Parolai et al.* [2007].

Hazard Inputs

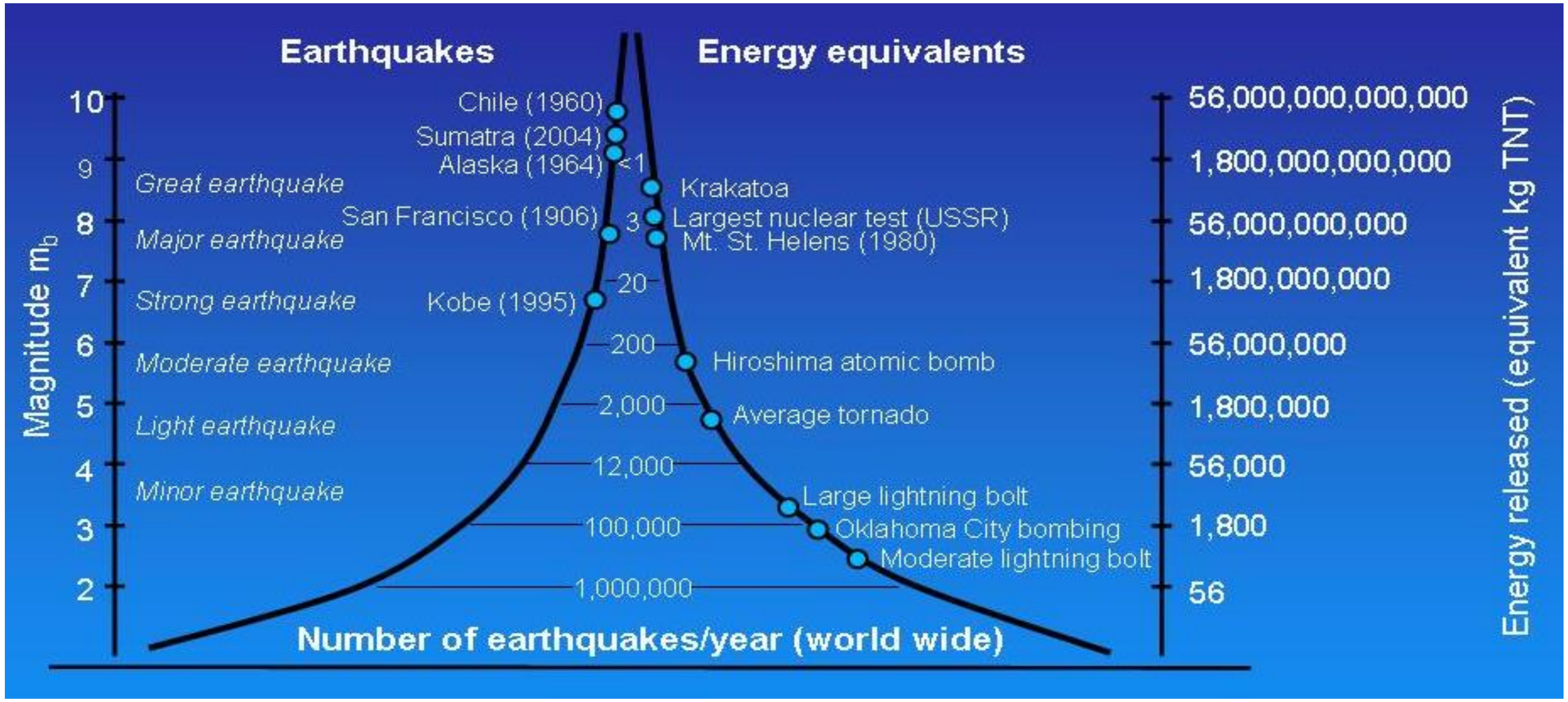

M			
to 2.9	Minor	Generally not felt but recorded	1000/day
3 to 3.9	Minor	Often felt, but rarely cause damage.	49000/year
4 to 4.9	Light	Noticeable shaking, damage unlikely.	6200/year
5 to 5.9	Moderate	Can cause damage to poor quality buildings	800/year
6 to 6.9	Strong	Destructive in areas up to *ca.*160 km.	120/year
7 to 7.9	Major	Serious damage over larger areas.	18/year
8 to 8.9	Great	Serious damage over areas of 100's km.	1/year
9 to 9.9	Great	Serious damage over areas of 1000' s km.	1/20 years

Hazard Inputs

Estimation of rupture rates

Seismicity based approaches

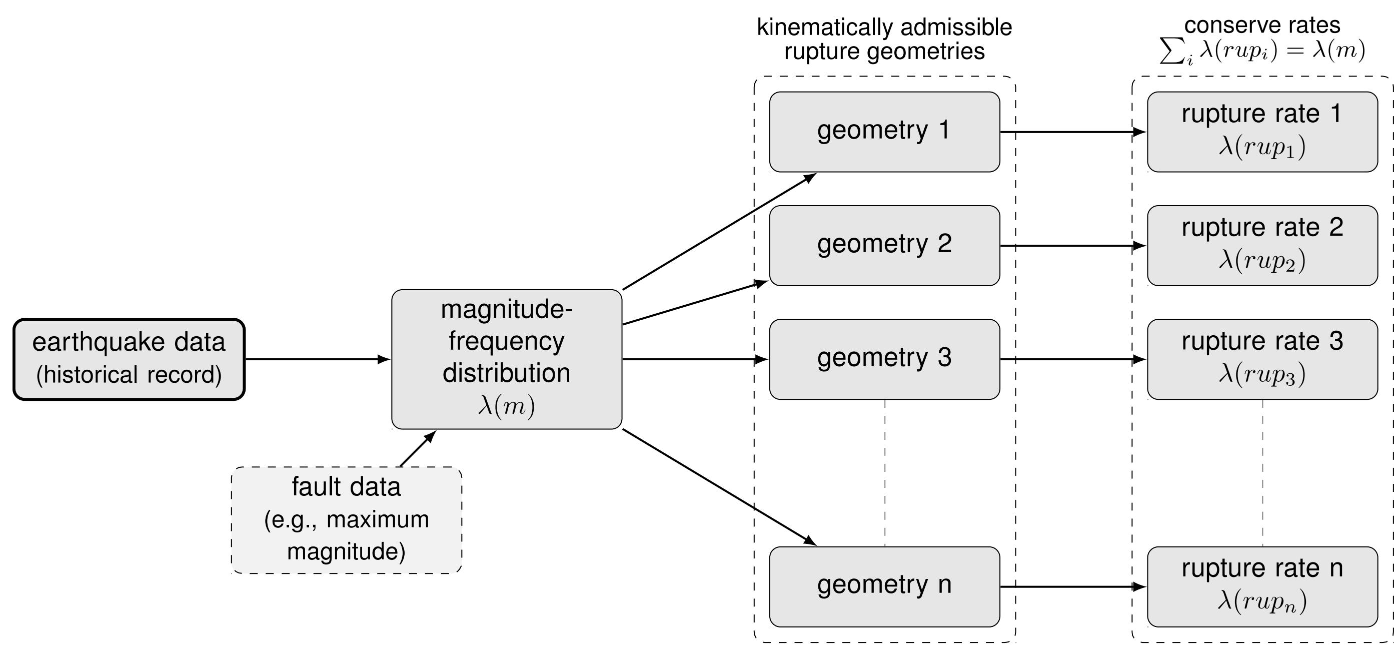

The rate of occurrence of the scenario is obtained by **partitioning the total rate of occurrence of the given magnitude over all plausible rupture geometries** that can exist for the respective source.

Geological approaches

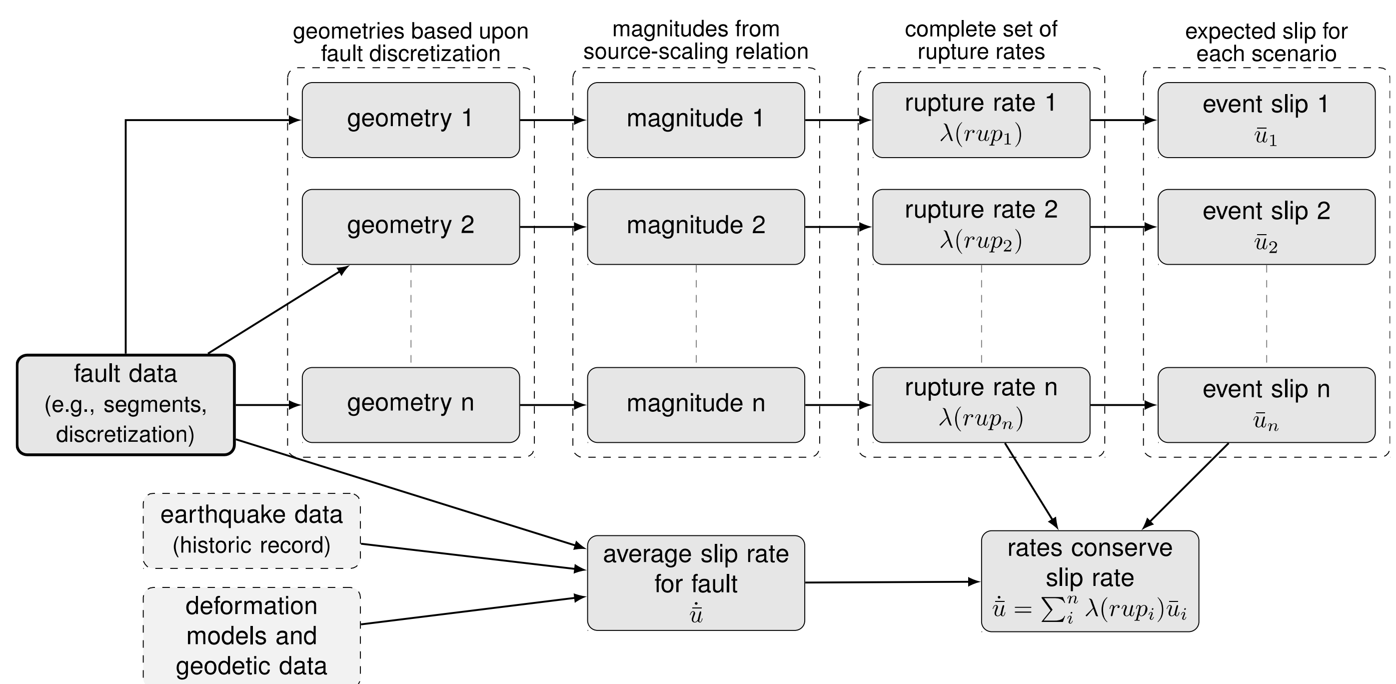

For each geometric rupture, a magnitude can be obtained from a source-scaling relation or from the definition of the seismic moment (if an associated estimate of the average slip for the rupture is available). Each scenario's rate of occurrence is then constrained by the overall slip rate for the fault.

Baker, Bradley and Stafford (2021), "Seismic Hazard and Risk Analysis." These images are provided for instructional and research use, with attribution. Not for commercial use.

Hazard Inputs

Gutenberg-Richter distribution

The number of earthquakes of a given size decreases by about an order of magnitude per magnitude unit increase.

N is the total number of events with magnitude M greater or equal to m

$$\log_{10} N(M \geq m) = a - bm.$$

the total number of earthquakes per year having $M \geq 0$ is $N(M \geq 0) = 10^a$

The parameter b is known as the Gutenberg–Richter b-value,

b ≅1 in the original study

Modern equivalent Gutenberg-Richter in a double bounded exponential distribution

$$f_M(m) = \frac{\beta \exp\left[-\beta\left(m - m_{\min}\right)\right]}{1 - \exp\left[-\beta\left(m_{\max} - m_{\min}\right)\right]}, \qquad m_{\min} \leq m \leq m_{\max}$$

$$\beta = \ln(10) \times b.$$

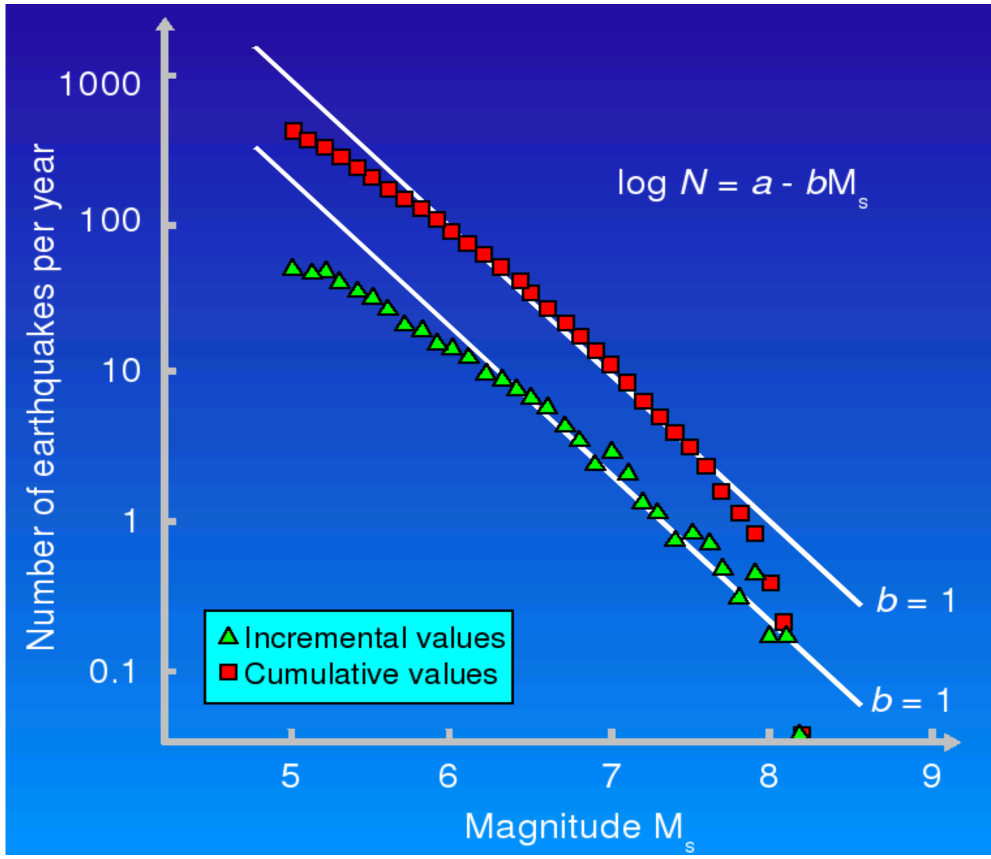

Stein & Wysession, 2003

UNIVERSITÀ DEGLI STUDI DI TRIESTE

Hazard Inputs

Gutenberg-Richter distribution

$$f_M(m) = \frac{\beta \exp\left[-\beta\left(m - m_{\min}\right)\right]}{1 - \exp\left[-\beta\left(m_{\max} - m_{\min}\right)\right]}, \qquad m_{\min} \le m \le m_{\max}$$

CDF

$$F_M(m) = \frac{1 - \exp\left[-\beta\left(m - m_{\min}\right)\right]}{1 - \exp\left[-\beta\left(m_{\max} - m_{\min}\right)\right]}, \qquad m_{\min} \le m \le m_{\max}.$$

Hazard Inputs

Gutenberg-Richter distribution

CDF

$$\begin{aligned} F_M(m) &= P(M \le m | M > m_{\min}) \\ &= \frac{\text{Rate of earthquakes with } m_{\min} < M \le m}{\text{Rate of earthquakes with } m_{\min} < M} \\ &= \frac{\lambda_{m_{\min}} - \lambda_m}{\lambda_{m_{\min}}} \\ &= \frac{10^{a-bm_{\min}} - 10^{a-bm}}{10^{a-bm_{\min}}} \\ &= 1 - 10^{-b(m-m_{\min})}, \qquad m > m_{\min} \end{aligned}$$

PDF

$$\begin{aligned} f_M(m) &= \frac{d}{dm} F_M(m) \\ &= \frac{d}{dm}\left[1 - 10^{-b(m-m_{\min})}\right] \\ &= b\ln(10)10^{-b(m-m_{\min})}, \qquad m > m_{\min} \end{aligned}$$

Hazard Inputs

Gutenberg-Richter distribution

CDF $$F_M(m) = \frac{1-10^{-b(m-m_{\min})}}{1-10^{-b(m_{\max}-m_{\min})}}, \qquad m_{\min} < m < m_{\max}$$

If an upper limit of M=m_{max} can be defined

PDF $$f_M(m) = \frac{b\ln(2.10)10^{-b(m-m_{\min})}}{1-10^{-b(m_{\max}-m_{\min})}}, \qquad m_{\min} < m < m_{\max}$$

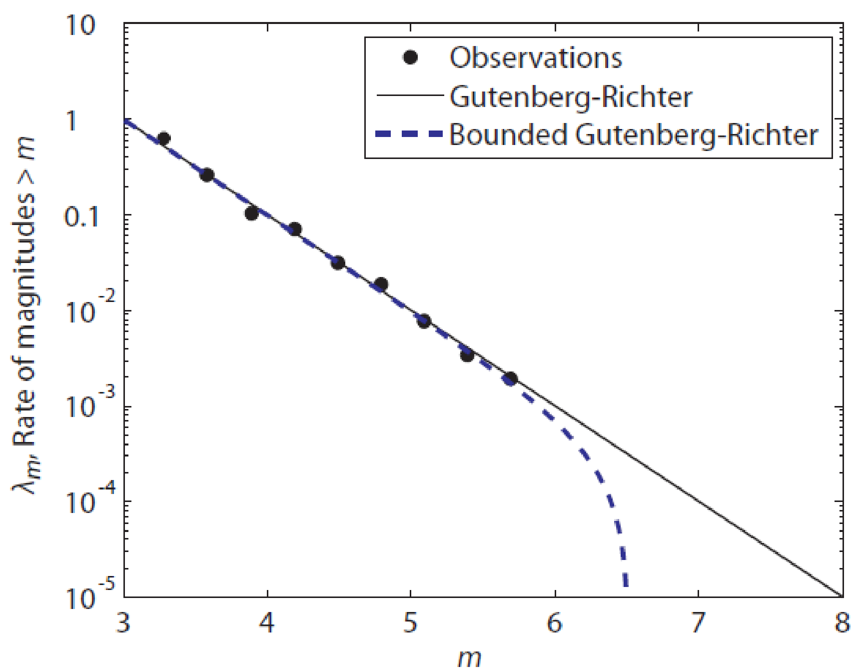

Since in PSHA we consider a discrete set of magnitude

$$P(M = m_j) = F_M(m_{j+1}) - F_M(m_j)$$

Baker, Bradley and Stafford (2021), "Seismic Hazard and Risk Analysis." These images are provided for instructional and research use, with attribution. Not for commercial use.

Hazard Inputs

Gutenberg-Richter distribution

Since in PSHA we consider a discrete set of magnitude

$$P(M = m_j) = F_M(m_{j+1}) - F_M(m_j)$$

$$\lambda_{y^*} = \sum_{i=1}^{N_S} \sum_{j=1}^{N_M} \sum_{k=1}^{N_R} \nu_i \int\int P[Y > y^* \mid m_j, r_k] P[M = m_j] P[R = r_k]$$

m_j	$F_M(m_j)$	$P(M = m_j)$
5.00	0.0000	0.4381
5.25	0.4381	0.2464
5.50	0.6845	0.1385
5.75	0.8230	0.0779
6.00	0.9009	0.0438
6.25	0.9447	0.0246
6.50	0.9693	0.0139
6.75	0.9832	0.0078
7.00	0.9910	0.0044
7.25	0.9954	0.0024
7.50	0.9978	0.0014
7.75	0.9992	0.0008
8.00	1.0000	0.0000

Continuous Probability Density function

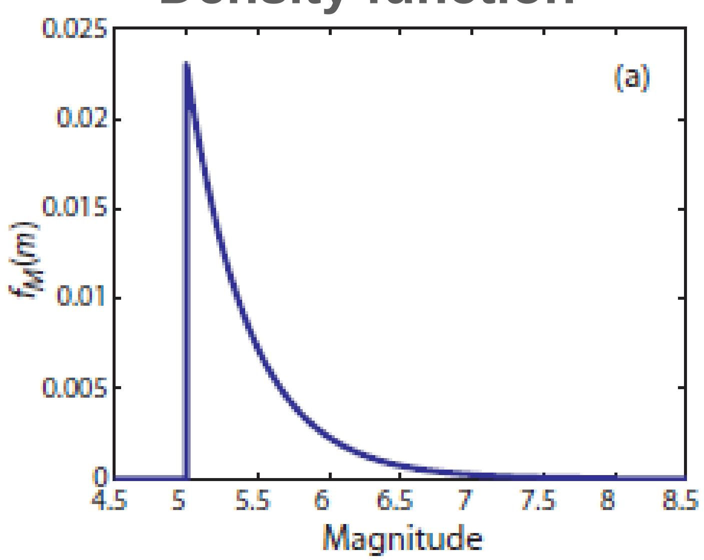

Discrete Probabilities

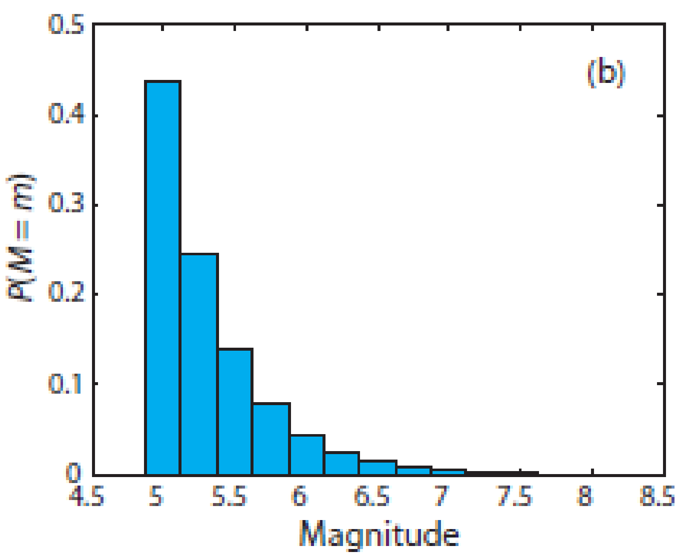

UNIVERSITÀ DEGLI STUDI DI TRIESTE

Empirical ground motion models

Also Attenuation relationships or Ground Motion Prediction Equation(GMPEs) in Literature

GMM can be empirical or physics-based

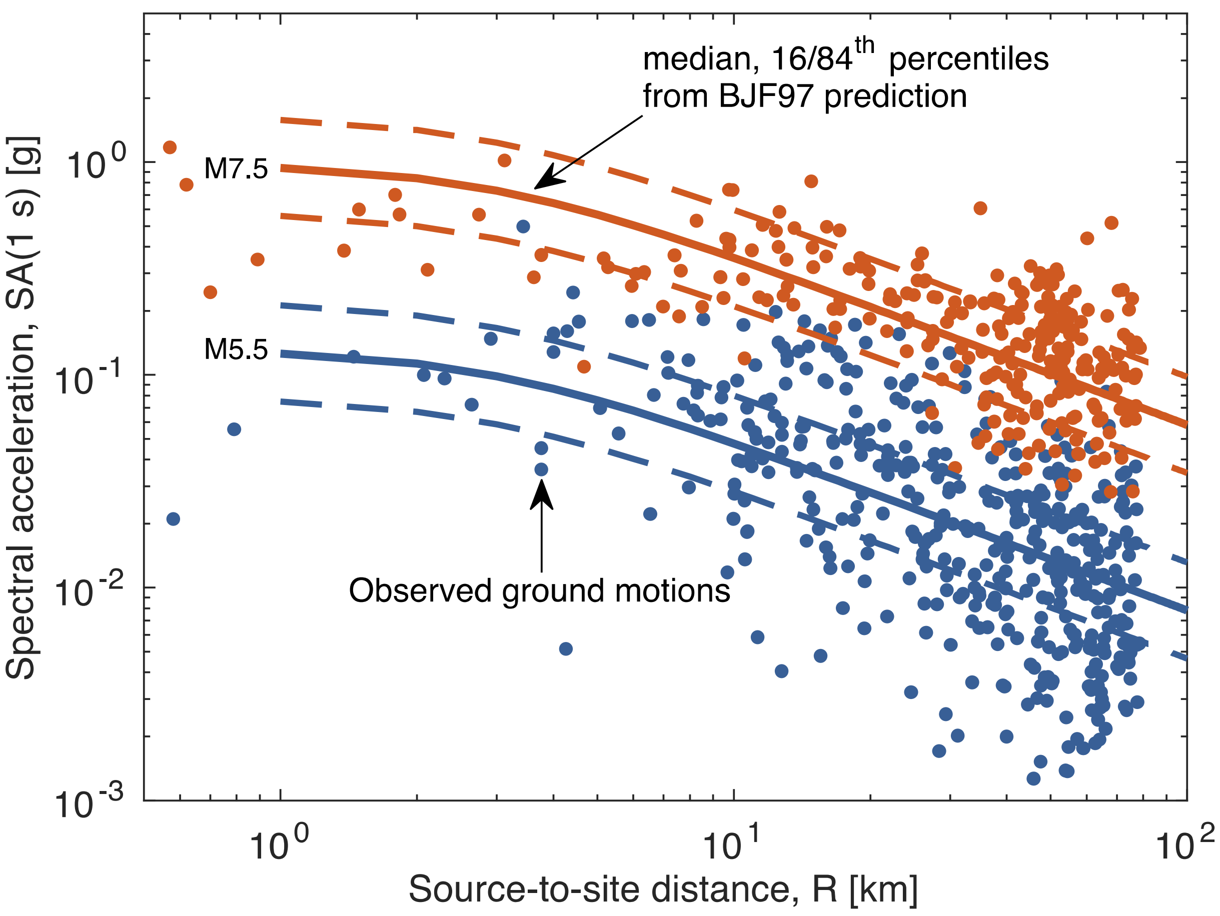

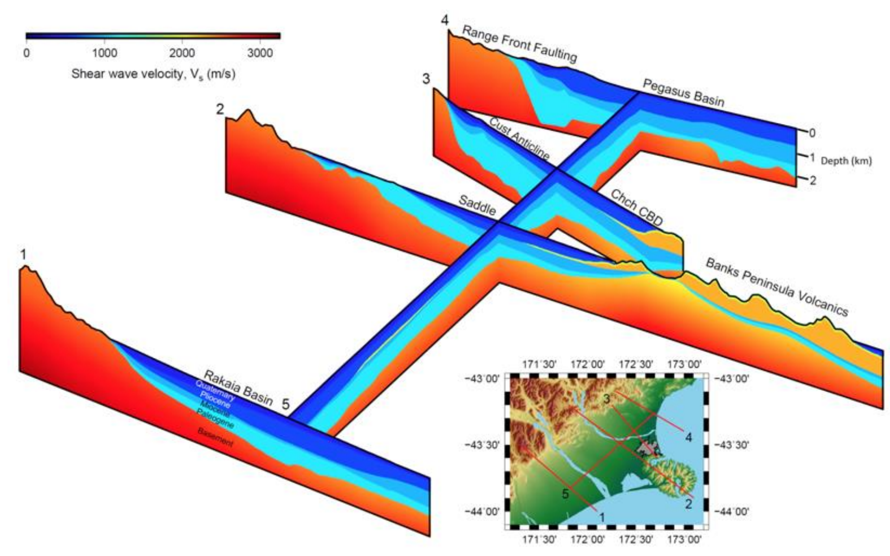

Baker, Bradley and Stafford (2021), "Seismic Hazard and Risk Analysis." These images are provided for instructional and research use, with attribution. Not for commercial use.

Empirical ground motion models

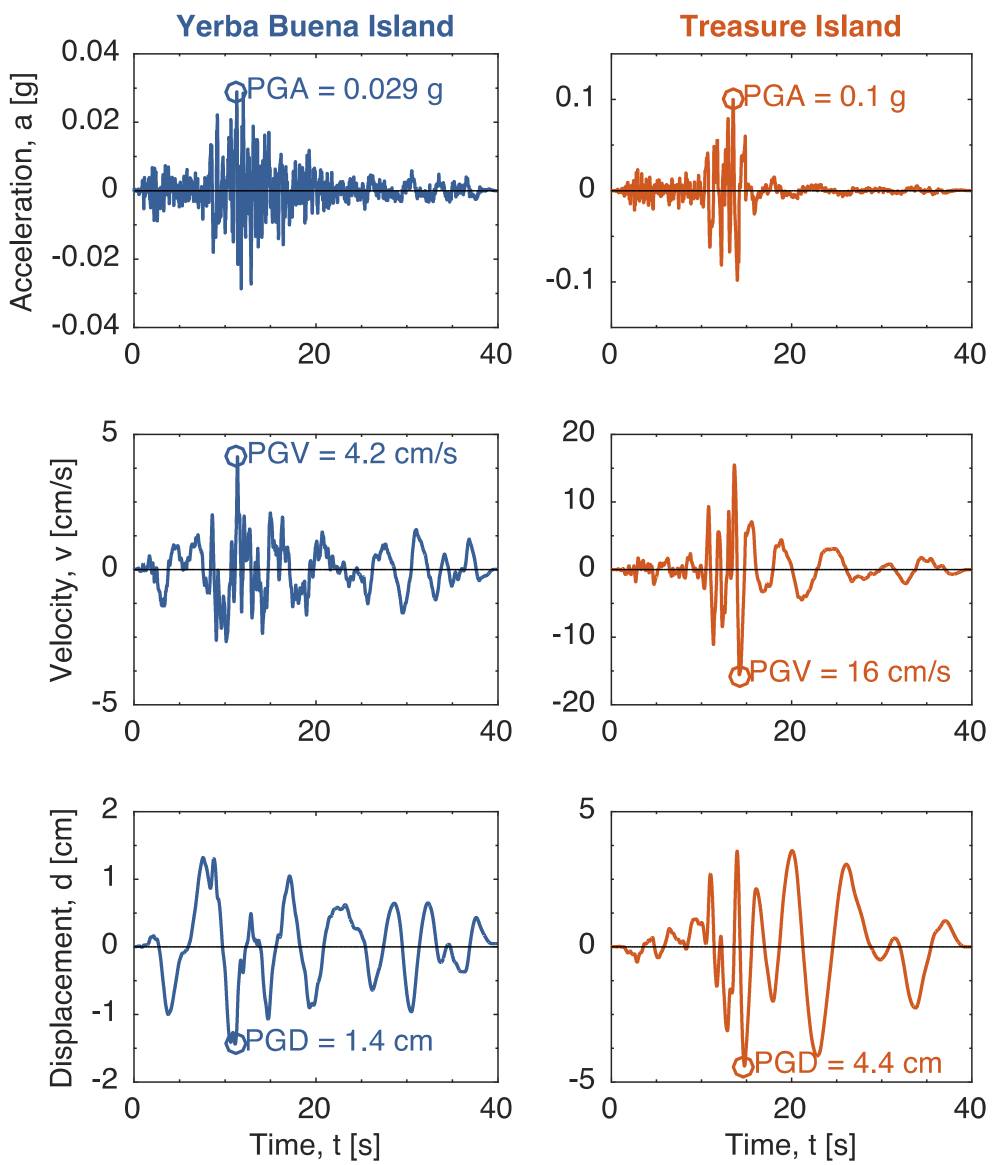

$$\ddot{x}(t) + 2\xi\omega_n\dot{x}(t) + \omega_n^2 x(t) = -a(t)$$

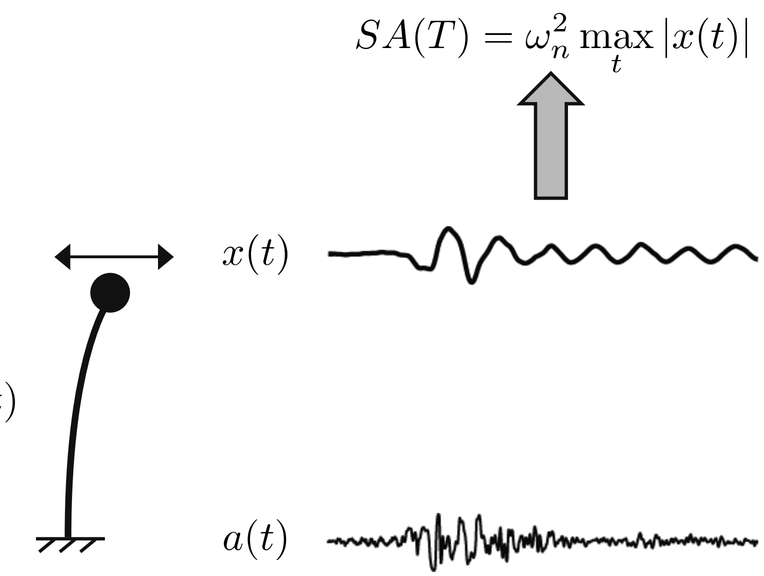

Oscillator with period T
and critical damping ratio ξ

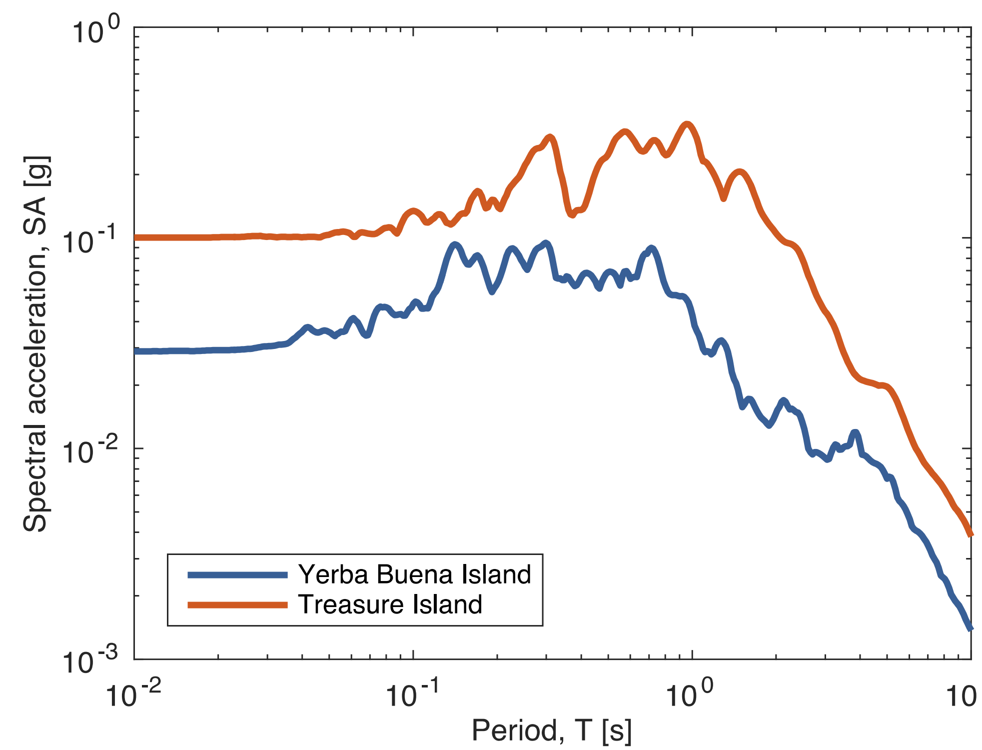

Empirical ground motion models

Bracket and Uniform Duration

$$D_B = \max(t_{|a(t)|>A_T}) - \min(t_{|a(t)|>A_T})$$

$$D_U = \int_t I[|a(t)| > A_T]dt$$

Significant Duration

$$\frac{\int_0^{t_X} [a(t)]^2 dt}{\int_0^{\infty} [a(t)]^2 dt} = \frac{X}{100}, \qquad D_{SX-Y} = t_Y - t_X.$$

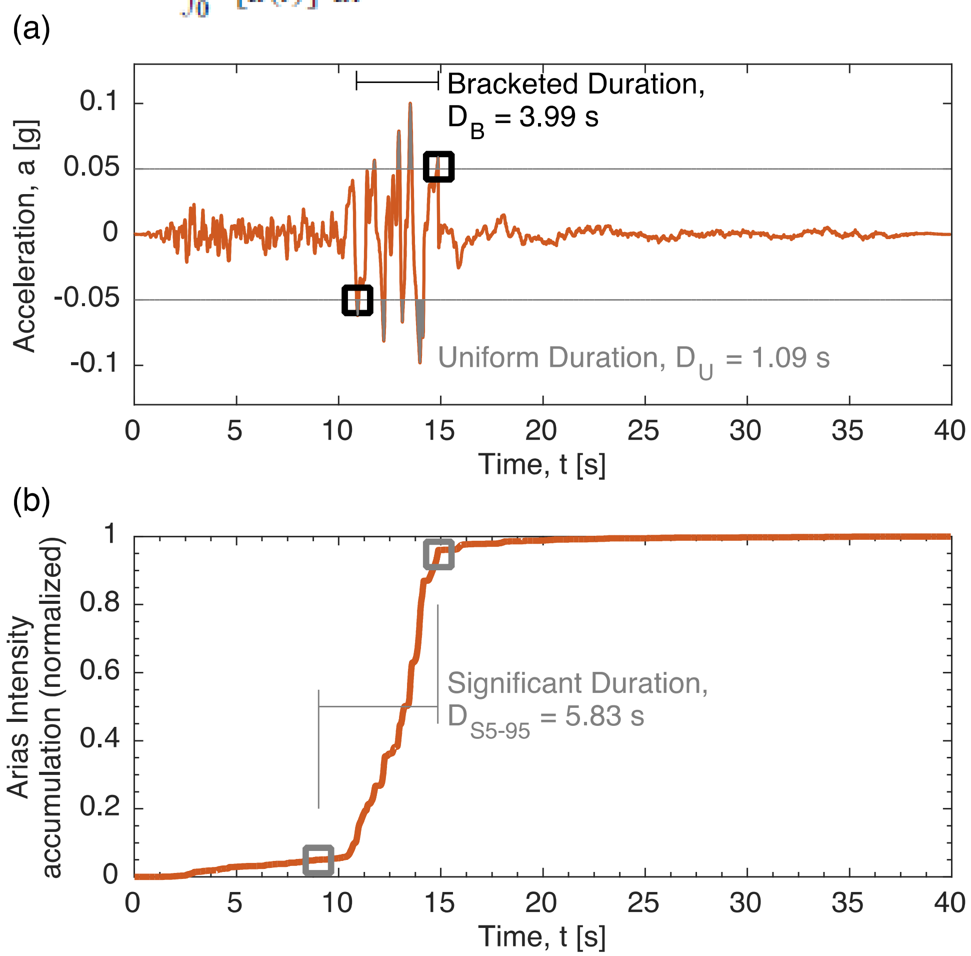

Fourier Spectrum

$$a(f_k) = \sqrt{\frac{\Delta t}{N_T}} \sum_{n=0}^{N_T-1} a(n\Delta t)e^{-i(2\pi f_k)n\Delta t}$$

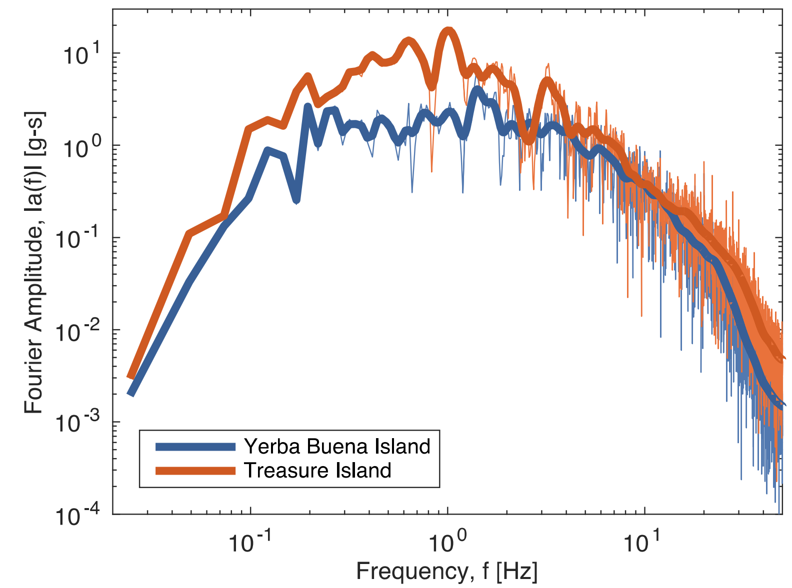

$$AI = \frac{\pi}{2g}\int_0^{t_{max}} a(t)^2 dt.$$

$$CAV = \int_0^{t_{max}} |a(t)| dt.$$

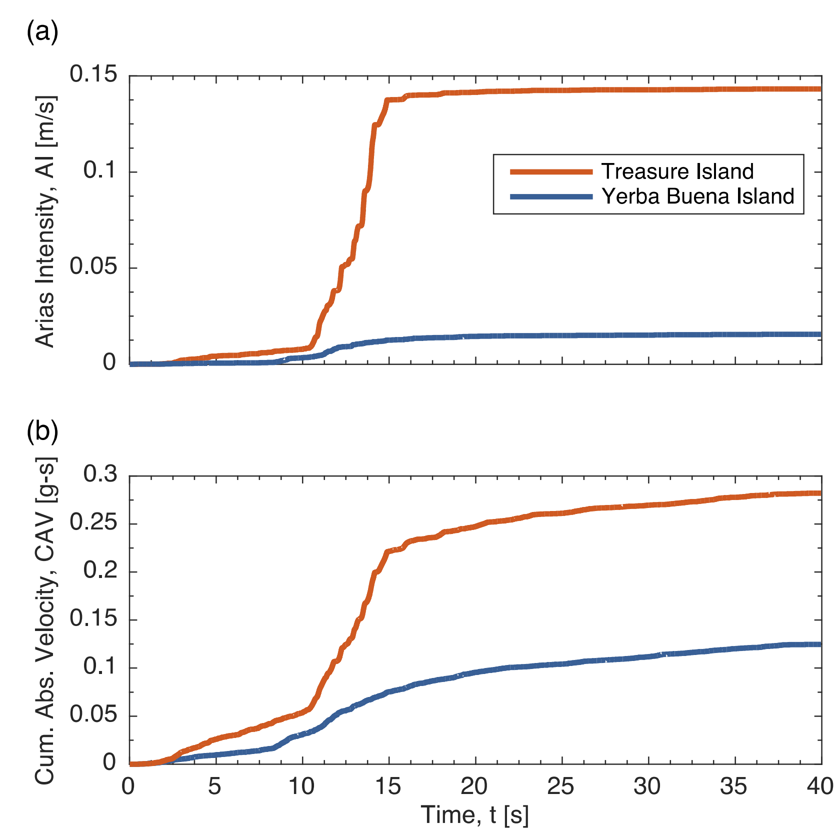

UNIVERSITÀ DEGLI STUDI DI TRIESTE

Empirical ground motion models (GMM)

Magnitude – Distance distribution

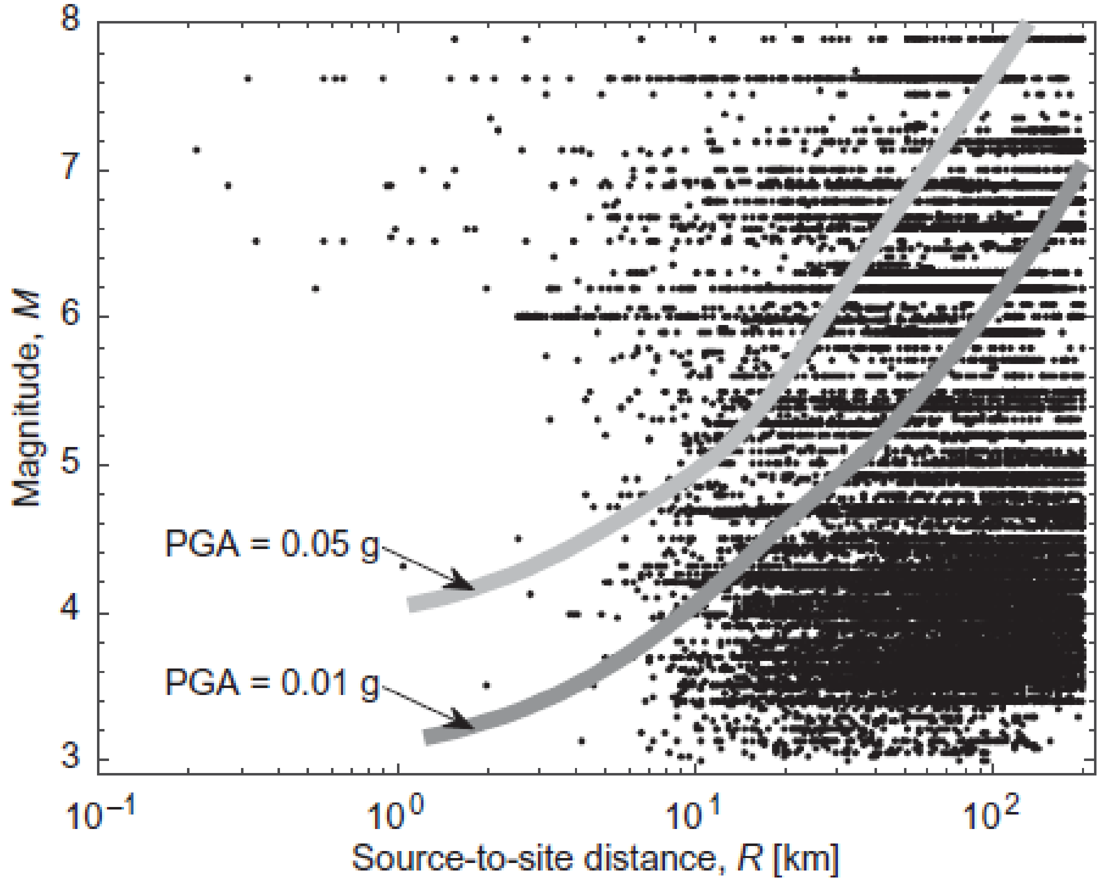

Maximum usable response spectral period

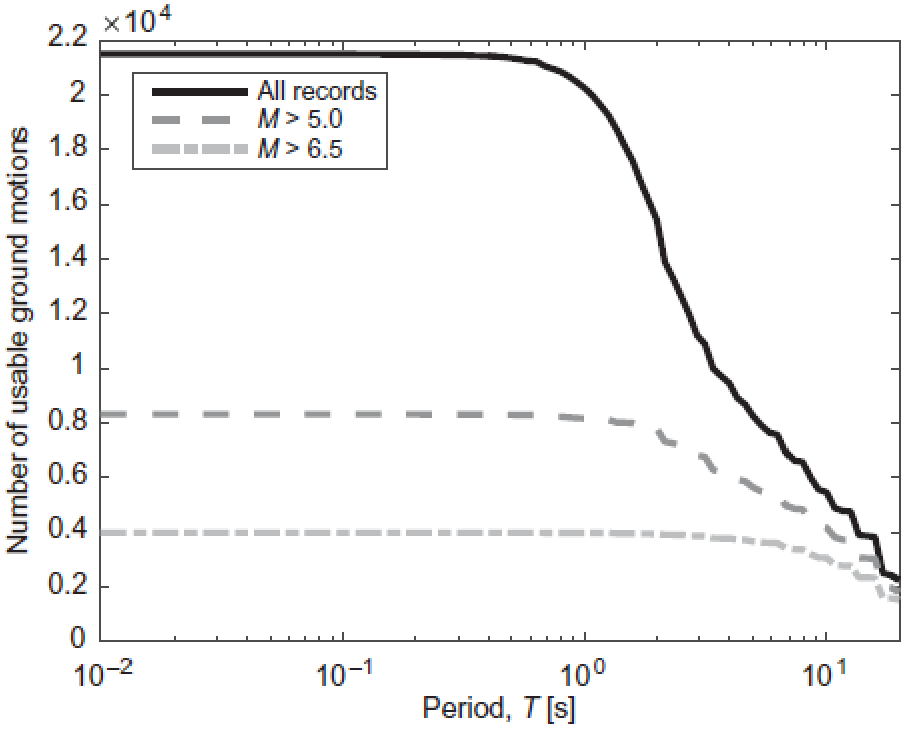

Baker, Bradley and Stafford (2021), "Seismic Hazard and Risk Analysis." These images are provided for instructional and research use, with attribution. Not for commercial use.

Empirical ground motion models (GMM)

Effect of site conditions

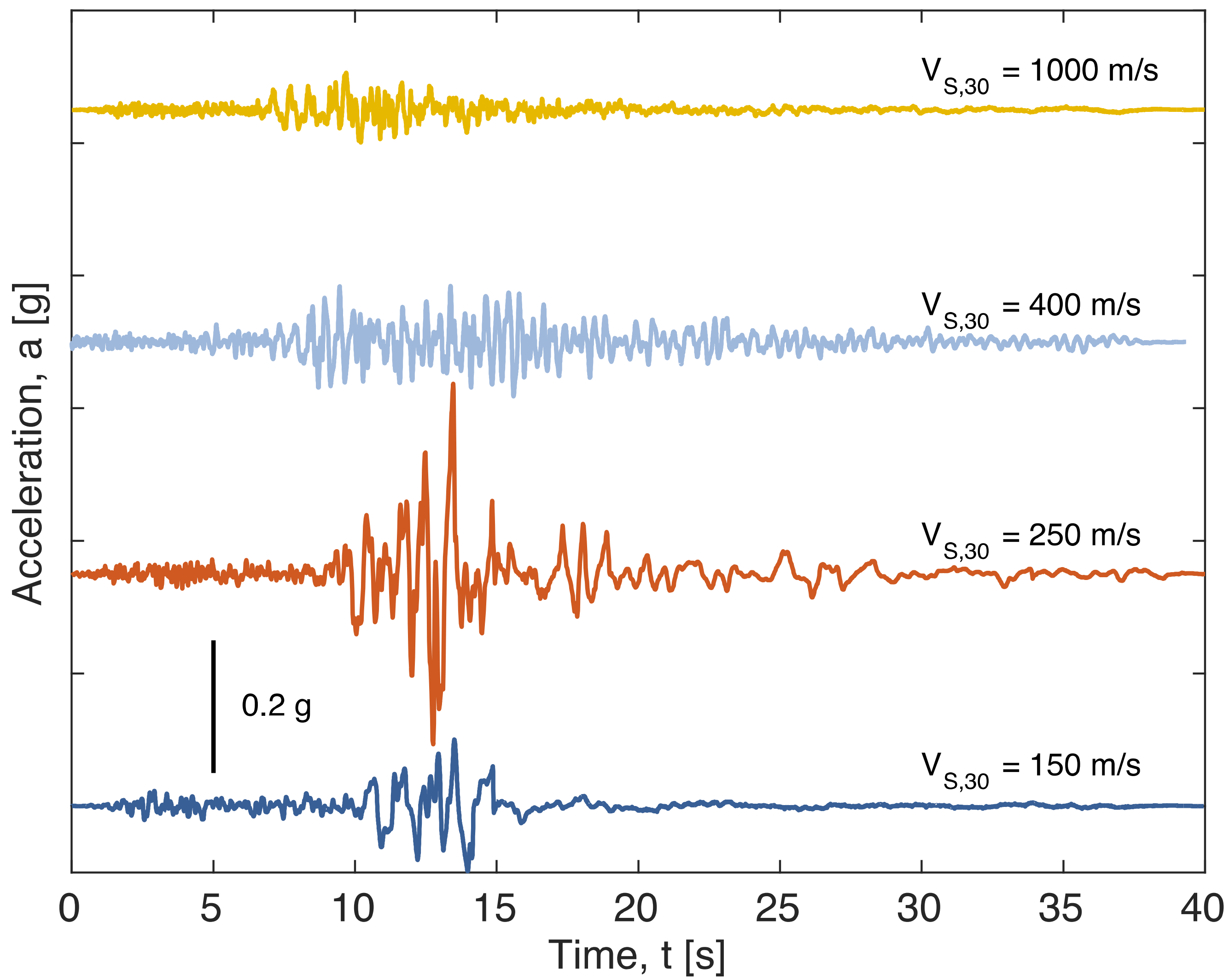

Effect of site conditions on recorded ground motions from the 1989 Loma Prieta (*M*6.9) earthquake at four nearly adjacent locations. Other than the variation in 30-m time-averaged shear wave velocity, $V_{S,30}$, the recordings all have source-to-site distances of approximately $R = 75$ km.

Baker, Bradley and Stafford (2021), "Seismic Hazard and Risk Analysis." These images are provided for instructional and research use, with attribution. Not for commercial use.

Disaggregation

Which earthquake rupture is most likely to cause IM>x?

Example of two ruptures influencing the site

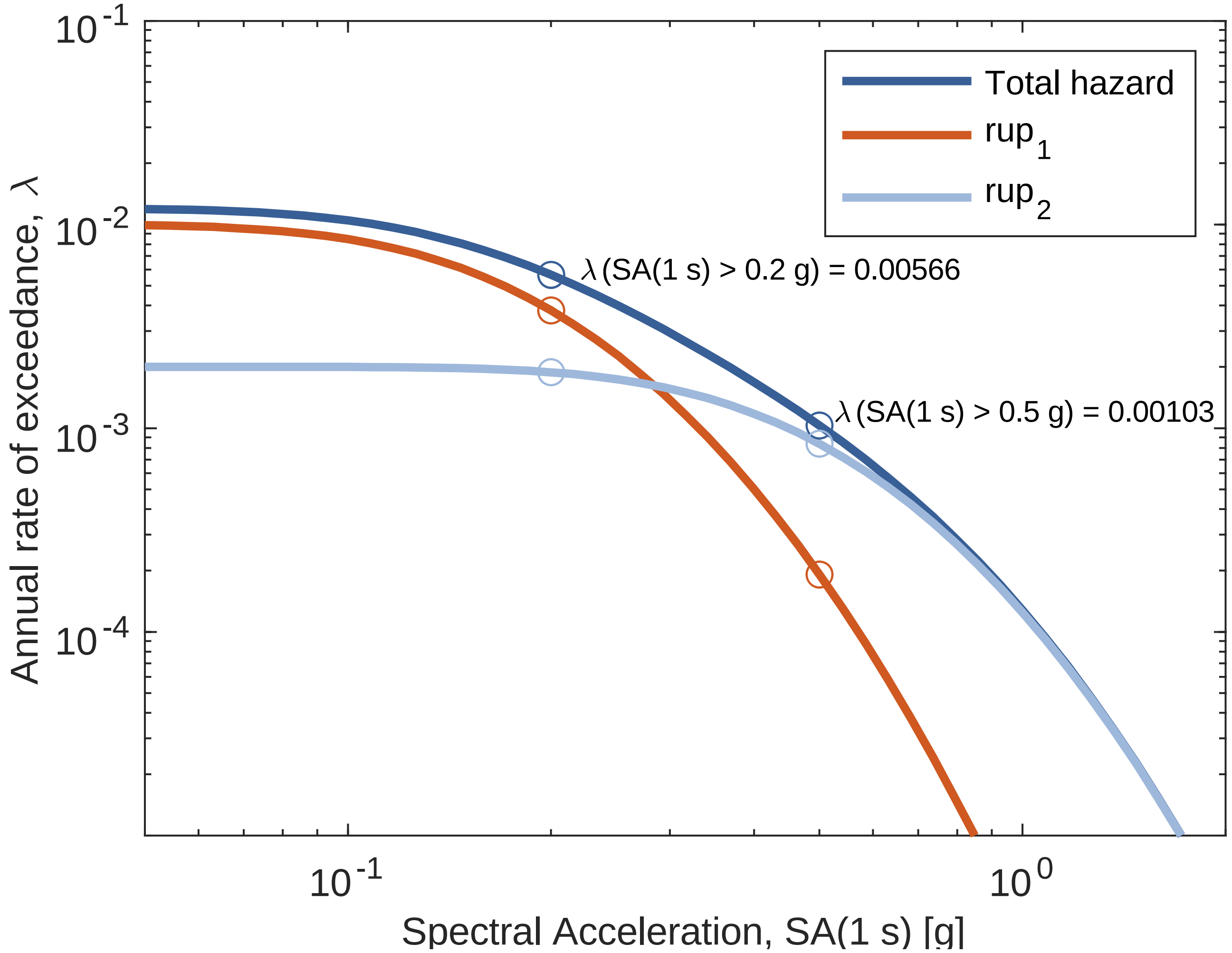

$$\lambda(SA(1\ \text{s}) > 0.2\ \text{g}, rup_1) = 0.00378$$
$$\lambda(SA(1\ \text{s}) > 0.2\ \text{g}, rup_2) = 0.00188$$

Taking the ratio of the exceedance rate from a given rupture to the overall exceedance rate, we can find the probablity that an exceedance is caused by that rupture:

$$P(rup_1 \mid SA(1\ \text{s}) > 0.2\ \text{g}) = 0.668 \quad (7.4)$$
$$P(rup_2 \mid SA(1\ \text{s}) > 0.2\ \text{g}) = 0.332. \quad (7.5)$$

Disaggregation

Which earthquake rupture is most likely to cause IM>x?

Example of two ruptures influencing the site

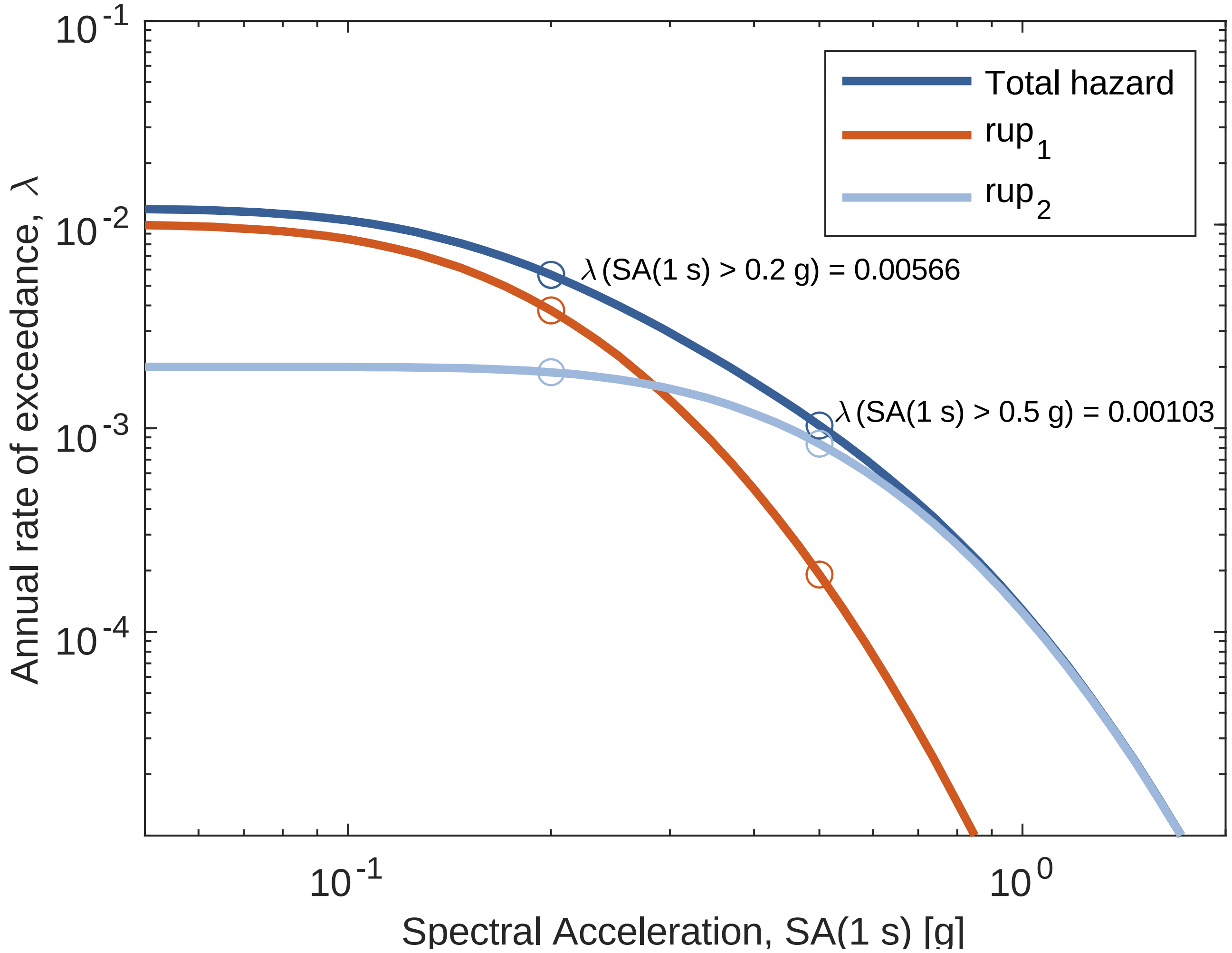

If we consider SA(1s)>0.5 g

$$P(rup_1 \mid SA(1\text{ s}) > 0.5\text{ g}) = 0.186$$

$$P(rup_2 \mid SA(1\text{ s}) > 0.5\text{ g}) = 0.814.$$

Baker, Bradley and Stafford (2021), "Seismic Hazard and Risk Analysis." These images are provided for instructional and research use, with attribution. Not for commercial use.

UNIVERSITÀ DEGLI STUDI DI TRIESTE

Disaggregation

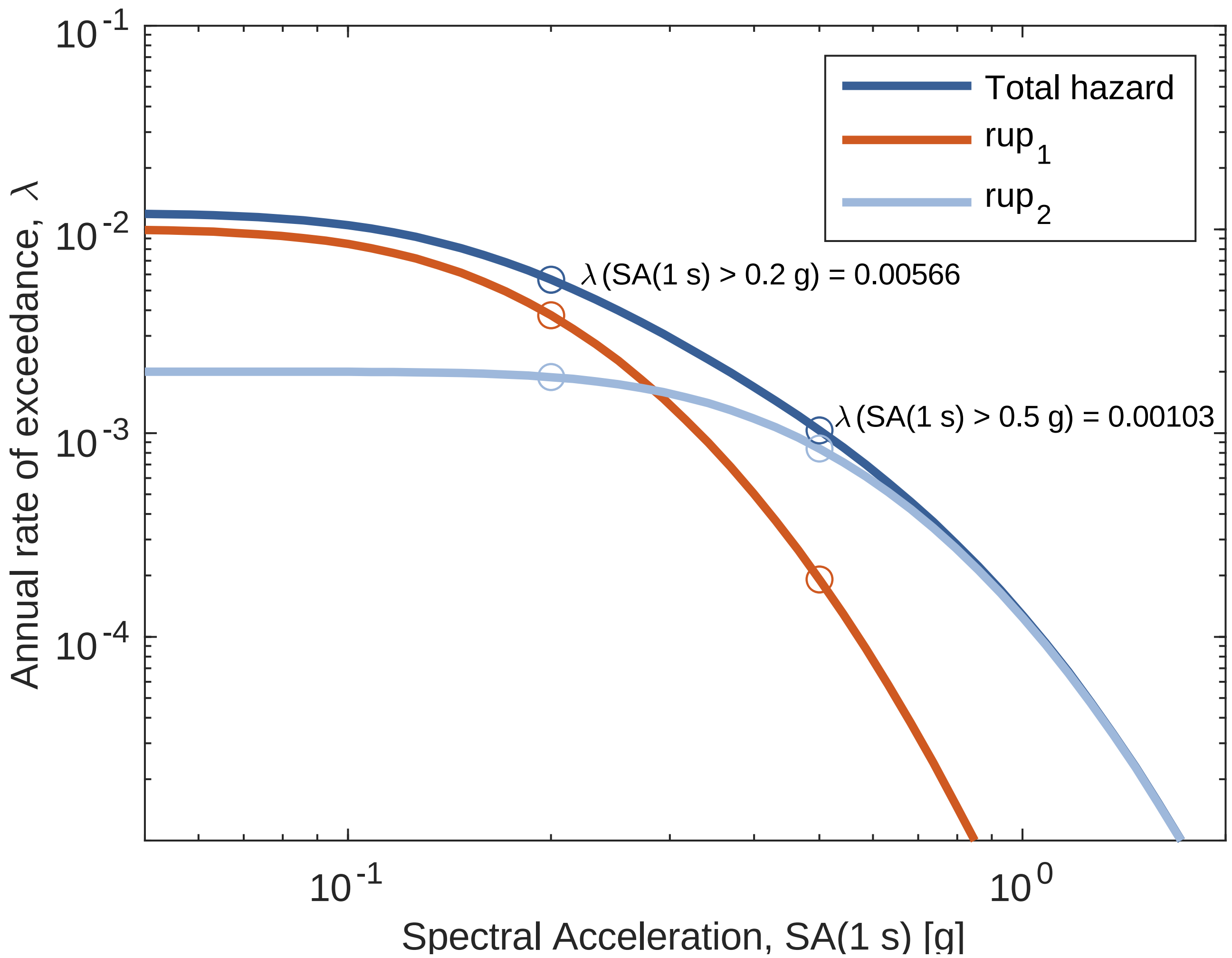

For the relatively lower SA(1s) value of 0.2 g, the more active source 1 has a high probability of being the causal rupture

At larger SA(1s) (0.5 g) the less acitive source 2 has the greater contribution to the exceedance of the SA(1s)

Baker, Bradley and Stafford (2021), "Seismic Hazard and Risk Analysis." These images are provided for instructional and research use, with attribution. Not for commercial use.

Disaggregation calculation

NOTE: This is site! specific

Annual rate of observing ground motion at a given site with Im>im, caused by the rupture rup$_i$

Rate of ground with Im>im

Probability that the ground motion comes from rupture rup$_i$

$$\lambda(IM > im, rup_i) = \lambda(IM > im) \times P(rup_i \mid IM > im).$$

OR

$$P(rup_i \mid IM > im) = \frac{\lambda(IM > im, rup_i)}{\lambda(IM > im)}.$$

$$P(rup_i \mid IM > im) = \frac{P(IM > im \mid rup_i)\lambda(rup_i)}{\lambda(IM > im)}.$$

The equations show that the probability of rup_i causing $IM > im$ is equal to the rate of rup_i earthquakes that cause $IM > x$, divided by the rate of *all* earthquakes that cause $IM > x$. The left-hand side of these equations always produces a valid probability distribution; that is, the sum over i of $P(rup_i | IM > im)$ always equals 1.

Disaggregation

Table 6.3. Intermediate calculations to compute $\lambda(SA(1\,s) > 0.2\,g)$ for the example of Section 6.3.3

i	m_i	$\lambda(rup_i)$	$P(SA(1\,s) > 0.2\,g \mid rup_i)$	$P(SA(1\,s) > 0.2\,g \mid rup_i)\lambda(rup_i)$
1	5.1	0.0185	0.001	1.59×10^{-5}
2	5.3	0.0117	0.003	3.85×10^{-5}
3	5.5	0.0074	0.011	7.84×10^{-5}
4	5.7	0.0046	0.029	1.35×10^{-4}
5	5.9	0.0029	0.068	1.99×10^{-4}
6	6.1	0.0018	0.137	2.54×10^{-4}
7	6.3	0.0012	0.242	2.82×10^{-4}
8	6.5	7.35×10^{-4}	0.378	2.78×10^{-4}
9	6.7	4.64×10^{-4}	0.529	2.45×10^{-4}
10	6.9	2.93×10^{-4}	0.674	1.97×10^{-4}
11	7.1	1.85×10^{-4}	0.795	1.47×10^{-4}
12	7.3	1.17×10^{-4}	0.884	1.03×10^{-4}
13	7.5	7.35×10^{-5}	0.940	6.91×10^{-5}
14	7.7	4.64×10^{-5}	0.972	4.51×10^{-5}
15	7.9	2.93×10^{-5}	0.988	2.90×10^{-5}
				Sum = 0.00212

Let's consider that the disaggregation over magnitude correspond to the disaggregragation on rupture rup$_i$

$$\lambda(SA(1\,s) > 0.2\,g, m_1) = \lambda(SA(1\,s) > 0.2\,g, rup_1).$$

The rate of M=5.1 causing SA(1s) >0.2 g $1.59X10^{-5}$

The rate of all ruptures causing SA(1s) >0.2 g 0.00212

Table 6.4. Intermediate calculations to compute $\lambda(SA(1\,s) > 0.5\,g)$ for the example of Section 6.3.3

i	m_i	$\lambda(rup_i)$	$P(SA(1\,s) > 0.5\,g \mid rup_i)$	$P(SA(1\,s) > 0.5\,g \mid rup_i)\lambda(rup_i)$
1	5.1	0.0185	0.000	9.04×10^{-9}
2	5.3	0.0117	0.000	4.39×10^{-8}
3	5.5	0.0074	0.000	1.77×10^{-7}
4	5.7	0.0046	0.000	5.93×10^{-7}
5	5.9	0.0029	0.001	1.67×10^{-6}
6	6.1	0.0018	0.002	3.98×10^{-6}
7	6.3	0.0012	0.007	8.07×10^{-6}
8	6.5	7.35×10^{-4}	0.019	1.40×10^{-5}
9	6.7	4.64×10^{-4}	0.046	2.12×10^{-5}
10	6.9	2.93×10^{-4}	0.095	2.78×10^{-5}
11	7.1	1.85×10^{-4}	0.175	3.23×10^{-5}
12	7.3	1.17×10^{-4}	0.285	3.32×10^{-5}
13	7.5	7.35×10^{-5}	0.419	3.08×10^{-5}
14	7.7	4.64×10^{-5}	0.562	2.61×10^{-5}
15	7.9	2.93×10^{-5}	0.695	2.04×10^{-5}
				Sum = 0.00022

The probability that ground motion SA(1s) >0.2 g is caused by a M=5.1 event is

$$P(5 \le M < 5.2 \mid SA(1\,s) > 0.2\,g) = \frac{\lambda(SA(1\,s) > 0.2\,g, m_1)}{\lambda(SA(1\,s) > 0.2)} = \frac{1.59 \times 10^{-5}}{0.00212} = 0.008.$$

Disaggregation

Repeating this for other magnitudes

Table 7.1. Results for the Section 6.3.3 disaggregation example

m_i	$P(m_i \mid SA(1\text{ s}) > 0.2\text{ g})$	$P(m_i \mid SA(1\text{ s}) > 0.5\text{ g})$
5.1	0.008	0.000
5.3	0.018	0.000
5.5	0.037	0.001
5.7	0.064	0.003
5.9	0.094	0.008
6.1	0.120	0.018
6.3	0.133	0.037
6.5	0.131	0.064
6.7	0.116	0.096
6.9	0.093	0.126
7.1	0.069	0.146
7.3	0.049	0.151
7.5	0.033	0.140
7.7	0.021	0.118
7.9	0.014	0.092
	Sum = 1.000	Sum = 1.000

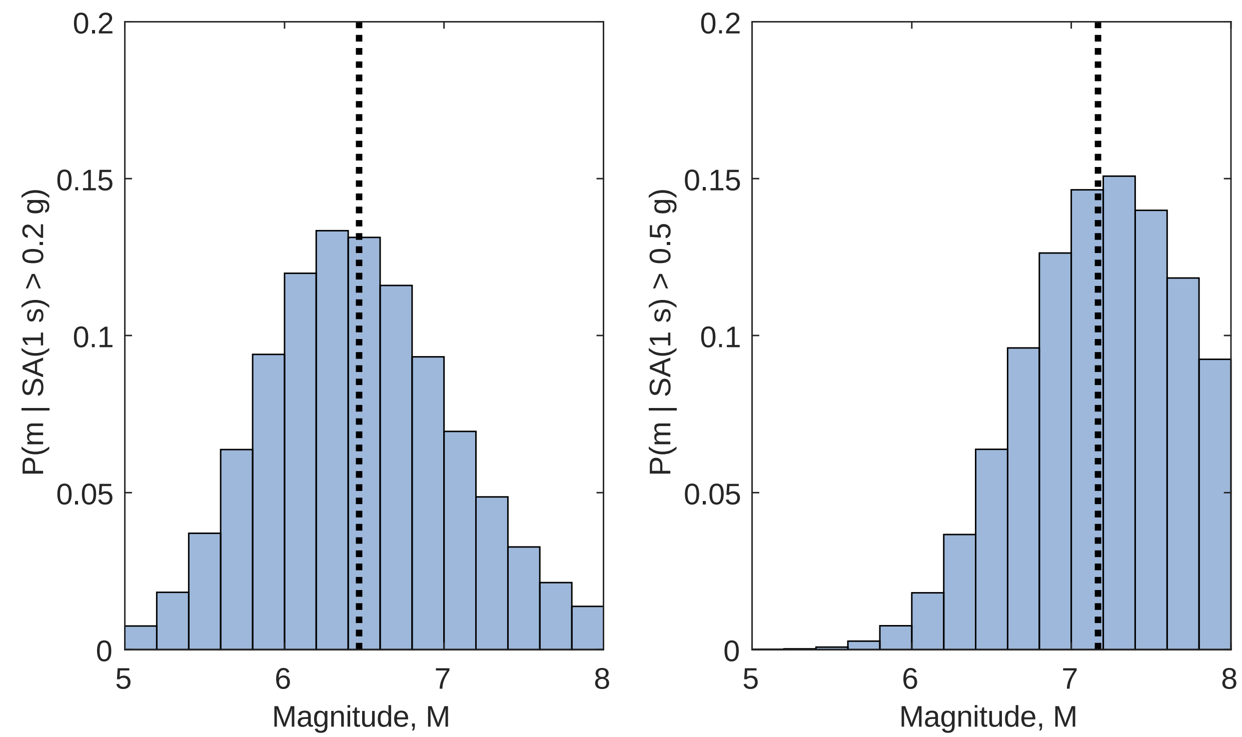

Smaller magnitude (i.e., M 6) earthquakes are likely to cause exceedances of SA(1 s) > 0.2 g, but are quite unlikely to cause exceedances of SA(1 s) > 0.5 g. This is because M 6 ruptures are relatively likely compared with larger-magnitude ruptures, and also likely to cause smaller-intensity ground motions. However, these M 6 ruptures are very unlikely to cause SA(1 s) > 0.5 g ground motions, so they contribute little at that higher intensity

Disaggregation

The disaggregation is also carried out to find probabilities of combination of Magnitude, Distance etc..

$$P(M = m | IM > x) = \frac{\lambda(IM > x, M = m)}{\lambda(IM > x)}$$

$$\lambda(IM > x, M = m) = \sum_{i=1}^{n_{sources}} \lambda(M_i > m_{\min}) \sum_{k=1}^{n_{R_i}} P(IM > x | m, r_k) P(M_i = m) P(R_i = r_k)$$

To find the conditional distribution of distance the equations above is modified to have summation over magnitude

Disaggregation

The conditional JOINT distribution of Magnitude and Distance is given by:

$$P(M=m,R=r|IM>x)=\frac{\lambda(IM>x,M=m,R=r)}{\lambda(IM>x)}$$

WITH

$$\lambda(IM>x,M=m,R=r)=\sum_{i=1}^{n_{sources}}\lambda(M_i>m_{\min})P(IM>x|m_j,r_k)P(M_i=m)P(R_i=r)$$

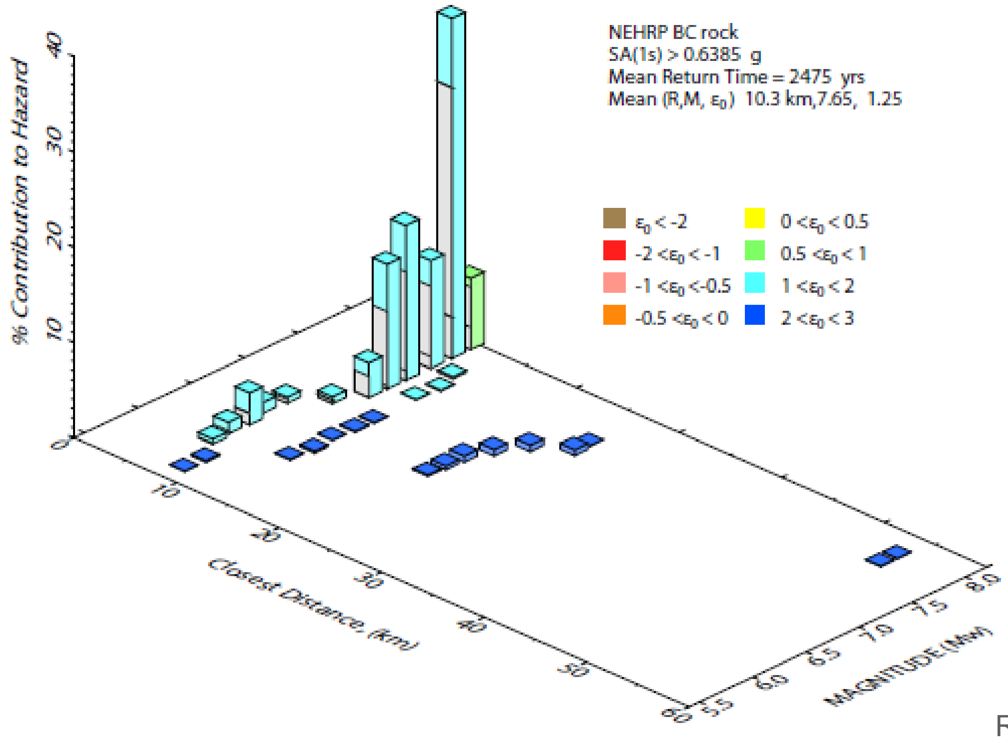

Baker, Bradley and Stafford (2021), "Seismic Hazard and Risk Analysis." These images are provided for instructional and research use, with attribution. Not for commercial use.

Basic of Probabilistic Seismic Hazard Assessment (1)

Disaggregation for hazard of 0.18×10^{-4}/yr for Pga=0.2 g

M=5 and distance <3.2 Km contribute for 0.06×10^{-4}/year that is nearly 1/3

M=6 contribution for distance <12 km (0.09×10^{-4}/year)
Part from distance <3.2 km (0.09×10^{-4}/year x $3.2^2/12^2$) and the rest between 3.2 and 12 km (0.09×10^{-4}/year X($12^2/12^2 - 3.2^2/12^2$)

M=7 contribution from distance <22 km must be divided in 3 contributions

If all numbers are divided by the total of 0.18×10^{-4}/year one get the fractional contribution to the total hazard of each magnitude and distance range

One M=5 per year
One M=6 per decade
One M=7 per century

Horizontal distance R (km) within which the given pga's are achieved or exceeded for the given magnitudes

	M=5	M=6	M=7
0.1 g	14	25	41
0.2 g	3.2	12	22
0.4 g	0	0	10

Mean rate of exceedance (MROES) x 10-4 per year, for given pga's for the given magnitudes

	M=5	M=6	M=7	$\sum$	$\sum^{\sigma}$
0.1 g	1.23	0.39	0.11	**1.73**	1.47
0.2 g	0.06	0.09	0.03	0.18	0.41
0.4 g	0	0	0.006	0.006	0.034

Uniform Hazard Spectrum

It is developed by:
- performing the PSHA calculation for spectral accelerations at a range of (oscillator) periods.
- Identifying the spectral acceleration value having the target rate or exceedance at each period.
- Plotting those spectral acceleration values versus their periods.

Since the spectrum ordinates all have the same exceedance rate (i.e., "hazard" level), it is called a *uniform hazard* spectrum.

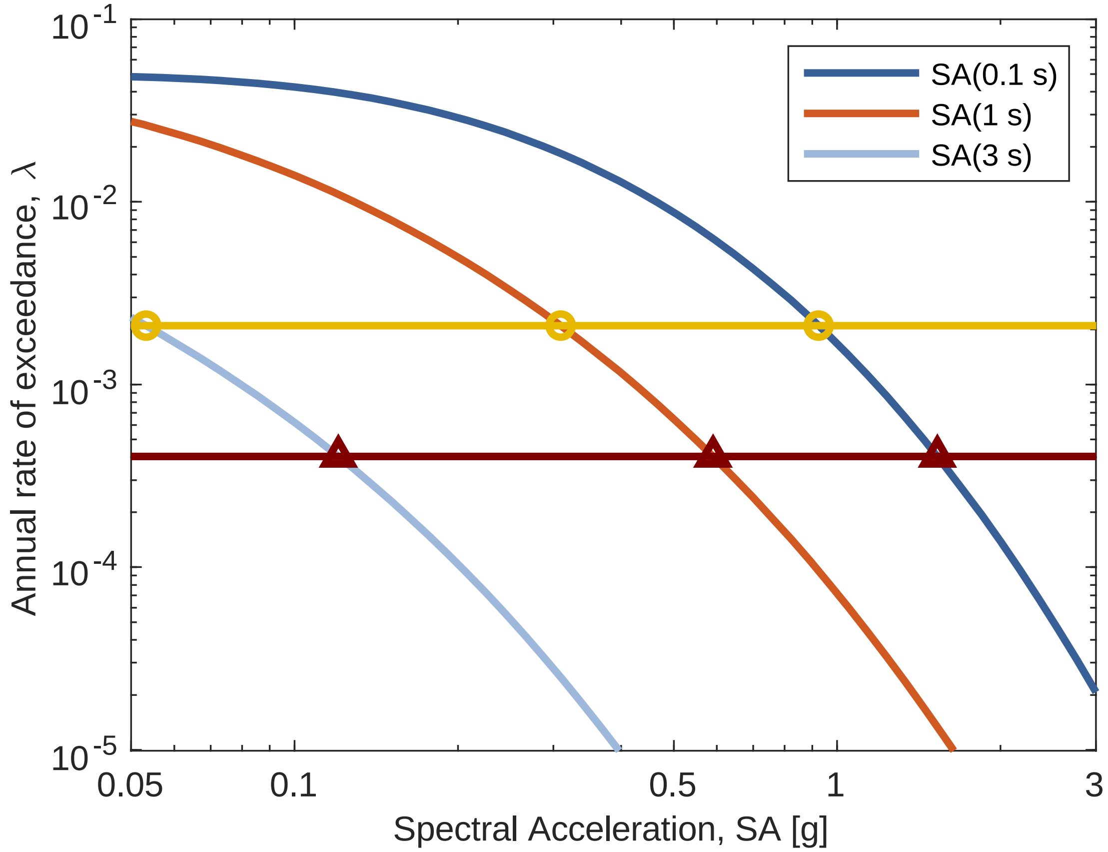

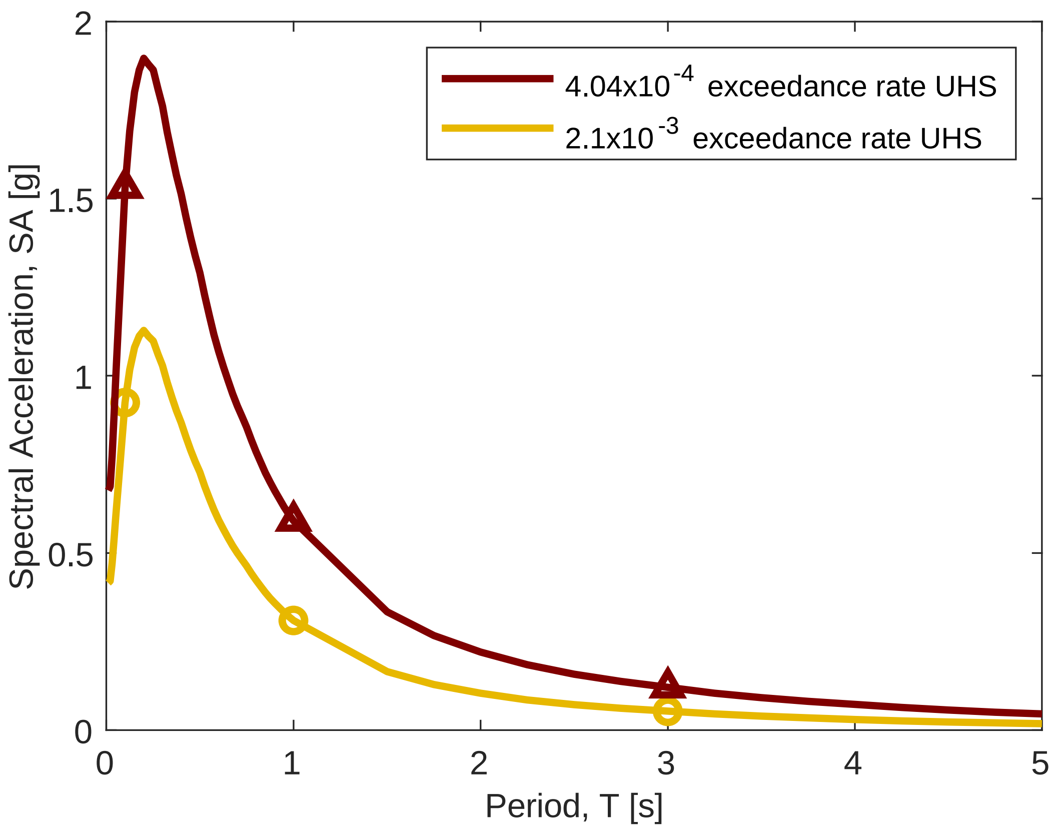

Baker, Bradley and Stafford (2021), "Seismic Hazard and Risk Analysis." These images are provided for instructional and research use, with attribution. Not for commercial use.

Fragility functions

A fragility function provides a prediction of a binary outcome, *F* (failure or nonfailure), as a function of ground-motion intensity.

$$P(F \mid IM = x) = \Phi\left(\frac{\ln(x/\theta)}{\beta}\right)$$

where $P(F \mid IM = x)$ is the probability that a ground motion with $IM = x$ will cause **failure** to occur, $\Phi()$ is the standard normal cumulative distribution function, θ is the median of the fragility function (the *IM* level with a 50% probability of failure), and β is the standard deviation of the ln *IM* level at which failure will occur

Table 9.1. Examples of binary failure criteria and continuous consequence metrics. Entries in a given row are not necessarily related

Failure criteria	*Consequence metrics*
Material yielding	Repair cost
Cracking of windows	Time to reopen a building
Reduction of x% capacity in an element	Time to repair a component
Exceedance of y floor acceleration	Number of fatalities
Structural collapse	Number of displaced people
Breakage in a pipe	Number of injuries
Breach of a levee	Amount of levee settlement
Soil liquefaction triggering	

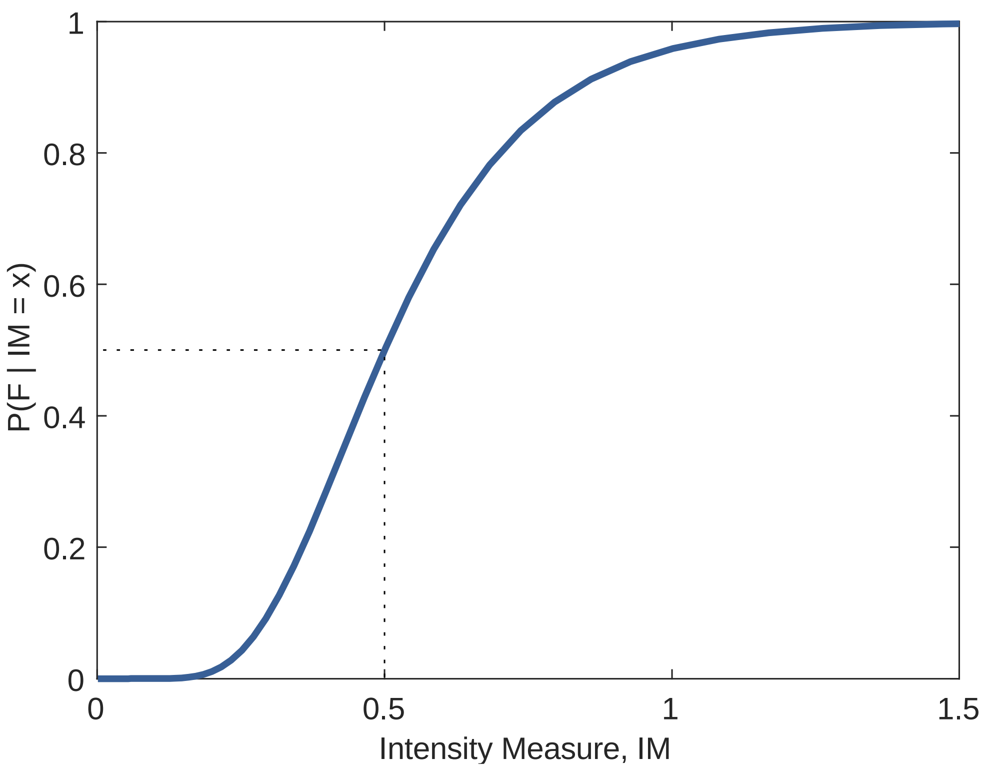

Seismic Risk

Fragility functions

Generally one considers discrete set of damage states (*DS*), and specify fragility functions for the probability of a structure reaching that damage state or worse:

$$P(DS \geq ds_i \mid IM = x) = \Phi\left(\frac{\ln(x/\theta_i)}{\beta_i}\right)$$

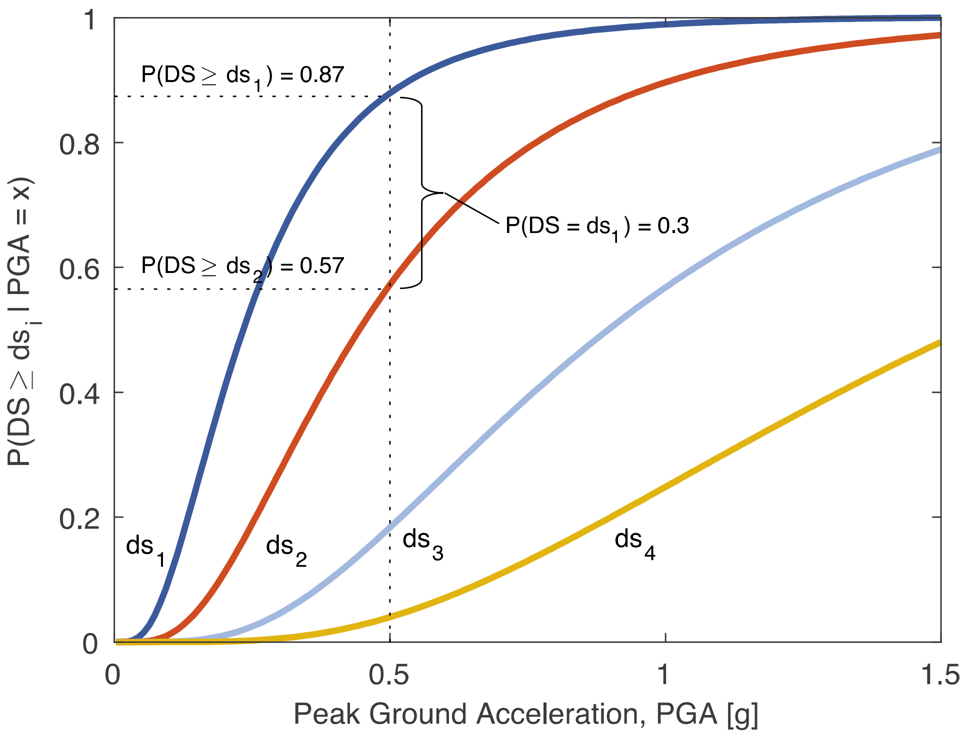

where *ds*i is the *i*th damage state, increasing values of *i* indicate more severe damage, and the fragility parameters θi and βi are specified for each damage state. The multiple damage states are typically assumed to be mutually exclusive and collectively exhaustive

Baker, Bradley and Stafford (2021), "Seismic Hazard and Risk Analysis." These images are provided for instructional and research use, with attribution. Not for commercial use.

UNIVERSITÀ DEGLI STUDI DI TRIESTE

Vulnerability functions

A vulnerability function is used to quantify outcomes when the **consequence** of interest is a continuous outcome, rather than a binary "failure" or "non failure.

$$P(C > c \mid IM = x) = 1 - F(c \mid x)$$

where *C* is the consequence metric of interest and *F*(*c* | *x*) is a cumulative distribution function for the consequence *C*, evaluated at *c* and dependent on the *IM* amplitude *x*.

Table 9.1. Examples of binary failure criteria and continuous consequence metrics. Entries in a given row are not necessarily related

Failure criteria	*Consequence metrics*
Material yielding	Repair cost
Cracking of windows	Time to reopen a building
Reduction of x% capacity in an element	Time to repair a component
Exceedance of y floor acceleration	Number of fatalities
Structural collapse	Number of displaced people
Breakage in a pipe	Number of injuries
Breach of a levee	Amount of levee settlement
Soil liquefaction triggering	

Seismic Risk

Failure rate

$$\lambda(F) = \int_0^{\infty} P(F \mid IM = x)|d\lambda(IM > x)|.$$

where $\lambda(F)$ denotes the annual rate of failure, F, $P(F \mid IM = x)$ is the fragility the failure limit state from

$$P(F \mid IM = x) = \Phi\left(\frac{\ln(x/\theta)}{\beta}\right)$$

$\lambda(IM > x)$ is the ground-motion hazard curve from

$$\lambda(IM > im) = \sum_{i=1}^{n_{rup}} P(IM > im \mid rup_i, site)\, \lambda(rup_i)$$

UNIVERSITÀ DEGLI STUDI DI TRIESTE

Seismic Risk

Failure rate

$$\lambda(F) = \int_0^{\infty} P(F \mid IM = x)|d\lambda(IM > x)|.$$

In discrete form:

$$\Delta\lambda_i = \lambda(IM > x_i) - \lambda(IM > x_{i+1})$$

$$\lambda(F) \approx \sum_{i=1}^{n} P(F \mid IM = x_i)\Delta\lambda_i.$$

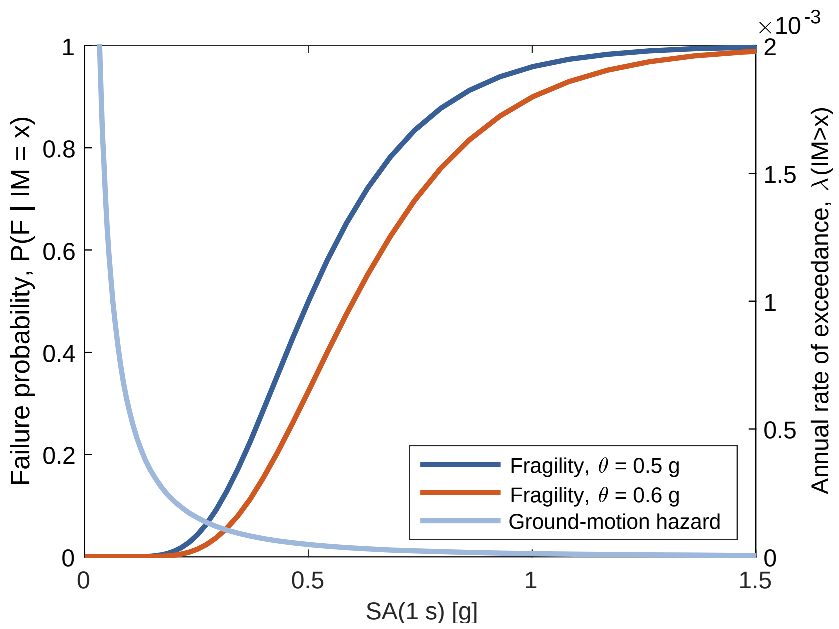

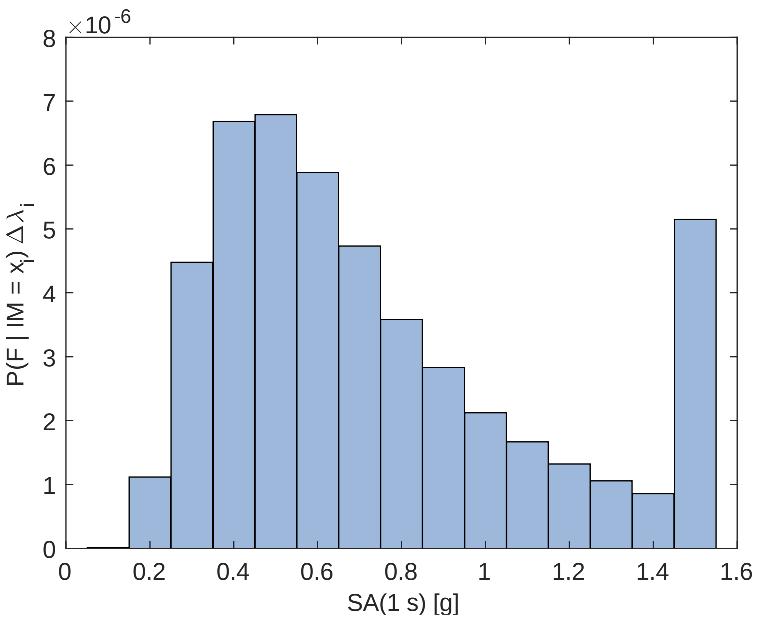

Baker, Bradley and Stafford (2021), "Seismic Hazard and Risk Analysis." These images are provided for instructional and research use, with attribution. Not for commercial use.

Seismic Risk

Loss exceedance curve

A *loss exceedance curve* provides the rates of exceeding various levels of losses (i.e., consequences) by combining a ground-motion hazard curve with a vulnerability function. The **exceedance rate** is computed for a particular loss level as

$$\lambda(C > c) = \int_0^{\infty} P(C > c \mid IM = x) |d\lambda(IM > x)|$$

where $\lambda(C > c)$ is the annual rate of consequence metric C exceeding threshold c, $P(C > c \mid IM)$ is a vulnerability and $\lambda(IM > x)$ is again the ground-motion hazard curve.

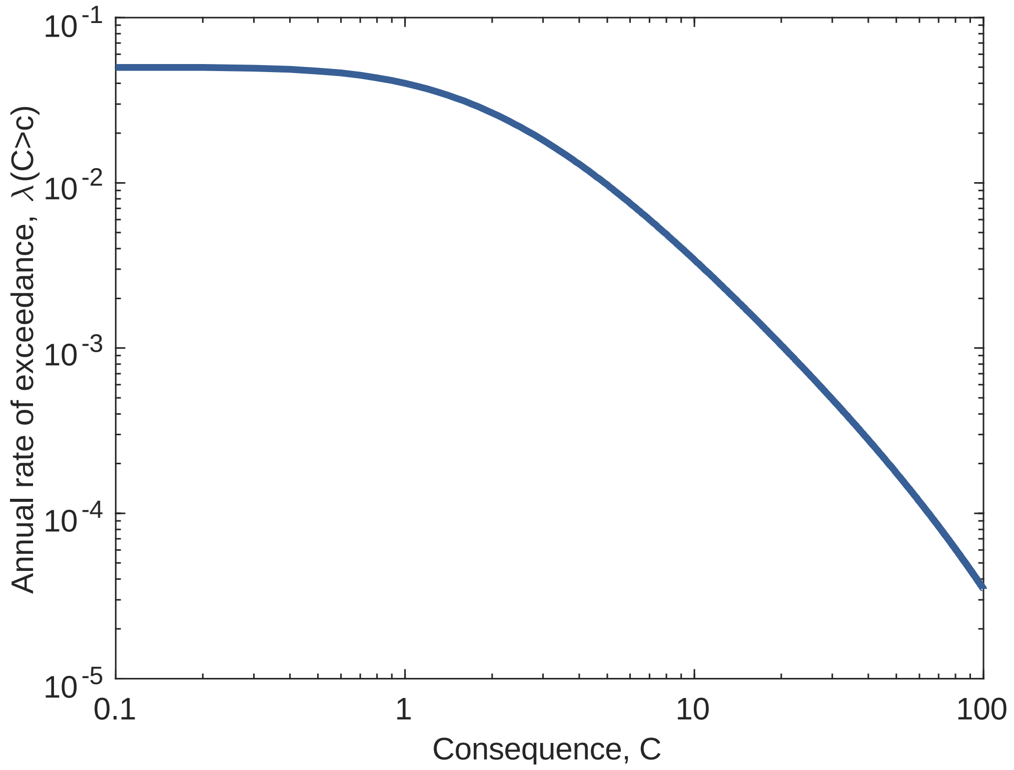

Seismic Risk

Exceedance probability curve

An ***exceedance probability*** **(EP)** curve (sometimes abbreviated as an 'EP Curve') provides the probability of exceeding various levels of loss during a specified window of time (often 1 year).

This connects the loss exceedance rates to the probability of an event occurring over some period of interest. The **exceedance rates** can be used to compute probabilities of exceedance over some time period *t*, assuming that the exceedances are Poissonian in nature and

$$P(C > c) = 1 - \exp\left[-\lambda(C > c)\,t\right].$$

Average annual Loss

The average annual loss (AAL) measures the expected amount of loss experienced per year. This metric is of interest for insurance transactions, as the annual cost of an insurance policy is influenced by the average payouts expected under the policy. It is also useful in evaluating risk reduction actions, as the cost of the action can be compared with the expected reduction of loss produced by the action.

$$E[C] = \int_0^{\infty} E[C \mid IM = x] |d\lambda(IM > x)|$$

where $E[C]$ is the expected loss (consequence) per unit time. Since $\lambda(IM > x)$ is typically an annual rate, these units persist and $E[C]$ is an expected annual loss.

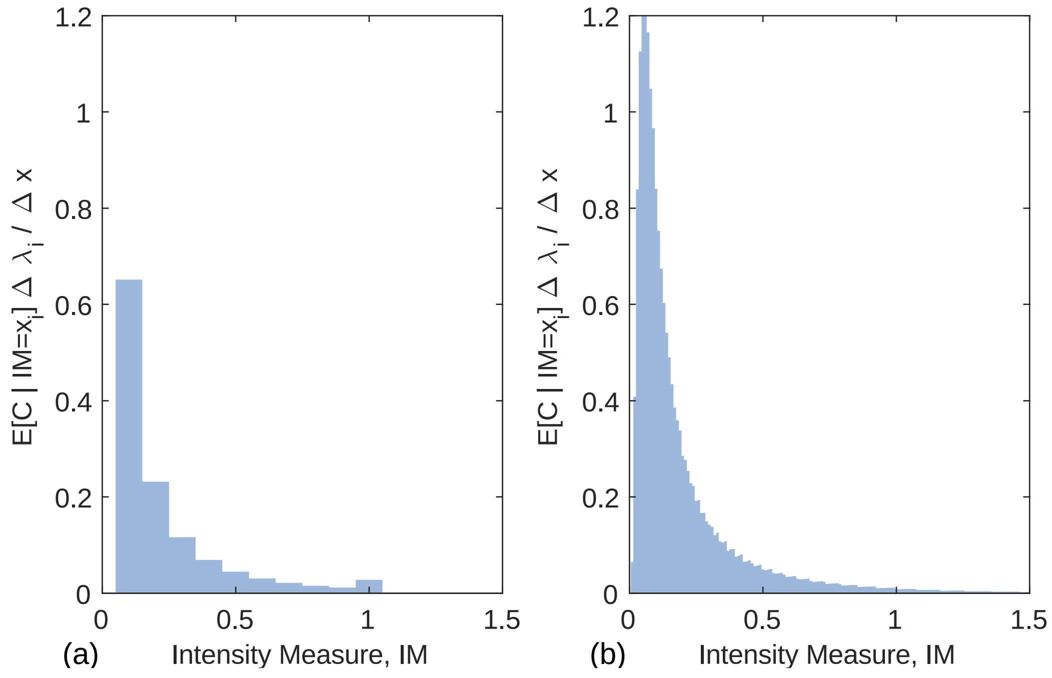

Baker, Bradley and Stafford (2021), "Seismic Hazard and Risk Analysis." These images are provided for instructional and research use, with attribution. Not for commercial use.

EMS Scale

ACCORD PARTIEL OUVERT
en matière de prévention, de protection et
d'organisation des secours contre les risques naturels
et technologiques majeurs du

CONSEIL DE L'EUROPE
Cahiers
du Centre Européen
de Géodynamique
et de Séismologie

Volume 15

European Macroseismic Scale 1998

Editor
G. GRÜNTHAL

Luxembourg 1998

The short form of the European Macroseismic Scale, abstracted from the Core Part, is intended to give a very simplified and generalized view of the EM Scale. It can, e.g., be used for educational purposes. *This short form is not suitable for intensity assignments.*

EMS intensity	Definition	Description of typical observed effects (abstracted)
I	Not felt	Not felt.
II	Scarcely felt	Felt only by very few individual people at rest in houses.
III	Weak	Felt indoors by a few people. People at rest feel a swaying or light trembling.
IV	Largely observed	Felt indoors by many people, outdoors by very few. A few people are awakened. Windows, doors and dishes rattle.
V	Strong	Felt indoors by most, outdoors by few. Many sleeping people awake. A few are frightened. Buildings tremble throughout. Hanging objects swing considerably. Small objects are shifted. Doors and windows swing open or shut.
VI	Slightly damaging	Many people are frightened and run outdoors. Some objects fall. Many houses suffer slight non-structural damage like hair-line cracks and fall of small pieces of plaster.
VII	Damaging	Most people are frightened and run outdoors. Furniture is shifted and objects fall from shelves in large numbers. Many well built ordinary buildings suffer moderate damage: small cracks in walls, fall of plaster, parts of chimneys fall down; older buildings may show large cracks in walls and failure of fill-in walls.
VIII	Heavily damaging	Many people find it difficult to stand. Many houses have large cracks in walls. A few well built ordinary buildings show serious failure of walls, while weak older structures may collapse.
IX	Destructive	General panic. Many weak constructions collapse. Even well built ordinary buildings show very heavy damage: serious failure of walls and partial structural failure.
X	Very destructive	Many ordinary well built buildings collapse.
XI	Devastating	Most ordinary well built buildings collapse, even some with good earthquake resistant design are destroyed.
XII	Completely devastating	Almost all buildings are destroyed.

EMS Scale

Differentiation of structures (buildings) into vulnerability classes (Vulnerability Table)

	Type of Structure	A	B	C	D	E	F
MASONRY	rubble stone, fieldstone	○					
	adobe (earth brick)	○	—				
	simple stone	·····	○				
	massive stone		—	○	·····		
	unreinforced, with manufactured stone units	·····	○	·····			
	unreinforced, with RC floors		—	○	·····		
	reinforced or confined			·····	○	—	
REINFORCED CONCRETE (RC)	frame without earthquake-resistant design (ERD)	·····	—	○	·····		
	frame with moderate level of ERD		·····	—	○	—	
	frame with high level of ERD			·····	—	○	—
	walls without ERD		·····	○	—		
	walls with moderate level of ERD			·····	○	—	
	walls with high level of ERD				·····	○	—
STEEL	steel structures			·····	—	○	—
WOOD	timber structures		·····	—	○	—	

○ most likely vulnerability class; — probable range;
····· range of less probable, exceptional cases

Grünthal (1998)

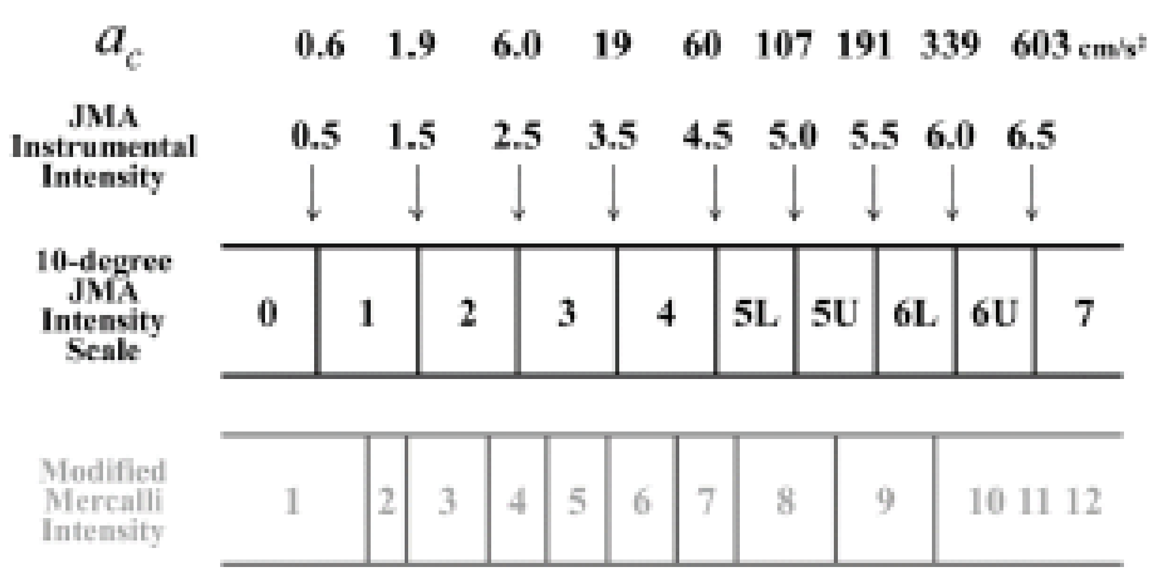

Kodera et al., 2016.

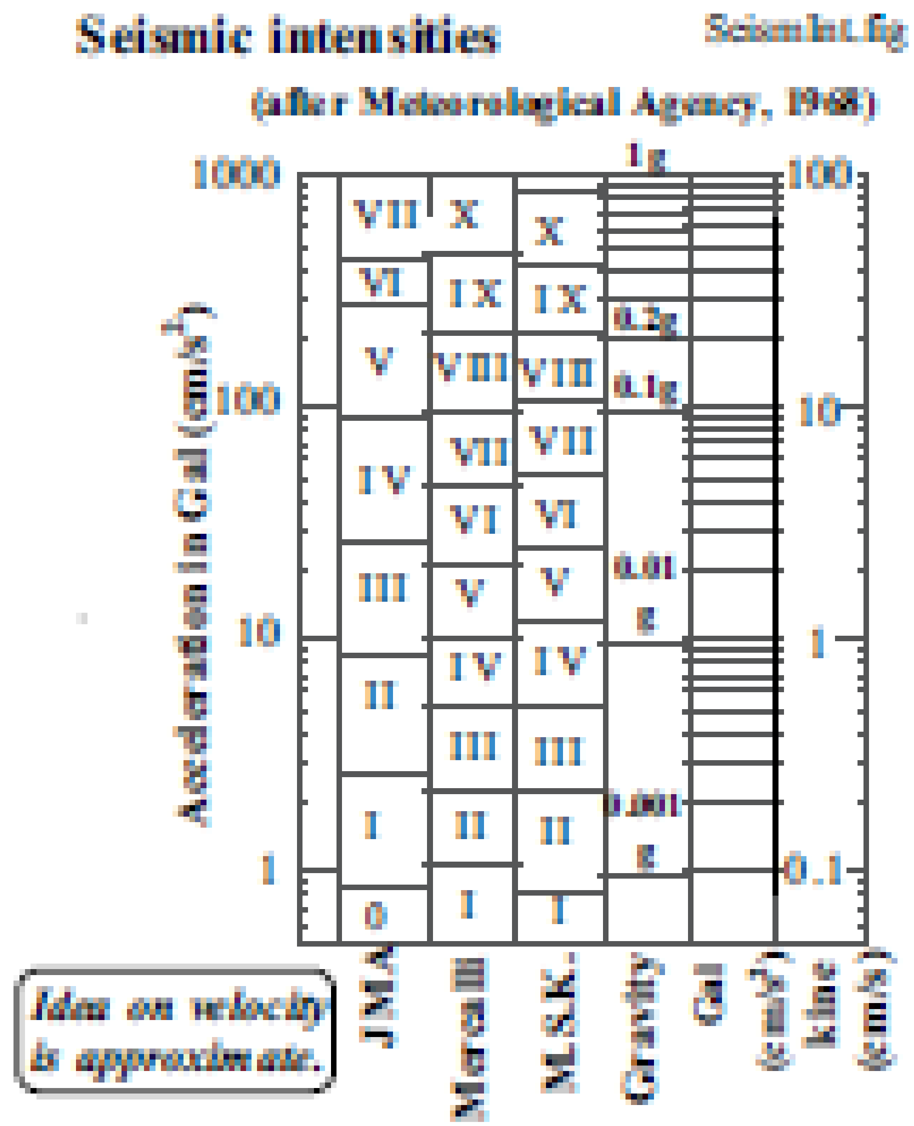

Towhata 2008.

SHAKING	Not felt	Weak	Light	Moderate	Strong	Very strong	Severe	Violent	Extreme
DAMAGE	None	None	None	Very light	Light	Moderate	Moderate/heavy	Heavy	Very heavy
PGA(%g)	<0.0555	0.232	1.21	3.38	7.46	14.5	26.1	44.4	>72.3
PGV(cm/s)	<0.0178	0.0939	0.686	2.08	5.06	10.9	21.6	40.3	>71.7
INTENSITY	I	II-III	IV	V	VI	VII	VIII	IX	X+

Scale based on Oliveti Faenza Michelini (2022) Version 2: Processed 2023-10-28T16:23:20Z

Damage Classification

Classification of damage to masonry buildings	
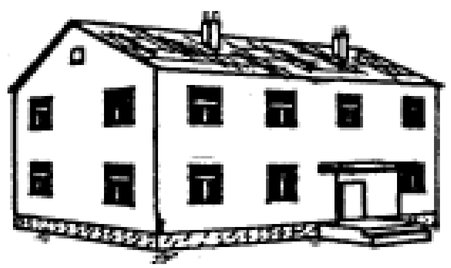	**Grade 1: Negligible to slight damage (no structural damage, slight non-structural damage)** Hair-line cracks in very few walls. Fall of small pieces of plaster only. Fall of loose stones from upper parts of buildings in very few cases.
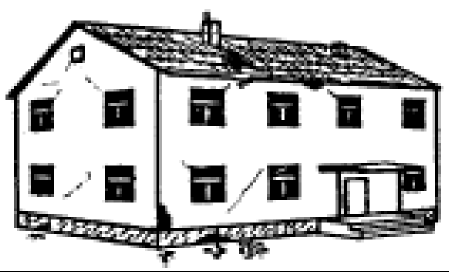	**Grade 2: Moderate damage (slight structural damage, moderate non-structural damage)** Cracks in many walls. Fall of fairly large pieces of plaster. Partial collapse of chimneys.
	**Grade 3: Substantial to heavy damage (moderate structural damage, heavy non-structural damage)** Large and extensive cracks in most walls. Roof tiles detach. Chimneys fracture at the roof line; failure of individual non-structural elements (partitions, gable walls).
	**Grade 4: Very heavy damage (heavy structural damage, very heavy non-structural damage)** Serious failure of walls; partial structural failure of roofs and floors.
	**Grade 5: Destruction (very heavy structural damage)** Total or near total collapse.

Classification of damage to buildings of reinforced concrete	
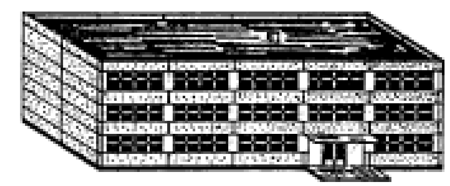	**Grade 1: Negligible to slight damage (no structural damage, slight non-structural damage)** Fine cracks in plaster over frame members or in walls at the base. Fine cracks in partitions and infills.
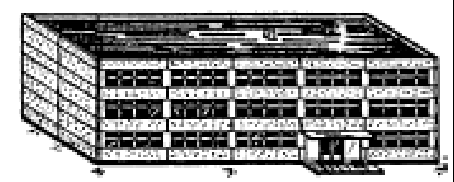	**Grade 2: Moderate damage (slight structural damage, moderate non-structural damage)** Cracks in columns and beams of frames and in structural walls. Cracks in partition and infill walls; fall of brittle cladding and plaster. Falling mortar from the joints of wall panels.
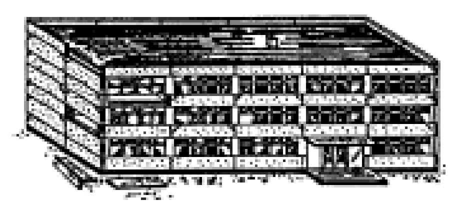	**Grade 3: Substantial to heavy damage (moderate structural damage, heavy non-structural damage)** Cracks in columns and beam column joints of frames at the base and at joints of coupled walls. Spalling of conrete cover, buckling of reinforced rods. Large cracks in partition and infill walls, failure of individual infill panels.
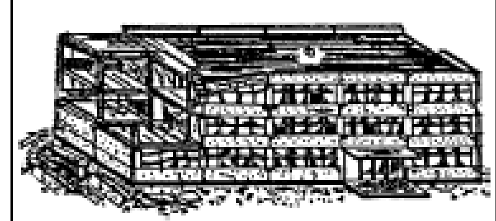	**Grade 4: Very heavy damage (heavy structural damage, very heavy non-structural damage)** Large cracks in structural elements with compression failure of concrete and fracture of rebars; bond failure of beam reinforced bars; tilting of columns. Collapse of a few columns or of a single upper floor.
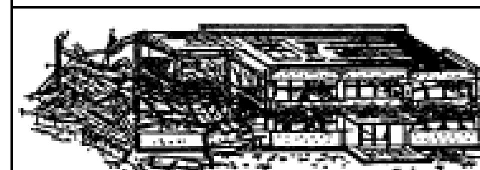	**Grade 5: Destruction (very heavy structural damage)** Collapse of ground floor or parts (e. g. wings) of buildings.

Definitions of quantity

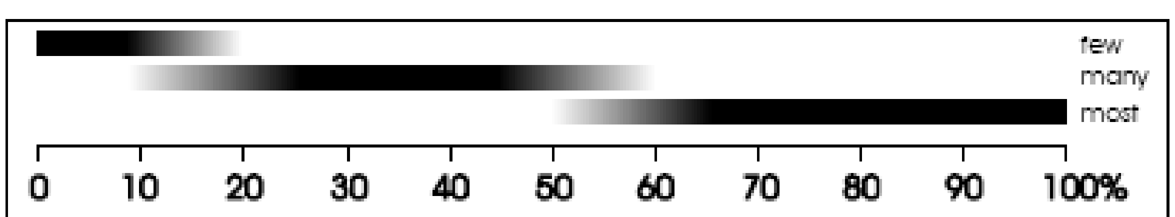

UNIVERSITÀ DEGLI STUDI DI TRIESTE

Grünthal (1998)

Damage classification

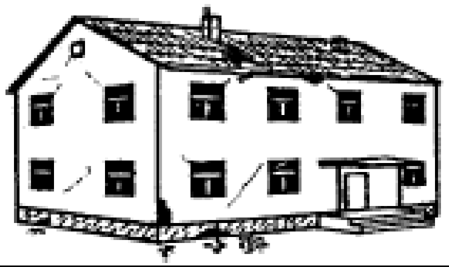

Grade 2: Moderate damage
(slight structural damage, moderate non-structural damage)
Cracks in many walls.
Fall of fairly large pieces of plaster.
Partial collapse of chimneys.

TYPE OF STRUCTURE	EARTHQUAKE / SITE	GRADE OF DAMAGE				
		1	2	3	4	5
Simple stone masonry	**Grison, Switzerland 1991 / Vaz**		●			

The long crack in this wall is large enough to constitute slight structural damage. The damage should be considered to be of grade 2

TYPE OF STRUCTURE	EARTHQUAKE / SITE	GRADE OF DAMAGE				
		1	2	3	4	5
Unreinforced masonry	**Roermond, The Netherlands 1992 / Heinsberg**		●			

Several chimneys have been damaged and tiles on the roof have been shifted. Large and extensive cracks in most walls were not observed, and therefore the damage is to be assessed as grade 2.

Note: The chimney on the left of the picture was broken due to the differential shaking behaviour of the two adjoining buildings. Parts of the broken chimney hit the roof and dislodged tiles; this damage to the tiles is therefore a secondary effect and not caused directly by the earthquake shaking.

UNIVERSITÀ DEGLI STUDI DI TRIESTE

Grünthal (1998)

Damage classification

Grade 3: Substantial to heavy damage (moderate structural damage, heavy non-structural damage)
Large and extensive cracks in most walls. Roof tiles detach. Chimneys fracture at the roof line; failure of individual non-structural elements (partitions, gable walls).

TYPE OF STRUCTURE	EARTHQUAKE / SITE	GRADE OF DAMAGE				
		1	2	3	4	5
Adobe masonry	**East Kazakhstan 1990 / Saisan**			●		

The large and extensive cracks in most walls suggest damage of grade 3.

TYPE OF STRUCTURE	EARTHQUAKE / SITE	GRADE OF DAMAGE				
		1	2	3	4	5
Unreinforced masonry	**Friuli, Italy 1976 / Gemona (Udine)**			●		

There are large diagonal cracks in most walls, but they are not so severe and the walls have not failed. In this case the damage is grade 3.

Grünthal (1998)

Damage classification

Grade 4: **Very heavy damage**
(heavy structural damage,
very heavy non-structural damage)
Serious failure of walls; partial structural failure of roofs and floors.

TYPE OF STRUCTURE	EARTHQUAKE / SITE	GRADE OF DAMAGE				
		1	2	3	4	5
Field stone masonry	**North Peloponissos, Greece 1995 / Aegion**				●	

The serious failure of walls in this example is indicative of damage grade 4. The vulnerability is affected by the poor quality of mortar and the non-effectiveness of the concrete elements in the construction.

TYPE OF STRUCTURE	EARTHQUAKE / SITE	GRADE OF DAMAGE				
		1	2	3	4	5
Simple stone masonry	**Montenegro, Yugoslavia 1979**				●	

Parts of the bearing walls have failed, causing partial collapse of the roof and floor slabs. This is heavy structural damage and therefore damage grade 4.

Grünthal (1998)

Damage classification

	**Grade 5: Destruction** **(very heavy structural damage)** Collapse of ground floor or parts (e. g. wings) of buildings.

TYPE OF STRUCTURE	EARTHQUAKE / SITE	GRADE OF DAMAGE				
		1	2	3	4	5
RC frame	**North Peloppônissos, Greece 1995 / Aegion**					●

The whole ground floor has collapsed completely. In such cases the damage grade is 5.

TYPE OF STRUCTURE	EARTHQUAKE / SITE	GRADE OF DAMAGE				
		1	2	3	4	5
RC frame	**Spitak, Armenia 1988 / Leninakan**					●

This is obviously very heavy structural damage and near-total collapse, and therefore damage grade 5.
Note: This RC frame structure incorporating a certain level of earthquake resistant design was adversely affected by the insufficient coupling between beams and columns. This building type is a typical example where one should assign a low vulnerability class, in this case B, which represents an exceptionally low class for this type of structure.

Grünthal (1998)

Italian building code (NTC08/18)

- Seismic classification

  https://rischi.protezionecivile.gov.it/it/sismico/attivita/classificazione-sismica

- Seismic hazard

  http://esse1.mi.ingv.it

- NTC08 Seismic code (§ 2.*; 3.2; 7.*)

  https://www.gazzettaufficiale.it/eli/id/2008/02/04/08A00368/sg

- NTC18 Seismic code (§ 2.*; 3.2; 7.*)

  https://www.gazzettaufficiale.it/eli/gu/2018/02/20/42/so/8/sg/pdf

  https://www.gazzettaufficiale.it/eli/id/2019/02/11/19A00855/sg

Site response

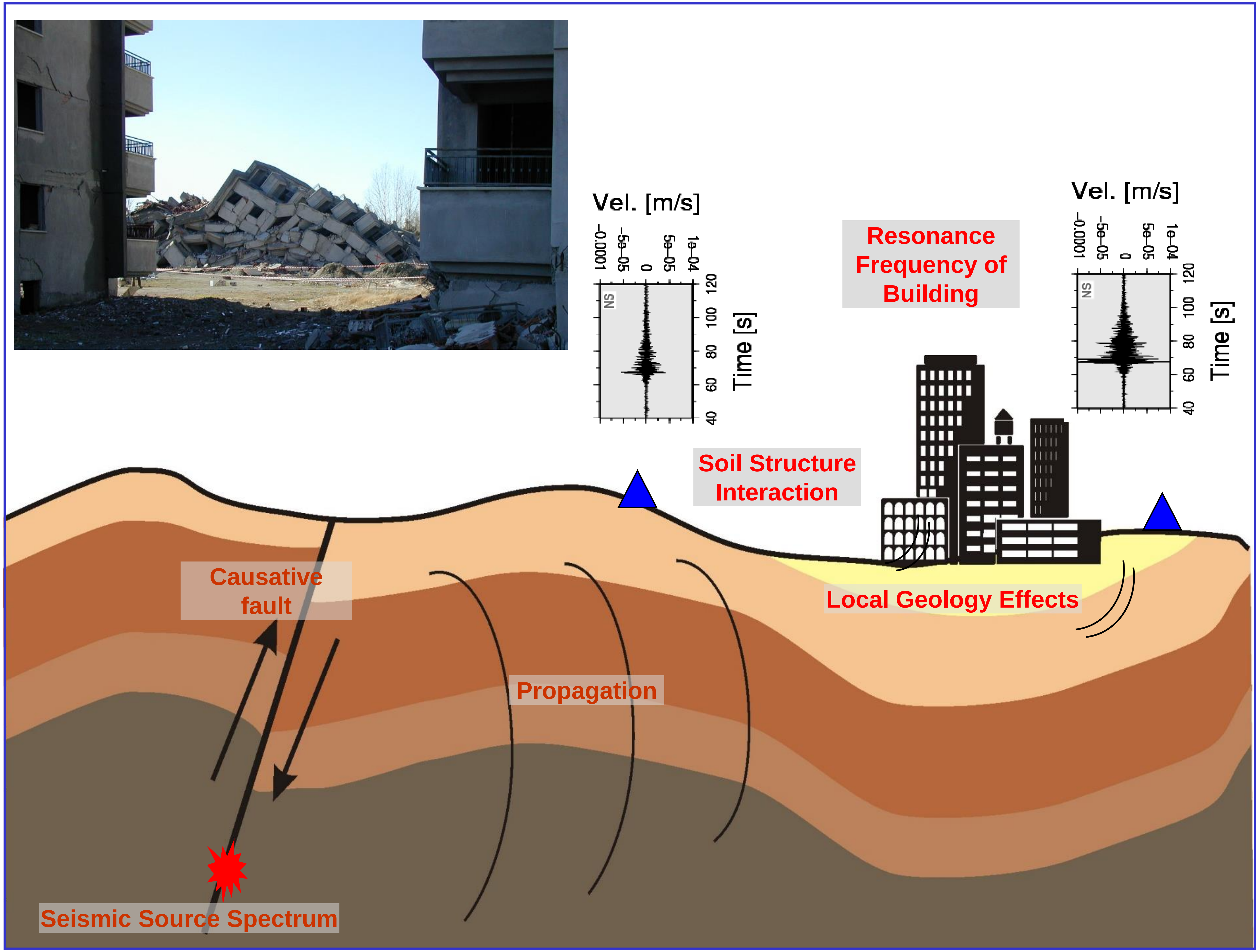
Vel. [m/s]
-0.0001
-5e-05
0
5e-05
1e-04
NS
Time [s]
40
60
80
100
120
Resonance Frequency of Building
Vel. [m/s]
Soil Structure Interaction
Causative fault
Local Geology Effects
Propagation
Seismic Source Spectrum

Site effects: Gubbio Valley (Italy)

Ground motion increasing with increasing distance from the source! (within the valley)

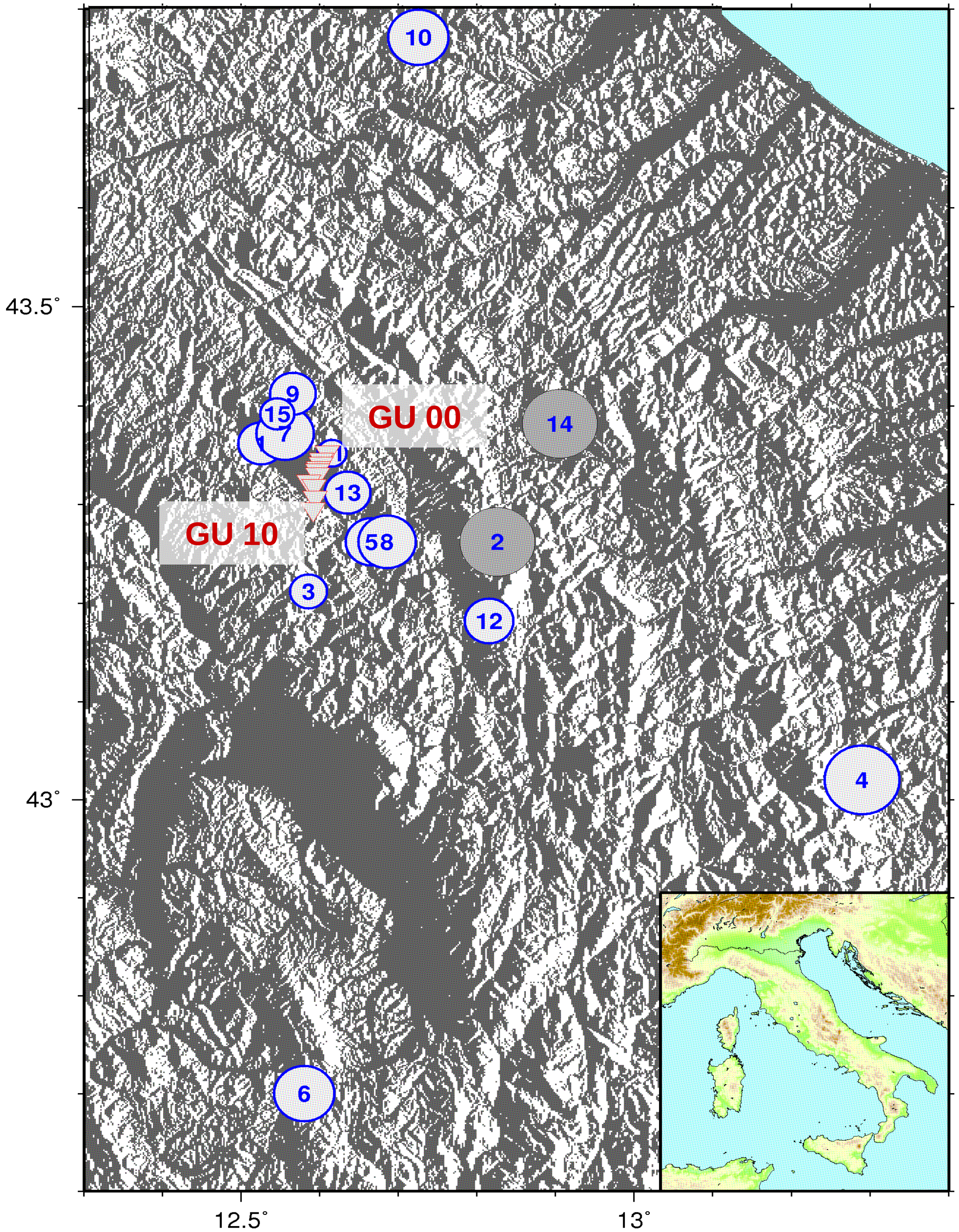

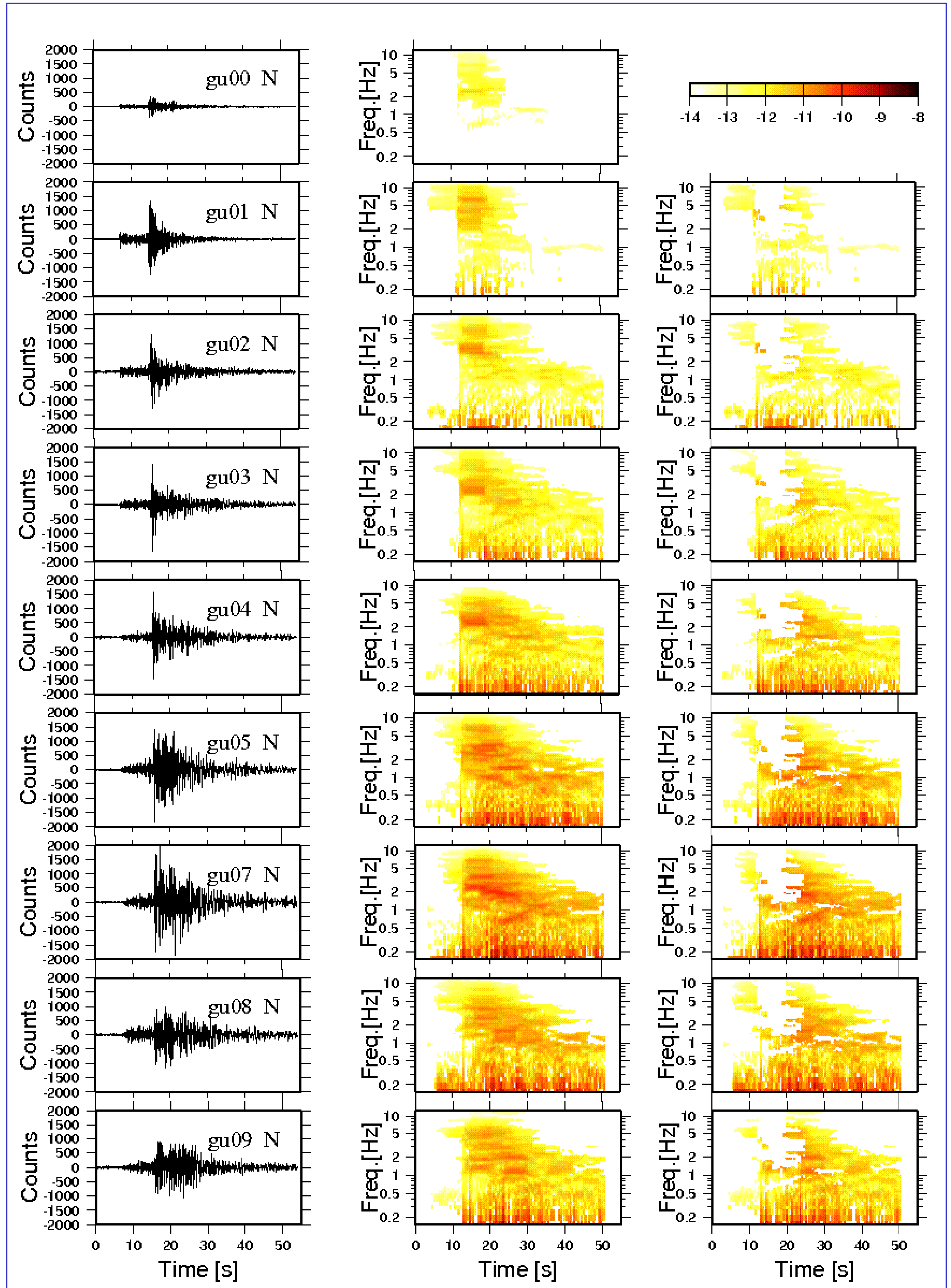

UNIVERSITÀ
DEGLI STUDI
DI TRIESTE

A simple model: site effects due to the seismic impedance contrast

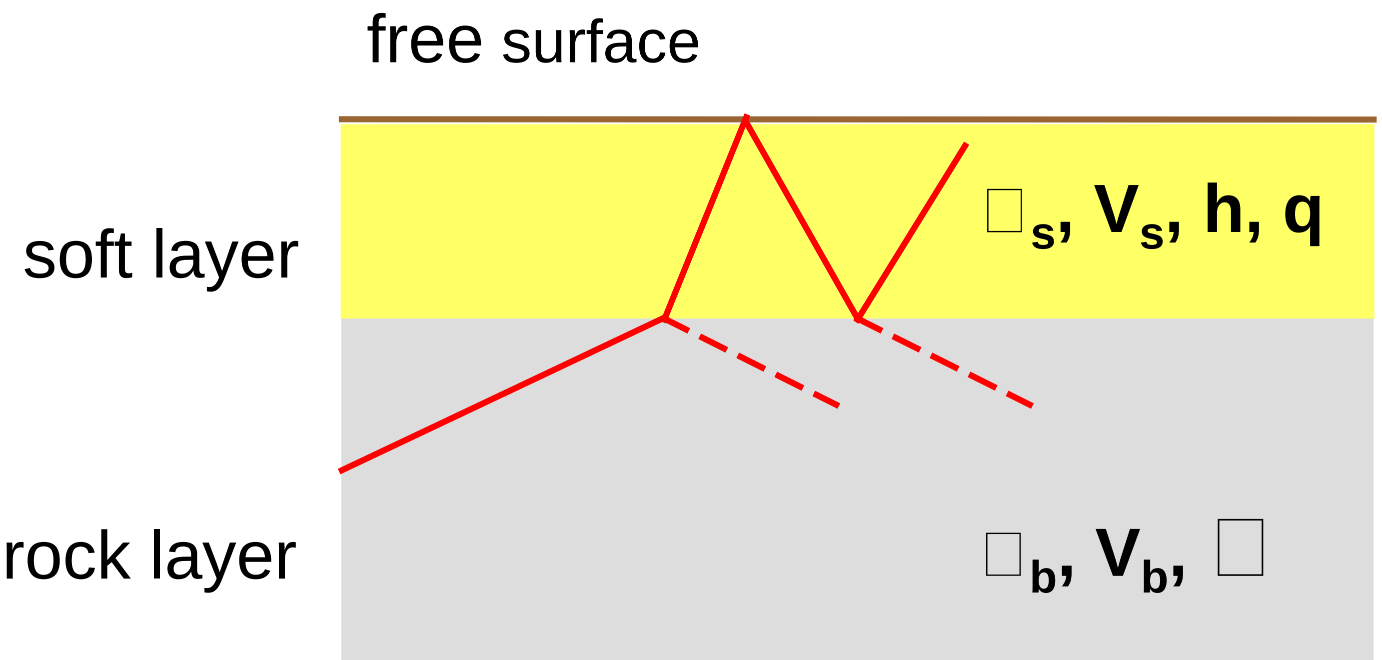

$C=(\square_2 V_2/\square_1 V_1)$ is impedance contrast

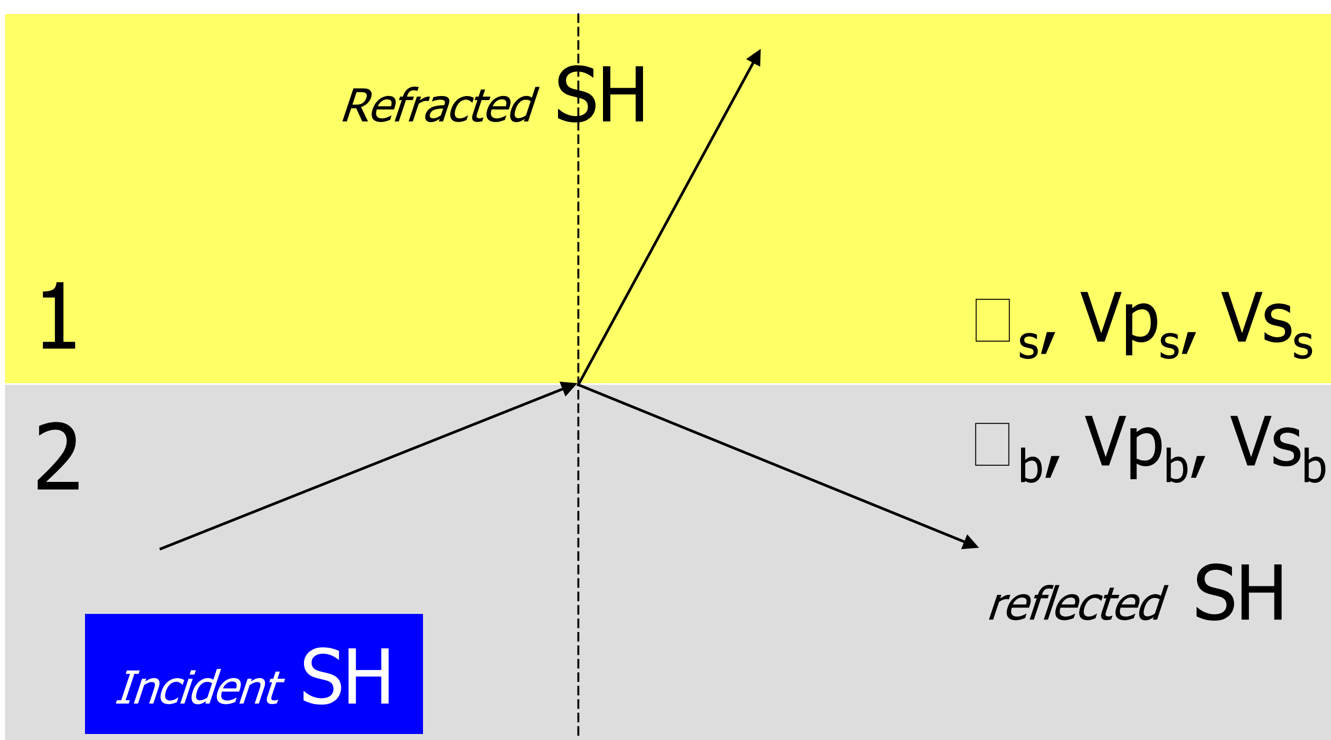

REFRACTION and REFLECTION

When a body wave encounters an ELASTIC boundary or discontinuity (change on seismic velocity), part of the energy will be transmitted through the boundary and part reflect.

SNELL'S LAW

sin(i) / V = constant = p

$\square$ $\sin(i_1) / V_1 = \sin(i_2) / V_2$

UNIVERSITÀ DEGLI STUDI DI TRIESTE

A simple model: site effects due to the seismic impedance contrast

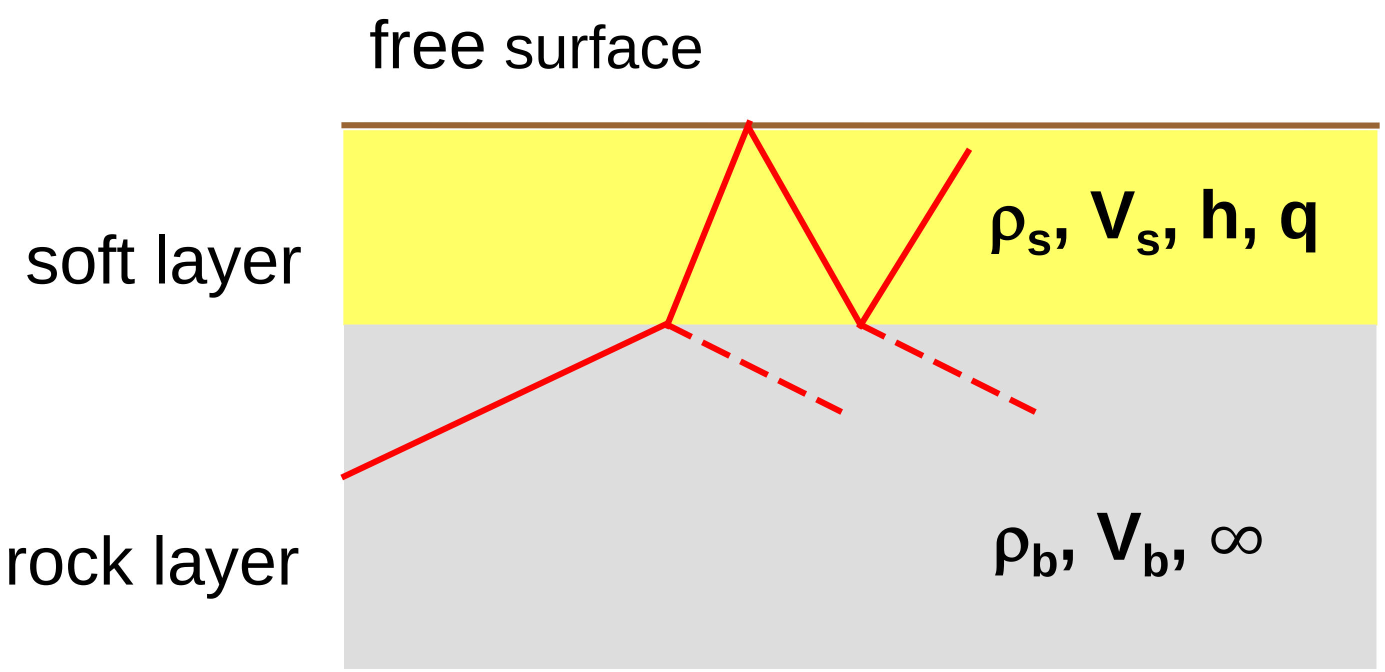

$C=(\rho_2 V_2/\rho_1 V_1)$ is impedance contrast

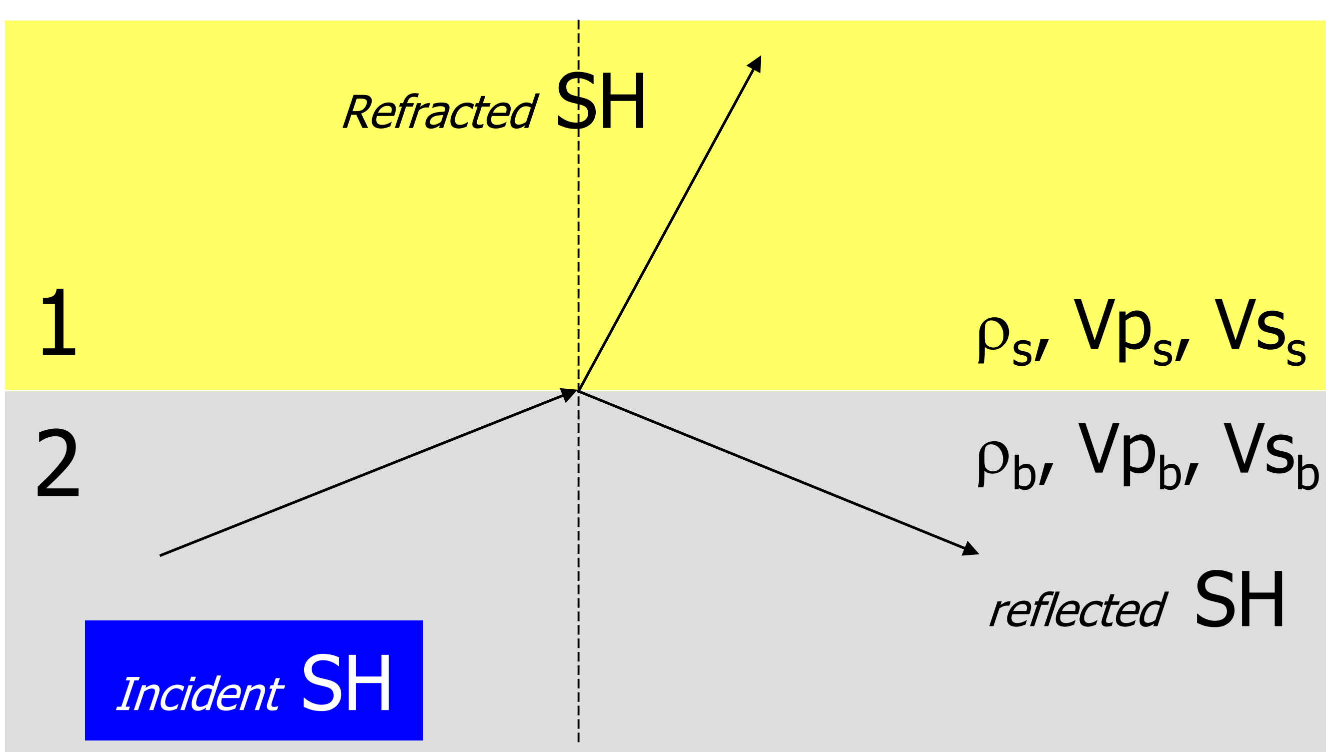

REFRACTION and REFLECTION

When a body wave encounters an ELASTIC boundary or discontinuity (change on seismic velocity), part of the energy will be transmitted through the boundary and part reflect.

SNELL'S LAW

sin(i) / V = constant = p

□ $\sin(i_1) / V_1 = \sin(i_2) / V_2$

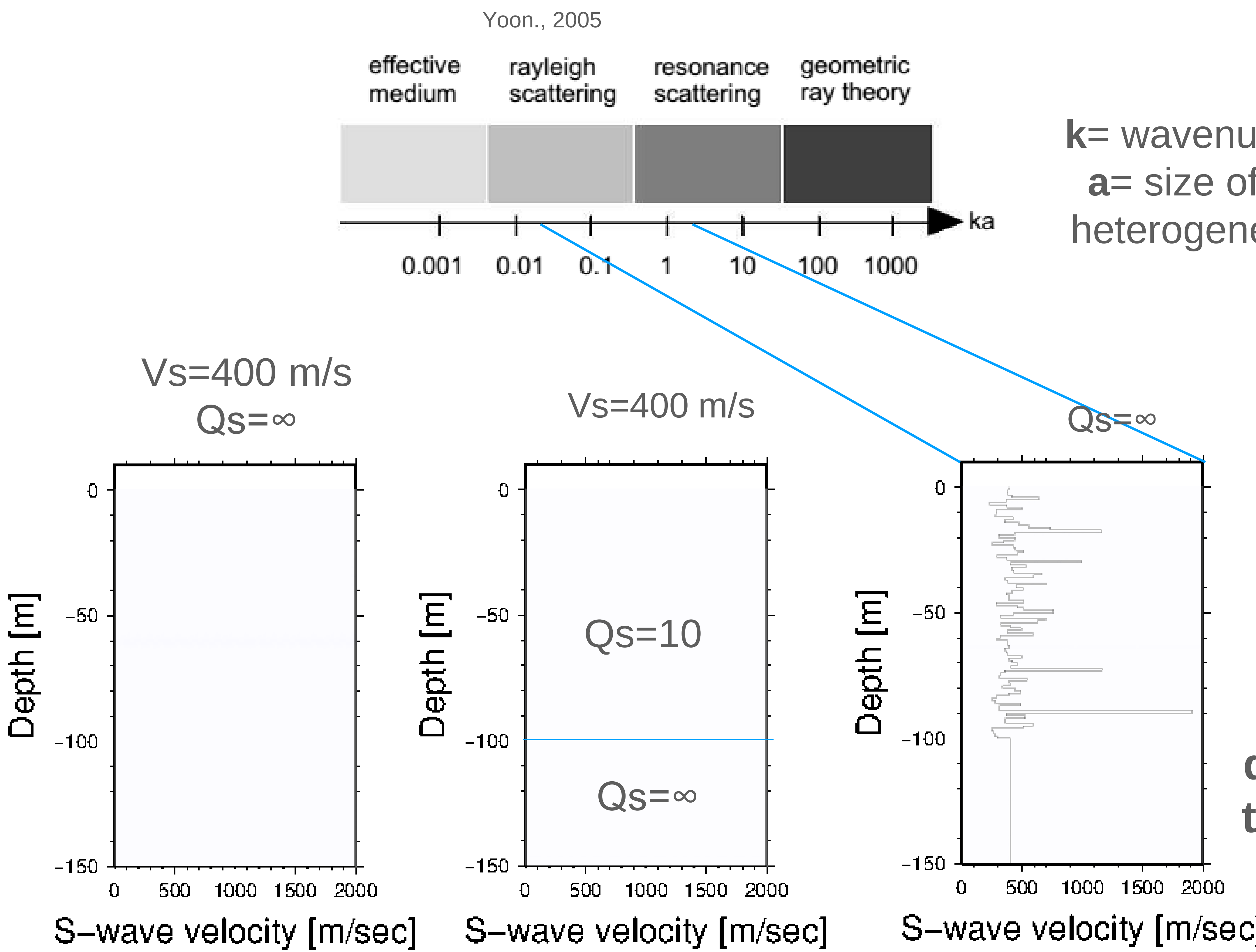

k= wavenumber
a= size of the heterogeneities

Combined effect of intrinsic, trasmission, scattering depending on the wavelegth

Contribution of the intrinsic attenuation and transmission properties of a media to the different portions of the seismic signal

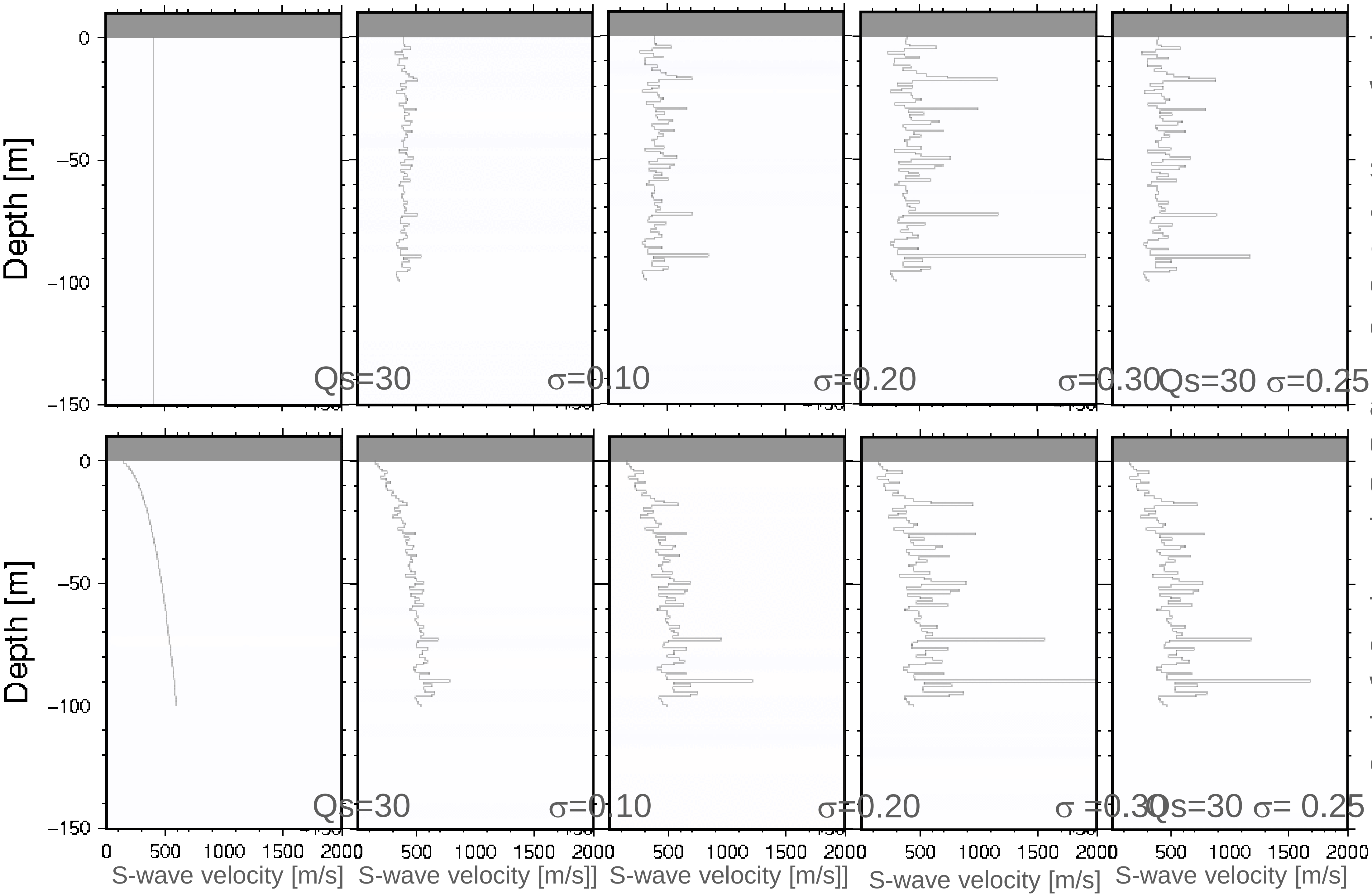

The travel time within each layer is perturbed randomly, starting from the average value (0.0025 s) **A Gaussian distribution of the perturbations with a st.dev. σ equal to 0.05, 0.10, 0.15, 0.2, 0.25, 0.30** of the average value is used. The sum of the travel times in each layer over the whole 100 m equals the original average one (0.25 s).

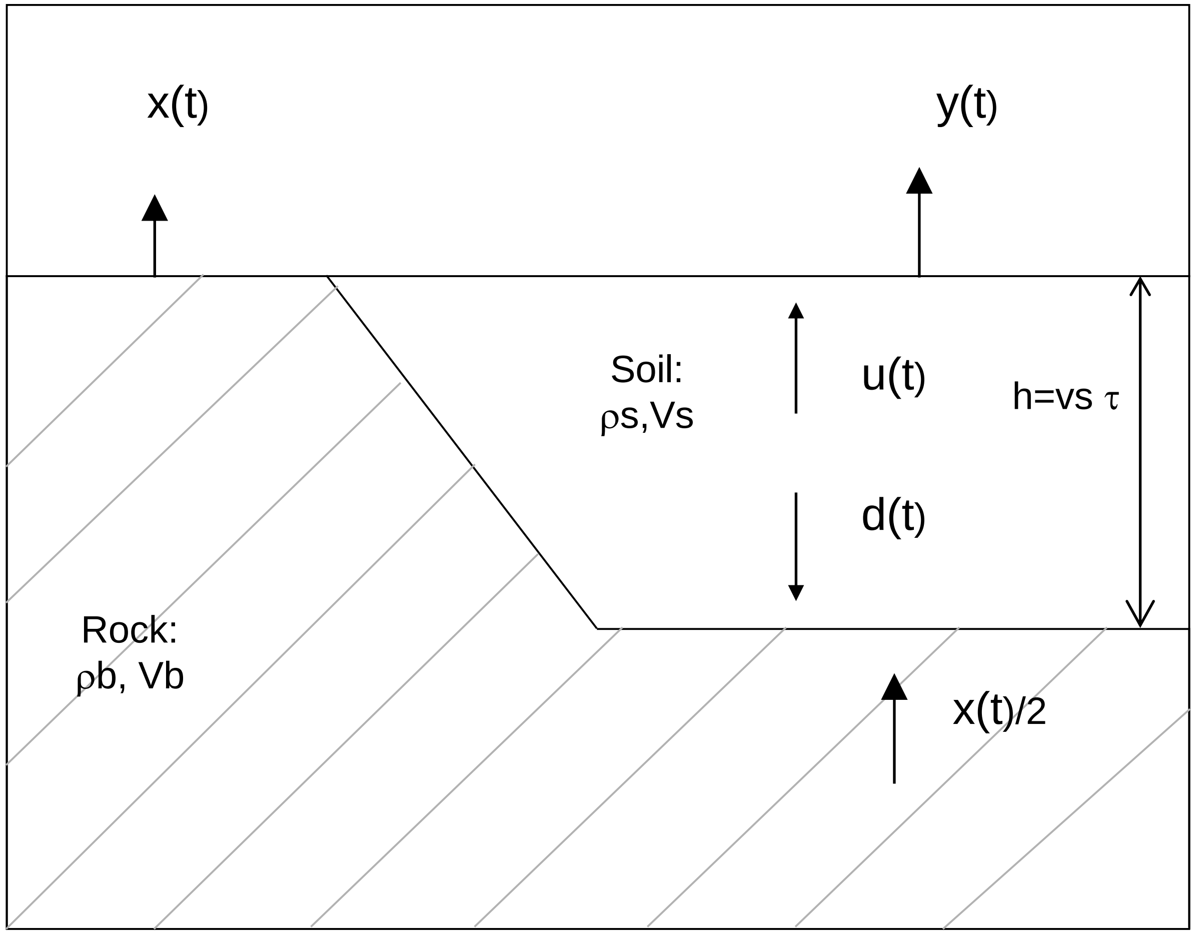

$C=(\rho_b V_v/\rho_s V_s)$ is the impedance contrast

$$r = \frac{pbVb - psVs}{pbVb + psVs} = \frac{c-1}{1+c}$$

$$u(t) = -rd(t-\tau) + (1+r)\frac{x(t-\tau)}{2}$$

$$d(t) = u(t-\tau) \quad y(t) = 2u(t)$$

Assuming that the free surface amplification is equal to 2 and eliminating u(t) and d(t) we obtain:

$$y(t) = -ry(t-2\tau) + (1+r)x(t-\tau)$$

Some properties of the Fourier Transform $\Im$

-Linearity: $\Im\left[a_1 f_1(t)+a_2 f_2(t)\right]=a_1\Im f_1(\omega)+a_2\Im f_2(\omega)$

-Derivative: $\Im\left[f^{(n)}(t)\right]=(i\omega)^n\,\Im f(\omega)$

-Shift: $\Im\left[f(t-a)\right]=e^{-i\omega a}\,\Im f(\omega)$

-Convolution: $\Im\left[f_1(t)*f_2(t)\right]=\Im\int_0^t f_1(\tau)f_2(t-\tau)\,d\tau=\Im f_1(\omega)\Im f_2(\omega)$

Applications: linear system (source*path*site*instrument), time-delay of propagation (e.g. array analysis), solving differential equations, etc…

Parseval identity
(sum of the square values)

$$\left\| f(t)\right\|_2=\left\|\Im f(\omega)\right\|_2$$

If X(f) is the Fourier transform of x(t) and Y(f) is the Fourier transform of y(t)

The Fourier transform of $x(t-\tau)$ is $X(f)e^{-i2\pi f\tau}$ and the Fourier transform of $y(t-2\tau)$ is $Y(f)e^{-i4\pi f\tau}$

The time delay τ correspond in the frequency domain to a phase shift $2\pi f\tau$

Multiplying the spectrum for the phasor $e^{-i2\pi f\tau}$ only modifies the phase but not the amplitude of the spectrum in fact:

$$e^{-i2\pi f\tau} = \cos\left(2\pi f\tau\right) - i\sin\left(2\pi f\tau\right)$$

$$\sqrt{\left(\cos\left(2\pi f\tau\right)\right)^2 + \left(\sin\left(2\pi f\tau\right)\right)^2} = 1$$

$$\phi\left(f\right) = \tan^{-1}\left(\frac{-\sin(2\pi f\tau)}{\cos(2\pi f\tau)}\right)$$

The Fourier trasform of Y(f) is then:

$$Y(f) = -rY(f)e^{-i4\pi f\tau} + (1+r)X(f)e^{-i2\pi f\tau}$$

If we define the transfer function H(f) as Y(f)/X(f) we obtain:

$$H(f) = \frac{(1+r)e^{-i2\pi f\tau}}{1+re^{-i4\pi f\tau}}$$

The modulus of H(f) can be simply calculated by computing the modulus of the numerator and of the denominator

The modulus of the numerator is:

$$\left|(1+r)e^{-i2\pi f\tau}\right| = \left|(1+r)\left(\cos\left(2\pi f\tau\right) - i\sin\left(2\pi f\tau\right)\right)\right| =$$

$$\sqrt{(1+r)^2\left(\left(\cos\left(2\pi f\tau\right)\right)^2 + \left(\sin\left(2\pi f\tau\right)\right)^2\right)} = 1+r$$

The modulus of the denominator is:

$$\left|1+re^{-i4\pi f\tau}\right| = \left|\left(1+r\cos\left(4\pi f\tau\right)\right) - ir\sin\left(4\pi f\tau\right)\right| =$$

$$\sqrt{\left(1+r\cos\left(4\pi f\tau\right)\right)^2 + \left(r\sin\left(4\pi f\tau\right)\right)^2} =$$

$$\sqrt{1+r^2\cos^2\left(4\pi f\tau\right) + 2r\cos\left(4\pi f\tau\right) + r^2\sin^2\left(4\pi f\tau\right)} =$$

$$\sqrt{1+r^2+2r\cos\left(4\pi f\tau\right)}$$

UNIVERSITÀ DEGLI STUDI DI TRIESTE

A simple model: site effects due to the seismic impedance contrast

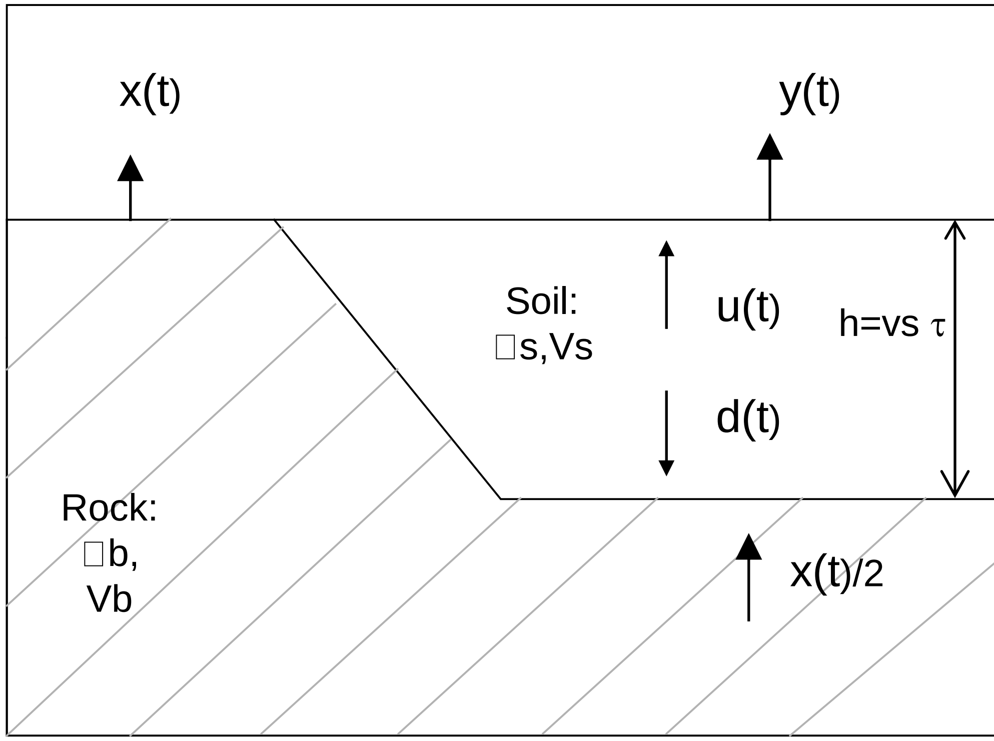

$$|H(f)| = \left(\frac{(1+r)^2}{1+2r\cos(4\pi f \tau)+r^2} \right)^{1/2}$$

$$r = \frac{p_b V_b - p_s V_s}{p_b V_b + p_s V_s} = \frac{c-1}{1+c}$$

□= h/V_s

f_o=400/(4*100)=1Hz

C = (2800*1200 / 2600*400) ~3.23

$|H(f)|$ maximum for f=f_o such that cos(4πfτ)=-1 $\Rightarrow$ $f_o = \dfrac{1}{4\tau} = \dfrac{V_s}{4h}$

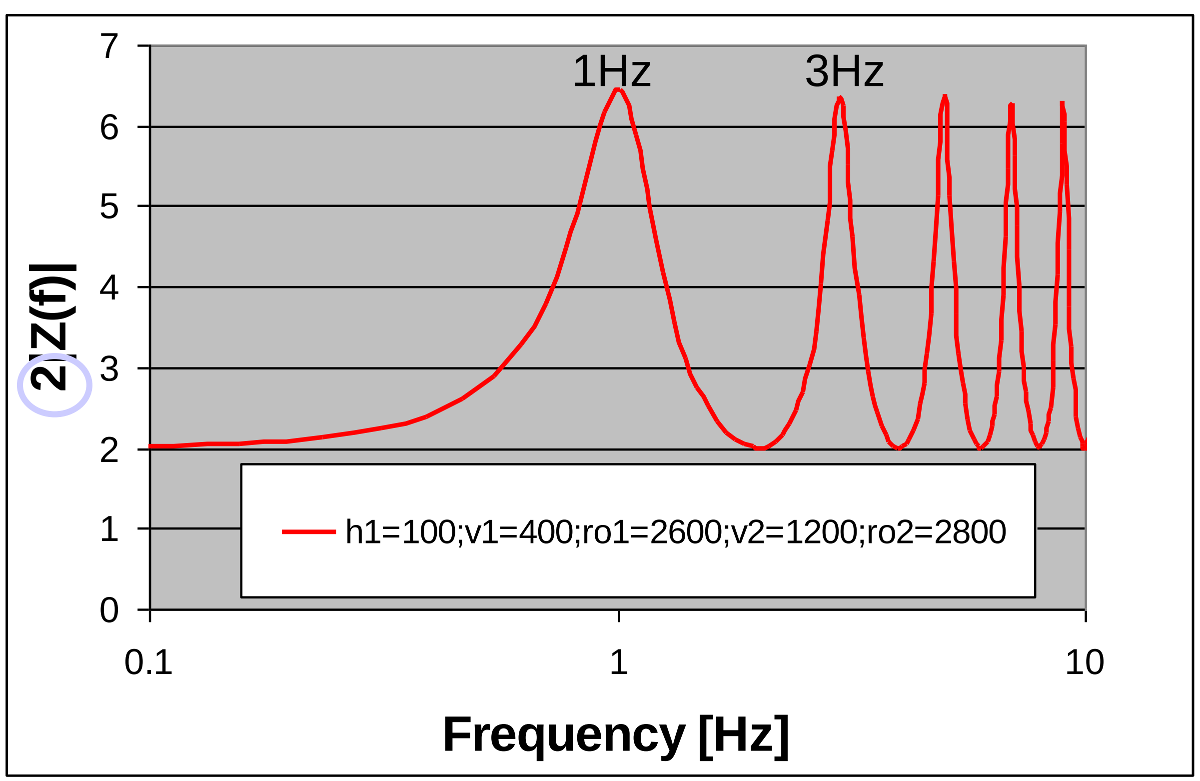

indeed we have a set of maximums at frequencies

$$f_n = \frac{V_s}{4h}(2n+1) \quad \text{with } n = 0, 1, 2, 3, \ldots$$

(n=0 fundamental mode
n>0 higher modes)

UNIVERSITÀ DEGLI STUDI DI TRIESTE

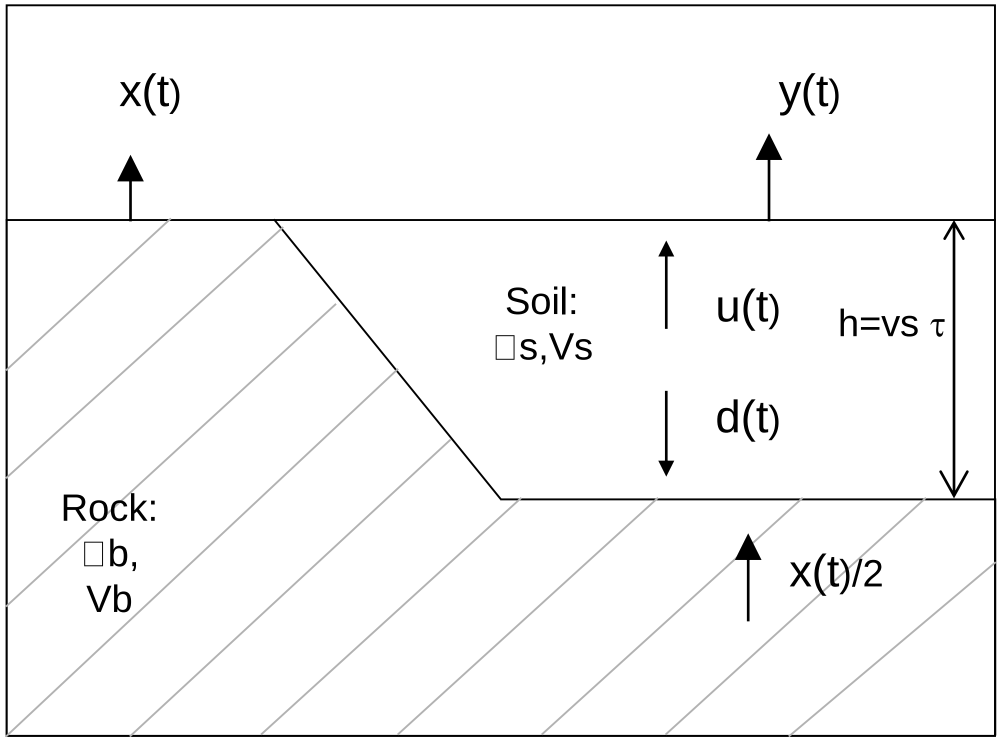

$$|H(f)| = \left(\frac{(1+r)^2}{1+2r\cos(4\pi f t)+r^2} \right)^{1/2}$$

For f=f_n $|H(f)|$ values

f_o=400/(4*100)=1Hz

C = ($\frac{2800*1200}{2600*400}$) ~3.23

$$|H(f_n)| = \left(\frac{(1+r)^2}{1-2r+r^2} \right)^{1/2} = \frac{1+r}{1-r} = c$$

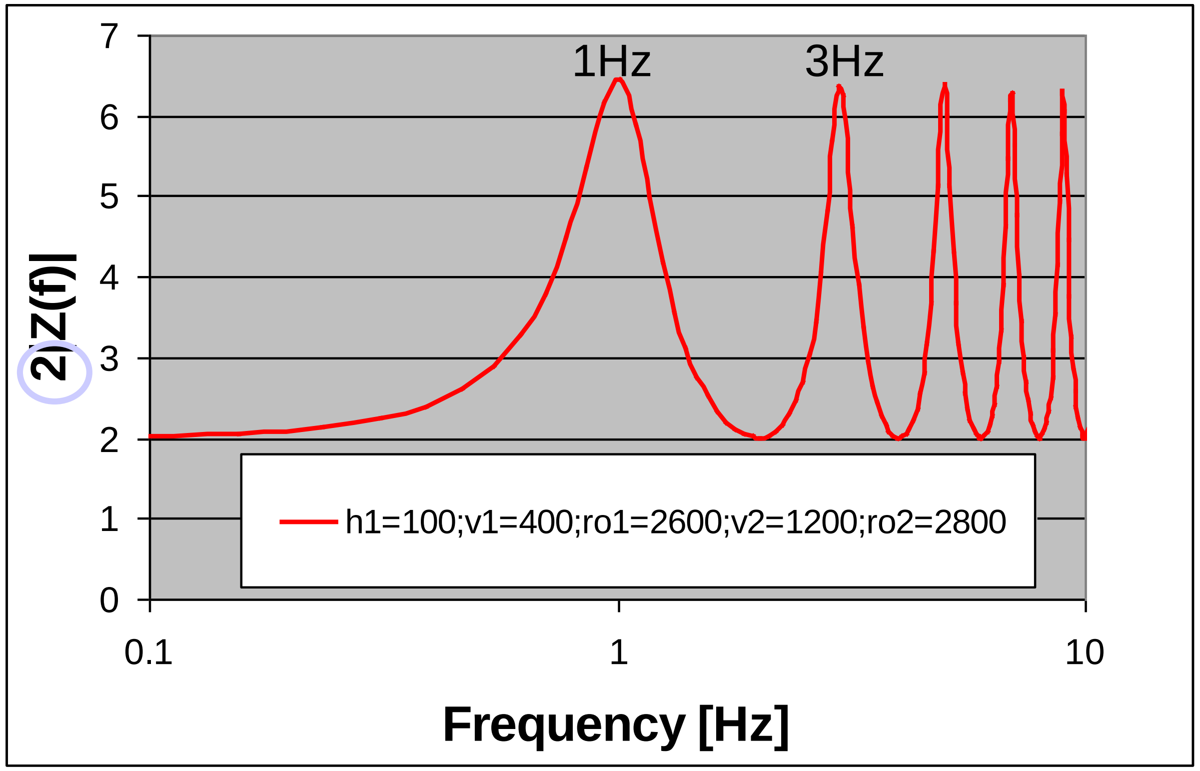

the impedance contrast determines the amplitude of the peaks (elastic layers)

If damping is accounted for and complex soil velocities are considered The reflection coefficients and the travel time become (for |r|<=1 and Q>>1):

$$r' = r - \frac{i}{4Q}$$

$$\tau' = \left(1 - \frac{i}{2Q}\right)\tau$$

Substituting these coefficients in the equation for H(f) we get:

$$H(f)=\frac{\left(1+r-\dfrac{i}{4Q}\right)e^{-i2\pi f\tau\left(1-\frac{i}{2Q}\right)}}{1+\left(r-\dfrac{i}{4Q}\right)e^{-i4\pi f\tau\left(1-\frac{i}{2Q}\right)}}$$

The modulus of the transfer function is :

$$\left|H(f)\right|=\left(\frac{\left[\left(1+r\right)^2+\dfrac{1}{\left(4Q\right)^2}\right]e^{-2\pi\tau f/Q}}{1+2\left[r\cos\left(4\pi f\tau\right)-\dfrac{1}{4Q}\sin\left(4\pi f\tau\right)\right]e^{-2\pi f\tau/Q}+\left(r^2+\dfrac{1}{\left(4Q\right)^2}\right)e^{-4\pi\tau f/Q}}\right)^{1/2}$$

UNIVERSITÀ DEGLI STUDI DI TRIESTE

For Q>0 assuming 1/4Q~0 does not cause significant errors and the modulus of the transfer function become:

$$\left|H(f)\right| = \frac{(1+r)e^{-\pi\tau f/Q}}{\left(1+2r\cos(4\pi f\tau)e^{-2\pi f\tau/Q}+r^2 e^{-4\pi\tau f/Q}\right)^{1/2}}$$

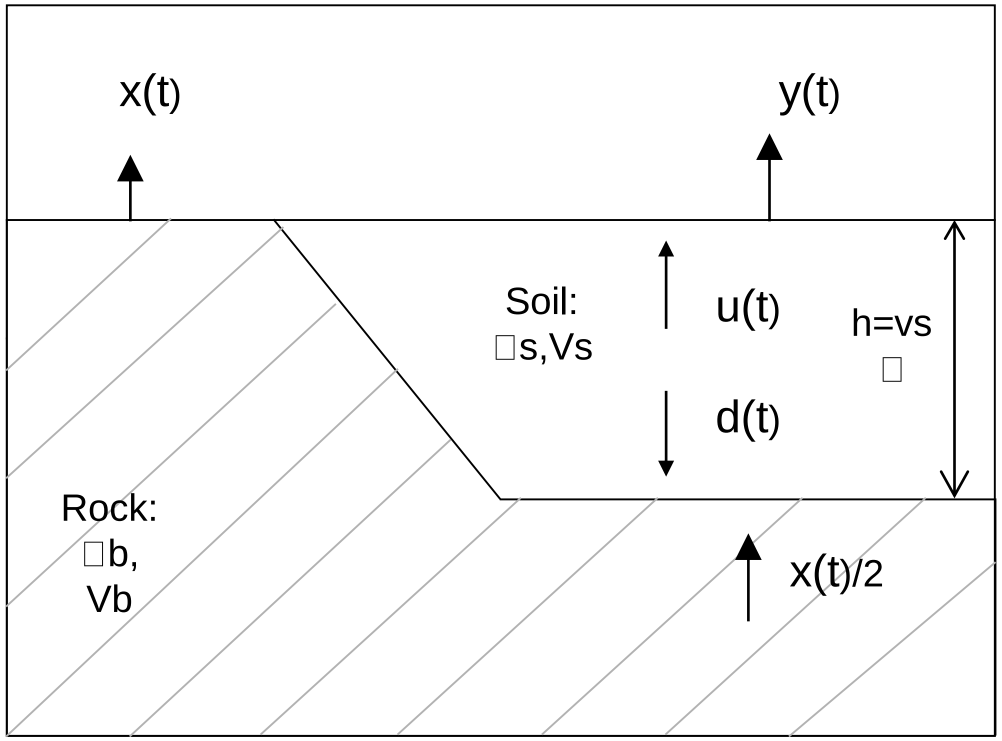

$$|H(f)| = \left(\frac{\left[(1+r)^2 + \frac{1}{(4Q)^2} \right] e^{-2\pi\tau t/Q}}{1 + 2\left[r\cos(4\pi f\tau) - \frac{1}{4Q}\sin(4\pi f\tau) \right] e^{-2\pi f\tau/Q} + \left(r^2 + \frac{1}{(4Q)^2} \right) e^{-4\pi\tau t/Q}} \right)^{1/2}$$

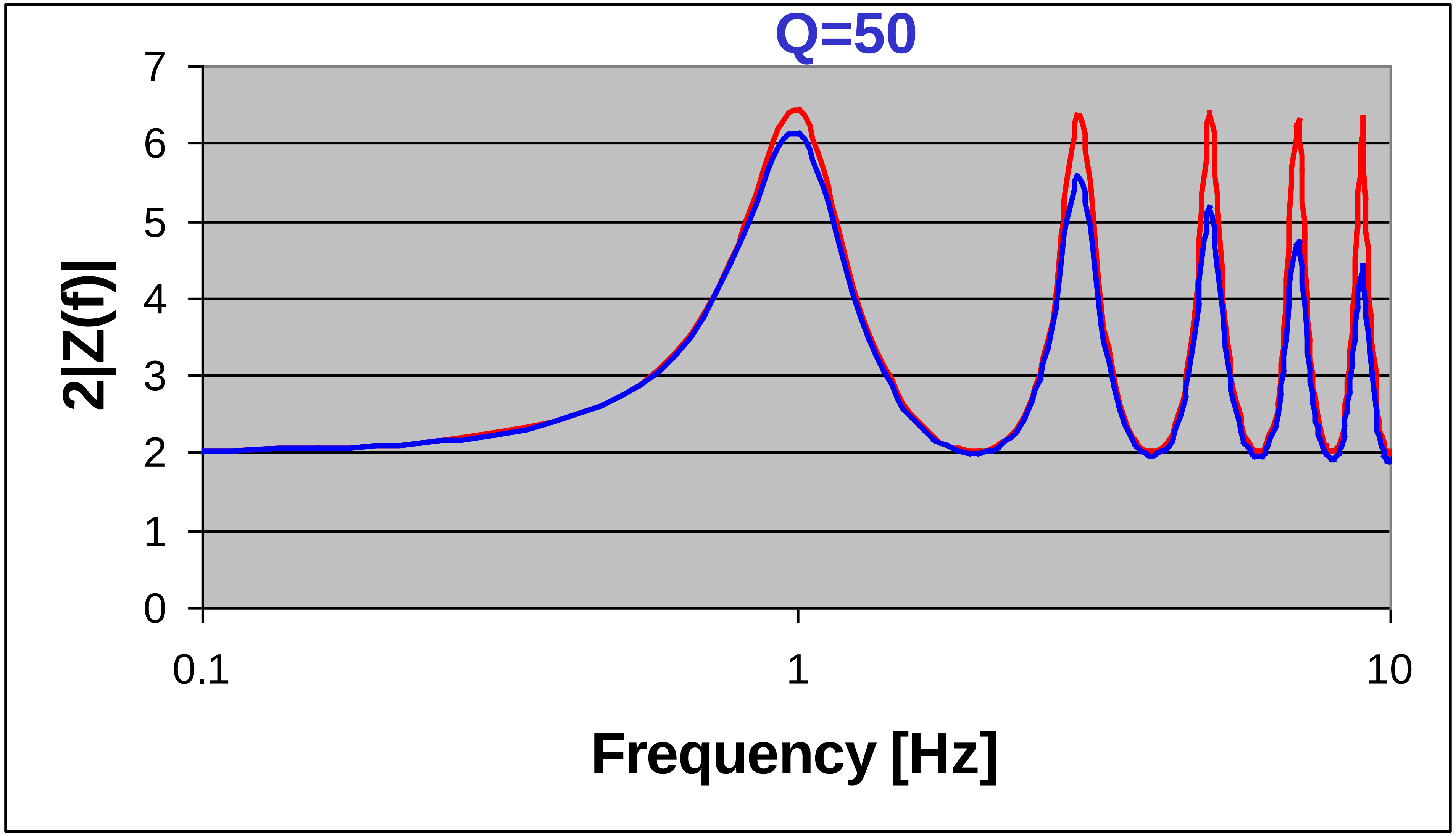

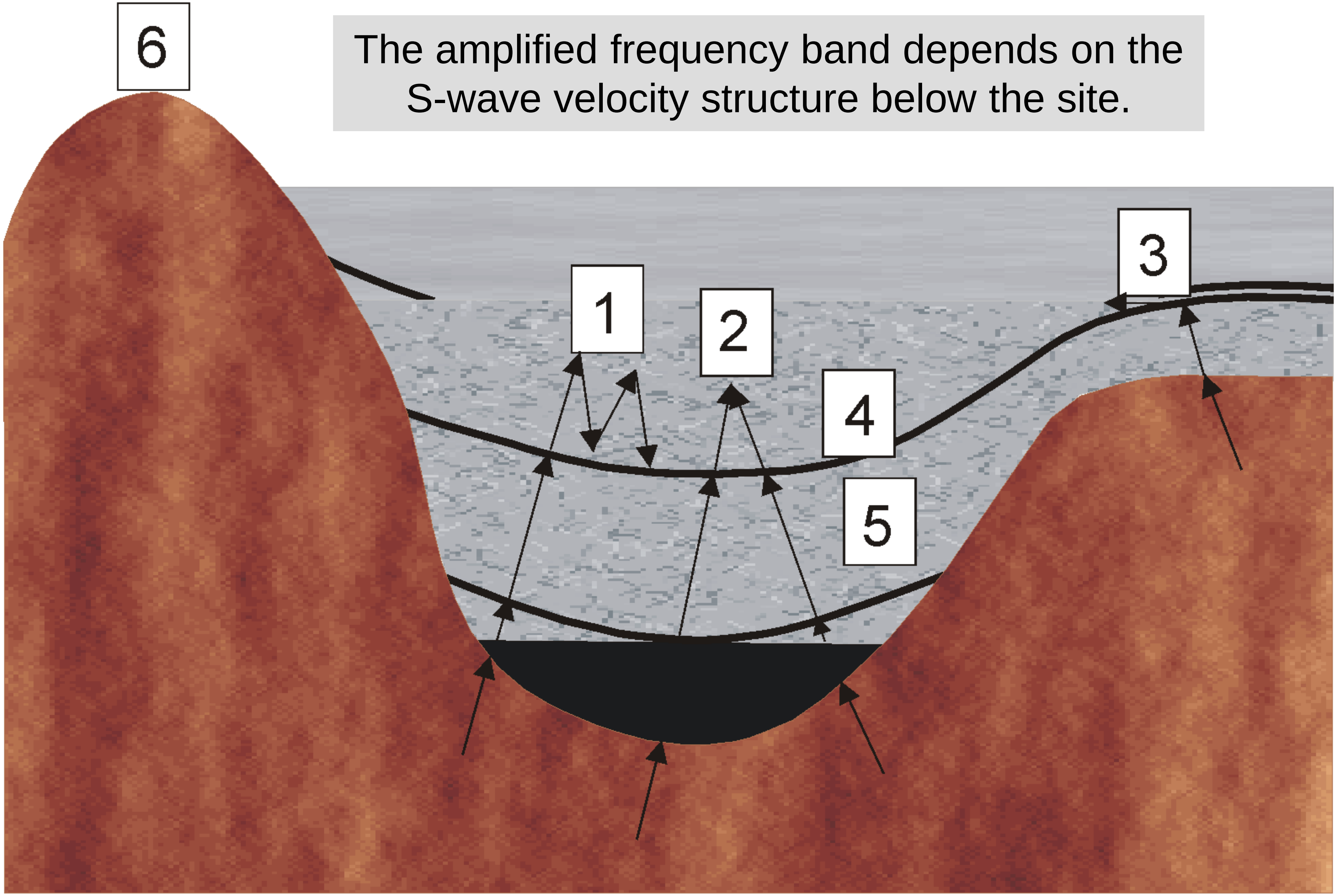

1 - Resonance due to impedance contrasts, 2 - Focusing due to subsurface topography, 3 - Body waves converted to surface waves, 4 - Water content, 5 - Randomness of the medium and 6 - Surface topography

Modified after Safak (2001)

Site effects and NTC18 - Soil classification

3.2.2 CATEGORIE DI SOTTOSUOLO E CONDIZIONI TOPOGRAFICHE

Categorie di sottosuolo

Ai fini della definizione dell'azione sismica di progetto, l'effetto della risposta sismica locale si valuta mediante specifiche analisi, da eseguire con le modalità indicate nel § 7.11.3. In alternativa, qualora le condizioni stratigrafiche e le proprietà dei terreni siano chiaramente riconducibili alle categorie definite nella Tab. 3.2.II, si può fare riferimento a un approccio semplificato che si basa sulla classificazione del sottosuolo in funzione dei valori della velocità di propagazione delle onde di taglio, V_S. I valori dei parametri meccanici necessari per le analisi di risposta sismica locale o delle velocità V_S per l'approccio semplificato costituiscono parte integrante della caratterizzazione geotecnica dei terreni compresi nel volume significativo, di cui al § 6.2.2.

Tab. 3.2.II – *Categorie di sottosuolo che permettono l'utilizzo dell'approccio semplificato.*

Categoria	Caratteristiche della superficie topografica
A	*Ammassi rocciosi affioranti o terreni molto rigidi* caratterizzati da valori di velocità delle onde di taglio superiori a 800 m/s, eventualmente comprendenti in superficie terreni di caratteristiche meccaniche più scadenti con spessore massimo pari a 3 m.
B	*Rocce tenere e depositi di terreni a grana grossa molto addensati o terreni a grana fina molto consistenti*, caratterizzati da un miglioramento delle proprietà meccaniche con la profondità e da valori di velocità equivalente compresi tra 360 m/s e 800 m/s.
C	*Depositi di terreni a grana grossa mediamente addensati o terreni a grana fina mediamente consistenti* con profondità del substrato superiori a 30 m, caratterizzati da un miglioramento delle proprietà meccaniche con la profondità e da valori di velocità equivalente compresi tra 180 m/s e 360 m/s.
D	*Depositi di terreni a grana grossa scarsamente addensati o di terreni a grana fina scarsamente consistenti*, con profondità del substrato superiori a 30 m, caratterizzati da un miglioramento delle proprietà meccaniche con la profondità e da valori di velocità equivalente compresi tra 100 e 180 m/s.
E	*Terreni con caratteristiche e valori di velocità equivalente riconducibili a quelle definite per le categorie C o D*, con profondità del substrato non superiore a 30 m.

Site effects and NTC18 - $V_{S,eq}$

Subsurface classification is made on the basis of stratigraphic conditions and values of the equivalent shear wave propagation velocity, $V_{S,eq}$ (in m/s), defined by :

$$V_{S,eq} = \frac{H}{\sum_{i=1,N} \frac{h_i}{V_{S,i}}} \quad [m/s]$$

With h_i thickness of the i-th layer; $V_{S,i}$ velocity of shear waves in the i-th layer; N number of layers; H depth of the substrate, defined as that formation consisting of very rigid rock or soil, characterized by VS not less than 800 m/s

For deposits with substrate depth H greater than 30 m, the equivalent shear wave velocity $V_{S,eq}$ is defined by the parameter $V_{S,30}$, obtained by placing H=30 m in the above expression and considering the properties of the soil layers up to that depth.

Multi Hazard and Multi Risk

FIGURE 2.19

From 'single-hazard' to 'multirisk' assessment and terminology adopted here.
Source: courtesy of author

Single-hazard Only one hazard considered	**Single-risk** Risk in a single-hazard framework
Multilayer single-hazard More than one hazard No hazard interactions	**Single-risk** Risk in a multilayer single-hazard framework No interactions on the vulnerability level
Multihazard More than one hazard Hazard interactions considered	**Multihazard risk** Risk in a multihazard framework No interactions on the vulnerability level
	Multirisk Risk in a multihazard framework Interactions on the vulnerability level considered

Difficulties arise because different hazards differ in their nature, return period and intensity, as well as the effects they may have on exposed elements

Zschau 2017

Multi Hazard and Multi Risk

In order to assist decision-makers in the field of DRM in their prioritizing of mitigation actions, one has to understand the relative importance of different hazards and risks for a given region.

A first step towards a full multirisk assessment, is to consider a **multilayer single-hazard/ risk assessment** approach, ignoring the interactions but harmonising and standardising the assessment procedures among the different perils.

Standardisation schemes use:

• **matrices** — hazard matrix, vulnerability
matrix and risk matrix;
• **indices** — hazard index, vulnerability index and risk index;
• **curves** — hazard curves, vulnerability curves and risk curves.

FIGURE 2.19

From 'single-hazard' to 'multirisk' assessment and terminology adopted here.
Source: courtesy of author

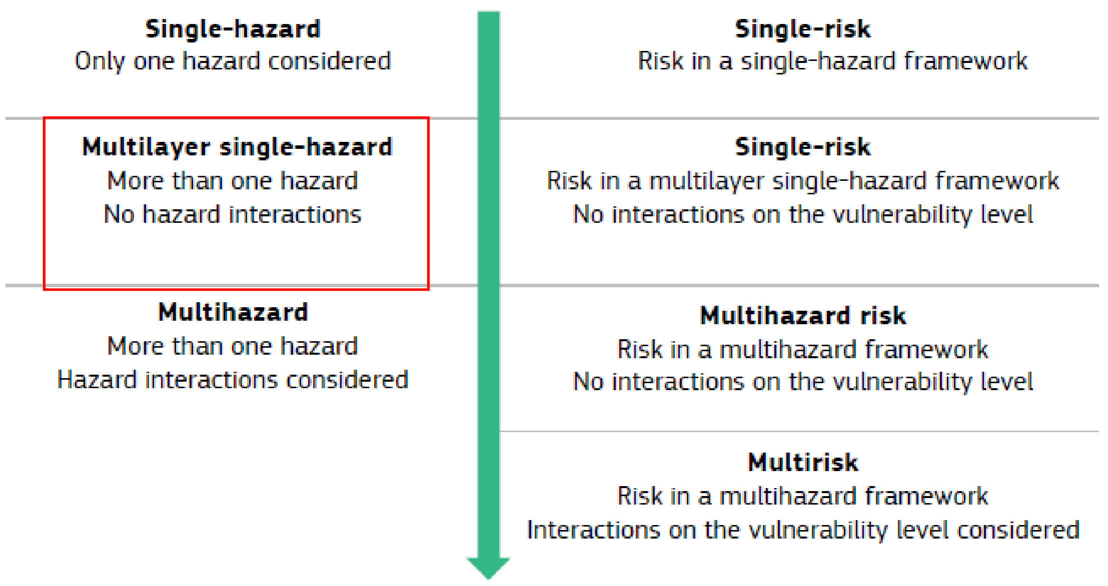

Zschau 2017

Multi Hazard and Multi Risk

Multilayer single risk hazard

A **hazard matr**ix applies a colour code to classify certain hazards by the intensity and frequency (occurrence probabilities) determined qualitatively, for instance ‘low’, ‘moderate’ and ‘high

If applied to vulnerability it is the damage matrix (e.g. link to the EMS-98 scale)

Swiss hazard matrix
Source: Kunz and Hurni (2008)

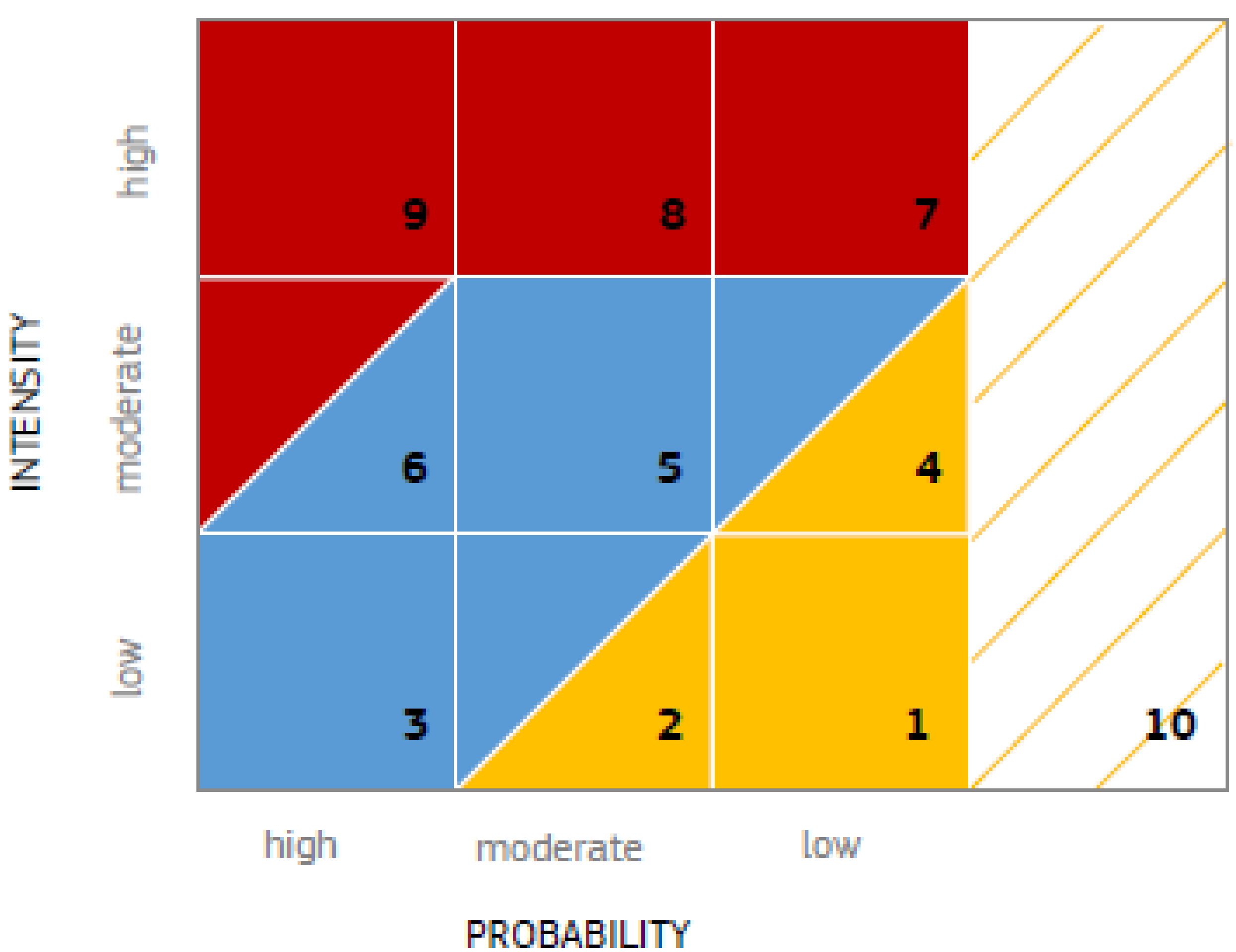

FIGURE 2.19

From ‘single-hazard’ to ‘multirisk’ assessment and terminology adopted here.
Source: courtesy of author

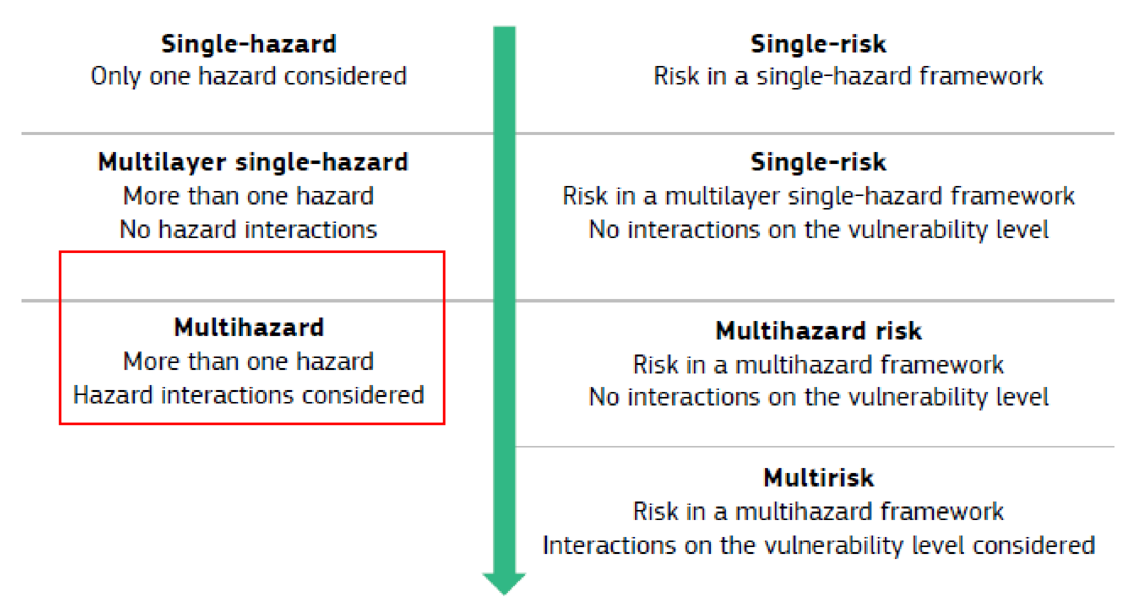

Zschau 2017

Multi Hazard and Multi Risk

Multilayer single risk hazard

For the aim of comparing and aggregating risks coming from multiple hazards, assessment procedures are required that combine both hazard and vulnerability information.

The European Commission (2010) proposed a risk matrix that relates the two dimensions, likelihood (probability) and impact (loss), for a graphical representation of multiple risks in a comparative way

Swiss hazard matrix
Source: Kunz and Hurni (2008)

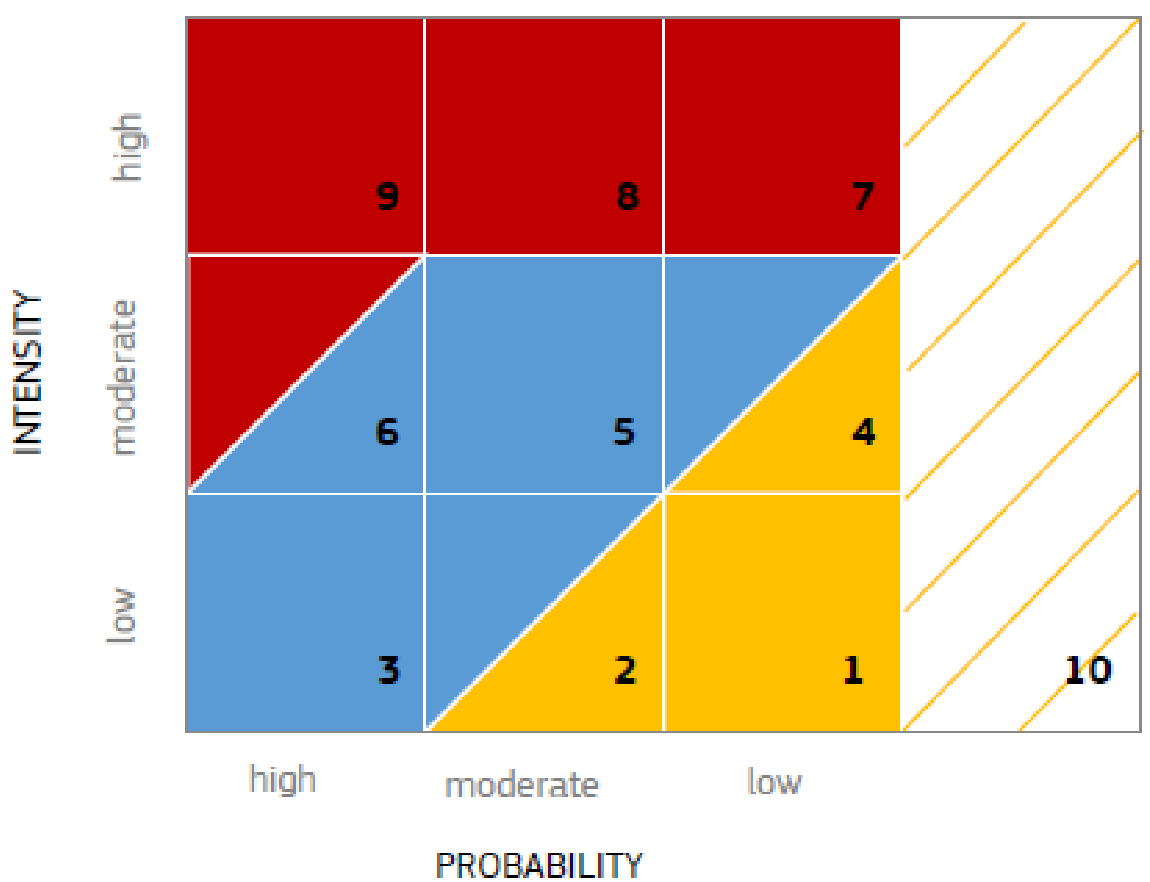

FIGURE 2.19

From 'single-hazard' to 'multirisk' assessment and terminology adopted here.
Source: courtesy of author

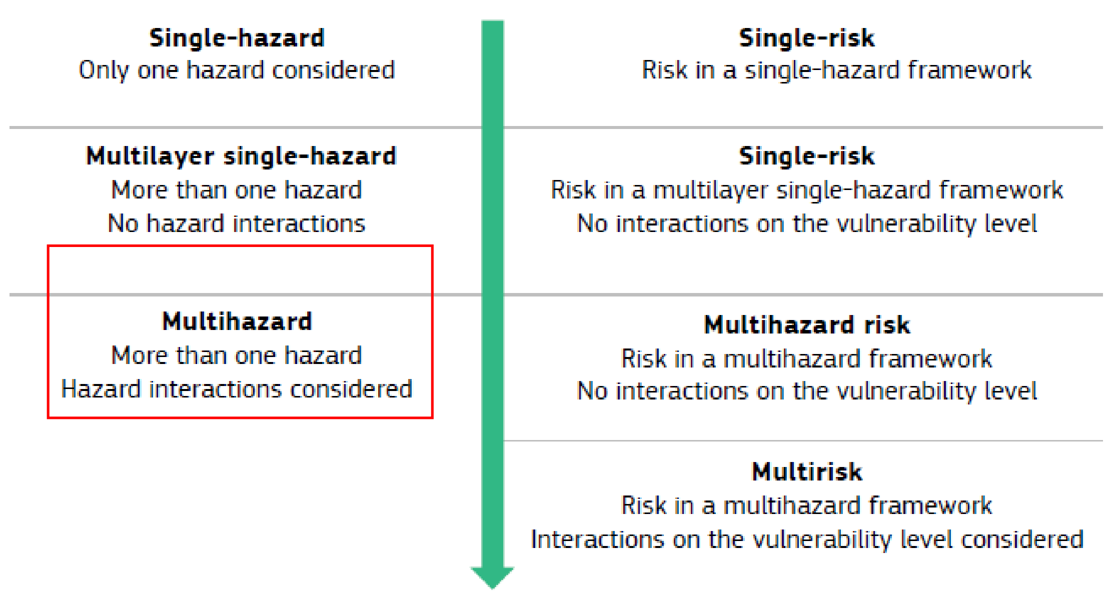

Zschau 2017

Multi Hazard and Multi Risk

Multilayer single risk hazard

More quantitative methods for assessing natural threats in a multilayer single-hazard approach are based on '**curves**' ('functions').

Hazard curves present the exceedance probabilities for a certain hazard's intensities in a given period. Vulnerability curves graphically relate the loss or the conditional probability of loss exceedance to the intensity measure of a hazard (for instance ground motion, wind speed or ash load) in order to quantify the vulnerability of elements at risk. When the probability of exceeding certain damage levels is considered, the curves are referred to as 'fragility curves'

One may easily combine vulnerability curves with the corresponding hazard curves to arrive at a measure of risk. This could be the average loss per considered period, the so-called average annual loss or expected annual loss, if the period is 1 year.

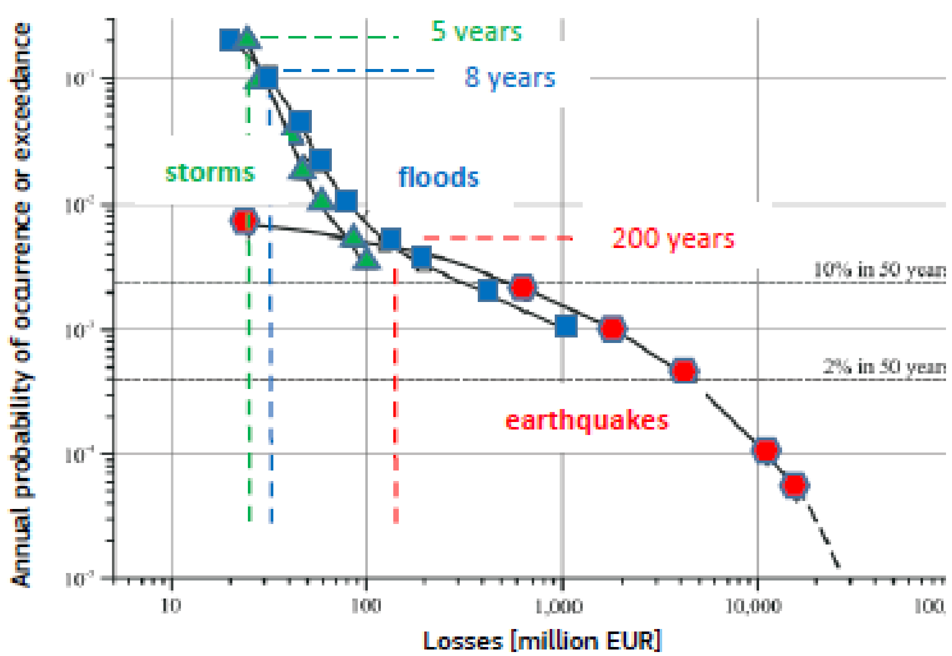

Risk curves and their aggregations for the city of Cologne
Source: Fleming et al. (2016)

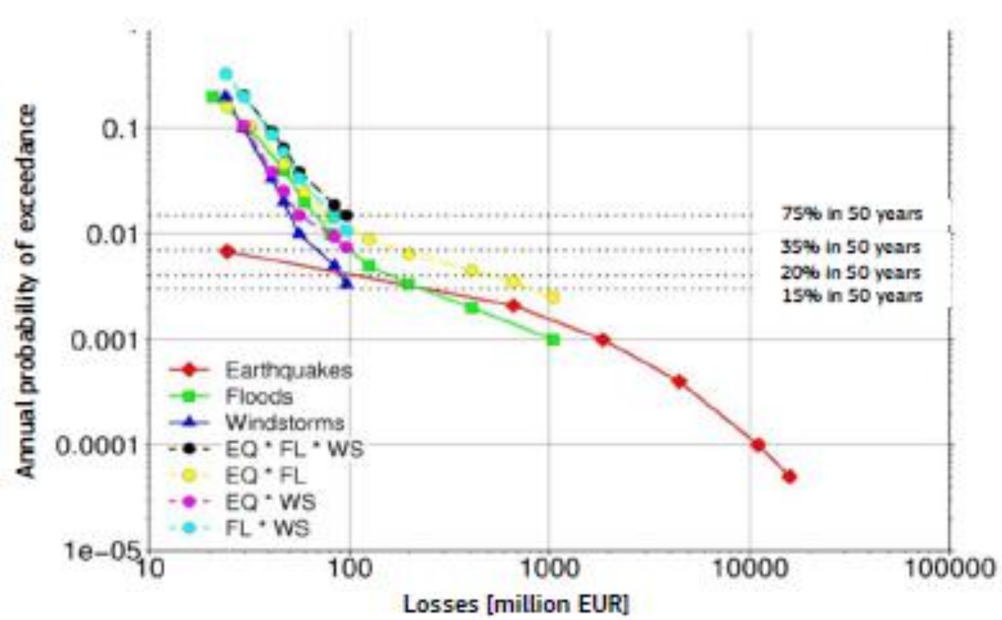

Zschau 2017

Multi Hazard and Multi Risk

Multilayer single risk hazard

To compare high-probability and low-consequences events with low-probability and high-consequences ones, probabilities and loss can simply be multiplied (P×L)

In the case of a single-risk scenario with a given annual probability, the loss-probability-product directly represents the average annual loss (impact). This is not the case for the risk curve, which includes the loss from all possible hazard intensities.

Thus, one may learn which curve, in terms of return periods, will contribute most to the average annual loss

Risk curves and P x L - curves for the city of Cologne (Exceedance probability versus loss (left) and versus its product with loss (right)
Source: courtesy of author

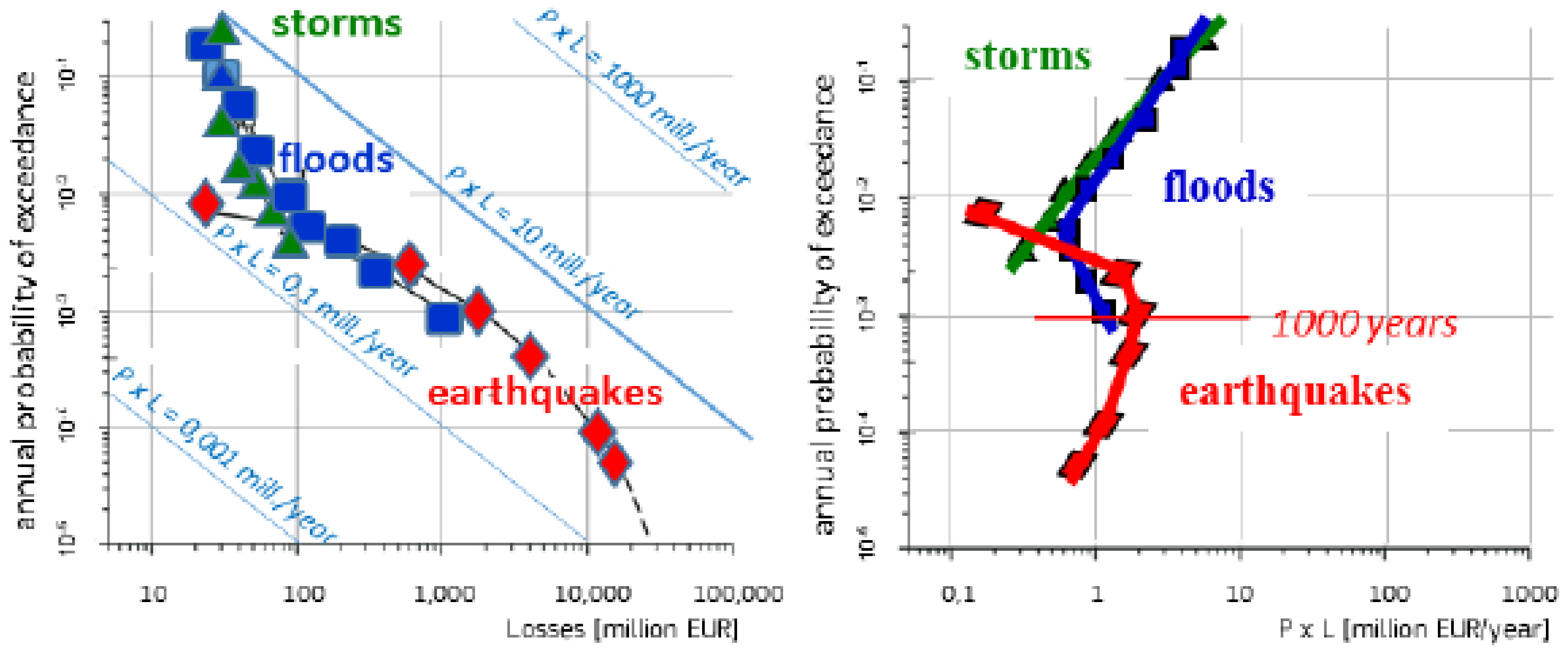

Zschau 2017

Multi Hazard and Multi Risk

Hazard interactions: cascading events and co.

In a complex system like nature, processes are very often dependent on each other, and interact. There are various kinds of interactions between hazards that often lead to significantly more severe negative consequences for the society than when they act separately. A multilayer single-risk perspective does not consider this, but a multihazard approach does.

BOX 2.1

Classification of hazard interactions

Source: Gill and Malamud (2014, 2016)

(1) Triggering relationship
(2) Increased probability relationship
(3) Decreased probability relationship
(4) Coincidence relationship
(5) Catalysis/ impedance relationship

Zschau 2017

Multi Hazard and Multi Risk

Hazard interactions: Semi-quantitative approach, hazard interaction matrices

Matrix approach for the identification of hazard interactions.
Source: Liu et al. (2015)

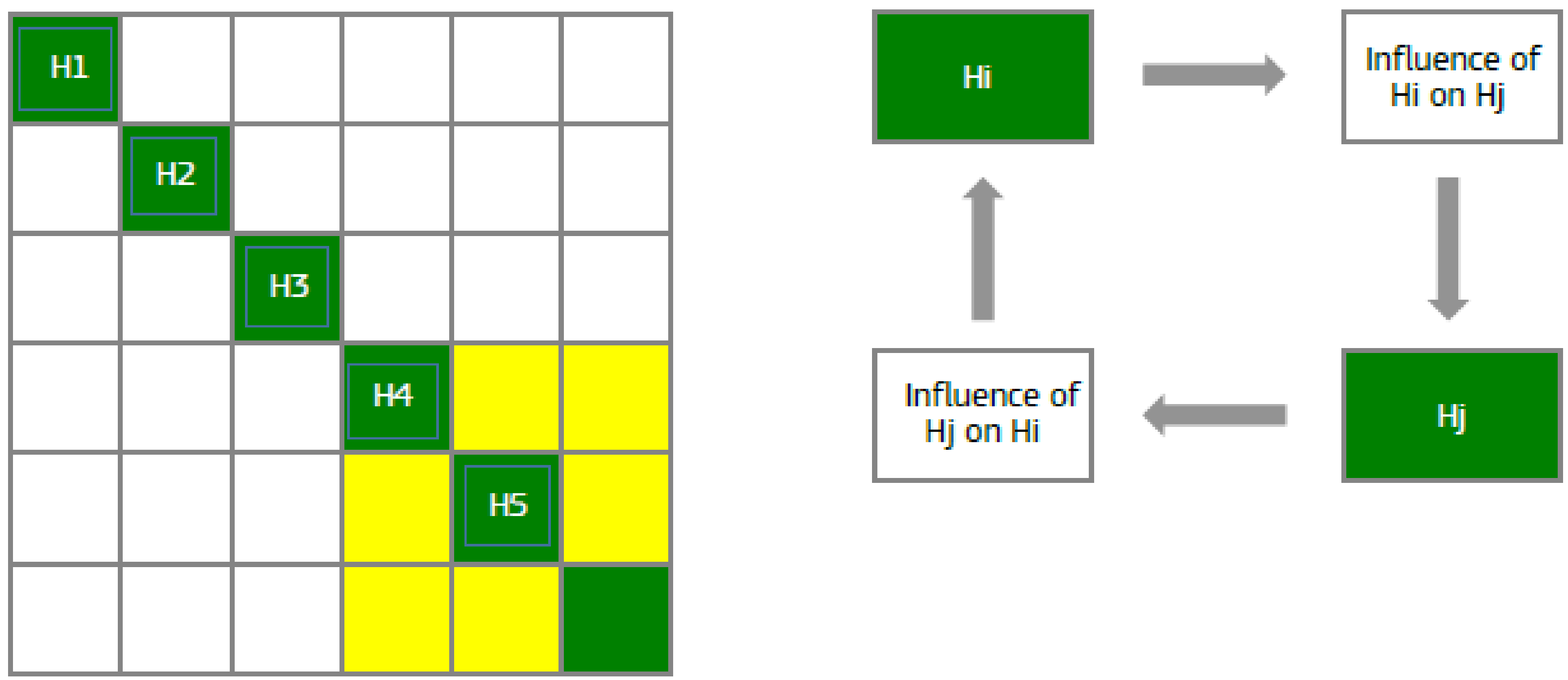

Slides (H4)	2	2	0 – No interaction
0	Debris flows (H5)	2	1 – Weak interaction 2 – Medium interaction
1	1	River floods (H6)	3 – Strong interaction

Slides (H4)	Deposits only	Cut off a flow in a water course
No interaction	Debris flows (H5)	Change of river bed morphology
Erosion / saturation of deposits	Re-mobilisation of deposits	River floods (H6)

Zschau 2017

Multi Hazard and Multi Risk

Hazard interactions: Quantitative method, tree and fault tree strategies

Event tree scheme for eruption forecasting
Source: Selva et al. (2012)

A probabilistic approach is used for quantifying each branch of the tree

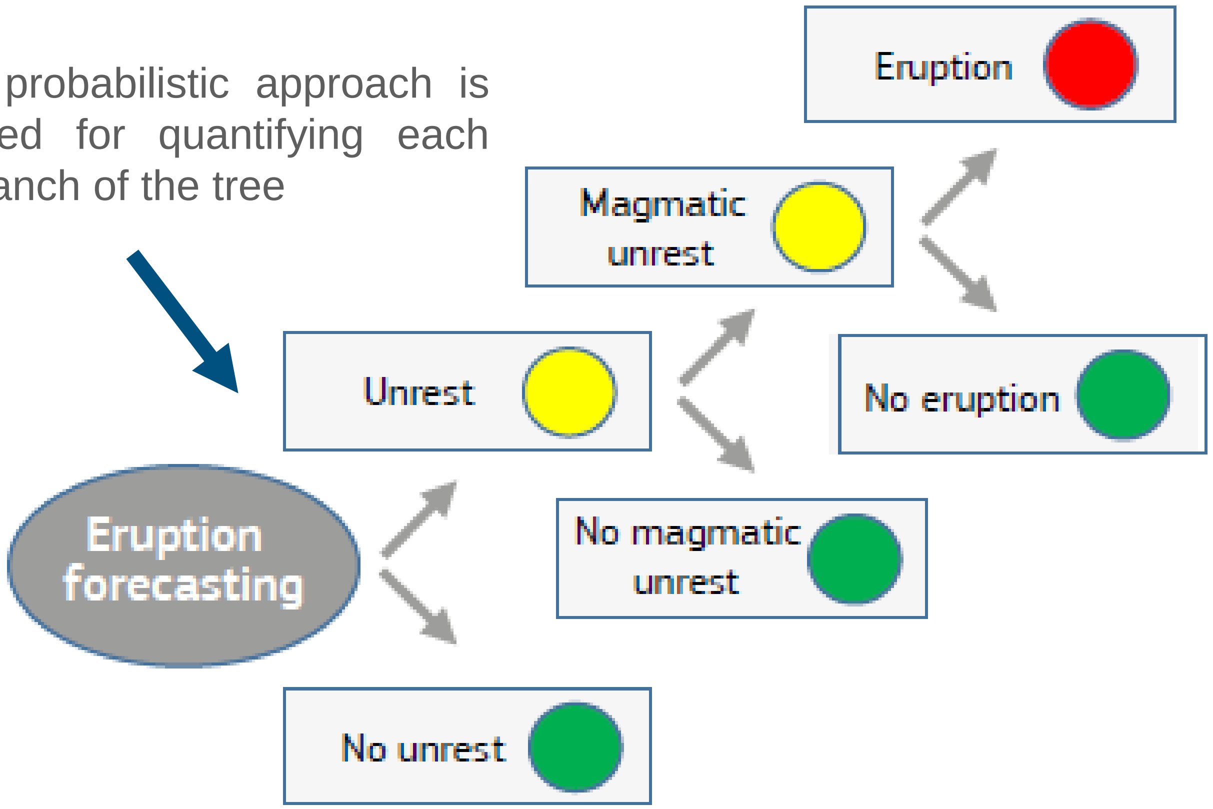

Example of a hazard surface, Hij, describing hazard interaction as a probability surface that depends on all possible intensities, Ai and Bj, of the primary event 'A' and of the secondary event 'B', respectively
Source: Garcia-Aristizabal and Marzocchi (2013)

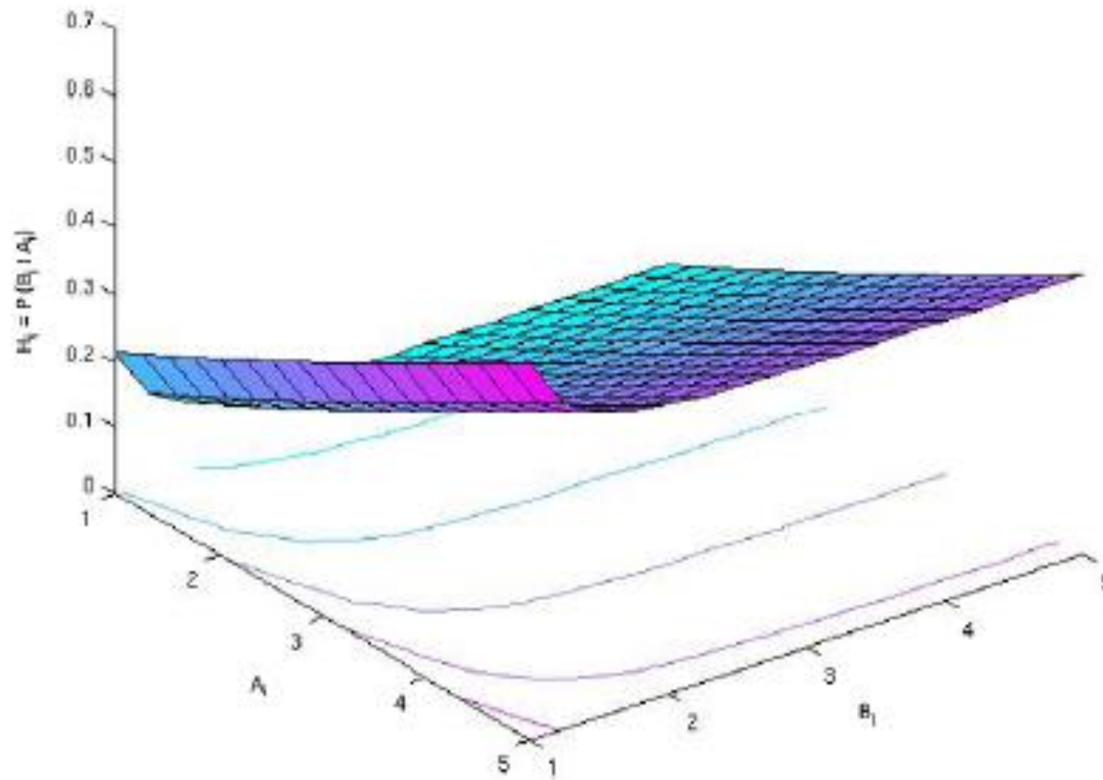

Zschau 2017

Multi Hazard and Multi Risk

Dynamic vulnerability: Time and state dependent

Time dependent: More or less gradual changes of vulnerability with time.

State dependent: depends on a certain state of a system that may change abruptly, due to a natural hazard event

Two examples of state-dependent seismic vulnerability: pre-damage-dependent vulnerability (above) and load-dependent vulnerability (below)
Source: Mignan (2013)

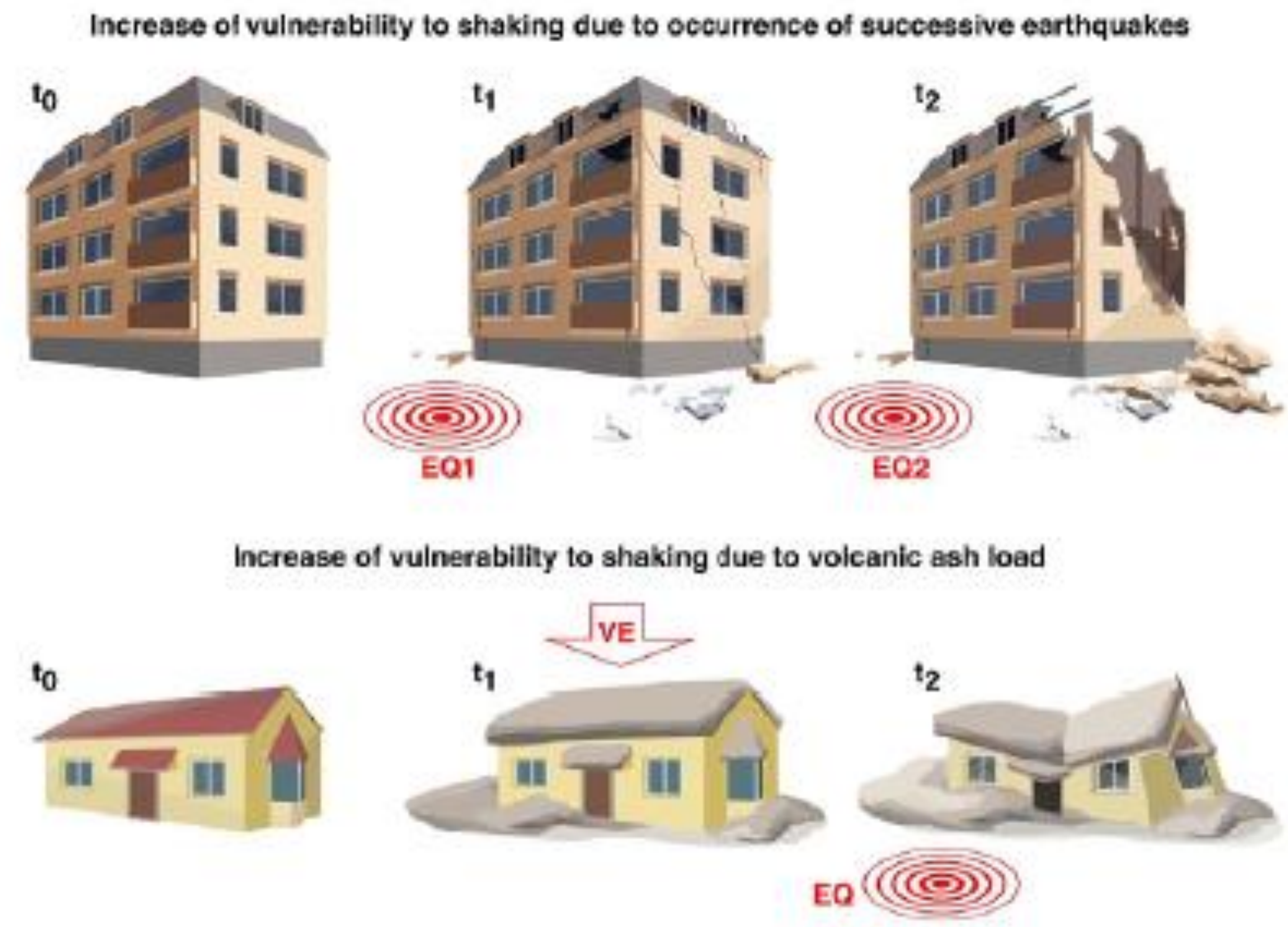

Zschau 2017

Multi Hazard and Multi Risk

Integration into a probabilistic framework
Multi risk framework

Integration of interaction on the vulnerability/fragility level: fragility/vulnerability surfaces

Ash load-dependent, two-dimensional seismic fragility surface
Source: Garcia-Aristizabal and Marzocchi (2013)

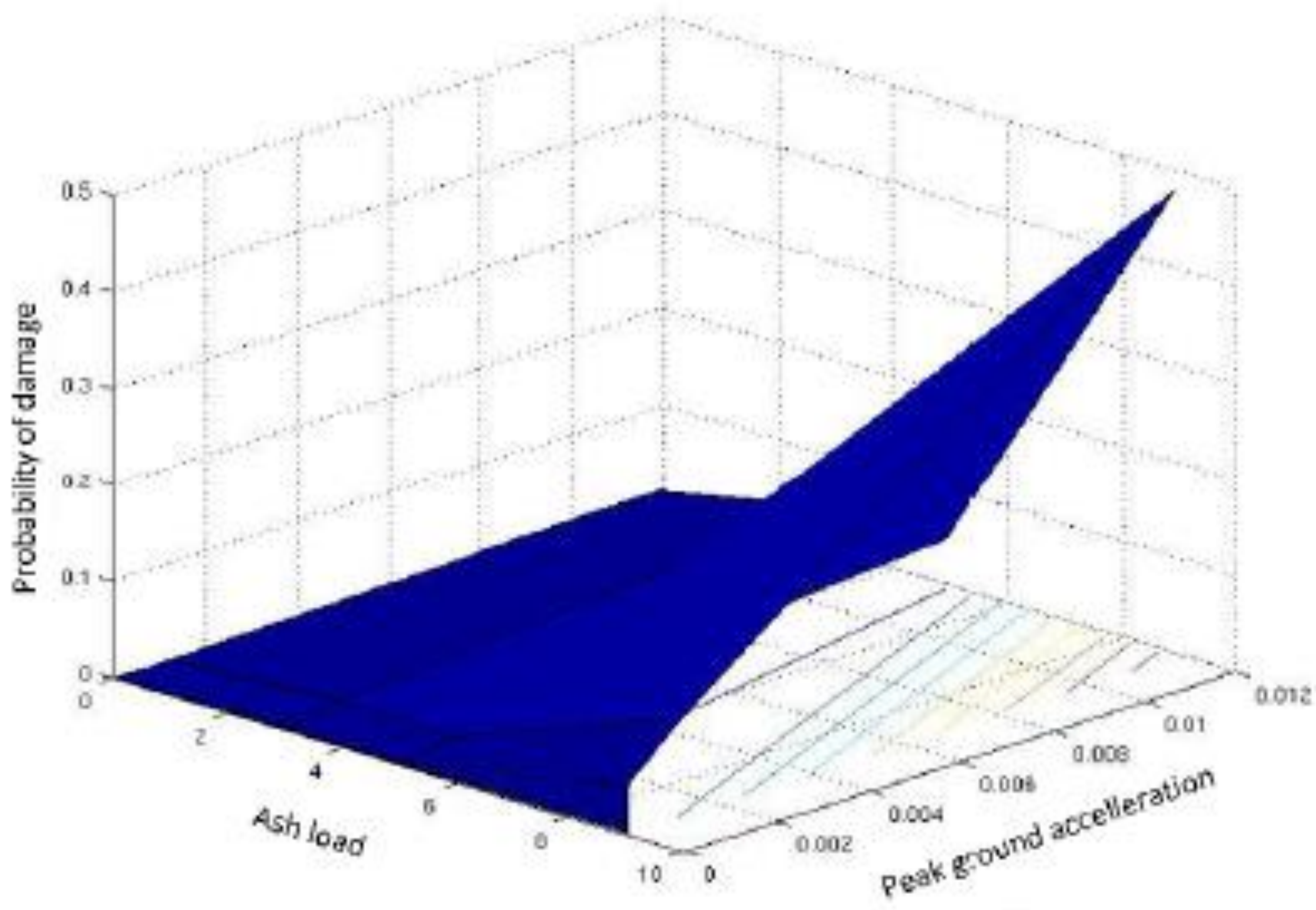

Zschau 2017

Uncertainties in single risk analysis: seismic risk

Two different types of uncertainties are usually identified, depending on their nature – namely, "**aleatory**" and "**epistemic**".

The part of the **total uncertainty** related to the inherent variability in the behaviour of a system is commonly known as **aleatory** uncertainty (sometimes referred to as "randomness").

The other part, which is related to the state of knowledge about the system under consideration, is known as **epistemic uncertainty**.

Epistemic uncertainty can be reduced by collecting additional relevant information and improving the state of knowledge, while the aleatory uncertainty is not reducible and, in principle, cannot be dealt with using deterministic approaches.

However, it should also be kept in mind that a given source of uncertainty cannot often be neatly separated into these types, with many sources containing elements of both.

Tyagunov et al., 2014

Uncertainties in single risk analysis: seismic risk

The example of Cologne (Germany)

Seismic Hazard: PSHA in terms of macroseismic intensities with respect to the European Macroseismic Scale (EMS-98, Grünthal, 1998)

Seismic vulnerability modelling is based on the vulnerability classification of EMS-98

The damage probability matrices were constructed following the guidelines of the EMS-98

Only direct monetary losses due to structural damage to residential buildings are taken into account.
The level of losses is estimated in terms of mean damage ratio (**MDR**), determined as the **cost of repair over the total cost of the damaged buildings**, as well as in monetary terms, taking into consideration the estimated construction costs of residential buildings in Germany

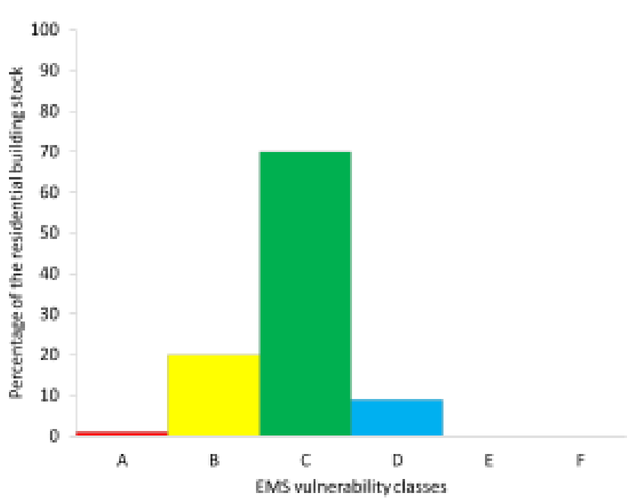

Figure 4. Vulnerability composition model of the residential building stock of Cologne as a percentage of the different vulnerability classes of EMS-98 (based on the INFAS database, 2010).

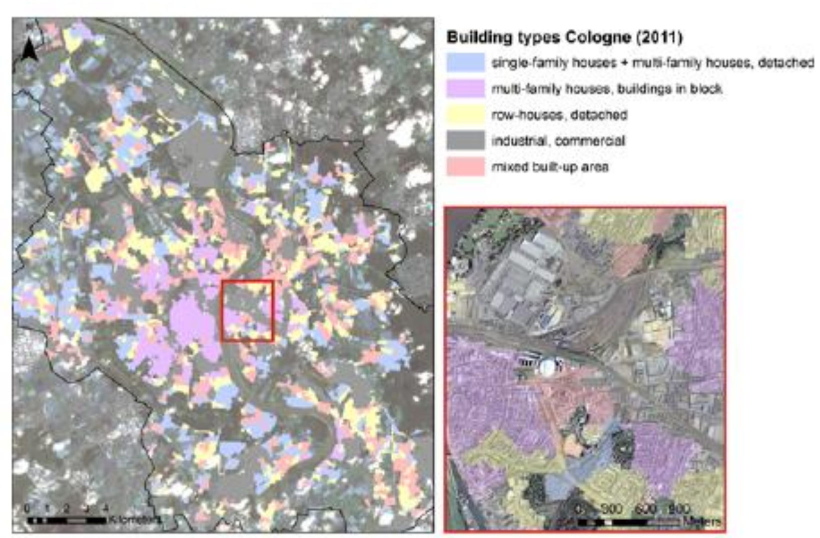

Figure 5. Building type stratification of the study area of Cologne: **(a)** superimposed on input Landsat image and **(b)** a magnification superimposed on Google Earth imagery.

Tyagunov et al., 2014

Uncertainties in single risk analysis: seismic risk

The example of Cologne (Germany)

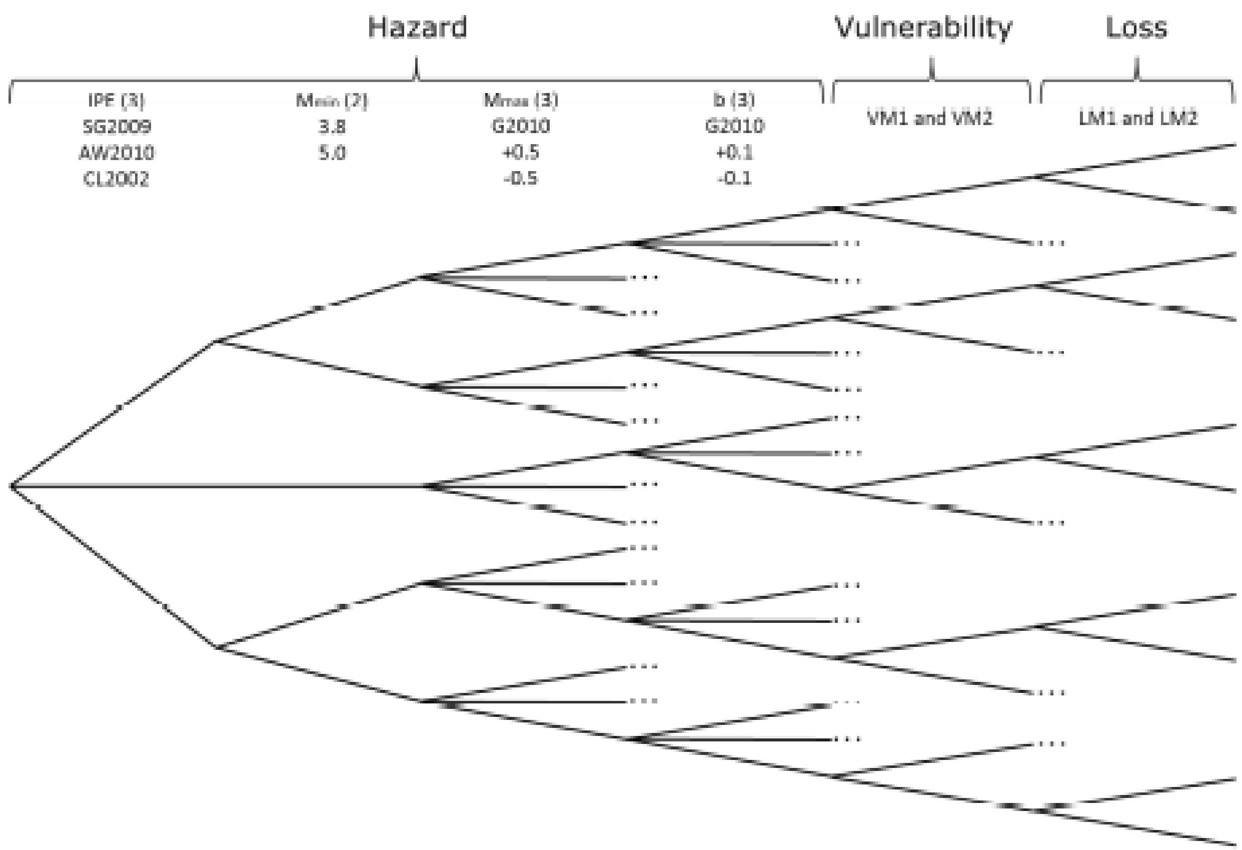

Figure 1. Logic tree scheme and number of input parameters for the different modules: Hazard: intensity prediction equations (IPEs) – 3, M_{min} – 2, M_{max} – 3, Gutenberg–Richter b – 3, Vulnerability: 2 models, Loss: 2 models. Equal weights are assigned to all the branches of the logic tree (more details in the text).

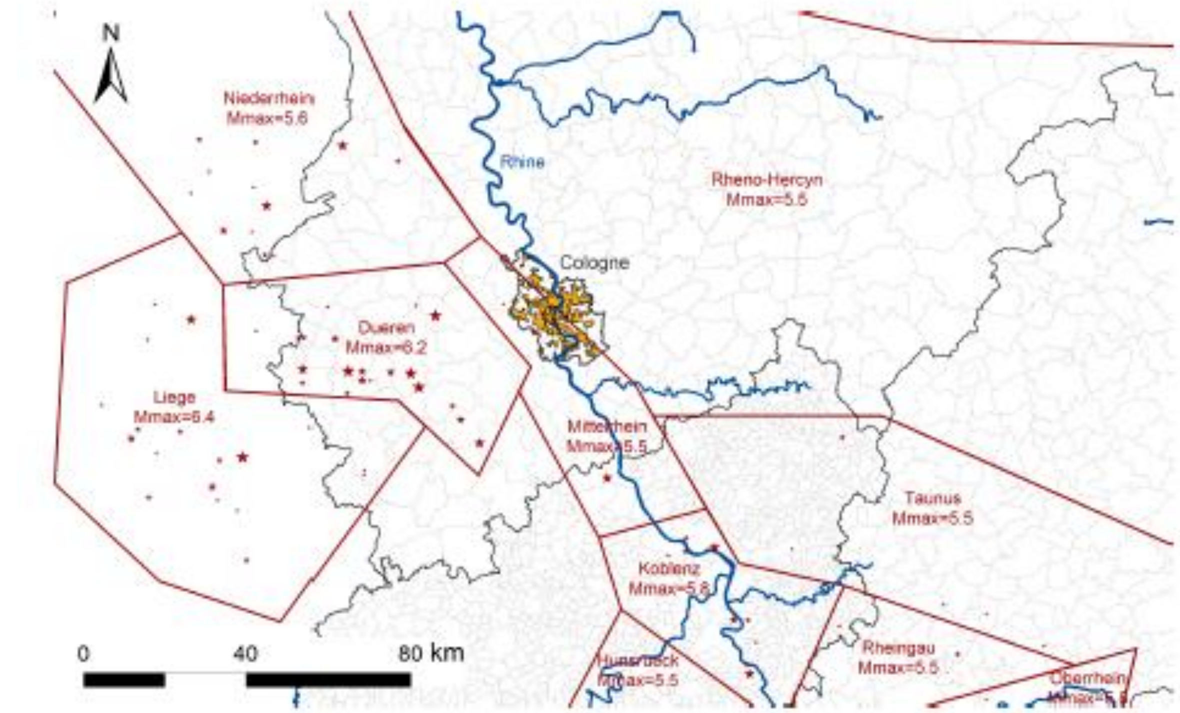

Figure 2. Seismic source zones (SSZs) around Cologne (according to Grünthal et al., 2010). The stars show the epicentres of past earthquakes in the area (from the CENEC earthquake catalogue, Grünthal et al., 2009). The grey lines show the administrative boundaries. The built-up area in Cologne is shown in yellow.

Tyagunov et al., 2014

Uncertainties in single risk analysis: seismic risk

The example of Cologne (Germany)

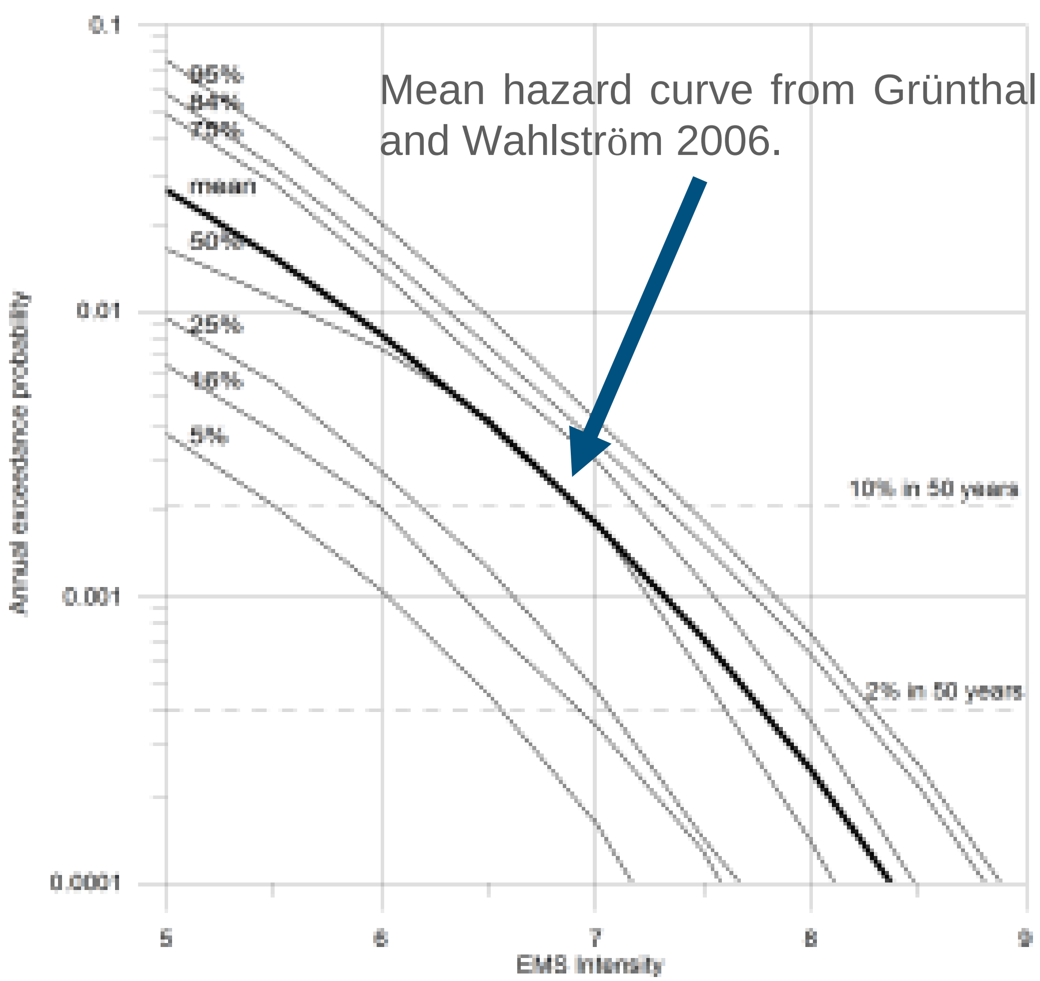

Figure 3. Calculated mean and quantile hazard curves, considering the whole range of the input parameters of the hazard part of the logic tree (Fig. 1).

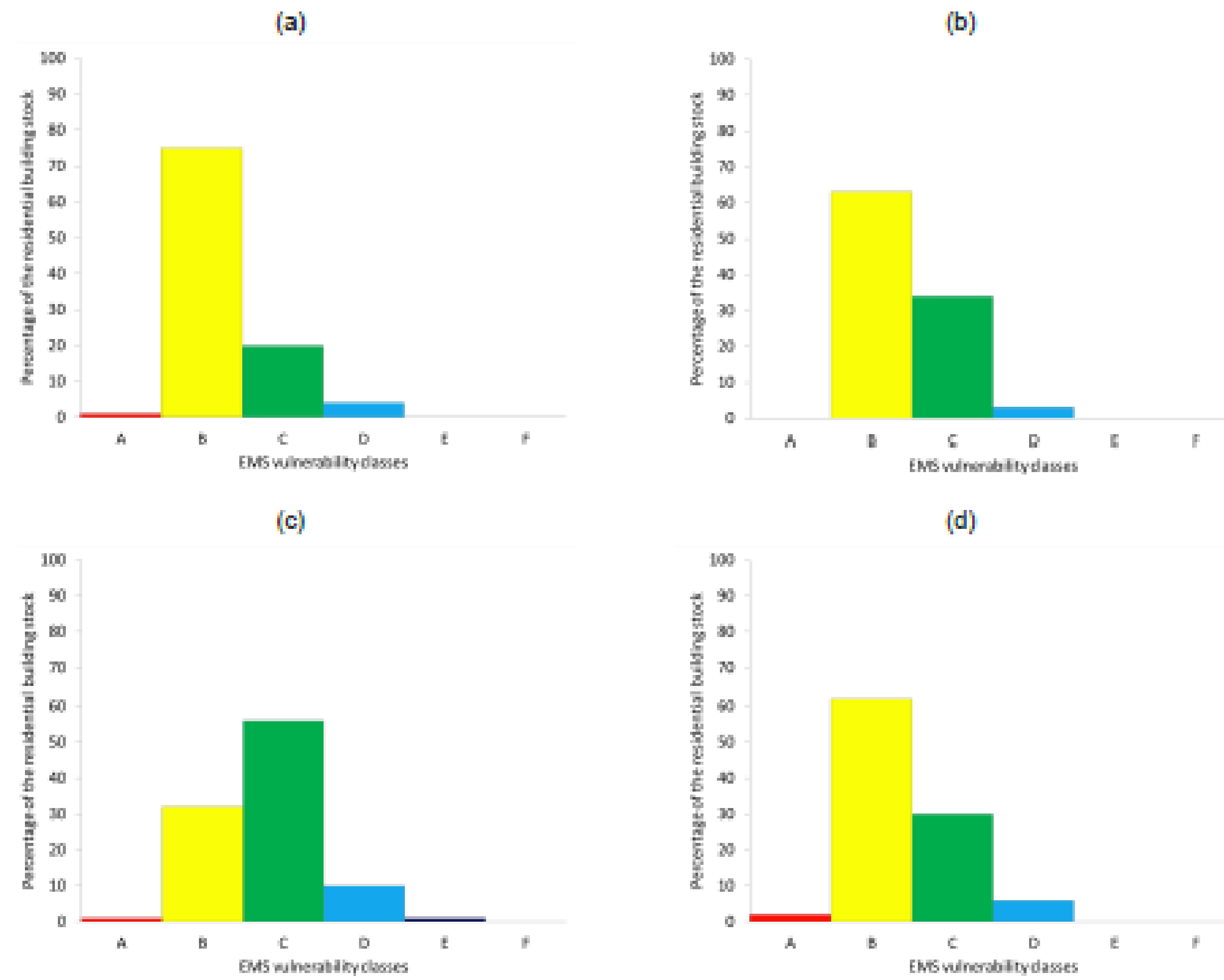

Figure 6. Vulnerability composition models (as a percentage of the vulnerability classes of EMS-98) for the classified urban typology strata of Cologne as outlined in Fig. 5: **(a)** mixed built-up area; **(b)** row houses, detached; **(c)** multi-family houses, buildings in blocks; **(d)** single-family houses and multi-family houses, detached.

Tyagunov et al., 2014

Uncertainties in single risk analysis: seismic risk

The example of Cologne (Germany)

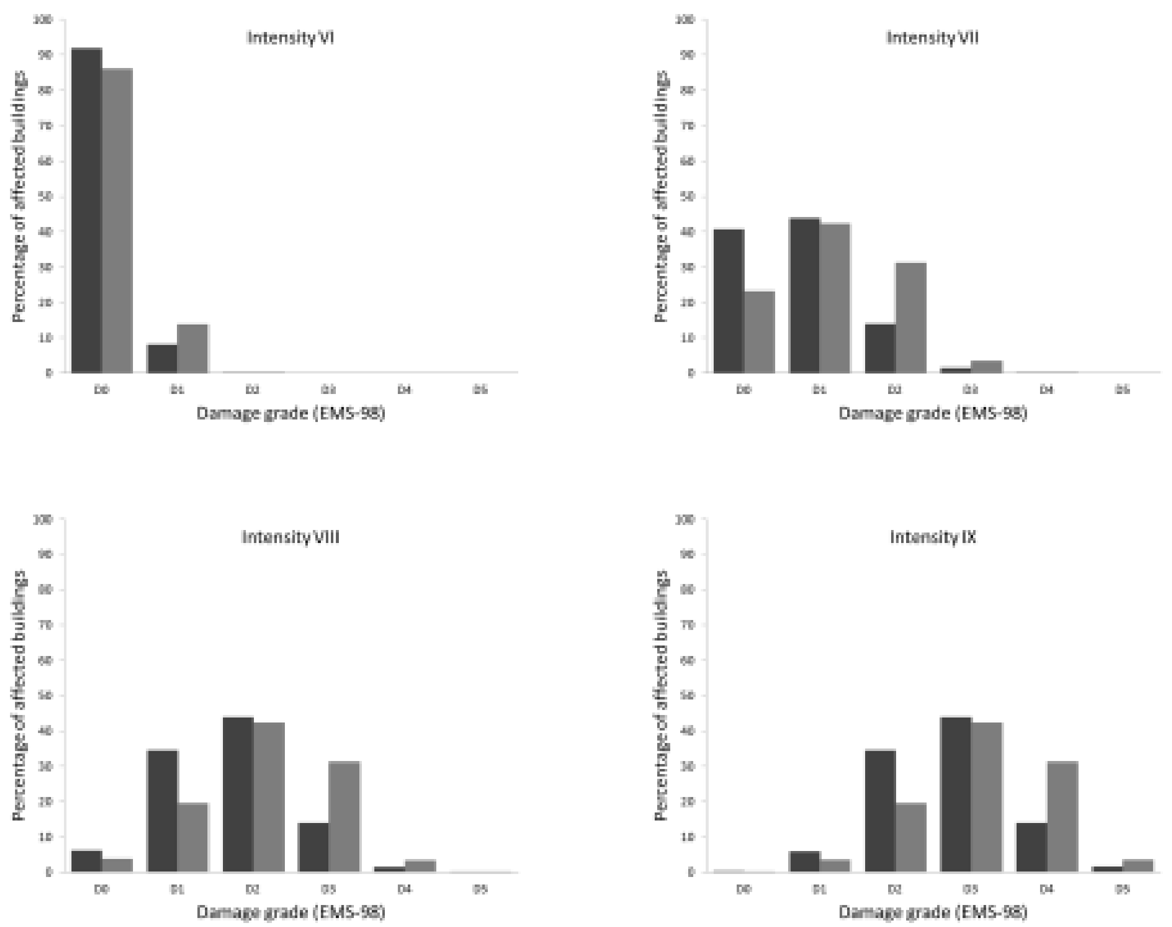

Figure 7. Structural damage distribution diagrams for the two vulnerability models for different levels of EMS intensity (VM1 – dark grey, VM2 – light grey).

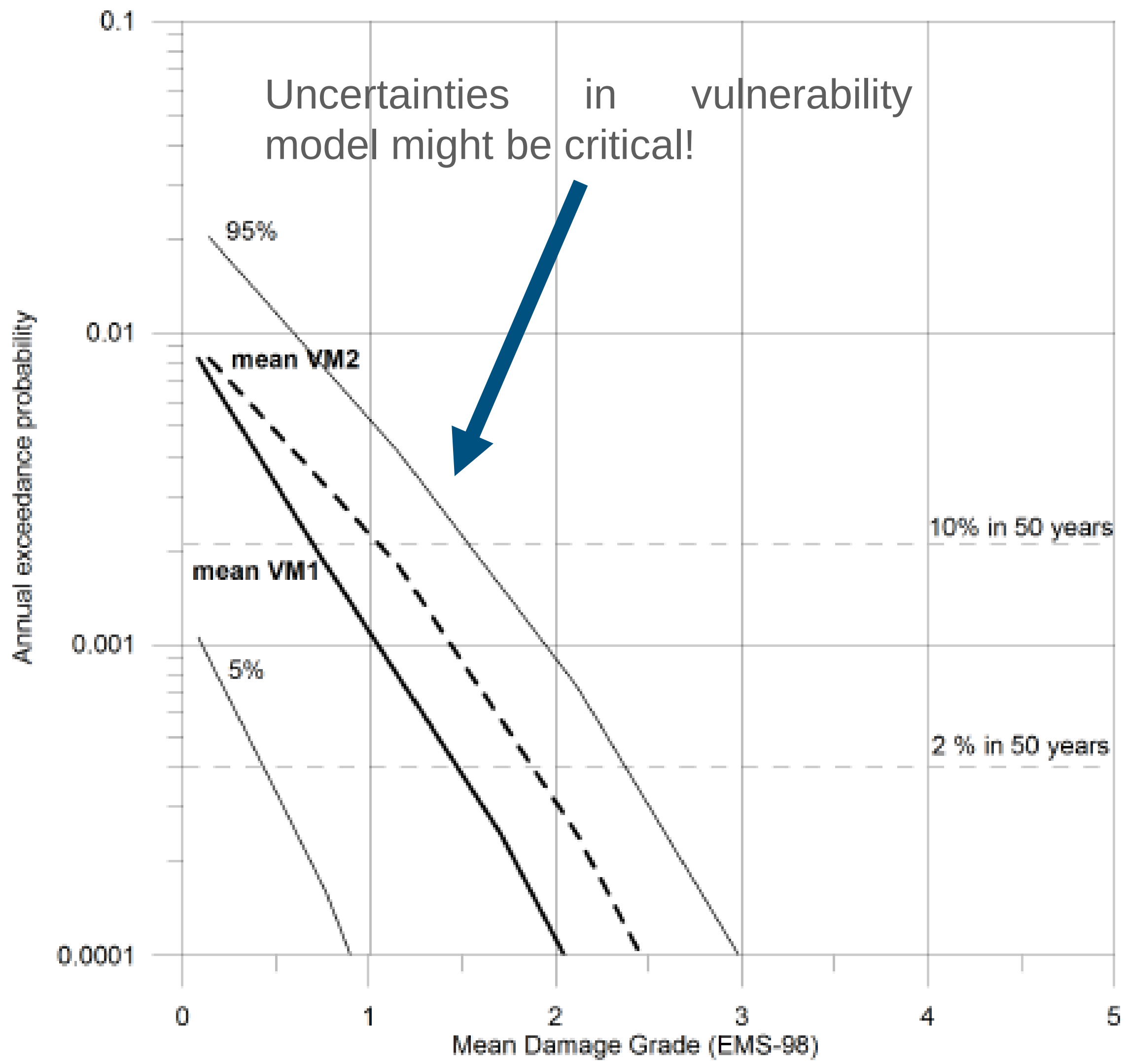

Figure 8. Structural damage probability estimation (in terms of mean damage grade) for the residential building stock of Cologne. The solid line corresponds to the mean estimate for VM1, the dashed line for VM2. The uncertainty bounds (5 and 95 %) correspond to the total uncertainty.

Tyagunov et al., 2014

Multi Hazard and Multi Risk

The example of Cologne (Germany)

Table 1. The loss models employed in this study.

Damage grade	Loss model 1 (Tyagunov et al., 2006a)		Loss model 2 (Hwang et al., 1994)	
	Loss ratio (%)	Central value (%)	Loss ratio (%)	Central value (%)
0	0	0	0	0
1	0–1	0.5	0.05–1.25	0.3
2	1–20	10	1.25–7.50	3.5
3	20–60	40	7.50–20	10
4	60–100	80	20–90	65
5	100	100	90–100	95

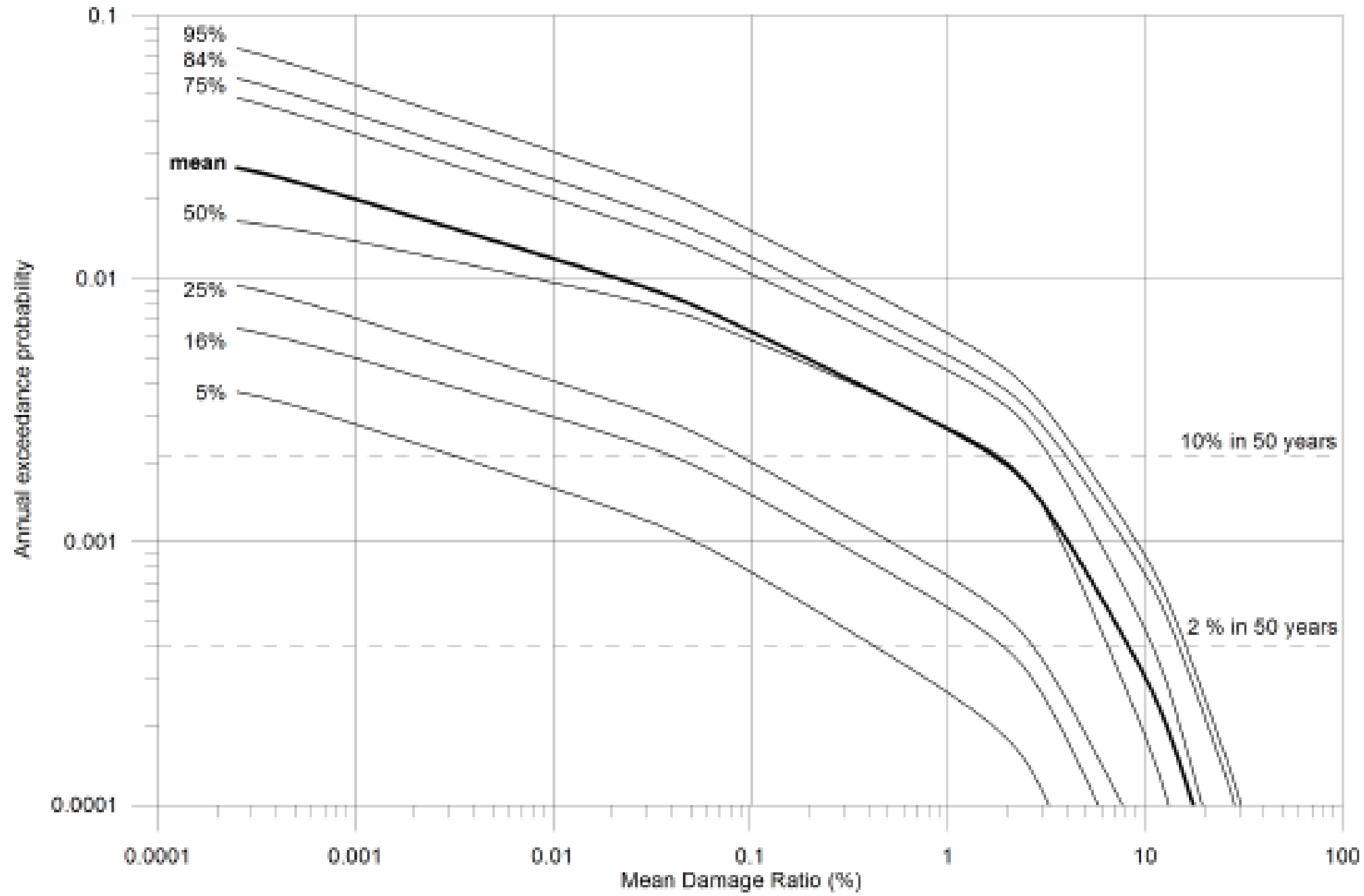

Figure 9. Calculated mean and quantile risk curves (in terms of MDR) for the whole range of the logic tree branches (Fig. 1).

Tyagunov et al., 2014

UNIVERSITÀ DEGLI STUDI DI TRIESTE

Multi Hazard and Multi Risk

The example of Cologne (Germany)

Sensitivity analysis

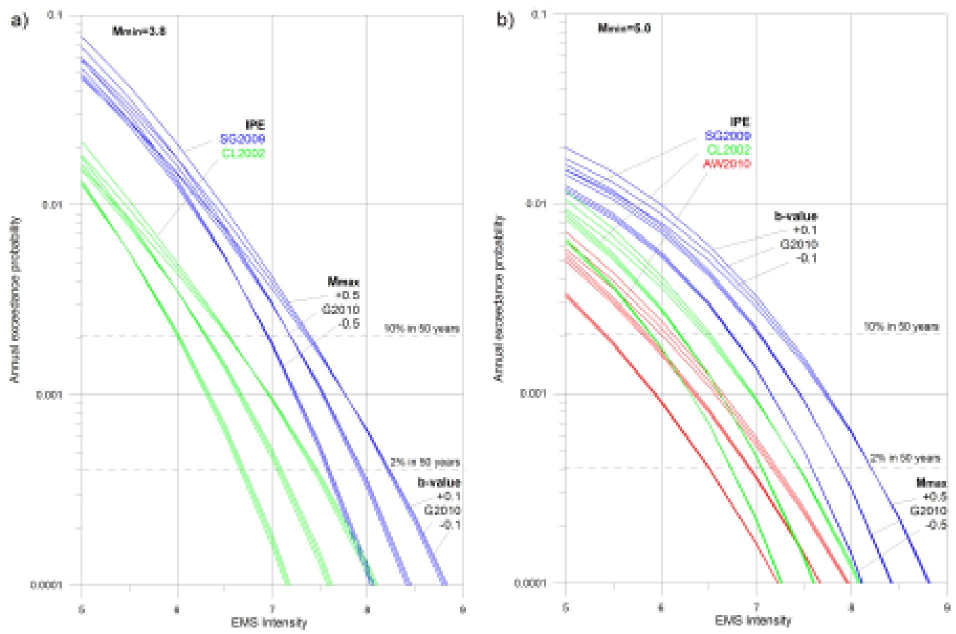

Figure 10. Hazard curves calculated for different combinations of the input parameters: **(a)** for $M_{\min} = 3.8$ and IPE from Stromeyer and Grünthal (2009) and Chandler and Lam (2002), **(b)** for $M_{\min} = 5.0$ and all three considered IPE.

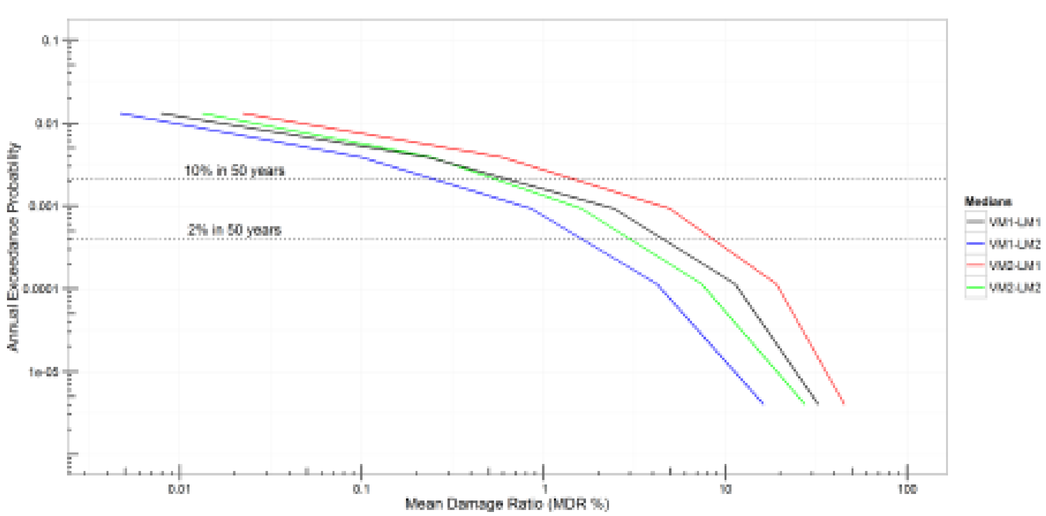

Figure 12. Comparison of the median estimates of seismic risk for the four different combinations of the vulnerability (VM) and loss (LM) models.

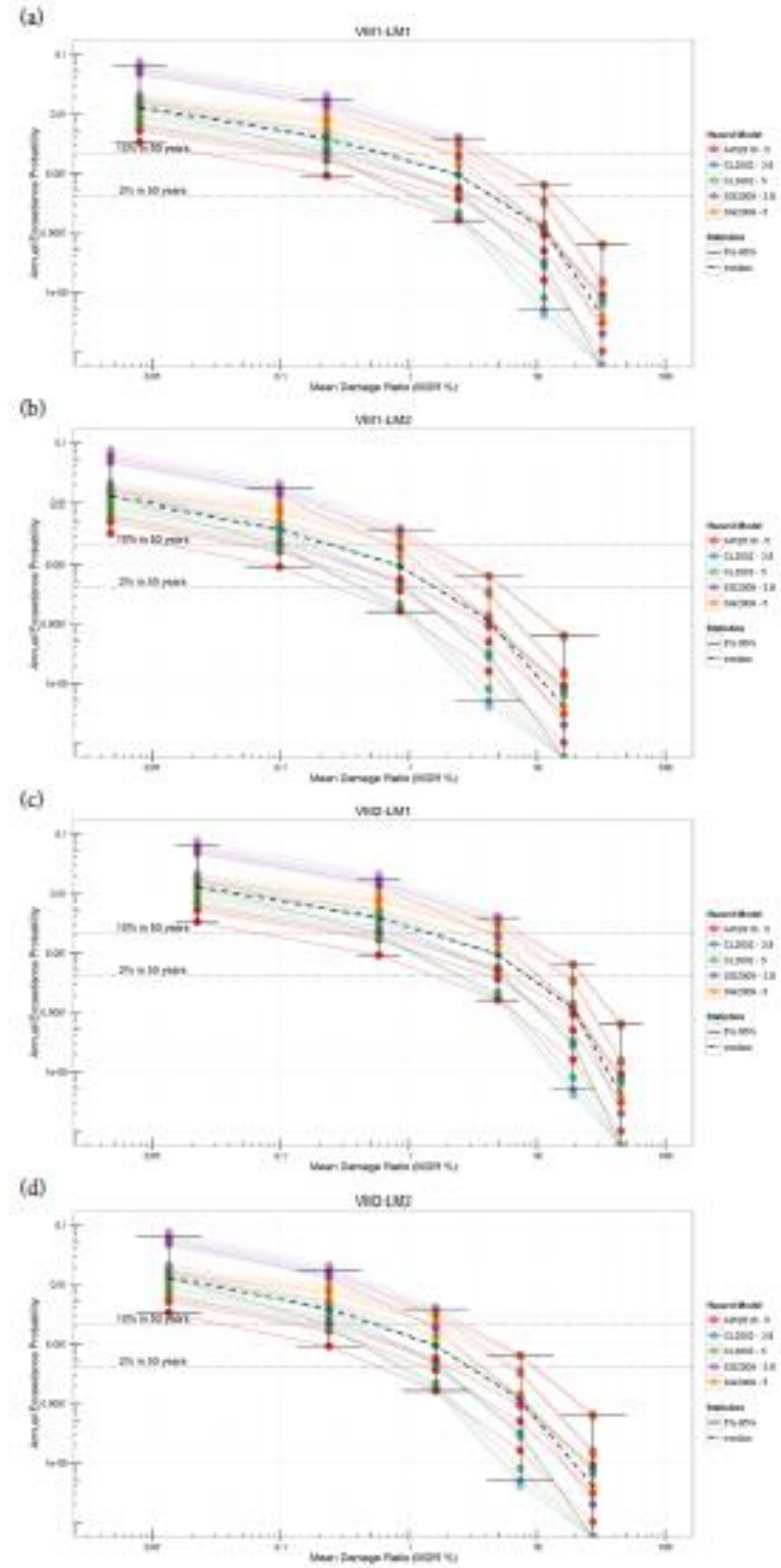

Figure 11. Comparison of the risk curves for different combinations of the vulnerability and loss models: **(a)** VM1 and LM1, **(b)** VM1 and LM2, **(c)** VM2 and LM1, **(d)** VM2 and LM2.

Tyagunov et al., 2014

Multi Hazard and Multi Risk

The example of Cologne (Germany)

Sensitivity analysis

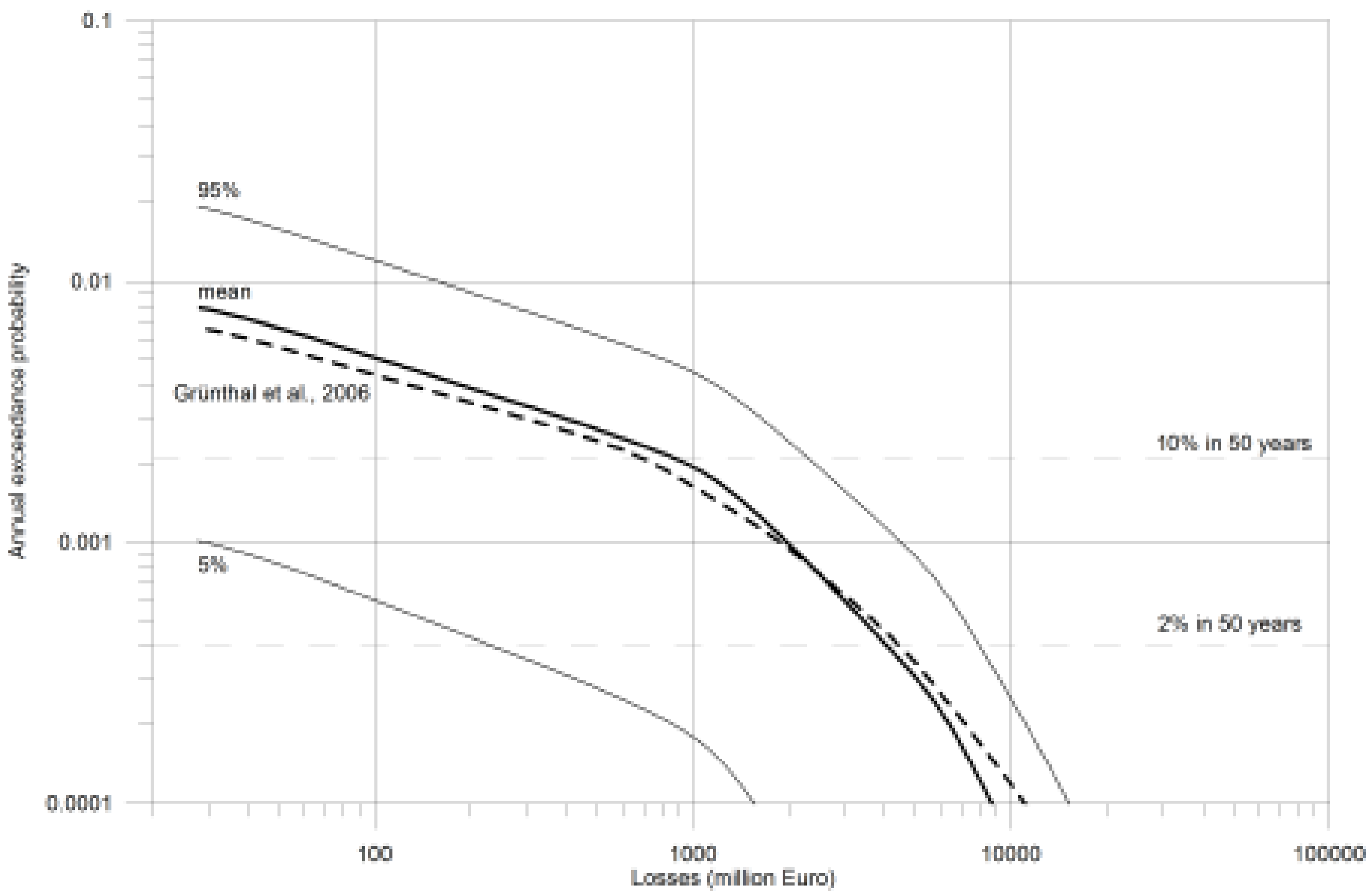

Figure 13. Seismic risk curves in terms of monetary losses (millions of Euros) due to structural damage to the residential building stock in Cologne (mean and 5–95 % percentiles). The dashed line shows the mean risk curve from the study of Grünthal et al. (2006), which also included the damage to commercial and industrial buildings.

Tyagunov et al., 2014

Multi Hazard and Multi Risk

Harmonizing and comparing single-type natural hazard risk estimations

The "total risk" curve relates the exceedance probability of a given loss value, independent of the risk source (or sources) causing it. If Pi(Lj) is the probability of exceedance of the jth loss *per* annum (Lj) for the ith risk source (e.g., earthquakes, floods, landslides, etc.), then the total annual exceedance probability curve can be calculated as:

$$\mathbf{P(Lj)tot = 1 - \Pi\ (1 - Pi(Lj))}$$

which is valid for *i* independent single-type risk sources (i.e., neglecting possible risk interactions)

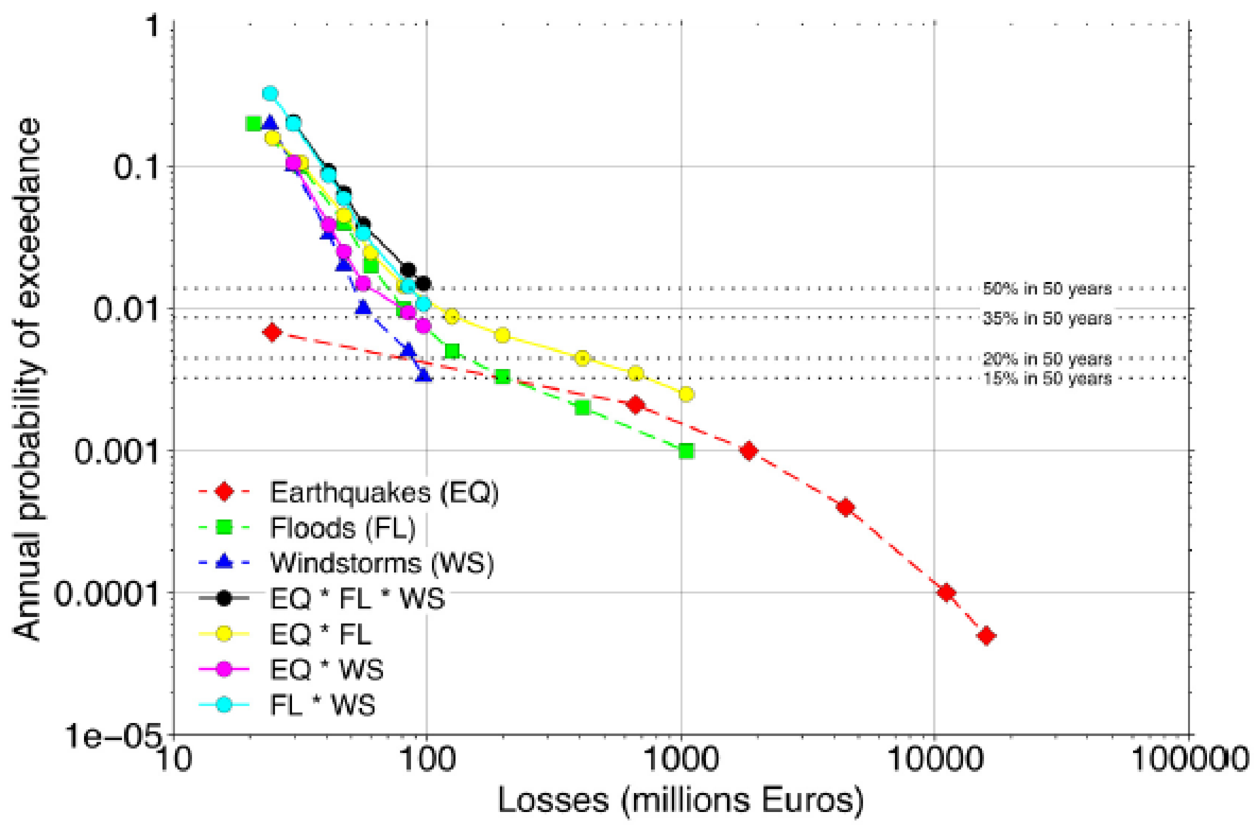

Figure 1. The individual risk curves for the three main hazards (earthquakes - EQ, floods - FL, windstorms - WS) that affect Cologne, as presented by Grünthal et al. [2006], and their various combinations derived using Equation (1).

Fleming et al., 2016

Multi Hazard and Multi Risk

Harmonizing and comparing single-type natural hazard risk estimations: visualization with a risk matrix

Value	Likelihood classification	Annual probability	Expected return period	Impact classification	Lower value ($\times 10^6$ euros)
5	Very likely	≤ 0.1	10	Disastrous	10,000
4	Likely	≤ 0.01	100	Significant	1,000
3	Conditionally likely	≤ 0.001	1,000	Moderate	100
2	Unlikely	≤ 0.0001	10,000	Minor	10
1	Very unlikely	≤ 0.00001	100,000	Insignificant	1

Table
hood a

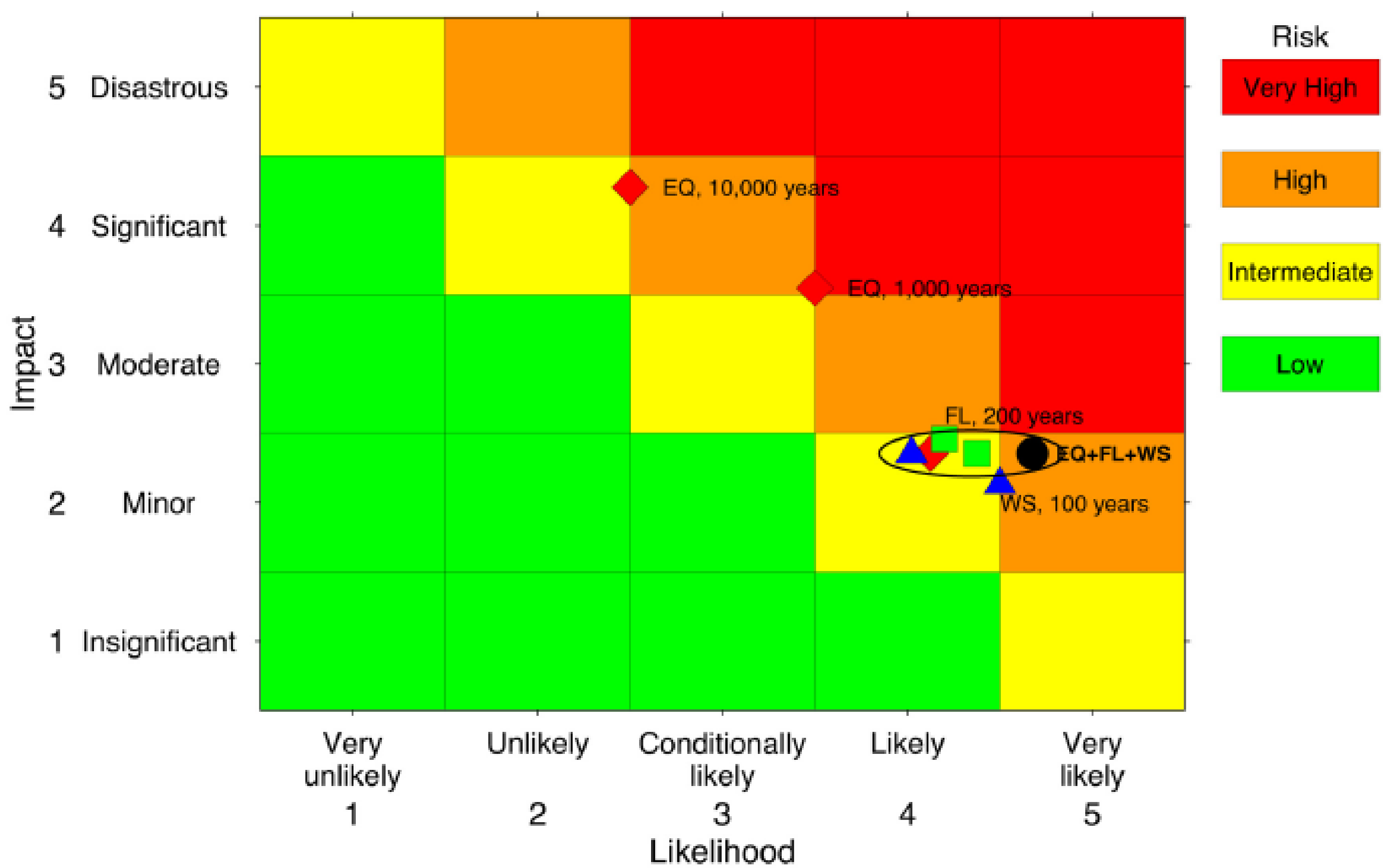

Figure 2. Risk matrix (exploiting the values presented in Figure 1) showing how combining the risk associated with individual perils (EQ - earthquake, FL - flood, WS - windstorm) can lead to a significantly higher probability of exceeding a given level of loss (EQ+FL+WS). The individual and combined risk estimates outlined by the ellipse correspond to the annual exceedance of losses of ⇔100 million, hence why they are all along the same Impact row. The ranges for the different classifications are presented in Table 1. The color scheme is derived from that used by BBK [2011].

Fleming et al., 2016

Multi Hazard and Multi Risk

Harmonizing and comparing single-type natural hazard risk estimations: Prioritization of risk under uncertainties

Are losses arising from two independent typologies of hazards for a specific return period are significantly different?

Distribution free ranking
Mann-Whitney test

is a nonparametric test of the null hypothesis that, for randomly selected values *X* and *Y* from two populations, the probability of *X* being greater than *Y* is equal to the probability of *Y* being greater than *X*.

Details on the test can be found in Barlow, R.J. (1989). Statistics A guide to the use of statistical methods in the physical sciences, John Wiley & Sons, 204 p. Available in the library

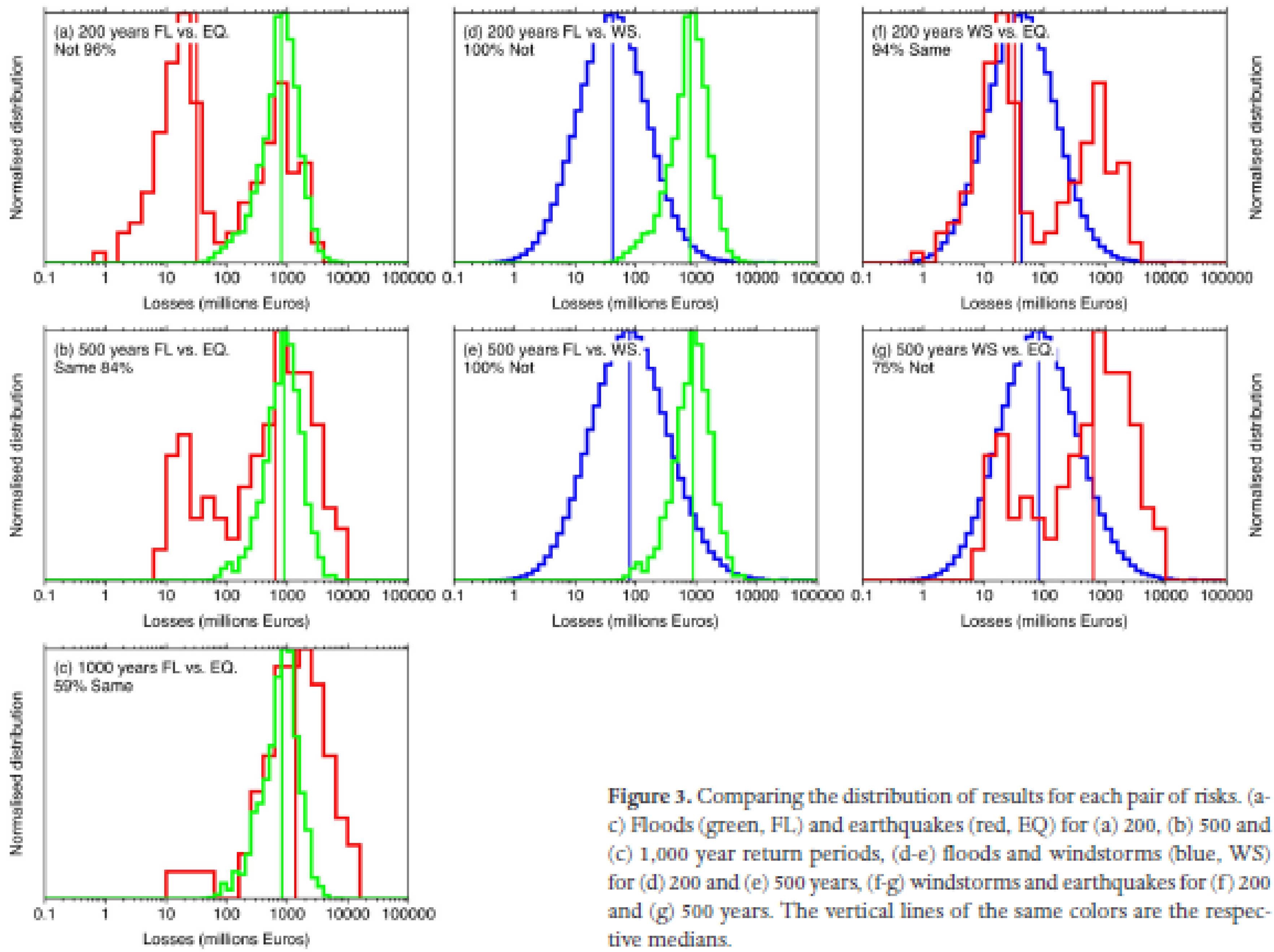

Figure 3. Comparing the distribution of results for each pair of risks. (a-c) Floods (green, FL) and earthquakes (red, EQ) for (a) 200, (b) 500 and (c) 1,000 year return periods, (d-e) floods and windstorms (blue, WS) for (d) 200 and (e) 500 years, (f-g) windstorms and earthquakes for (f) 200 and (g) 500 years. The vertical lines of the same colors are the respective medians.

Fleming et al., 2016

Multi Hazard and Multi Risk

Multihazard analysis fragility analysis

Example for fluvial earthen dikes in earthquake and flood-prone areas due to liquefaction.

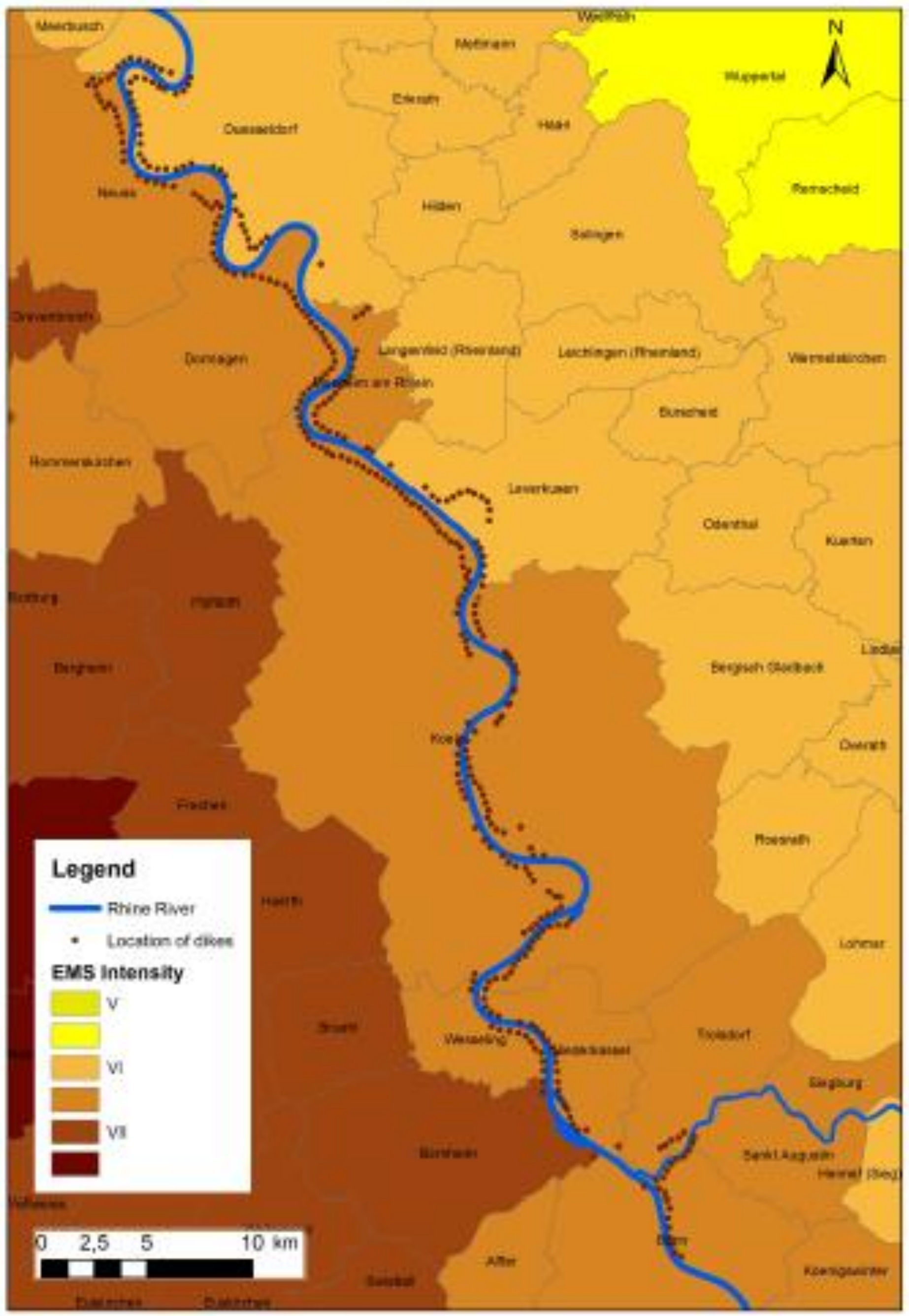

Figure 1. Location of flood protection dikes along the Rhine and the spatial distribution of seismic hazard in the study area in terms of EMS intensities for an exceedance probability of 10 % in 50 years (Grünthal et al., 1998).

Soil properties	Mean	Standard deviation	Minimum	Maximum
Specific weight γ (k N m^{-3})	18	1	13	21
Friction angle ϕ	29.2	0.3	20.8	37.6
Fines content, FC (%)	5	1	3	11

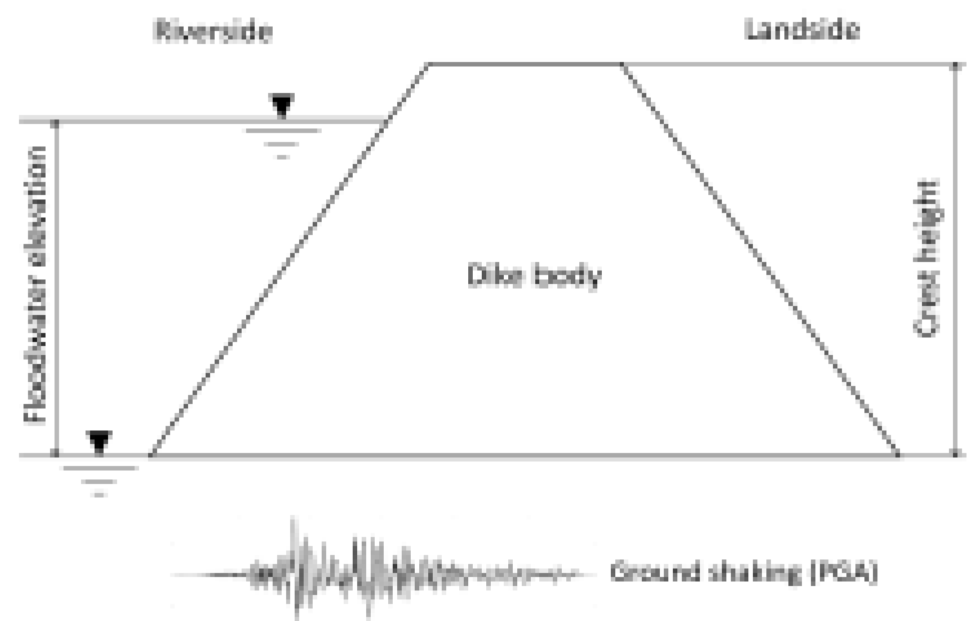

Figure 2. Generic dike model to illustrate the earthquake–flood–dike interaction.

Tyagunov et al., 2018

Multi Hazard and Multi Risk

Multihazard analysis fragility analysis

Example for fluvial earthen dikes in earthquake and flood-prone areas due to liquefaction.

The liquefaction potential, estimated using the method of Seed and Idriss (1971). The liquefaction potential can be assessed with a **factor of safety (FS)** against liquefaction, which is determined as the ratio of the capacity of the soil to resist liquefaction **(CRR, cyclic resistance ratio)** and the seismic demand placed on the soil layer **(CSR, cyclic stress ratio)**.
The CSR value can be estimated using the following expression:

$$\mathrm{CSR} = 0.65 \times \frac{a_{\max}}{g} \times \frac{\sigma_{\mathrm{vo}}}{\sigma'_{\mathrm{vo}}} \times r_{\mathrm{d}},$$

(PGA), g is the gravitational acceleration, σ_{vo} and σ'_{vo} are the total and effective overburden stresses (pressure imposed by above layers) of the soil, respectively, and rd is a stress reduction factor that depends on the depth.
For the calculation of the vertical stresses as a function of depth, the variations in the water level in the river, which influences the phreatic surface and degree of saturation in the dike core is considered.

As for the CRR value, probably the most common method based on standard penetration testing (SPT). Here, due to the lack of SPT data, an approach based on the correlation between penetration resistance and the angle of internal friction for sandy soils was used

Table 1. Relationship between the angle of internal friction and SPT values (Peck, 1974).

SPT, *N* value	Density of sand	φ (degrees)
< 4	Very loose	< 29
4–10	Loose	29–30
10–30	Medium	30–36
30–50	Dense	36–41
> 50	Very dense	> 41

Tyagunov et al., 2018

Multi Hazard and Multi Risk

Multihazard analysis fragility analysis

Example for fluvial earthen dikes in earthquake and flood-prone areas due to liquefaction.

The performance of dikes under seismic ground motion loading is analysed using a simplified one-dimensional model assuming that below the water level the soil is in a saturated state.

CSR (reflecting the level of seismic ground shaking) and CRR (depending on the dike material properties and the water level) are calculated for all points of the dike cross-section from the crest to the bottom (with a discretization interval of 5 cm). Once both the CSR and CRR values have been determined at a certain point under certain load conditions, one can calculate the factor of safety (FS) against liquefaction employing the following relationship (Seed and Idriss, 1971):

$$FS = \frac{CRR}{CSR}.$$

Computations of the liquefaction potential are done in a **Monte Carlo simulation** (MCS) considering the variability (uncertainty) of the geotechnical parameters of the dikes

Based on a frequency analysis of the MCS results, **dike failure probabilities** are computed for different points of the discretized two-dimensional load space, considering possible combinations of peak ground acceleration and floodwater level.

Tyagunov et al., 2018

Multi Hazard and Multi Risk

Multihazard analysis fragility analysis

Example for fluvial earthen dikes in earthquake and flood-prone areas due to liquefaction.

The fragility results are presented in a three-dimensional form, with seismic and hydraulic load described by peak ground acceleration and water level

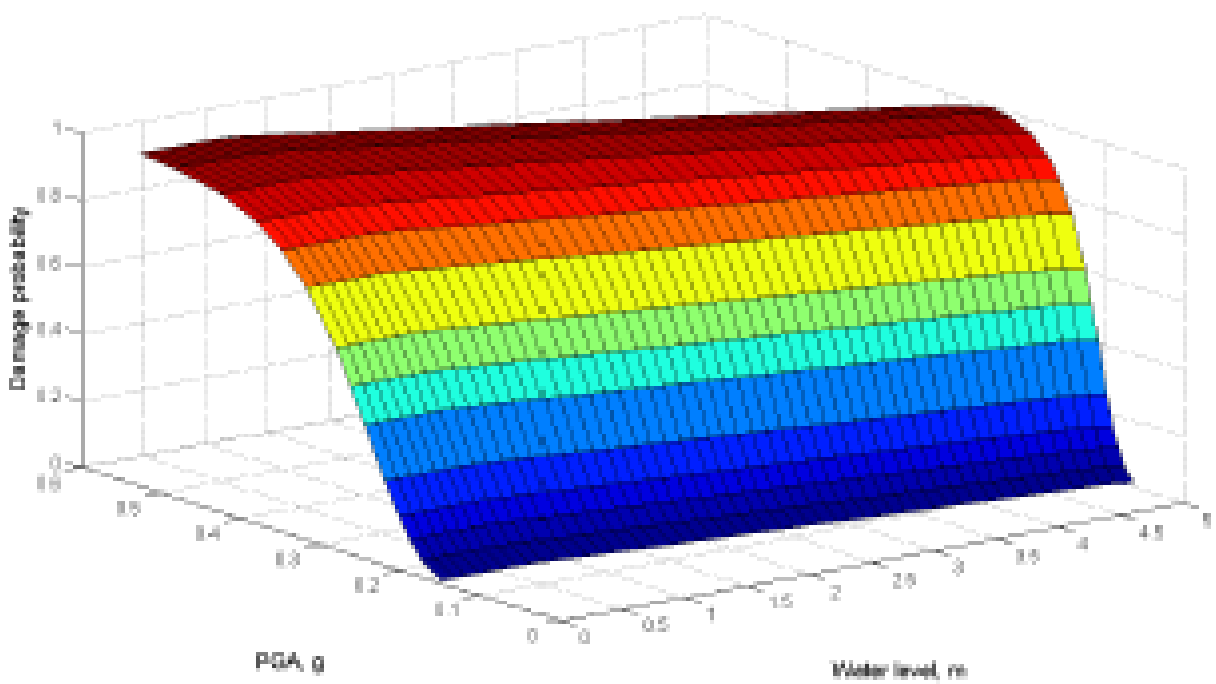

Figure 3. Multi-hazard fragility surface for liquefaction failure of a dike.

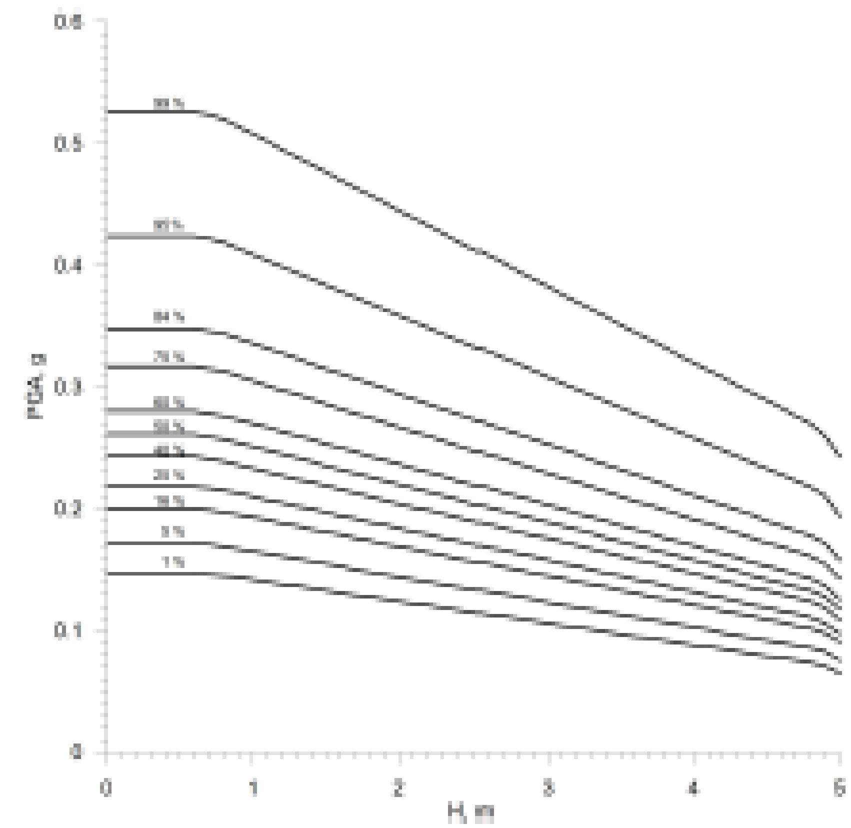

Figure 4. Dike failure probability in the PGA and water level space.

Tyagunov et al., 2018
Tyagunov et al., 2018

Multi Hazard and Multi Risk

Multihazard analysis fragility analysis

Example for fluvial earthen dikes in earthquake and flood-prone areas due to liquefaction.

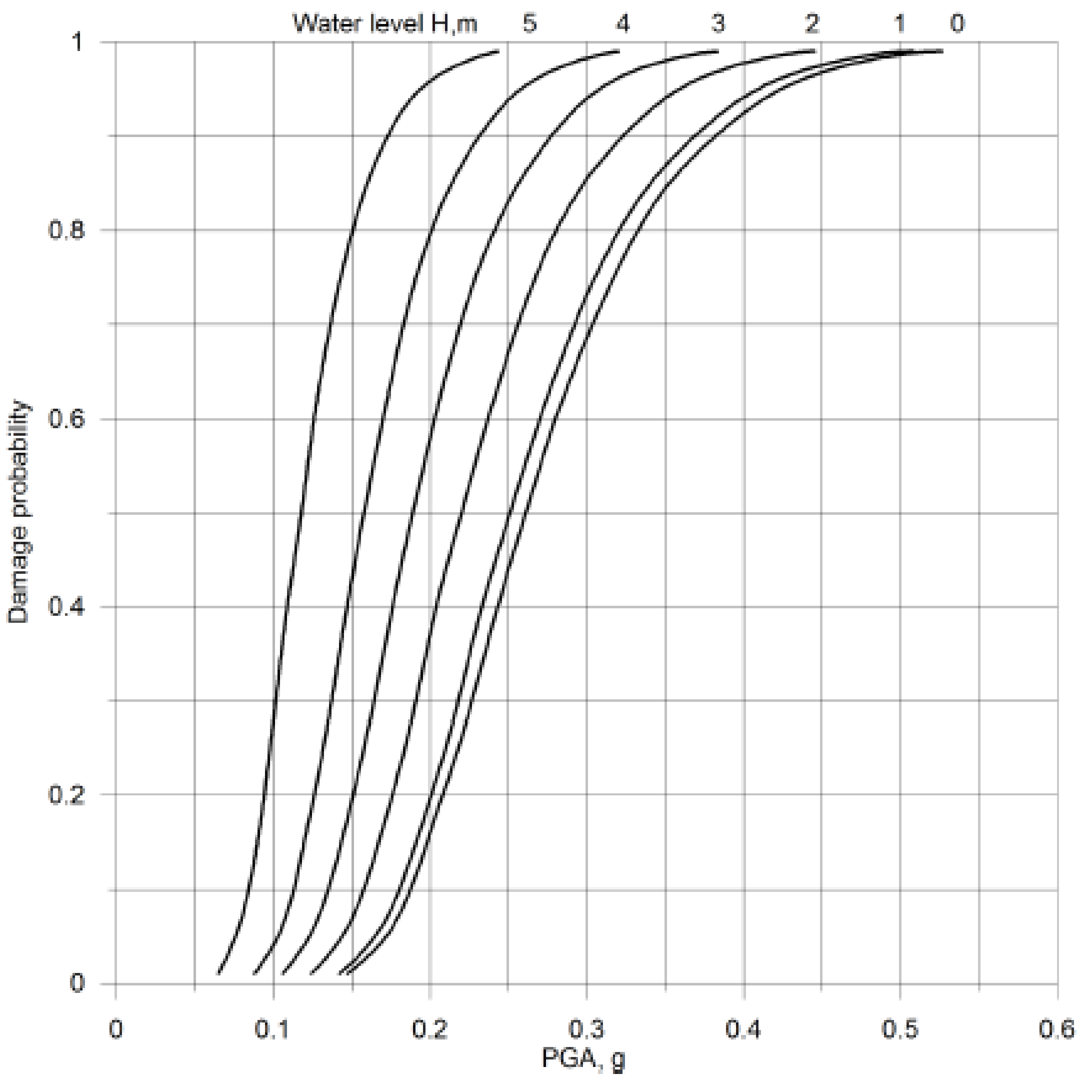

Figure 5. Fragility functions for earthen dikes for different water levels ranging from the dike toe to the assumed crest height.

Tyagunov et al., 2018

Multi Hazard and Multi Risk

Multihazard analysis fragility analysis

Example for fluvial earthen dikes in earthquake and flood-prone areas due to liquefaction

Integrating seismic and hydraulic load for the calculation of the multi-hazard failure probability

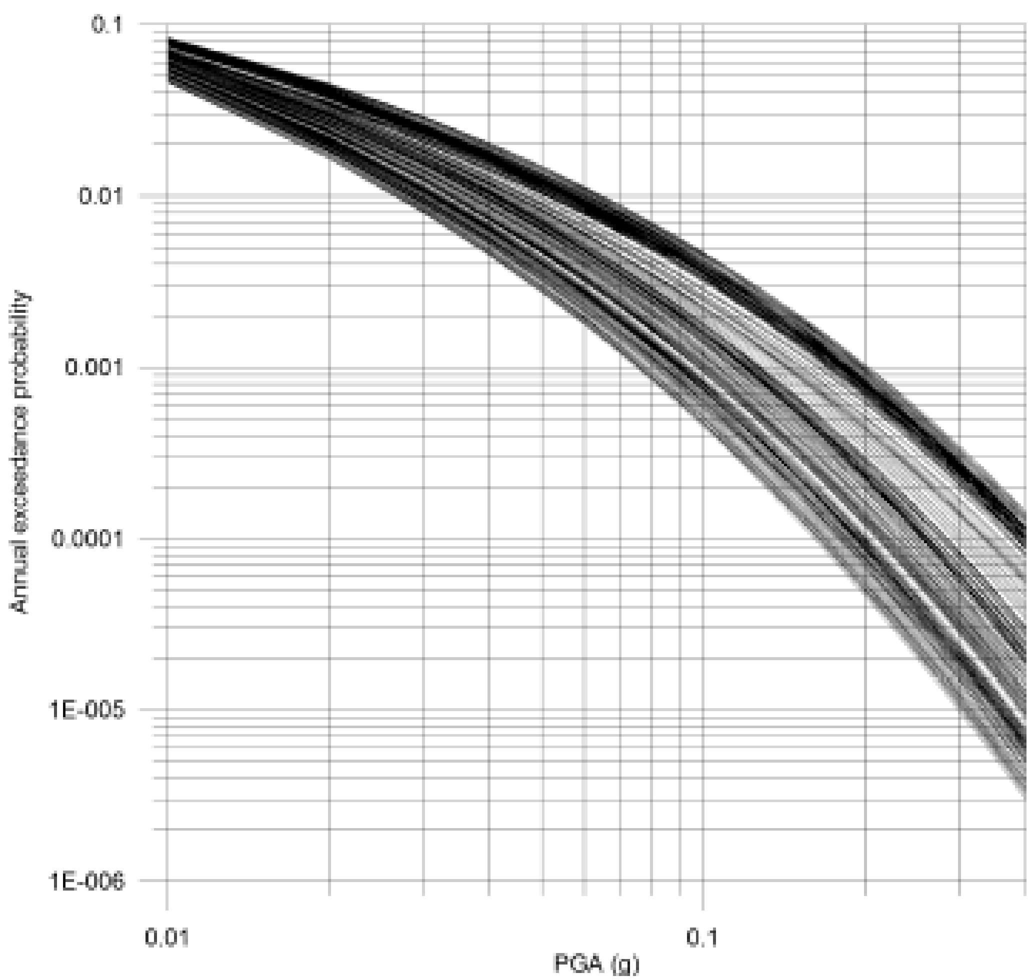

Figure 6. Seismic hazard (mean) curves for the locations of the dikes along the Rhine River. Each curve corresponds to one dike segment.

The actual dike failure probabilities can be quantified by considering the probabilities of occurrence of the earthquake ground shaking level and flood return periods at different dike locations combined with the presented fragility curves

The simultaneous occurrence of a flood and an earthquake should be assumed. The typical duration of a flood wave of 30 days is considered for the Rhine. It is assumed that no dike repair actions are undertaken in this period, which may affect the probability of failure. Thus, the earthquake probability is computed for this period to be combined in the following expression to determine the actual failure probability

$$P(F) = \iint P(F|S_i^{30}, W_j) \times P(S_i^{30}) \times P(W_j)\, \mathrm{d}S\mathrm{d}W,$$

where $P\left(F|S_i^{30}, W_j\right)$ is the conditional failure probability given the combination of the seismic ground shaking S_i^{30} within a time window of 30 days and the water level W_j; $P\left(S_i^{30}\right)$ is the probability of occurrence of the seismic input S (peak ground acceleration) of the level i within a time window of 30 days; $P(W_j)$ is the probability that the water level W corresponds to the level j.

Tyagunov et al., 2018